AD_____

Award Number: DAMD17-02-1-0375

TITLE: CBP and Extracellular Matrix-Induced Apoptosis in p53(-) HMECs: A Model of Early Mammary Carcinogenesis

PRINCIPAL INVESTIGATOR: Victoria Seewaldt, M.D.

CONTRACTING ORGANIZATION: Duke University Medical School
Durham, NC 27710

REPORT DATE: September 2006

TYPE OF REPORT: Final

PREPARED FOR: U.S. Army Medical Research and Materiel Command
Fort Detrick, Maryland 21702-5012

REPORT DOCUMENTATION PAGE

Form Approved
OMB No. 0704-0188

1. REPORT DATE	2. REPORT TYPE	3. DATES COVERED
01-09-2006	Final	1 Sep 2002 – 31 Aug 2006

4. TITLE AND SUBTITLE

CBP and Extracellular Matrix-Induced Apoptosis in p53(-) HMECs: A Model of Early Mammary Carcinogenesis

5a. CONTRACT NUMBER

5b. GRANT NUMBER
DAMD17-02-1-0375

5c. PROGRAM ELEMENT NUMBER

6. AUTHOR(S)

Victoria Seewaldt, M.D.

5d. PROJECT NUMBER

5e. TASK NUMBER

5f. WORK UNIT NUMBER

7. PERFORMING ORGANIZATION NAME(S) AND ADDRESS(ES)

Duke University Medical School
Durham, NC 27710

8. PERFORMING ORGANIZATION REPORT NUMBER

9. SPONSORING / MONITORING AGENCY NAME(S) AND ADDRESS(ES)
U.S. Army Medical Research and Materiel Command
Fort Detrick, Maryland 21702-5012

10. SPONSOR/MONITOR'S ACRONYM(S)

11. SPONSOR/MONITOR'S REPORT NUMBER(S)

12. DISTRIBUTION / AVAILABILITY STATEMENT
Approved for Public Release; Distribution Unlimited

13. SUPPLEMENTARY NOTES
Original contains colored plates: ALL DTIC reproductions will be in black and white.

14. ABSTRACT

Interactions between normal mammary epithelial cells (HMECs) and extracellular matrix (ECM) are important for mammary gland homeostasis and loss of ECM-sensitivity is an early event in mammary carcinogenesis. The purpose of this grant is to investigate how the CREBP-binding protein (CBP) might target the elimination of damaged HMECs. We have observed that 1) suppression of CBP results in apoptosis-resistance through impaired laminin expression and 2) CBP promotes induction of interferon-regulated genes during apoptosis. These findings will provide novel targets for chemoprevention and are being used to develop markers for response to current prevention strategies.

15. SUBJECT TERMS
prevention, CREBP-binding protein, extracellular matrix, apoptosis

16. SECURITY CLASSIFICATION OF:				18. NUMBER OF PAGES	19a. NAME OF RESPONSIBLE PERSON
					USAMRMC
a. REPORT	b. ABSTRACT	c. THIS PAGE			19b. TELEPHONE NUMBER *(include area code)*
U	U	U	UU	129	

Table of Contents

INTRODUCTION:
Interactions between normal mammary epithelial cells (HMECs) and extracellular matrix (ECM) are important for mammary gland homeostasis; loss of ECM-sensitivity is thought to be an early event in mammary carcinogenesis. The CREBP binding protein (CBP) is known to regulate both proliferation and apoptosis but the role of CBP in ECM-signaling is poorly characterized. **The purpose of this grant is to investigate how CBP might regulate apoptosis in HMECs. Major findings to date and progress in fulfillment of Specific Aim I: YEAR 1-2 FINDINGS:** We investigated the relationship between CBP expression and sensitivity to prepared ECM (rECM)-induced growth arrest and apoptosis in an *in vitro* model of early mammary carcinogensis. Suppression of CBP expression in HMECs by antisense oligonucleotides (ODNs) resulted in loss of rECM-mediated growth regulation, polarity, and apoptosis. Chromatin immunoprecipitation studies (ChIP) and reporter studies demonstrated that inhibition of CBP protein expression resulted in 1) loss of CBP-occupancy of the *LAMA3A* promoter and 2) a decrease in *LAMA3A* promoter activity. rECM-resistance correlated with 1) loss of CBP occupancy of the *LAMA3A* promoter, 2) decreased *LAMA3A* promoter activity, and 3) loss of laminin-5 α3-chain mRNA and protein expression. These observations suggest a critical role for CBP in rECM-mediated growth regulation, polarity, and apoptosis through modulation of *LAMA3A* activity and laminin-5 α3-chain expression. Expression of CBP in rECM-resistant cells resulted in induction of laminin-5 α3-chain expression and restoration of apoptosis-sensitivity. Suppression of CBP expression in apoptosis-resistant cells resulted in 1) loss of CBP occupancy of the LAMA3A promoter, 2) loss of laminin-5 α3-chain expression, and 3) apoptosis-resistance. **YEAR 3-4 FINDINGS:** To further test the role of laminin-5 signaling in promoting apopotosis, we developed anti-sense oligonucleotides (ODS) directed against laminin-5. These constructs suppressed laminin-5 expression by over 60% and resulted in loss of apoptosis. In addition we **Major findings to date and progress in fulfillment of Specific Aim II: YEAR 1-2 FINDINGS:** CBP is a known regulator of interferon **(**IFN)-signaling and dysregulated expression of IFN-signal transduction genes has been observed during mammary carcinogeneis. We hypothesize that the level of CBP expression is critical for the induction of IFN-activated transcription during rECM-mediated apoptosis in HMEC-E6 cells. We observed that CBP regulates induces expression of interferon regulated genes in the absence of interferon release. rECM promotes CBP occupancy of the IRF-1 promoter and upregulation of IRF-1 mRNA and protein. Inhibition of IRF-1 signaling by siRNA directed against IRF-1 blocks IRF-1 expression, induction of interferon regulated genes, and apoptosis resistance. **YEAR 3-4 FINDINGS:** We further investigated the composition of co-activator complex necessary to induce IRF-1 expression. We observe that the nuclear regulator, STAT1 as CBP well as CBP were recruited to the gamma-interferon activation sequence (GAS) element of the IRF-1 promoter. Inhibition of CBP expression resulted in loss of CBP recruitment to the GAS element and inhibited IRF-1 expression. We next investigated co-activator recruitment to the interferon signaling gene 6-16. 6-16 is known to be downstream from IRF-1 but the exact mechanism of 6-16 induction is poorly understood. Here we observed that CBP, IRF-1, and STAT1 were all required to be recruited to the 6-16 promoter in order to induce 6-16 expression. Results have been accepted for publication in Oncogene. These finding have allowed us to develop new markers for breast cancer risk that are currently being translated in our high-risk clinic.

BODY:

SPECIFIC AIM I: Does the level of the CREBP binding protein (CBP) protein expression in normal human mammary epithelial cells (HMECs) determine sensitivity to prepared extracellular matrix (rECM)-mediated apoptosis? [See appended manuscript Dietze et al. Journal of Cell Science, 2005]

1a) Suppression of CBP in early passage HMECs by antisense oligonucleotides (ODNs). Antisense ODNs were utilized to suppress CBP protein expression in HMECs to test whether the level of CBP protein expression might be important for rECM-sensitivity. Relative levels of CBP protein expression were tested by Western analysis. Early passage HMEC vector controls (HMEC-LXSN) and early passage apoptosis-sensitive HMECs transduced with human papillomavirus-16 E6 protein (HMEC-E6) treated with the active, CBP-specific ODN, A3342V, exhibited a 65% and 72% respective decrease in CBP protein expression relative to untreated controls. Cells treated with the inactive CBP ODN, scrA3342V, did not exhibit a significant decrease in CBP protein expression.

1b) Suppression of CBP enhances proliferation in rECM. Treatment of early passage HMEC-LXSN controls and HMEC-E6 cells with CBP-specific ODNs resulted in enhanced proliferation in rECM-culture as measured by 1) physical growth parameters and 2) Ki-67 staining. Both early passage HMEC-LXSN controls and HMEC-E6 cells treated with active CBP-specific ODNs (A33243V) demonstrated a continued increase in sphere diameter from Day 7-9 in rECM culture. In contrast, early passage HMEC-LXSN controls and HMEC-E6 cells treated with inactive ODNs (scrA33243V) did not exhibit an increase in sphere diameter after Day 7. Treatment of early passage HMEC-LXSN and HMEC-E6 cells with CBP-specific ODNs (A33243V) resulted in continued Ki-67 staining at 9 and 11 days in rECM culture. In contrast, Ki-67 staining at 9 and 11 days were markedly reduced in HMEC-LXSN and HMEC-E6 cells treated with inactive ODNs (scrA33423V). These observations show that suppression of CBP protein expression in early passage HMEC-E6 cells and HMEC-LXSN controls resulted in enhanced proliferation in rECM culture.

1c) Suppression of CBP protein results in altered localization and expression of biochemical markers of polarity. Early passage HMEC-E6 cells and HMEC-LXSN controls treated with active CBP ODNs (A33423V) exhibited a loss of epithelial polarity as evidenced by dispersed and intracellular staining of 1) E-cadherin and 2) the tight junction-associated protein, ZO-1. In contrast, early passage HMEC-LXSN controls and HMEC-E6 cells treated with inactive CBP ODNs (scrA33423V) demonstrated expression of E-cadherin and ZO-1 at the cell-cell junction, consistent with a correctly polarized epithelium. These observations indicate that suppression of CBP protein expression in HMECs by antisense ODNs promotes a loss of epithelial polarity in rECM culture.

1d) Suppression of CBP inhibits apoptosis in rECM culture. Early passage HMEC-E6 cells were treated with CBP-specific antisense ODNs to test whether suppression of CBP protein expression blocked apoptosis in rECM culture. Early passage HMEC-E6 treated with CBP-specific antisense ODNs (A33423V) formed large irregular clusters in rECM and did not undergo apoptosis as assessed by either electron microscopy or TUNEL-staining. In contrast, early passage HMEC-E6 cells treated with inactive CBP ODNs underwent apoptosis on Day 7

as assessed by either morphologic criteria or TUNEL-staining. Similar to early passage HMEC-E6 cells, early passage HMEC-LXSN cells treated CBP-specific, antisense ODNs (A33423V) formed large irregular clusters in rECM. Early passage HMEC-LXSN controls treated with inactive ODN (scrA33423V) formed a morphologically organized, ascinus-like structure and did not undergo apoptosis consistent with what has been previously observed for early passage HMEC-LXSN untreated controls. These observations demonstrate that suppression of CBP protein expression in early passage HMEC-E6 cells by antisense ODNs blocks apoptosis in rECM culture.

A second HMEC strain, AG11134, was tested to ensure that these observations were not HMEC strain-specific. Similar to observations made in HMEC strain AG11132 above, 1) early passage AG11134-E6 cells treated with inactive CBP ODN (scrA33423V) were sensitive to rECM-growth regulation and underwent apoptosis at Day 7, 2) early passage AG1134-LXSN controls treated with antisense-CBP ODN (A99424V) were resistant to rECM growth arrest and did not undergo apoptosis at Day 7-9, and 3) early passage AG11134-LXSN controls treated with CBP-specific antisense ODNs were resistant to rECM-mediated growth regulation and did not undergo apoptosis (data not shown).

1e) Laminin-5 expression is decreased in rECM resistant, late passage HMEC-E6 cells. We previously observed that sensitivity to rECM-apoptosis in early passage HMEC-E6 cells required polarized expression of α3/β1-integrin. Differential gene expression studies, semi-quantitative RT-PCR, and Western analysis were performed to test whether the loss of sensitivity to rECM-mediated growth regulation, polarity, and apoptosis observed in late passage HMEC-E6 cells correlated with altered expression of laminin-5 and/or α3/β1-integrin mRNA. Differential gene expression studies demonstrated decreased expression of all three laminin-5 chains (α3, β3, and γ2) in apoptosis-resistant, late passage HMEC-E6 cells relative to early passage HMEC-LXSN controls and early passage HMEC-E6 cells grown in rECM. Semi-quantitative RT-PCR confirmed a 98% decrease in laminin-5 α3-chain ($p \leq 0.01$), an 88% decrease in laminin-5 β3-chain ($p \leq 0.01$), and a 75% decrease in laminin-5 γ2-chain ($p \leq 0.01$) mRNA expression relative to early passage HMEC-LXSN controls. There was no significant change in the level of α3/β1-integrin mRNA expression. Western analysis similarly demonstrated an 85% ($p < 0.001$) decrease in laminin-5 α3-chain protein expression in apoptosis-resistant, late passage HMEC-E6 cells relative to early passage HMEC-LXSN controls. Expression of laminin-5 α3-chain protein did not significantly vary between early passage HMEC-LXSN cells and early passage HMEC-E6 cells. There was a 130% ($p < 0.002$) increase in laminin-5 α3-chain protein in late passage HMEC-LXSN controls relative to early passage HMEC-LXSN cells. These observations demonstrate that the presence of rECM-resistance in late passage HMEC-E6 cells correlates with a loss of laminin-5 mRNA and protein expression.

1f) Lack of polarized expression of laminin-α3 and integrin-α3 proteins in late passage HMEC-E6 cells grown in rECM. Early and late passage HMEC-LXSN controls and HMEC-E6 cells were grown in rECM and tested for 1) laminin-5 α3-chain and 2) α3- and β1-integrin expression by immunohistochemistry (clones P5H10, P1F2, and P4C10, respectively). Early and late passage HMEC-LXSN controls and early passage HMEC-E6 cells exhibited polarized basal expression of laminin-5 α3-chain and α3- and β1-integrins. In contrast, late passage,

CBP-"poor" HMEC-E6 cells grown in rECM demonstrated disorganized plasma membrane and cytosolic expression of both laminin-5 α3-chain and α3-integrin. As predicted by differential gene expression studies and Western analysis, there was also a qualitative decrease in laminin-5 α3-chain expression in late passage HMEC-E6 cells relative to controls. Late passage HMEC-E6 cells grown in rECM exhibited polarized basal β1-integrin expression but had an increase in the amount of cytosolic expression relative to early passage cells. These observations demonstrate a loss of polarized expression of laminin-5 α3-chain and α3-integrin in rECM-resistant late passage HMEC-E6 cells.

1g) Suppression of CBP expression in HMECs alters both laminin-α3 and integrin-α3 protein expression in rECM culture. We observed that late passage HMEC-E6 cells grown in rECM culture exhibit 1) reduced levels of CBP protein expression and 2) disorganized expression of both laminin-5 α3-chain and α3-integrin. This observation led us to hypothesize that suppression of CBP in HMECs would alter laminin-5 α3-chain and α3-integrin expression and/or distribution. CBP protein expression was suppressed in early passage HMEC-E6 cells and HMEC-LXSN controls by treatment with CBP-specific, antisense ODN (A99424V). HMECs with suppressed CBP expression exhibited disorganized plasma membrane and cytosolic distribution of laminin-5 α3-chain and α3-integrin. β1-integrin expression was observed at the basal surface. In contrast, early passage HMEC-LXSN controls and HMEC-E6 cells treated with inactive CBP ODN (scrA99424V) exhibited polarized basal expression of laminin-5 α3-chain and α3- and β1-integrins . These observations demonstrate that suppression of CBP protein expression in HMECs alters the distribution of both laminin-5 α3-chain and α3-integrin.

1h) Decreased CBP expression in rECM-resistant late passage HMEC-E6 cells correlates with decreased LAMA3A promoter activity. We tested whether the observed decrease in CBP and laminin-5 α3-chain expression in late passage HMEC-E6 cells correlated with decreased LAMA3A promoter activity. Early and late passage HMEC-E6 and passage-matched HMEC-LXSN controls were transiently transfected with a CAT reporter coupled to the *LAMA3A* promoter sequence (1403 bp, GenBank Accession Number AF279435) and grown in rECM culture. rECM-sensitive early passage HMEC-E6 cells and early and late passage HMEC-LXSN controls exhibited a similar level of *LAMA3A* activity. In contrast, rECM-resistant, late passage HMEC-E6 cells with decreased CBP and laminin-5 α3-chain expression exhibited a 91% decrease in *LAMA3A* promoter activity relative to early passage HMEC-E6 cells ($p \leq 0.01$). These experiments demonstrate in HMECs a positive correlation between 1) the level of CBP and laminin-5 α3-chain protein expression and 2) *LAMA3A* promoter activity.

1i) LAMA3A promoter activity in HMECs with suppressed CBP protein expression. We next tested whether suppression of CBP protein expression resulted in decreased *LAMA3A* promoter activity. LAMA3A-CAT reporter activity was compared in early passage HMEC-LXSN and HMEC-E6 cells treated with either CBP-specific antisense ODNs (A33423V) or inactive ODNs (scrA33423V). A 92% and 89% decrease ($p<0.01$) in *LAMA3A* promoter activity was observed, respectively, in early passage HMEC-LXSN and HMEC-E6 cells grown in rECM and treated with CBP-specific ODNs (A33423V) relative to cells treated with inactive ODNs (scrA33423V). No significant difference in *LAMA3A* promoter activity was observed in

HMECs treated with or without inactive ODNs. These observations demonstrate that suppression of CBP expression in HMECs results in a reduction in *LAMA3A* promoter activity.

1j) Lack of CBP occupancy of the human laminin 5 (LAMA3A) promoter correlates with rECM-resistance. The human *LAMA3A* promoter contains three AP-1 sites at positions –387, –185, and –127. The AP-1 site, at position –185, has been previously shown to be critical for basal activity in mammary epithelial cells. Chromatin immunopreciptation (ChIP) was performed in rECM-resistant, CBP-"poor" late passage HMEC-E6 cells and controls to test whether the observed 1) decrease in laminin-5 α3-chain expression and 2) loss of *LAMA3A* activity correlated with a lack of CBP binding to the 277 bp AP-1-"rich" site of the *LAMA3A* promoter (position -402 to –125). Early and late passage HMEC-LXSN control cells and rECM-sensitive, early passage HMEC-E6 cells grown in rECM demonstrated CBP binding to the AP-1-"rich" site of the *LAMA3A promoter*. In contrast, rECM-resistant, late passage HMEC-E6 cells, with decreased CBP and laminin-5 α3-chain expression, failed to demonstrate CBP binding. These observations suggest that a decrease in CBP expression might promote loss of CBP occupancy of the AP-1-"rich" site of the *LAMA3A* promoter.

1k) Suppression of CBP expression in HMECs results in loss of CBP occupancy of the LAMA3A promoter. Early passage HMEC-E6 cells were treated with active CBP ODNs and tested by ChIP to determine whether suppression of CBP protein expression resulted a loss of CBP occupancy of the AP-1-"rich" region of the *LAMA3A* promoter. Early passage HMEC-E6 cells treated with CBP-specific ODNs, and grown in rECM, did not demonstrate CBP occupancy of the *LAMA3A* promoter. In contrast, early passage HMEC-E6 controls, treated with inactive ODNs, and grown in rECM demonstrated CBP-occupancy. These observations demonstrate that suppression of CBP expression in HMEC-E6 cells by antisense ODNs results in a loss of CBP occupancy of the AP-1-"rich" site of the *LAMA3A* promoter. Since the AP-1 site, at position –185, is critical for basal activity in mammary epithelial cells, these observations provide a mechanism by which loss of CBP expression might promote loss of *LAMA3A* promoter activity and laminin-5 α3-chain expression in HMECs.

1e) Expression of CBP in apoptosis-resistant cells results in increased expression of laminin-5 and restoration of apoptosis-sensitivity in rECM culture. We used retroviral-mediated gene transfer to express CBP in late passage rECM-resistant cells with suppressed levels of CBP. Protein levels of CBP in our transduced were comparable to that observed in parental and rECM-sensitive HMEC-E6 cells. Expression of CBP in rECM-resistant cells resulted in restoration of 1) laminin-5 α3-chain expression and 2) apoptosis sensitivity. These observations highlight a critical role for CBP in regulating rECM-apoptosis and laminin-5 expression.

SPECIFIC AIM II: Does CBP modulate interferon (IFN)-signal transduction during rECM-mediated apoptosis in HMEC-E6 cells? Please see Bowie et al. Oncogene, 2006 which is now in press.

2a) Prepared extracellular matrix (rECM) activates caspases-1/-3 and induces apoptosis in HMEC-E6 cells

We have previously shown that 1.0 μM Tam promotes p53-independent apoptosis in HMEC-E6 cells through activation of caspases-1 and -3. Here we tested in large-scale 3-dimensional, high-density liquid rECM culture (3-hD) whether rECM, similar to Tam, activates caspases-1 and -3 and promotes apoptosis in *HMEC-E6 cells.

3-hD culture is an adaptation of the large-scale culture system developed by the laboratory of Mina Bissell. HMECs are plated at high density ($2.5 \times 10^7/25$ cm^2) on a non-adhesive substrate, and treated with a 1:100 dilution of growth factor-depleted rECM in Standard Media. In this system, HMEC-E6 cells and passage matched HMEC-LX controls detach from the non-adhesive substrate starting at 6 hr and spontaneously form 20-30 micron cellular aggregates in a liquid solution of growth-factor depleted rECM diluted in tissue culture media. HMEC-LX controls and HMEC-E6 cells undergo growth arrest starting between 6 and 7 hr ($p < 0.01$) while only HMEC-E6 cells undergo apoptosis which occurs at 12-24 hr ($p < 0.05$). This contrasts with our prior studies employing small scale 3-D rECM culture where HMECs are plated as single cell suspension in semi-solid growth factor-depleted rECM. In small scale 3-D rECM culture, HMEC-E6 cells and HMEC-LX controls proliferate for 6 days until they form 20-30 micron ascinus-like structures, and then undergo growth arrest. While HMEC-LX controls undergo growth arrest alone starting on Day 6, passage-matched HMEC-E6 cells undergo growth arrest on Day 6 followed by apoptosis on Day 6-7. For the experiments described here, large-scale 3-hD culture was chosen over small-scale 3-D culture due to the need to precisely synchronize our cells for promoter recruitment and differential gene expression studies. In large-scale 3-hD culture, apoptosis occurs starting at 12 hrs and occurs during a narrow window of time (versus 6-7 days for small-scale 3-D culture). Therefore, 3-hD culture allows for both precise temporal control and synchronization of gene expression prior to and during the induction of apoptosis.

We previously observed that 1.0 uM Tam promotes growth arrest and apoptosis in HMEC-E6 cells but growth arrest alone in HMEC-LX cells. Evidence of apoptosis in Tam-treated HMEC-E6 cells was first observed at 12 hr and maximally at 24 hr, as demonstrated by electron microscopy and Annexin V binding. Similarly, *HMEC-E6 cells grown in 3-hD culture demonstrated Annexin V binding first at 12 hr ($p < 0.05$) and maximally at 24 hr ($p < 0.001$) . In contrast, a significant increase in Annexin V binding was not observed in rECM-treated, passage-matched HMEC-LX vector controls at 24 hr ($p > 0.10$). These observations provide evidence that *HMEC-E6 cells undergo apoptosis in 3-hD culture starting at 12 hr.

We also previously demonstrated that Tam-induced apoptosis in *HMEC-E6 cells was dependent on sequential activation of caspase-1 and -3. In addition, we have shown that rECM culture 1) promotes apoptosis in *HMEC-E6 cells through laminin-5/α3β1-integrin signaling and 2) interruption of laminin-5/α3β1-integrin signaling blocked apoptosis. Here we tested whether rECM-induced apoptosis was similarly associated with caspase-1 and -3 activation, and whether α3- or β1-integrin blocking antibodies could inhibit this caspase activation. *HMEC-E6 cells grown in 3-hD culture demonstrated caspase-1 activation first at 3 hr ($p < 0.0001$), with maximal activation at 4 hr ($p < 0.0001$), and pre-treatment of *HMEC-E6 cells with α3- or β1-integrin blocking

antibodies inhibited the activation of caspase-1 ($p < 0.05$). The effector-caspase, caspase-3, was activated in *HMEC-E6 cells starting at 12 hr ($p < 0.001$), maximally at 24 hr ($p < 0.001$), and pre-treatment with α3- or β1-integrin blocking antibodies blocked the activation of caspase-3 ($p < 0.01$). Control non-immune mouse IgG did not block activation of caspases-1 and -3 ($p < 0.05$). These data show that 1) rECM, similar to Tam, promotes apoptosis in *HMEC-E6 cells associated with activation of caspases-1 and -3 and 2) pre-treatment of *HMEC-E6 with α3- or β1-integrin blocking antibodies inhibited the activation of caspases-1 and -3.

2b) cDNA microarray analysis of rECM-induced gene transcripts

To investigate the molecular mechanism of rECM-induced apoptosis in HMEC-E6 cells, we analyzed the expression profiles of early passage HMEC-E6 cells and passage-matched HMEC-LX vector controls in 3-hD rECM culture. Analysis was performed using HuGeneFL cDNA microarrays (Affymetrix™). We previously reported that treatment with 1.0 μM Tam induced interferon-stimulated genes (ISGs) in *HMEC-E6 cells. Surprisingly, rECM treatment induced a similar subset of ISGs. Eighteen genes involved in the interferon pathway were significantly up-regulated by rECM (fold change >1.5 and p-value <0.05); 16 of these 18 rECM-induced ISGs were also induced in *HMEC-E6 cells by Tam, including interferon regulatory factor (IRF-1). This latter finding is important because we have previously shown that IRF-1 regulates Tam-induced, p53-independent apoptosis in HMEC-E6 cells.

Differential gene expression was confirmed by semi-quantitative RT-PCR in triplicate, and normalized to beta-actin, for 5 ISGs. HMEC-E6 cells showed up-regulation of all 5 ISGs upon 6 hr rECM treatment. Unlike Tam-induced ISG expression, some ISGs were also slightly induced by rECM in HMEC-LX controls at 6 hr. However, the absolute levels of these transcripts in rECM-treated HMEC-LX cells are significantly lower than the absolute transcript levels in rECM-treated HMEC-E6 early cells. Importantly, even though some ISGs are slightly induced by rECM in HMEC-LX controls, IRF-1 was not induced. Based on these similar patterns of ISG induction, we hypothesized that both Tam- and rECM-mediated apoptosis in HMEC-E6 cells may activate a similar downstream pathway that utilizes IRF-1 and possibly other ISGs.

2c) rECM does not induce interferon-α, -β, or -γ and does not increase ERα expression

As in our previous work with Tam, we investigated whether rECM-mediated induction of IRF-1 was due to the production and/or release of interferon (IFNs). Differential gene expression of HMEC-E6 cells treated with rECM for 6 hr in 3-hD culture showed that transcription of IFN-α, -β, and -γ was not increased. ELISA assays tested for IFN production. Passage-matched apoptosis-sensitive HMEC-E6 cells and HMEC-LX controls were cultured in rECM and media was tested at 0, 30 min, 1 hr, 2 hr, and 4 hr. IFN-α, -β, and -γ production was not detected in either HMEC-E6 cells or HMEC-LX controls grown in 3-hD rECM culture. These observations are consistent with our previous observation that Tam promotes induction of IRF-1/ISGs and apoptosis in HMEC-E6 cells in the absence of IFN production or secretion. These data show that

induction of IRF-1/ISGs, in HMEC-E6 cells grown in 3-hD rECM culture, occurs in the absence of IFN-α, -β, and -γ transcriptional activation and/or release.

Unlike ER(+) human breast cancers, HMECs typically express low nuclear levels of ER (ER-"poor"). While HMECs are ER-"poor", unlike ER(-) breast cancer cells, HMECs are not Tam-resistant and express low but detectable levels of ERα protein. Previous studies demonstrated that rECM increased expression of ERα in primary mouse mammary epithelial cells, but only in the presence of prolactin. Differential gene expression and western analysis was performed to test whether rECM similarly increased ERα protein expression in HMEC-E6 cells. We observed that there was no increase in ERα mRNA or protein expression in HMEC-E6 cells grown in contact with rECM. The lack of ERα induction is the expected result, as we do not culture our cells in the presence of prolactin, and prior investigators observed that prolactin was essential for induction of ERα.

2d) Testing for Upstream Convergence of Tam and rECM Signaling

The upregulation of a similar subset of ISG genes lead us to investigate whether both Tam and rECM signal through the same upstream target or converge downstream at the level of transcription in HMEC-E6 cells. Apoptosis sensitive HMEC-E6 cells were pretreated with either estrogen and then cultured in rECM or pretreated with alpha3- or beta1-integrin blocking antibodies and then treated with 1.0 uM Tam. Caspase-3 activation was measured 24 hr later. None of the pretreatments inhibited the rECM and Tam activation of caspase-3 in the HMEC-E6 early cells ($p > 0.05$). These experiments demonstrated that rECM and 1.0 uM Tam initiate apoptosis through different upstream targets. Based on these observations, we hypothesized that rECM- and Tam-induced apoptosis converged at the level of transcriptional activation of IRF-1.

2e) rECM promotes recruitment of CBP and STAT1 to the* IRF-1 *GAS element

Type II-IFN (IFN-gamma) signaling has been shown to promote p53-independent apoptosis. We previously demonstrated that treatment of HMEC-E6 cells with 1.0 uM Tam promotes formation of a STAT1 complex on the *IRF-1* gamma-inteferon activating sequence (GAS) element, recruitment of cofactor CBP, and up-regulation of IRF-1 mRNA. Here we investigated whether induction of IRF-1 by rECM in HMEC-E6 cells grown in 3-hD culture was due to the formation of a similar transcriptional complex on the *IRF-1* GAS element. Western analysis was conducted to test for STAT1 expression and its phosphorylation. There are two known phosphorylation sites within STAT1, Tyr701 and Ser727. It has been shown that phosphorylation of Ser727 induces the highest transcriptional activation for STAT1. As we previously reported for Tam-induced apoptosis, STAT1 was active at baseline in untreated *HMEC-E6 cells. Treatment of *HMEC-E6 cells with rECM increased STAT1 phosphorylation at Ser727 by 2.5-fold ($p < 0.005$) at 1 hr, while total STAT1 levels remained unchanged.

Chromatin immunoprecipitation (ChIP) studies were performed to test whether rECM, similar to Tam, promotes the formation of a STAT1/CBP complex on the *IRF-1* GAS element. HMEC-LX control and *HMEC-E6 cells were grown in 3-hD rECM culture. Chromatin lysates were screened for STAT1 and CBP bound to the *IRF-1* GAS element.

STAT1 was bound to the *IRF-1* GAS element in the HMEC-E6 cells at baseline and during rECM treatment while CBP was recruited to the GAS element only after rECM treatment. In contrast, neither STAT1 nor CBP were recruited to the *IRF-1* GAS element in HMEC-LX control cells. These observations indicate that STAT1 and CBP binding to the *IRF-1* GAS element may play a role in IRF-1 induction during rECM-mediated apoptosis in HMEC-E6 cells.

To further test the association of STAT1 with the *IRF-1* GAS element, immunoprecipitation using a biotin-labeled oligonucleotide containing the *IRF-1* GAS promoter element was performed in HMEC-E6 cells grown in 3-hD culture. Consistent with the ChIP results, STAT1 was associated with the GAS element at baseline. rECM promoted increased STAT1 association with the *IRF-1* promoter GAS element by 1 hr. These results show that 1) HMEC-E6 cells exhibit baseline association of STAT1 binding to the *IRF-1* GAS element and 2) rECM promotes recruitment of CBP to the GAS element complex in HMEC-E6 but not HMEC-LX cells.

2f) IRF-1 induction and rECM

To further investigate the role of rECM in promoting apoptosis in HMEC-E6 cells, we tested for mRNA and protein levels as a function of rECM treatment. Semi-quantitative RT-PCR showed that rECM promoted significant induction of IRF-1 mRNA in HMEC-E6 cells at 1 hr (9.1-fold, p-value <0.05) but not in HMEC-LX cells. Consistent with mRNA expression results, rECM promoted a 2.5-fold increase in IRF-1 protein expression in HMEC-E6 cells at 1 hr ($p < 0.0001$).

2g) Suppression of IRF-1 inhibits caspase-1 and -3 activation in HMEC-E6 cells

We previously demonstrated that suppression of IRF-1 in HMEC-E6 cells blocked Tam-induced activation of caspase-1 and -3 and apoptosis. Here we similarly investigated whether suppression of IRF-1 in *HMEC-E6 cells blocked rECM-mediated caspase-1 and -3 activation and apoptosis in 3-hD culture. IRF-1 was suppressed using our previously published siRNA oligo sequences directed against IRF-1. Consistent with our prior results, treatment with IRF-1 #1 and IRF-1 #4 siRNA oligos for 12 hr suppressed baseline IRF-1 1) mRNA expression by 60% and 75%, respectively and 2) protein expression by 95% and 97%, respectively. IRF-1 siRNAs #1 and #4 also blocked rECM-mediated induction of IRF-1 mRNA in *HMEC-E6 cells.

Suppression of IRF-1 with siRNA oligos in HMEC-E6 cells blocked rECM-mediated apoptosis as evidenced by a lack of caspase-1 or -3 activation in 3-hD rECM culture. HMEC-E6 cells pretreated with IRF-1 #1 or IRF-1 #4 siRNA oligos for 12 hr and grown in 3-hD rECM did not show activation of caspase-1 ($p < 0.002$). Similarly, HMEC-E6 cells pretreated with IRF-1 siRNA oligos also failed to fully activate caspase-3 at 12-24 hr after rECM culturing ($p < 0.002$). In addition, we tested whether stable suppression of IRF-1 would inhibit rECM-induced activation of caspase-3 in HMEC-E6 cells at 48 hr. *HMEC-E6 cells were transfected with the pSilencer4.1-CMV puro vector containing either the IRF-1 #1 siRNA target sequence or the Control siRNA non-specific sequence, and IRF-1 suppression was confirmed by western analysis. As shown, HMEC-E6 cells with stable suppression of IRF-1 failed to activate caspase-3 upon 48h of rECM culturing

($p < 0.01$). These data show that IRF-1 expression is required for rECM-mediated activation of caspases-1 and -3 in HMEC-E6 cells and are consistent with our previous observations demonstrating that suppression of IRF-1 in HMEC-E6 cells blocked Tam-induced activation of caspase-1 and -3 as well as apoptosis.

Based on the above observations, we next tested if overexpression of IRF-1 in HMEC-LX control cells sensitized them to rECM-mediated apoptosis. An exogenous IRF-1 construct was expressed in HMEC-LX cells using an IRES2 DsRed2 vector; control cells expressed the IRES2 DsRed2 empty vector alone. Transfection was confirmed by red fluorescence emission at 24 hr and overexpression of IRF-1 in HMEC-LX cells expressing exogenous IRF-1 was confirmed by western analysis at 12 hr. Overexpression of IRF-1 in HMEC-LX cells induced apoptosis in HMEC-LX cells 24 hr after transfection as evidenced by Annexin V binding ($p < 0.01$) and caspase-3 activation ($p < 0.01$). This result is in line with recent reports showing that overexpression of IRF-1 induces apoptosis.

2h) rECM induces IFI 6-16 mRNA

IRF-1 expression induces transcription of IFI 6-16, and it has been previously shown that IRF-1 directly binds to the interferon-stimulated response element (ISRE) within the *IFI 6-16* promoter. We previously demonstrated that treatment of HMEC-E6 cells with 1.0 μM Tam promotes recruitment of IRF-1, STAT1, and CBP to the *IFI 6-16* IFN-stimulated response element (ISRE) promoter element followed by induction of IFI 6-16 mRNA. These observations suggest that IFI 6-16 transcriptional activation can occur during Tam-induced apoptosis, associated with recruitment of IRF-1 to the *IFI 6-16* ISRE. We observe that Tam and rECM, as shown above, promote apoptosis through recruitment of CBP to the *IRF-1* promoter, induction of IRF-1, and induction of apoptosis. Here we tested whether the downstream target of IRF-1, IFI 6-16 was activated by rECM, similar to our previously observations with Tam.

Differential gene expression data and semi-quantitative RT-PCR studies of HMEC-E6 cells demonstrated that rECM, similar to Tam, induced a subset of ISGs, including IFI 6-16. Since both Tam and rECM signals converge on the induction of IRF-1, we further investigated whether a downstream target of IRF-1, IFI 6-16, was similarly upregulated by rECM culturing in our HMEC-E6 cells. Passage-matched HMEC-LX control and apoptosis-sensitive HMEC-E6 cells were grown in 3-hD rECM culture and mRNA lysate harvested. Semi-quantitative RT-PCR was performed in triplicate and normalized to β-actin. IFI 6-16 mRNA was induced in HMEC-E6 cells at 1 hr ($p < 0.01$), while HMEC-LX control cells showed no induction of IFI 6-16 ($p > 0.05$).

2i) ISGF3 and IRF-1 binding to the ISRE in the* IFI 6-16 *promoter temporally correlates with transcriptional activation of IFI-6-16

IFI 6-16 has been shown to be strongly induced by Type I-IFN (IFN-α/β) signaling and weakly induced by Type II-IFN (IFN-γ) signaling. Induction of IFI 6-16 expression by Type I IFNs has been shown to be mediated by binding of the ISGF3 complex (STAT1/STAT2/IRF-9) to the ISRE element of the *IFI 6-16* promoter (Kelly et al, 1986). It has been shown that upon IFN-α treatment, ISGF3 binds rapidly to the *IFI 6-16* ISRE, followed by the recruitment of IRF-1 at 1-2 hr. Furthermore, the binding of IRF-1 upon

IFN-α treatment corresponds to maximal and sustained IFI 6-16 transcription. Without IRF-1 binding the level of IFI 6-16 transcription falls off suggesting that IRF-1 is required to stabilize the ISGF3 complex. However, following treatment with IFN-γ, recruitment of IRF-1 alone to the *IFI 6-16* ISRE site also has been shown to promote IFI 6-16 expression.

Here we tested in rECM-treated *HMEC-E6 cells whether the transcriptional activation of IFI 6-16 temporally correlated with recruitment of either the ISGF3 complex (STAT1/STAT2/IRF-9) or IRF-1/CBP to the *IFI 6-16* ISRE. *HMEC-E6 cells and HMEC-LX controls were grown in 3-hD rECM culture, cells harvested, and lysates tested for protein content and transcriptional factor binding. Western analysis demonstrated that exposure to rECM for 30 min was associated with a 3.1-fold and 2.2-fold respective increase in IRF-9 and STAT2 protein expression in *HMEC-E6 cells at 30 min. ChIP analysis demonstrated that in rECM-treated *HMEC-E6 cells, IRF-9 and STAT1 were recruited to the *IFI 6-16* ISRE promoter element by 30 min. IRF-9 is the final DNA binding factor recruited to the ISGF3 complex and is required for transcriptional activation. Therefore, these observations show that treatment of *HMEC-E6 cells with rECM for 30 min promotes recruitment of the ISGF3 complex to the *IFI 6-16* ISRE promoter element and precedes transcriptional activation of IFI 6-16 at 60 min.

We previously demonstrated that treatment of *HMEC-E6 cells with 1.0 μM Tam promoted recruitment of IRF-1, STAT1, and CBP to the *IFI 6-16* ISRE promoter element (Bowie *et al*, 2004). As described above, we observed that STAT1 was recruited to *IFI 6-16* ISRE promoter element in HMEC-E6 cells after 30 min rECM treatment. We next tested the same lysates from HMEC-E6 cells for the recruitment of IRF-1 and CBP to the *IFI 6-16* ISRE element. Both IRF-1 and CBP were recruited to the *IFI 6-16* ISRE promoter element in *HMEC-E6 cells at 60 min, respectively. Recruitment was temporally associated with IFI 6-16 mRNA induction at 60 min. Taken together, these data show the ISGF3 complex is recruited to the *IFI 6-16* ISRE promoter element at 30 min, followed by IRF-1 and CBP recruitment by 60 min. The presence of this transcriptional complex correlates with the transcriptional activation of IFI 6-16 at 60 min. Since Tam also promotes recruitment of STAT1/CBP/IRF-1 to the *IFI 6-16* ISRE during the induction of IFI 6-16, this provides evidence that Tam- and rECM-signaling through IRF-1/CBP and target a common set of down-stream genes.

2j) AKT activity is critical for induction of rECM-mediated apoptosis: AKT is an important regulator of cell survival and loss of AKT activity is known to promote apoptosis. We observe that rECM-induced apoptosis is associated with loss of AKT-activity and phosphorylation at Ser-473. This is an important observation since we also observe that AKT phosporylation at Ser-473 is critical cell surface-regulated, tamoxifen-induced apoptosis in HMEC-E6 cells. Expression of a constitutively active AKT blocked the induction of apoptosis and resulted in loss of rECM-regulated growth arrest. Inhibition of α3/β1-integrin signaling also resulted in loss of AKT phosphorylation at Ser-473. These results highlight a potential role for AKT in regulating rECM-mediated apoptosis. Work is on-going to investigate whether AKT plays a role in activating CBP.

KEY RESEARCH ACCOMPLISHMENTS:

1) Demonstration that suppression of the CREBP binding protein (CBP) results in loss of cellular polarity and apoptosis resistance.
2) Evidence that CBP regulates expression of laminin-5 through binding to the laminin 5 promoter (*LAMA3A*).
3) Demonstration that suppression of CBP exprsesion blocks CBP recruitment to *LAMA3A*.
4) Demonstration that prepared extracellular matrix (rECM) promotes induction of interferon regulated genes (IRGs), including interferon regulatory factor-1 (IRF-1) in the absence of interferon production.
5) Identifying that IRF-1 expression is critical for interferon regulated gene (IRG) expression and induction of apoptosis.
6) Demonstration that AKT is important for rECM-mediated apoptosis.

Reportable Outcomes:

a) Manuscripts: Dietze, E.C., Troch, M.M., Heffner, J.B., Bean, G.R., and Seewaldt, V.L. Tamoxifen and Tamoxifen Ethyl Bromide Induce Apoptosis in Acutely Damaged Mammary Epithelial Cells Through Modulation of AKT Activity. Oncogene, 23: 3851-3862, 2004.

b) Bowie, M., Dietze, E.C., Delrow, J., Bean, G.R., Troch, M.M., Marjoram, R.J., and Seewaldt, V.L. Interferon Regulatory Factor-1 is Critical for Tamoxifen-Mediated Apoptosis in Human Mammary Epithelial Cells. *Oncogene*, 23:8743-8755, 2004.

c) Bean, G.R., Scott, V., Yee, L., Ratliff-Daniel, B., Troch, M.M., Seo, P., Bowie, M.L., Marcom, P.K., Slade, J., Kimler, B., Fabian, C.J., Zalles, C.M., Broadwater, G., Baker Jr., J.C., and Seewaldt, V.L. Retinoic Acid Receptor-β2 Promoter Methylation in Random Periareolar Fine Needle Aspriration. *Cancer Epidemiology Biomarkers Prevention*, 14:790-813, 2005.

d) Dietze, E.C., Bowie, M.L., Mrózek, K., Caldwell, L.E., Neal, C., Marjoram, R.J., Troch, M.M., Bean, G.R., Yokoyama, K.K., Ibarra, C.A., and Seewaldt, V.L. CREB-Binding Protein Regulates Apoptosis and Growth of HMECs in Reconstituted ECM via Laminin-5. *J. Cell Sci*., 118: 5005-5022, 2005.

e) Bowie, M.L., Troch, M.M., Delrow, J., Dietze, E.C., Bean, G.R., Ibarra, C.A., Pandiyan, G., and Seewaldt, V.L. Interferon Regulatory Factor-1 Regulates Reconstituted Extracellular Matrix (rECM)-Mediated Apoptosis in Human Mammary Epithelial Cells. In press, *Oncogene*, 2006.

f) Seewaldt, V.L. Redefining Translational Research. *Cancer Biology and Therapy*. In press, 2006.

g) Troch, M.M., Dietze, E.C., Bean, G.R., Bowie, M.L, Pandiyan, G., Ibarra, C.A., and Seewaldt, V.L. AKT Regulates Apoptosis in 3-D Culture. Submitted, *J. Biol. Chem.*, 2006.

1) **Funding granted:**
   a) AVON/NCI Developing markers of breast cancer risk in breast fine needle aspiration. NIH/NCI CA6843-AV13.

b) AVON/NCI Contralateral risk markers in women with primary breast cancer. NIH/NCI CA6843-AV43.
c) R01 CA114703 Markers of Breast Cancer Risk and Prevention.
d) Mentorship awards
BC050373 (Bilsaka-Wolek, A.) 03/01/06-04/01/09
Combined models mammographic density and stromal composition as predictors of short-term breast cancer risk.
BC051099 (Rowell, C.) 03/01/06-04/01/08
Predictive markers of response to tamoxifen breast cancer chemoprevention
F32CA112844 (Ostrander, J.) 10/01/06-9/30/07
Investigating the role of NF-kappaB in mammary gland homeostasis
P50CA68438-PDF 05 CDA (Ibarra, C) 10/01/06-9/30/07
Risk-Biomarker Development in Early Mammary Carcinogenesis
BC060943 DoD (Pandiyan, G.) 03/01/07-04/01/10
CBP Promoter Characterization and Biomarker Development

3) Funding pending:
a. DOD SIDA.

Conclusions:
In this report we demonstrate that suppression of the CREBP binding protein (CBP) results in apoptosis-resistance and loss of epithelial polarity and that CBP is critical for laminin-5 expression. These observations are important for 1) identifying improved targets for breast cancer prevention and 2) developing novel markers to test for response to chemoprevention agents. Information gained in this report is currently being translated to benefit women at risk for breast cancer prevention in our multi-institutional cohort. We have obtained funding for this cohort and are currently using markers in developed in this proposal to identify risk in high-risk women.

References:
None.

Appendices

1) Dietze, E.C., Troch, M.M., Bean, G.R., Heffner, J.B., Bowie, M.L., Rosenberg, P., Ratliff, B., and Seewaldt, V.L. Tamoxifen and Tamoxifen Ethyl Bromide Induce Apoptosis in Acutely Damaged Mammary Epithelial Cells Through Modulation of AKT Activity. *Oncogene*, 23:3851-3862, 2004.
2) Bowie, M.L., Dietze, E.C., Delrow, J., Bean, G.R., Troch, M.M., Marjoram, R.J., and Seewaldt, V.L. Interferon Regulatory Factor-1 is Critical for Tamoxifen-Mediated Apoptosis in Human Mammary Epithelial Cells. *Oncogene*, 23:8743-8755, 2004.
3) Bean, G.R., Scott, V., Yee, L., Ratliff-Daniel, B., Troch, M.M., Seo, P., Bowie, M.L., Marcom, P.K., Slade, J., Kimler, B., Fabian, C.J., Zalles,

C.M., Broadwater, G., Baker Jr., J.C., Wilke, L.G., and Seewaldt, V.L. Retinoic Acid Redeptor-β2 Promoter Methylation in Random Reiareolar Fine Needle Aspiration. *Cancer Epidemiology Biomarkers Prevention*, 14:790-813, 2005.

4) Dietze, E.C., Bowie, M.L., Mrózek, K., Caldwell, L.E., Neal, C., Marjoram, R.J., Troch, M.M., Bean, G.R., Yokoyama, K.K., Ibarra, C.A., and Seewaldt, V.L. CREB-Binding Protein Regulates Apoptosis and Growth of HMECs Grown in Reconstituted ECM via Laminin-5. *J. Cell Sci*., 118: 5005-5022, 2005.
5) Bowie, M.L., Troch, M.M., Delrow, J., Dietze, E.C., Bean, G.R., Ibarra, C.A., Pandiyan, G., and Seewaldt, V.L. Interferon Regulatory Factor-1 Regulates Reconstituted Extracellular Matrix (rECM)-Mediated Apoptosis in Human Mammary Epithelial Cells. In press, *Oncogene*, 2006.

Oncogene (2004) 23, 3851–3862

www.nature.com/onc

Tamoxifen and tamoxifen ethyl bromide induce apoptosis in acutely damaged mammary epithelial cells through modulation of AKT activity

Eric C Dietze[1], Michelle M Troch[1], Gregory R Bean[1], Joshua B Heffner[1], Michelle L Bowie[1], Paul Rosenberg[2], Brooke Ratliff[1] and Victoria L Seewaldt*[,1]

[1]*Division of Medical Oncology, Department of Medicine, Duke University Medical Center, Durham, NC 27710, USA;* [2]*Division of Cardiology, Department of Medicine, Duke University Medical Center, Durham, NC 27710, USA*

Normal human mammary epithelial cells (HMECs), unlike estrogen receptor-positive (ER +) breast cancers, typically express low nuclear levels of ER (ER-'poor'). We previously demonstrated that 1.0 μM tamoxifen (Tam) induced apoptosis in ER-'poor' HMECs acutely transduced with human papillomavirus-16 E6 (HMEC-E6) through a rapid mitochondrial signaling pathway. Here, we show that plasma membrane-associated E2-binding sites initiate the rapid apoptotic effects of Tam in HMEC-E6 cells through modulation of AKT activity. At equimolar concentrations, Tam and tamoxifen ethyl bromide (QTam), a membrane impermeant analog of Tam, rapidly induced apoptosis in HMEC-E6 cells associated with an even more rapid decrease in phosphorylation of AKT at serine-473. Treatment of HMEC-E6 cells with 1.0 μM QTam resulted in a 50% decrease in mitochondrial transmembrane potential, sequential activation of caspase-9 and -3, and a 90% decrease in AKT Ser-473 phosphorylation. The effects of both Tam and QTam were blocked by expression of constitutively active AKT (myristoylated AKT or AKT-Thr308Asp/Ser473-Asp). These data indicate that Tam and QTam induce apoptosis in HMEC-E6 cells through a plasma membrane-activated AKT-signaling pathway that results in (1) decreased AKT phosphorylation at Ser-473, (2) mitochondrial membrane depolarization, and (3) activated caspase-9 and -3.

Oncogene (2004) **23,** 3851–3862. doi:10.1038/sj.onc.1207480
Published online 1 March 2004

Keywords: tamoxifen; apoptosis; AKT; plasma membrane; mammary epithelial cells

Introduction

The mechanism of both estrogen (E2) and tamoxifen (Tam) action in normal mammary epithelial cells (HMECs) and early proliferative breast lesions is poorly characterized. Typically, greater than 90% of normal HMECs express low levels of estrogen receptor (ER) and are considered ER-'poor' (Anderson *et al*., 1998). It has been observed that ER-'poor', but not ER-positive (ER +), HMECs proliferate in response to E2 (Anderson *et al*., 1998). The National Surgical Adjuvant Breast and Bowel Project Breast Cancer Prevention Trial (BCPT) demonstrated that Tam markedly reduced the incidence of breast cancers in patients with atypical hyperplasia (Fisher *et al*., 1998). While many of the benefits of Tam in the BCPT appear to be mediated through ER, it is unclear how Tam acted in ER-'poor' atypical mammary epithelial cells (Friedman, 1998).

We previously developed an *in vitro* model of Tam action in acutely damaged, ER-'poor' HMECs. In this model system, we demonstrated that 1.0 μM Tam promotes apoptosis in ER-'poor' HMECs acutely transduced with HPV-16 E6 (HMEC-E6), but not in HMEC vector controls (HMEC-LX) (Dietze *et al*., 2001; Seewaldt *et al*., 2001a). Disruption of mitochondrial electron transport is an early feature of apoptosis. We observed in our model of acute cellular damage that Tam rapidly induced mitochondrial membrane depolarization and activation of caspase-9. Both the loss of mitochondrial membrane potential ($\Delta\Psi_m$) and caspase-9 induction occurred within 30–60 min (Dietze *et al*., 2001). Effects observed at later times included mitochondrial condensation and caspase-3 activation at 6–12 h and morphologic and biochemical evidence of effector-phase apoptosis starting at 12 h.

Rapid signaling by E2, and E2 agonists/antagonists such as Tam, have been demonstrated in numerous cell types and are thought to be initiated by membrane-associated ER (Marquez and Pietras, 2001; Pietras *et al*., 2001; Behl, 2002; Ho and Liao, 2002; Kousteni *et al*., 2002; Levin, 2002; Ropero *et al*., 2002; Segars and Driggers, 2002; Doolan and Harvey, 2003; Li *et al*., 2003). Plasma-membrane association of ERα is ablated by mutation at Ser-522 (Razandi *et al*., 2003a) and may require palmitoylation (Li *et al*., 2003). ERs have also been shown to associate with caveolin-1, a major component of caveoli in the plasma membrane (Schlegel *et al*., 1999; Chambliss *et al*., 2002; Razandi *et al*., 2002). Rapid, membrane-associated ERα-linked E2 signaling has been shown to activate signal-transduction pathways involving cAMP, Ca^{+2}, NO, Ras, AKT, and mitogen-activated protein kinase (MAPK) (Aronica *et al*., 1994; Improta-Brears *et al*., 1999; Linford *et al*.,

*Correspondence: VL Seewaldt, DUMC, Box 2628, Durham, NC 27710, USA; E-mail: seewa001@mc.duke.edu
Received 3 October 2003; revised 23 December 2003; accepted 24 December 2003; Published online 1 March 2004

2000; Pietras *et al*., 2001; Behl, 2002; Ho and Liao, 2002). In turn, some of these signaling pathways have been shown to activate ERα. For example, ERα is phosphorylated on Ser-118 and -167 by MAPK and AKT, respectively (Kato *et al*., 1995; Campbell *et al*., 2001).

AKT activity is critical for normal mammary gland homeostasis and overexpression of AKT is frequently observed in primary mammary tumors (Sun *et al*., 2001). E2 promotes mammary epithelial cell survival through AKT activation; loss of AKT activity promotes apoptosis and mammary gland involution (Kandel and Hay, 1999; Okano *et al*., 2000; Aoudjet and Vuori, 2001; Hutchinson *et al*., 2001; Schwartfeger *et al*., 2001; Strange *et al*., 2001; Sun *et al*., 2001; Testa and Bellacosa, 2001). ER has been shown to directly interact with the regulatory subunit of phosphatidylinositol-3-OH kinase (PI3K) which results in the activation of AKT (Simoncini *et al*., 2000). Association between the pleckstrin homology domain of AKT and the PI3K lipid product results in two events leading to AKT activation: (1) recruitment of AKT to the plasma membrane and (2) phosphorylation of Thr-308 in the kinase domain and of Ser-473 in the C-terminal hydrophobic motif domain by membrane bound kinases (Brazil and Hemmings, 2001; Whitehead *et al*., 2001; Scheid and Woodgett, 2003). Overexpression of AKT and increased AKT-1 activity is frequently observed in primary breast cancer (Sun *et al*., 2001) and dysregulation of AKT signaling appears to be an important event in mammary carcinogenesis.

Activation of AKT by plasma membrane-associated ERα has been recently shown to play an important role in proliferation, survival, and signal transduction in MCF-7 cells. E2 activation of AKT and MAPK in MCF-7 cells by plasma membrane-associated ERα has been shown to promote increased proliferation (Marquez and Pietras, 2001). Membrane-associated ERα has been shown to rapidly activate AKT following E2 treatment and thereby protect MCF-7 cells against proapoptotic stimuli (Razandi *et al*., 2000; Marquez and Pietras, 2001; Stocia *et al*., 2003a). Membrane-associated E2 activation of AKT also blocked both taxol- and UV-irradiation-induced apoptosis in MCF-7 cells (Razandi *et al*., 2000). Rapid AKT activation appears to require ErbB2 activity (Stocia *et al*., 2003a, b) and may be G-protein coupled (Razandi *et al*., 2003b). In MCF-7 cells, E2 binding promotes ERα association with Shc which is then phosphorylated by Src and activates MAPK (Song *et al*., 2002). An ERα construct targeted to the plasma membrane showed an increased ability to activate MAPK (Zhang *et al*., 2002). Taken together, these observations suggest that activation of AKT through E2 binding to plasma membrane-associated ERα may play an important role in E2-related signal transduction in ER + breast cancer cells.

The potential role of membrane-associated ERα regulation of AKT activity during Tam-induced apoptosis in ER-'poor' HMECs has not been studied. In our *in vitro* model of acute cellular damage, we tested the hypothesis that Tam rapidly induces a decrease in mitochondrial membrane potential ($\Delta\Psi_m$) and an increase in caspase-9 and -3 activities by a mechanism that involves binding of Tam to plasma membrane-associated E2-binding sites and subsequent inactivation of AKT. We show that HMEC-E6 cells bound E2 on the cell surface and that this binding was blocked by either Tam or tamoxifen ethyl bromide (QTam), a membrane impermeant analog of Tam. Furthermore, both Tam and QTam induced a rapid decrease in $\Delta\Psi_m$ and rapid caspase-9 activation. These changes were preceded by loss of AKT phosphorylation at Ser-473 and followed by induction of apoptosis. Inhibition of AKT with SH-6 (Kozikowski *et al*., 2003) mimicked and expression of constitutively active AKT blocked these events. These observations demonstrate an important role for plasma membrane-associated E2-binding sites in modulating AKT activity and apoptosis in ER-'poor' HMECs.

Results

Plasma membrane-association of tamoxifen aziridine (Taz) and tamoxifen in HMEC-E6 cells

[^{3}H]Taz was found to distribute throughout HMEC-E6 cells (Figure 1). Of the Taz recovered, 43% was found in the nuclear fraction and 20, 18, 13, and 6% were

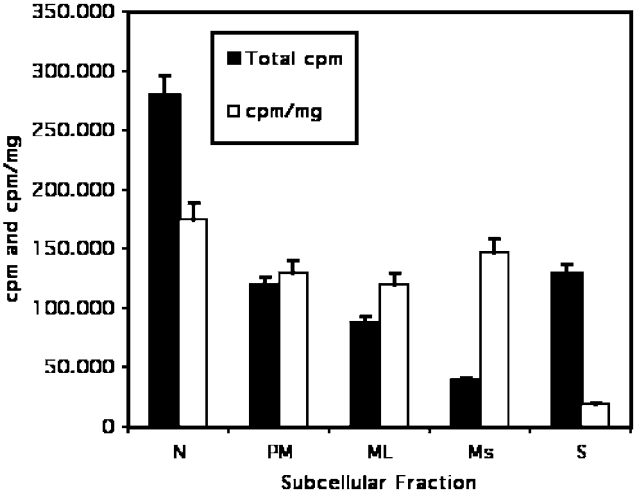

Figure 1 Distribution of [^{3}H]Taz binding (c.p.m.) to HMEC-E6 subcellular fractions and the specific activity (c.p.m./mg protein) of [^{3}H]Taz in each fraction. Cells were preincubated with 6.0 μM unlabeled Tam and then incubated with 0.5 μM [^{3}H]Taz (Perkin-Elmer) for another 15 min. Next, the cells were washed with ice-cold PBS, trypsinized, pelleted, and resuspended in ice-cold homogenization buffer (50 mM Tris/10 mM sodium pyrophosphate/5 mM EDTA (pH 7.5), 150 mM NaCl, 1.0 mM Na orthovanadate, 10 mM NaF, 2 × Complete protease inhibitor). The resuspended cells were homogenized at 4°C and the lysate, or respective supernatants, were centrifuged at 4°C for 10 min at 1000, 3000, and 20 000 *g*. The final supernatant was centrifuged for 60 min at 4°C and 100 000 *g* to produce microsomal and cytosolic fractions (N – nuclei; PM – plasma membrane; ML – mitochondria/lysosome; Ms – microsome; and S – soluble). All pellets were washed once by resuspending in homogenization buffer and repelleting. The washed pellets were resuspended in homogenization buffer and an aliquot counted. The crude nuclear fraction (1000 *g*) was subfractionated into an enriched nuclear fraction and a plasma membrane fraction by discontinuous sucrose density gradient centrifugation. The mean of two experiments with s.d. is shown

found in the soluble, plasma membrane, mitochondrial/lysosomal, and microsomal fractions, respectively. The specific activity of Taz binding to the nuclear, enriched plasma membrane, mitochondrial/lysosomal, and microsomal fractions was similar, approximately 150 000 c.p.m./mg protein. The specific binding to the soluble fraction was much lower, 15 000 c.p.m./mg protein. The high percentage of Taz binding to the plasma membrane fraction at a specific activity of binding similar to subcellular compartments known to contain Taz-binding proteins was similar to observations made by Marquez and Pietras (2001) in Tam-treated MCF-7 cells. Taken together, these observations raised the possibilities that (1) the plasma membrane fraction of HMEC-E6 cells contained a Tam-binding protein and (2) Tam might, in part, induce apoptosis through a plasma membrane-associated binding site.

We tested for (1) the presence of E2-binding sites on the HMEC-E6 cell surface and (2) the ability of Tam to compete for potential plasma membrane-associated E2-binding sites using competitive binding with a membrane impermeable derivative of E2. Estradiol conjugated to BSA/fluoroscene isothiocyanate (E2-BSA/FITC) does not cross the plasma membrane and has been extensively used to characterize plasma membrane binding of E2 (Razandi *et al*., 2000; Marquez and Pietras, 2001; Segars and Driggers, 2002). Incubation of HMEC-E6 cells with 0.2 μM E2-BSA/FITC resulted in ligand binding to the cell surface, predominantly at cell–cell interfaces (Figure 2a). This binding required the presence of E2 as BSA/FITC did not bind to HMEC-E6 cells (Figure 2b). Binding of E2-BSA/FITC to the cell surface of HMEC-E6 cells was blocked by 0.1 μM E2 (Figure 2c). However, E2-BSA/FITC binding was not blocked by 1.0 μM E2-17-hemisuccinate-BSA, a ligand that should not interfere with the specific binding of E2 (Figure 2d). These data clearly demonstrate the presence of specific binding sites for E2-BSA/FITC on the plasma membrane surface of HMEC-E6 cells.

We next tested whether Tam blocked the binding of E2-BSA/FITC to HMEC-E6 cells. Binding of E2-BSA/FITC to the cell surface of HMEC-E6 cells was specifically blocked by 1.0 μM Tam (Figure 2e). These observations demonstrated that Tam competitively binds to cell surface-associated E2-binding sites in HMEC-E6 cells.

QTam blocks E2-BSA/FITC binding to and promotes apoptosis in HMEC-E6 cells

We observed that (1) a significant amount of Taz bound to the plasma membrane fraction of HMEC-E6 cells and (2) Tam blocked the E2-BSA/FITC binding to the cell surface. These observations raised the possibility that Tam might, in part, be inducing apoptosis through a plasma membrane-associated site. QTam, a quaternary ammonium derivative of Tam, does not cross the plasma membrane and has been extensively used to test for plasma membrane-mediated effects of Tam

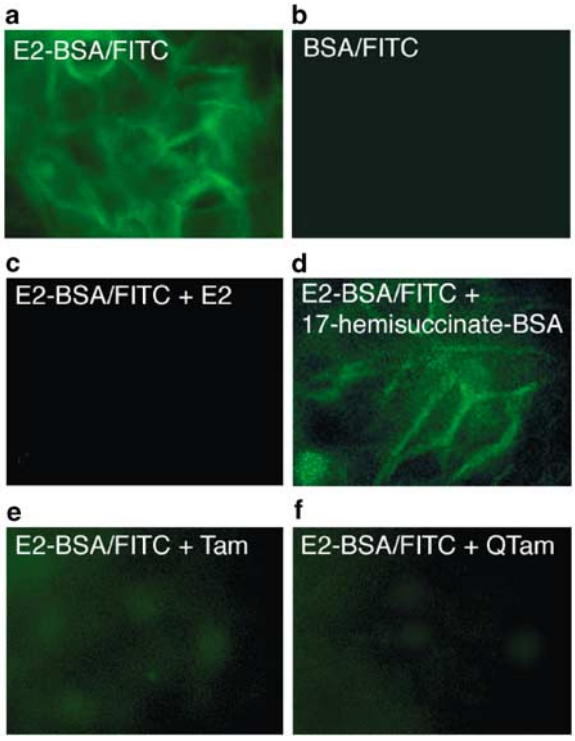

Figure 2 Binding of 200 nM E2-BSA/FITC to HMEC-E6 cells. (**a**) E2-BSA alone. (**b**) 1.0 μM BSA/FITC alone. (**c**) E2-BSA/FITC with (0.1 μM) E2. (**d**) E2-BSA/FITC with 1.0 μM E2-17-hemisuccinate-BSA. (**e**) E2-BSA/FITC with 1.0 μM Tam. (**f**) E2-BSA/FITC with 1.0 μM QTam. The HEMC-E6 cells were plated and allowed to grow for 1 day, fixed for 10 min with 1% formaldehyde, washed with PBS, and incubated with the indicated ligand(s) for 15 min. The cells were then washed two times with ice-cold PBS and observed with a Nikon TE2000 microscope. Representative images are shown

(Fernandez *et al*., 1993; Kirk *et al*., 1994; Allen *et al*., 2000; Dick *et al*., 2002). Similar to observations with Tam (Figure 2e), 1.0 μM QTam blocked the binding of E2-BSA/FITC to the cell surface of HMEC-E6 cells (Figure 2f). These observations demonstrated that QTam, similar to Tam, competitively binds to cell surface-associated E2-binding sites on HMEC-E6 cells.

We previously observed that 1.0 μM Tam induced apoptosis in HMEC-E6 cells but promoted growth arrest alone in HMEC-LX controls (Dietze *et al*., 2001). Similar to our observations in Tam-treated HMEC-E6 cells, apoptosis-sensitive HMEC-E6 cells treated with 1.0 μM QTam for 18 h underwent apoptosis as evidenced by (1) Annexin V binding and (2) morphologic criteria demonstrated by electron microscopy (Figure 3a and data not shown). In contrast, a majority of HMEC-LX cells treated with 1.0 μM QTam (similar to our prior observations utilizing Tam) underwent growth arrest but did not undergo apoptosis (Figure 3 and data not shown). HMEC-E6 cells treated with Tam or QTam had a 690 and 610% increase in the percentage of apoptotic cells, respectively. However, HMEC-LX cells demonstrated no change in the percentage of apoptotic cells.

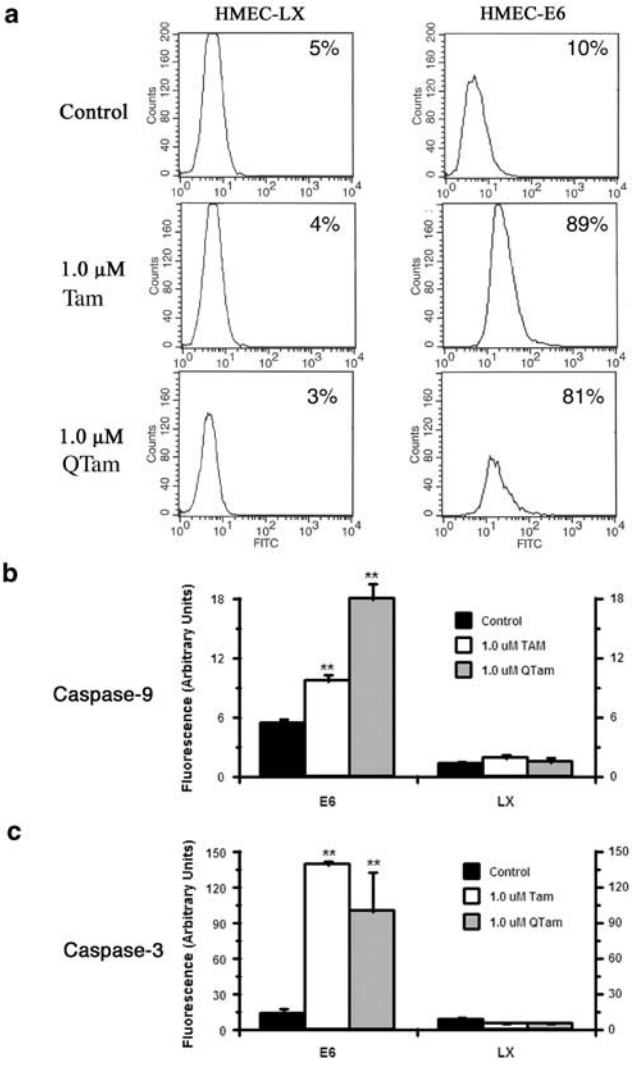

Figure 3 Tam and QTam induce apoptosis in HMEC-E6 cells and caspase-9 and -3 are activated. (**a**) HMEC-LX vector controls (passage 10) and HMEC-E6 cells (passage 10) treated with either 1.0 μM Tam (TAM) or 1.0 μM QTam (Q-Tam) for 18 h. Untreated control cells (Control) received an equivalent volume of ethanol. (**b**) Caspase-9 activity in apoptosis-sensitive HMEC-E6 cells (passage 11) and HMEC-LX controls (passage 11) treated with either 1.0 μM Tam (Tam) or QTam (QTam) for 1 h. (**c**) Caspase-3 activity in HMEC-E6 cells and HMEC-LX controls (both passage 10) treated with either 1.0 μM Tam (Tam) or 1.0 μM QTam (QTam) for 18 h. Detection of apoptotic cells was with FITC-conjugated Annexin V as described in Materials and methods. These data are representative of three experiments. Cells for caspase assays were harvested by trypsinization, washed, and pelleted. The pellets were lysed and assayed according to the manufacturer's instructions (Clontech, Caspase 3 assay kit/K2026 and Caspase9/6 assay kit/K2015). Assays were performed in duplicate. Data are the mean of three separate experiments with s.d. (**: $P<0.025$)

QTam promotes mitochondrial membrane depolarization and activates caspase-9 and -3 in HMEC-E6 cells

Disruption of mitochondrial electron transport is an early feature of apoptosis. We previously observed that 1.0 μM Tam promoted a decrease in $\Delta\Psi_m$ starting at 1 h in apoptosis-sensitive HMEC-E6 cells but not in HMEC-LX controls (Dietze *et al*., 2001). The ability of membrane impermeable QTam to induce a decrease in $\Delta\Psi_m$ in HMEC-E6 cells was tested by rhodamine 123 staining (Johnson *et al*., 1980).

As previously observed (Dietze *et al*., 2001), baseline $\Delta\Psi_m$ of apoptosis-sensitive HMEC-E6 cells was 25% lower than that of HMEC-LX controls (Table 1). Treatment of HMEC-E6 cells with either Tam or QTam for 6 h resulted in a dose-dependent decrease in $\Delta\Psi_m$. Treatment with 0.1 μM Tam or QTam decreased $\Delta\Psi_m$ by 28 and 29%, respectively ($P<0.02$) (Table 1). Treatment with 1.0 μM Tam or QTam resulted in a 43 and 58%, respectively, decrease in $\Delta\Psi_m$ ($P<0.01$) (Table 1). When HMEC-LX cells were treated with either 0.1 or 1.0 μM Tam or QTam, there was no significant change in $\Delta\Psi_m$ ($P>0.05$) (Table 1). Mitochondrial mass was measured by staining with nonyl-acridine orange (NAO), a fluorescent dye that specifically binds to the mitochondrial inner membrane independent of $\Delta\Psi_m$ (Boserma *et al*., 1996). The mitochondrial mass of apoptosis-sensitive HMEC-E6 cells and HMEC-LX controls was the same as judged by NAO staining (Table 1). Thus, 1.0 μM QTam, similar to 1.0 μM Tam (Dietze *et al*., 2001), promoted a decrease in $\Delta\Psi_m$ in apoptosis-sensitive HMEC-E6 cells but not in HMEC-LX controls.

Previously, we also observed that 1.0 μM Tam promoted activation of caspase-9 and -3 in apoptosis-sensitive HMEC-E6 cells but not in HMEC-LX controls (Dietze *et al*., 2001). Caspase-9 and -3 activations were maximal at 1 and 12–18 h, respectively. Here, we tested whether equimolar concentrations of Tam or membrane impermeable QTam similarly activated caspase-9 and -3 in HMEC-E6 cells at 1 and 18 h, respectively (Figure 3b, c). Caspase-9 activation was increased by 80 and 230% ($P<0.01$) by Tam or QTam treatment, respectively, relative to untreated controls. Neither 1.0 μM Tam nor QTam increased caspase-9 activity ($P>0.05$) in HMEC-LX controls.

Caspase-3 activation gave similar results (Figure 3c). Activity was measured 18 h after treatment as above and was found to be significantly increased ($P<0.01$) by 1000 and 670%, respectively, by treatment with either 1.0 μM Tam or QTam. As observed with caspase-9 activity, caspase-3 activity was not increased

Table 1 Baseline mitochondrial membrane potential ($\Delta\Psi_m$) is decreased in HMEC-E6 cells relative to HMEC-LX vector control cells

	Treatment	***E6***	***LX***
NAO	0 h 1.0 μM Tam	1.00±0.05	0.98±0.04
Rhodamine/NAO	0 h 1.0 μM Tam	1.00±0.05	1.34±0.04
	6 h 0.1 μM Tam	0.72±0.04	1.41±0.06
	6 h 1.0 μM Tam	0.57±0.06	1.36±0.03
	6 h 0.1 μM QTam	0.71±0.05	1.32±0.07
	6 h 1.0 μM QTam	0.42±0.07	1.28±0.09

HMEC-E6 cells (passage 11, E6) and HMEC-LX cells (passage 11, LX) treated with 0.1 or 1.0 μM tamoxifen (Tam) for 0 or 6 h. $\Delta\Psi_m$ is measured by rhodamine 123 staining and normalized to mitochondrial mass, measured by NAO staining. Fluorescence values are reported relative to ethanol-treated controls. Reported values represent the average of three separate experiments

in HMEC-LX controls after treatment for 18 h with either 1.0 μM Tam or QTam. These observations showed that 1.0 μM QTam, similar to Tam, activates caspase-3 in apoptosis-sensitive HMEC-E6 cells but not in HMEC-LX controls.

Tam and QTam reduce AKT phosphorylation at Ser-473 in HMEC-E6 cells

Phosphorylated AKT serves as a cell-survival signal that modulates mitochondrial depolarization and caspase-9 activation; decreased AKT-phosphorylation at Ser-473 is observed during apoptosis (Brazil and Hemmings, 2001; West *et al*., 2002). We hypothesized that membrane-associated effects of Tam might inhibit AKT activity in apoptosis-sensitive HMEC-E6 cells.

AKT Ser-473 phosphorylation showed a rapid, time-dependent loss of phosphorylation ($P<0.01$) when HMEC-E6 cells were incubated with 1.0 μM Tam (Figure 4a). Ser-473 phosphorylation was tested at 0, 5, 15, and 30 min. A 15 and 88% decrease was observed at 5 and 15 min, respectively. At 30 min, the relative degree of phosphorylation was not significantly different ($P>0.1$) than at 15 min. Identically treated HMEC-LX cells showed no significant decrease ($P>0.1$). At baseline, passage-matched apoptosis-sensitive HMEC-E6 cells and HMEC-LX controls expressed similar levels of total AKT protein (Figure 4b). Treatment of HMEC-E6 cells with either 1.0 μM Tam or QTam for 60 min resulted in a 98 and 90%, respectively, decrease in AKT phosphorylation at Ser-473 relative to untreated controls (Figure 4b, d). The loss of phosphorylation observed is similar to that seen after 30 min treatment with 1.0 μM Tam. AKT activity was similarly decreased in HMEC-E6 cells treated with 1.0 μM Tam or QTam by 93 and 91%, respectively (Figure 4c, e). Total AKT protein levels remained relatively constant and were not decreased by treatment with Tam or QTam in HMEC-E6 cells (Figure 4b, d). In contrast, treatment of HMEC-LX controls with either 1.0 μM Tam or QTam had a much smaller decrease in levels of AKT Ser-473 phosphorylation, 20 and 54%, respectively, or in AKT activity, 0.0 and 8.0%, respectively (Figure 4b–e).

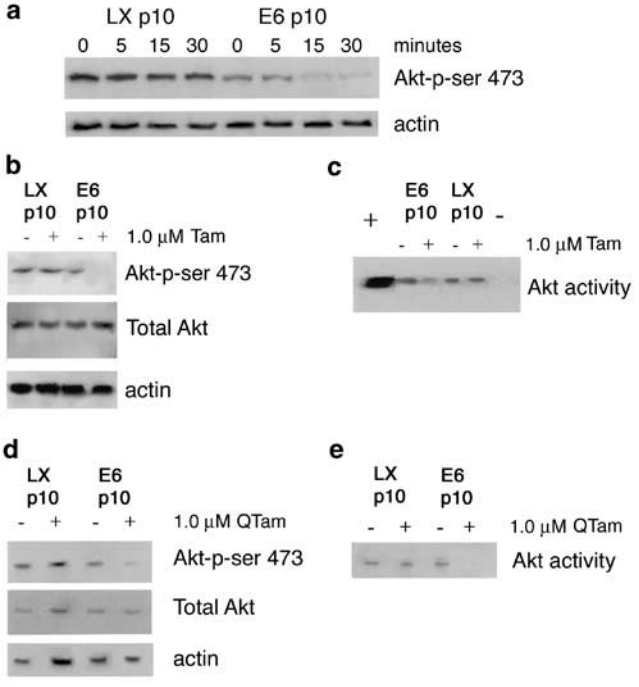

Figure 4 Loss of AKT Ser-473 phosphorylation and AKT activity were observed in Tam- and QTam-treated HMEC-E6 cells. (**a**, **b**, **c**) Equal amounts of protein lysate were loaded in each lane. Actin serves as a loading control. Membranes were incubated with antibody specific for AKT phosphserine-473 (Akt-p-Ser 473) and AKT (Total Akt). HMEC-E6 cells were treated for the indicated time with (**a**) 1.0 μM Tam (Tam). (**b**, **d**) HMEC-E6 cells were treated for the 1 h with (**b**) 1.0 μM Tam (Tam) or (**d**) 1.0 μM QTam (QTam). (**c**, **e**) AKT was immunoprecipitated from equal amounts of cell lysate and assayed. Lanes 1 and 6 of panel c show AKT-positive and -negative controls, respectively. AKT was assayed with a Cell Signaling Technology AKT assay kit according to the manufacturer's instructions. Bound antibodies were visualized using the appropriate secondary antibody-AP conjugate (Santa Cruz) and LumiPhos (Pierce). Luminescence was recorded using a Kodak Digital Science IS 440 system (Eastman Kodak)

Inhibition of AKT activity promotes apoptosis and caspase-9/-3 activation in HMEC-E6 cells

As demonstrated above, we observed a temporal association between Tam/QTam-induced (1) induction of apoptosis, loss of $\Delta\Psi_m$, and caspase-9 and -3 activation and (2) loss of AKT-phosphorylation and AKT-activity (Figures 3 and 4). To test whether inhibition of AKT-activity could promote apoptosis and casapse-9 and -3 activation, apoptosis-sensitive HMEC-E6 cells were treated with SH-6, a specific inhibitor of AKT activity (Kozikowski *et al*., 2003). Treatment of HMEC-E6 cells with 12 μM SH-6 resulted in apoptosis as evidenced by Annexin V-binding at 18 h (Figure 5a). In contrast, an equal volume of DMSO did not promote apoptosis. Treatment of apoptosis-sensitive HMEC-E6 cells with SH-6 also resulted in 780 and 1100% activation of caspase-9 at 1 h and caspase-3 at 12 h ($P<0.025$), respectively (Figure 5b, c). As expected, treatment of HMEC-LX controls with SH-6 did not result in activation of caspase-9 or -3 (data not shown). Like Tam/QTam treatment, direct inhibition of AKT activity promotes apoptosis and activation of caspase-9 and -3 in HMEC-E6 cells but not in HMEC-LX controls.

Constitutively active AKT blocks Tam- and QTam-induced apoptosis in HMEC-E6 cells

To directly test whether a decrease in AKT activity was required for Tam- and QTam-induced apoptosis, constitutively active AKT constructs, AKT1-myr and AKT1-DD, were transduced into HMEC-E6 cells (Figure 6a). The resulting transduced cells were designated HMEC-Myr/E6 and HMEC-DD/E6, respectively. HPV-16 E6 and the empty retroviral vector LXSN were also simultaneously expressed in

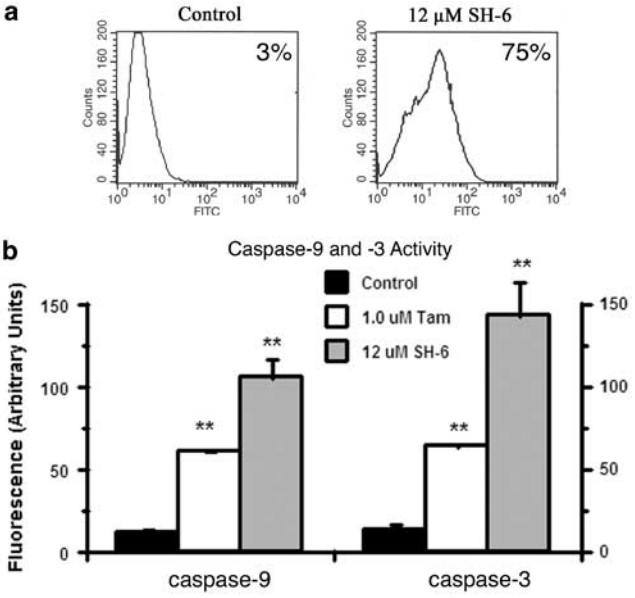

Figure 5 AKT inhibitor SH-6 promotes apoptosis and activation of both caspase-9 and -3 activity in HMEC-E6 cells. (**a**) Annexin V binding in HMEC-E6 cells treated with 12 μM SH-6 for 18 h (SH-6). Detection of apoptotic cells was with FITC-conjugated Annexin V as described in Materials and methods. Data are representative of two experiments. (**b**) Caspase-9 activity in HMEC-E6 cells (passage 11) treated with either 12 μM SH-6 (SH-6) or 1.0 mM Tam (Tam) for 1 h and caspase-3 activity in HMEC-E6 cells (passage 11) with identical treatment for 12 h. Experiments were performed in duplicate. Data are expressed as the mean of two separate experiments with s.d. (**: $P<0.025$)

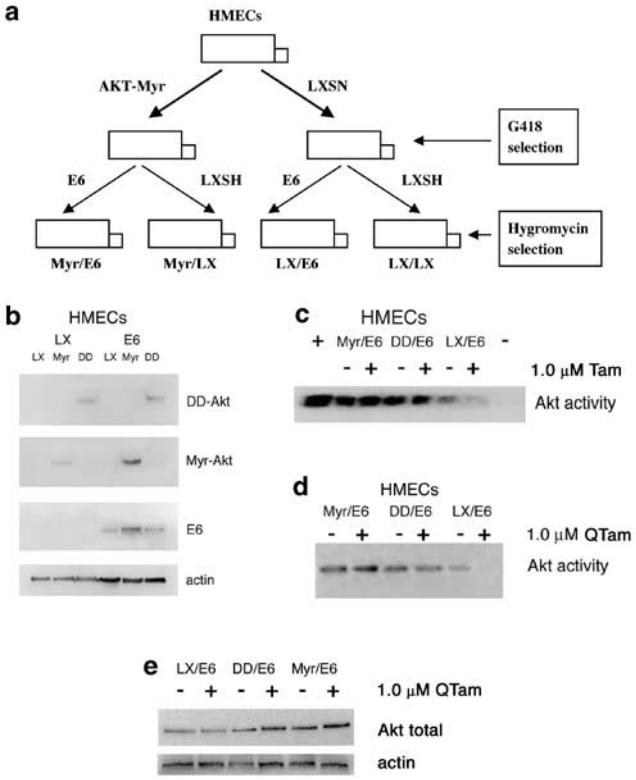

Figure 6 Constitutively active AKT expression in HMEC-E6 cells blocks loss of AKT activity on treatment with either Tam or QTam. (**a**) Illustration of the selection scheme used to produce the HMEC double transfectants, (**b**) Expression of the transfected gene products in the double transfectants as demonstrated by Western blotting, and the AKT activity of double transfectants (**c**) treated with 1.0 μM Tam or (**d**) treated with 1.0 μM QTam. For expression of gene products, cells were harvested, equal amounts of protein were loaded in each lane, and the proteins separated by SDS–PAGE. The membrane was sequentially probed with anti-HA, anti-Myc myristoylation sequence, anti-HPV16 E6, and anti-β-actin antibodies (first two antibodies from Cell Signaling Technology, second two antibodies from Santa Cruz). For AKT activity, cells were treated for 1 h and harvested by trypsinization. Equal amounts of cell lysate were immunoprecipitated and assayed using a Cell Signaling Technology AKT assay kit according to the manufacturer's instructions. Lanes 1 and 6 of panel a show AKT-positive and -negative controls, respectively. Bound antibodies were visualized using the appropriate secondary antibody-AP conjugate (Santa Cruz) and LumiPhos (Pierce). Luminescence was recorded using a Kodak Digital Science IS440 system (Eastman Kodak)

HMECs (HMEC-LX/E6) to ensure that apoptosis sensitivity was not abrogated by retroviral transduction or cell selection. All experiments were conducted within three passages of retroviral transduction. Expression of the constitutively active AKT constructs and HPV-16 E6 were confirmed by Western analysis using antibodies specific for each construct (Figure 6b).

HMEC-Myr/E6 and HMEC-DD/E6 cells had significantly ($P<0.01$) increased AKT activity relative to HMEC-LX/E6 cells (Figure 6c). The modest, but significant, increase in AKT activity seen in HMEC-LX/Myr and -LX/DD is due to the ability of the LXSN transduction system to stably insert one copy of the transduced gene into target cells. In untreated cells, AKT activity was 400% higher in HMEC-Myr/E6 and 300% higher in HMEC-LX/DD cells than HMEC-LX/E6 cells. As expected, neither 1.0 μM Tam or QTam treatment had a significant ($P>0.1$) effect on AKT activity in either HMEC-LX/Myr or -LX/DD cells (Figure 6c, d). However, consistent with results obtained with HMEC-E6 cells (Figure 4c, e), treatment with either Tam or QTam resulted in, respectively, 93 and 87% decreases ($P<0.01$) in the AKT activity of HMEC-LX/E6 cells. In addition, the expression of AKT was not decreased by treatment with either Tam (data not shown) or QTam for 1 h (Figure 6e).

Annexin V binding was utilized to test whether constitutive activation of AKT in HMEC-E6 cells blocked Tam- or QTam-induced apoptosis. Similar to results obtained in apoptosis-sensitive HMEC-E6 cells (Figure 3a), Tam and QTam induced apoptosis in HMEC-LX/E6 cells (Figure 7a). Treatment of HMEC-LX/E6 cells with either 1.0 μM Tam or QTam for 18 h resulted in a majority of cells undergoing apoptosis, 85 and 53%, respectively, compared to 6% in untreated controls. In contrast, when HMEC-Myr/E6 or HMEC-DD/E6 cells were treated with either 1.0 μM Tam or QTam, there was no significant difference ($P>0.05$) in the number of apoptotic cells, 13–18%, when compared to untreated controls, 5–8% (Figure 7a).

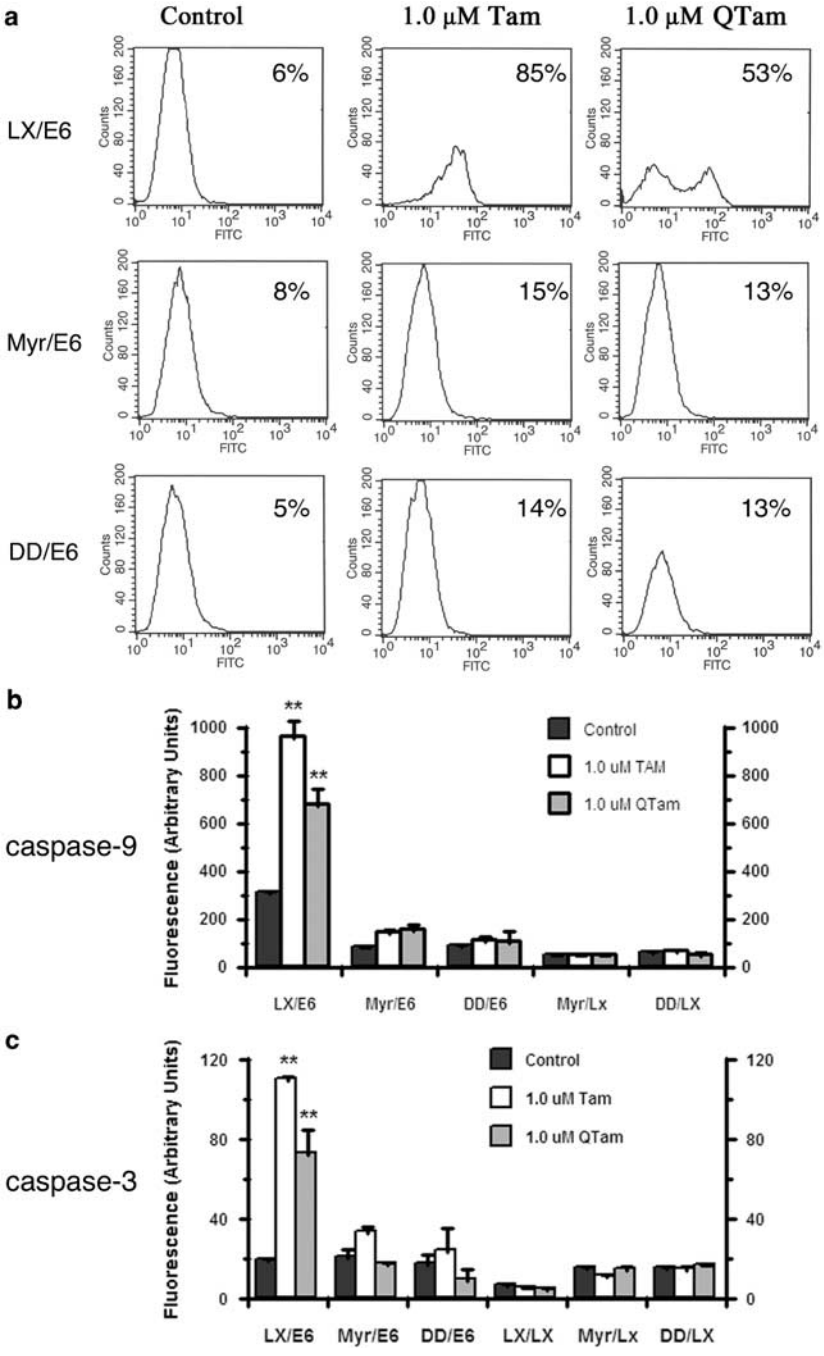

Figure 7 Tam- and QTam-induced apoptosis and caspase-9 and -3 activation in HMEC-LX/E6 cells but not in HMEC-Myr/E6 or -DD/E6 cells. (**a**) HMEC-LX/E6 controls (passage 11), HMEC-Myr/E6 cells (passage 11), and HMEC-DD/E6 cells (passage 11) treated with either 1.0 μM Tam (Tam) or 1.0 μM QTam (Q-Tam) for 18 h. Untreated control cells (Control) received an equivalent volume of ethanol. (**b**) Caspase-9 activity in apoptosis-sensitive HMEC-LX/E6 cells (passage 12) and apoptosis-insensitive HMEC-Myr/E6 and -DD/E6 cells (both passage 12) treated with either 1.0 μM Tam (Tam) or QTam (QTam) for 1 h. (**c**) Caspase-3 activity in apoptosis-sensitive HMEC-LX/E6 cells (passage 12) and apoptosis-insensitive HMEC-Myr/E6 and –DD/E6 cells (both passage 12) treated with either 1.0 μM Tam (Tam) or 1.0 μM QTam (QTam) for 12 h. Detection of apoptotic cells was with FITC-conjugated Annexin V as described in Materials and methods. These data are representative of three experiments. Cells for caspase assays were harvested by trypsinization, washed, and pelleted. The pellets were lysed and assayed according to the manufacturer's instructions (Clontech, Caspase 3 assay kit/K2026 and Caspase9/6 assay kit/K2015). Assays were performed in duplicate. Data are the mean of three separate experiments with s.d. (**: $P<0.025$)

Constitutively active AKT blocks Tam- and QTam-induced mitochondrial membrane depolarization and activation of caspase-9 and -3 in HMEC-E6 cells

Expression of the constitutively active AKT-Myr and AKT-DD constructs in HMEC-E6 cells blocked the ability of 1.0 μM Tam or QTam to decrease $\Delta\Psi_m$. $\Delta\Psi_m$ remained unchanged in HMEC-Myr/E6 and HMEC-DD/E6 cells after treatment for 1 or 3 h with either Tam or QTam ($P>0.05$) (Table 2b, c). However, apoptosis-sensitive HMEC-LX/E6 cells showed a 20 and a 30% decrease in $\Delta\Psi_m$ when treated with 1.0 μM Tam or QTam, respectively (Table 2b, c). The mitochondrial mass was similar in each untreated cell type (Table 2a). Interestingly, HMEC-Myr/E6 and HMEC-DD/E6 cells had 51 and 30% higher baseline levels of $\Delta\Psi_m$, respectively, than HMEC-LX/E6 cells.

Expression of the constitutively active AKT-Myr and AKT-DD constructs in HMEC-E6 cells also blocked the ability of Tam and QTam to activate caspase-9. Apoptosis-resistant HMEC-Myr/E6 and HMEC-DD/E6 cells treated with either 1.0 μM Tam or QTam for 1 h exhibited only a slight increase (81–94 and 11–24%, respectively, $P>0.05$) in caspase-9 activation (Figure 7b). This was in marked contrast to HMEC-LX/E6 cells that, similar to HMEC-E6 cells, exhibited a significant increase ($P<0.01$) in caspase-9 activation after treatment with either Tam or QTam, 210 and 120%, respectively. As expected, treated HMEC-Myr/LX and HMEC-DD/LX controls did not exhibit an increase in caspase-9 activation. Baseline caspase-9 activity was significantly ($P<0.01$) lower in control HMEC-Myr/E6 and HMEC-DD/E6 cells when compared to control HMEC-LX/E6 cells (Figure 7b).

Similar to results obtained for caspase-9, expression of the constitutively active AKT-Myr and AKT-DD constructs in HMEC-E6 cells blocked the ability of Tam and QTam to activate caspase-3. Apoptosis-resistant HMEC-Myr/E6 and HMEC-DD/E6 cells treated with either 1.0 μM Tam or QTam for 12 h exhibited no significant change ($P>0.05$) in caspase-3 activation (Figure 7c). In contrast, HMEC-LX/E6 cells, similar to HMEC-E6 cells, exhibited a significant increase in caspase-3 activation after treatment with either 1.0 μM Tam or QTam, 480 and 280%, respectively. As expected, Tam and QTam treated HMEC-Myr/LX and HMEC-DD/LX controls did not exhibit a significant ($P>0.05$) increase in caspase-3 activation. Unlike results obtained for caspase-9, baseline caspase-3 activity was similar in HMEC-Myr/E6, HMEC-DD/E6, and HMEC-LX/E6 cells (Figure 7c).

Discussion

The 'classic' or genomic mechanism of tamoxifen action requires the presence of ER and changes in both transcription and translation due to alteration(s) in promoter site occupancy. The interaction between Tam and nuclear ER has been well characterized (O'Regan and Jordan, 2002). However, there is evidence that E2, and perhaps antiestrogens, act through rapid, nongenomic signaling pathways that are initiated by ligand binding to plasma membrane-associated E2-binding sites (Marquez and Pietras, 2001; Pietras *et al*., 2001; Behl, 2002; Ho and Liao, 2002; Koustni *et al*., 2002; Levin, 2002; Ropero *et al*., 2002; Segars and Driggers, 2002; Doolan and Harvey, 2003; Li *et al*., 2003). Both E2 and Tam have been found to have specific binding sites on the plasma membrane. While there have been many reports of plasma membrane ER, there have been few reports of plasma membrane mediated effects of Tam in normal breast cells or breast cancer cell lines (Kirk *et al*., 1994).

Table 2 Baseline mitochondrial membrane potential ($\Delta\Psi_m$) is decreased in HMEC-Myr/E6 and -DD/E6 cells relative to HMEC-LX/E6, -Myr/LX, and -DD/LX control cells. (a) Baseline mitochondrial mass (NAO), potential (Rhodamine), and normalized potential (Rhodamine/NAO). (b) HMECs treated with 1.0 μM Tam for 1 or 3 h. (c) HMECs treated with 1.0 μM QTam for 1 or 3 h. $\Delta\Psi_m$ is measured by rhodamine 123 staining and normalized to mitochondrial mass, measured by NAO staining

	LX	*LX/E6*	*Myr/LX*	*DD/LX*	*Myr/E6*	*DD/E6*
(a)						
NAO	0.71±0.07	0.71±0.05	0.75±0.07	0.69±0.07	0.61±0.07	0.72±0.03
Rhodamine	0.88±0.05	0.76±0.04	0.98±0.06	1.01±0.06	0.85±0.06	0.87±0.09
Rhod/NAO	1.23±0.07	0.92±0.05	1.30±0.06	1.46±0.06	1.39±0.06	1.20±0.09
(b)						
	Treatment	*LX/E6*	*Myr/LX*	*DD/LX*	*Myr/E6*	*DD/E6*
Rhod/NAO	0 h TAM	1.00±0.05	1.83±0.06	1.98±0.06	1.76±0.06	2.23±0.09
	1 h TAM	0.83±0.04	1.78±0.03	2.11±0.05	1.69±0.07	2.39±0.07
	3 h TAM	0.80±0.03	1.79±0.04	1.93±0.05	1.75±0.06	2.27±0.08
(c)						
	Treatment	*LX/E6*	*Myr/LX*	*DD/LX*	*Myr/E6*	*DD/E6*
Rhod/NAO	0 h QTam	1.00±0.09	1.21±0.10	1.24±0.07	1.37±0.07	1.26±0.05
	1 h QTam	0.69±0.07	1.32±0.08	1.19±0.05	1.35±0.08	1.32±0.05
	3 h QTam	0.70±0.06	1.32±0.05	1.23±0.09	1.37±0.05	1.32±0.09

Fluorescence values are reported relative to ethanol-treated controls. Reported values represent the average of three separate experiments

The molecular mechanism(s) of Tam action in ER-'poor' HMECs is not well characterized. We previously developed an *in vitro* model of early mammary carcinogenesis and acute cellular damage of ER-'poor' HMECs. In this system, acute cellular damage was modeled by transduction with a retroviral vector coding for the HPV-16 E6 protein. We observed that Tam-treated HMEC-E6 cells rapidly underwent apoptosis, while HMEC-LX vector controls underwent growth arrest alone (Dietze *et al*., 2001). Tam-induced apoptosis in HMEC-E6 cells was associated with a rapid decrease in $\Delta\Psi_m$ followed by sequential activation of caspase-9 and -3 (Dietze *et al*., 2001). The rapidity of Tam's action in HMEC-E6 cells raised the possibility that Tam might act through a 'nonclassic', plasma membrane-associated signaling pathway.

Here, we provide evidence for (1) the presence of plasma membrane-associated E2-binding sites, (2) Tam initiation of apoptosis in HMEC-E6 cells by binding to plasma membrane-associated sites, and (3) the association of apoptosis with decreased AKT activity and Ser-473 phosphorylation. Initial experiments demonstrated that (1) Taz was enriched in a plasma membrane fraction prepared from Taz-treated HMEC-E6 cells (Figure 1) and (2) incubation of HMEC-E6 cells with 0.2 μM E2-BSA/FITC resulted in specific binding to the cell surface that was blocked by coincubation with 0.1 μM E2 (Figure 2c) but not by 1.0 μM E2-17-hemisuccinate-BSA (Figure 2d). These observations suggested the presence of plasma membrane-associated binding sites in HMEC-E6 cells for both Tam and E2. QTam (1) is a quaternized derivative of Tam which does not cross the plasma membrane (Fernandez *et al*., 1993; Kirk *et al*., 1994; Allen *et al*., 2000; Dick *et al*., 2002), (2) has similar binding characteristics to Tam (Jarman *et al*., 1986; Allen *et al*., 2000), and (3) like Tam, rapidly induced apoptosis in HMEC-E6 cells associated with mitochondrial membrane depolarization and caspase-9/-3 activation (Figure 3 and Table 1). Binding of E2-BSA/FITC to the plasma membrane surface of HMEC-E6 cells was specifically blocked by either 1.0 μM Tam or QTam (Figure 2e, f). These observations demonstrated that Tam and QTam competitively bound to cell surface-associated E2-binding sites on HMEC-E6 cells.

Phosphorylation of Thr-308 and Ser-473 activate AKT and serve as a cell-survival signal. Loss of AKT phosphorylation at Ser-473 is observed during apoptosis (Brazil and Hemmings, 2001; West *et al*., 2002). Recently, plasma membrane-associated sites for E2 have been shown to modulate AKT activity and signaling (Marquez and Pietras, 2001). Here, we provide evidence that membrane-associated effects of Tam decrease AKT activity and promote apoptosis in HMEC-E6 cells. Tam treatment of HMEC-E6 cells, but not HMEC-LX cells, resulted in a rapid, time-dependent loss of Ser-473 phosphorylation (Figure 4a). Loss of Ser-473 phosphorylation was complete at approximately 15 min. Treatment of apoptosis-sensitive HMEC-E6 cells with either 1.0 μM Tam or QTam resulted in (1) a decrease in AKT Ser-473 phosphorylation and AKT activity at 1 h (Figure 4b–e) and (2) biochemical and morphologic evidence of effector-phase apoptosis at 18 h (Figure 3 and data not shown).

SH-6 is a recently described specific inhibitor of AKT (Kozikowski *et al*., 2003). AKT activity is blocked without inhibition of PI3K or PDK1. HMEC-E6 cells treated with SH-6 demonstrated both increased caspase-9 and -3 activities and apoptosis (Figure 5). This demonstrated that direct inhibition of AKT had the same effects on HMEC-E6 cells as treatment with either Tam or QTam. We next explored whether or not constitutively active AKT constructs were able to block Tam- or QTam-induced decrease in $\Delta\Psi_m$, activation of caspase-9 and -3, and apoptosis.

Two constitutively active AKT constructs were used to test whether active AKT blocked Tam- and QTam-induced apoptosis in HMEC-E6 cells (Figure 6). The first construct incorporates the Myc myristoylation sequence into AKT1 (AKT-Myr). The expressed protein is inserted into the plasma membrane and, as a result, resides in proximity to activator kinases, which by mass action phosphorylate and activate AKT without the need of elevated PI3K activity. The second construct, AKT308D/S473D (AKT-DD), was generated by mutating the wild-type AKT phosphorylation sites Thr-308 and Ser-473 to Asp (Hutchinson *et al*., 2001). Expression of either AKT-Myr or AKT-DD in HMEC-E6 cells blocked the ability of Tam and QTam to induce apoptosis (Figure 7a). HMEC-Myr/E6 or HMEC-DD/E6 cells treated with either 1.0 μM Tam or QTam did not exhibit (1) a decrease in $\Delta\Psi_m$ (Table 2b) or (2) increased caspase-9/-3 activation (Figure 7b, c). Thus, both AKT-Myr and -DD were able to block the effects of either 1.0 μM Tam or QTam in apoptosis-sensitive HMEC-E6 cells.

Unexpectedly, HMEC-E6 and -LX/E6 cells showed a decrease in $\Delta\Psi_m$ and elevated caspase-9 activity without an accompanying increase in caspase-3 activity when compared to HMEC-LX cells (Tables 1 and 2; Figures 3b, c and 7b, c). The decrease in $\Delta\Psi_m$ was blocked by the expression of either of the constitutively active AKT constructs (Table 2). Increased caspase-9 activity was also blocked (Figure 7b). Thus, there appears to be an increase in the basal level of mitochondrial depolarization and caspase-9 activation in HMECs expressing E6 that is blocked by constitutively active AKT.

Taken together, these data indicate that Tam-induced apoptosis in HMEC-E6 cells is mediated through a plasma membrane-associated site and subsequent rapid inhibition of AKT activity. Tam did not directly inhibit AKT since QTam had the same effect on AKT. The results also indicate that a second, nongenomic pathway exists by which Tam might act as a chemoprevention/chemotherapeutic agent in breast cancer, possibly in ER-'poor' mammary epithelial cells. Membrane-bound ER has been shown to activate AKT when MCF-7 cells were stimulated with E2 (Marquez and Pietras, 2001; Razandi *et al*., 2003b). However, we have previously shown that while Tam induced apoptosis in this system but 4-hydroxyTam did not (Dietze *et al*., 2001). 4-HydroxyTam binds ER with higher affinity than Tam and would also be expected to induce apoptosis

mediated by ER binding. Thus, this AKT inhibition pathway may involve ER localized to the plasma membrane or an as yet uncharacterized receptor. We are now determining the properties of the receptor involved as well as the mechanism by which Tam or QTam inhibit AKT activity by binding a plasma membrane-associated receptor.

Materials and methods

Materials

All chemicals were obtained from Sigma-Aldrich (St Louis, MO, USA), DNA primers from GibcoBRL (Bethesda, MD, USA), and cell culture plasticware from Corning (Corning, NY, USA) unless otherwise noted. A 1.0 mM Tam stock solution was prepared in ethanol and stored in opaque tubes at −70°C. Tam was only used under reduced yellow lighting. AKT inhibitor SH-6 was obtained from CalBiochem (San Diego, CA, USA). Complete protease inhibitor was obtained from Roche (Indianapolis, IN, USA).

QTam was synthesized according to established methods (Allen *et al*., 2000) and stored desiccated in amber vials at −20°C. Tam and QTam were resolved with a 25 cm × 2.1 mm ID pkb100 column (Supelco, Bellefonte, PA, USA). The mobile phase was 40% aqueous 0.05% trifluoroacetic acid (TFA) and 60% aqueous 95% acetonitrile with 0.05% TFA. The flow rate was 1.0 ml/min and each run was 15 min with 5 min between injections. The column effluent was monitored at 280 nm and the retention time of Tam and QTam were 4.3 and 4.8 min, respectively. QTam was >95% pure by reverse phase HPLC. The high-resolution FAB-MS and [^{1}H]NMR spectra were consistent with reported values (data not shown).

Construction of retroviral vectors

Two retroviral vectors containing the coding sequences for constitutively active AKT were generated. The pAkt1-Myr plasmid (Upstate Biotechnology, Lake Placid, New York, USA) was digested with Tsp509I; the AKT308D/S473D (AKT-DD) plasmid (generous gift of J Woodgett) was digested with *Xho*I and *Eco*R1 (Hutchinson *et al*., 2001). The released inserts were inserted into the cloning site of the LXSN retrovirus as previously described (Seewaldt *et al*., 1995; Seewaldt *et al*., 1997b). Correct orientation and sequence were verified by direct sequencing. Transducing virions were derived as previously described (Seewaldt *et al*., 1995).

Cell culture conditions and retroviral transduction

Cell culture Normal HMEC strain AG11132 (M Stampfer #172R/AA7) was purchased from the National Institute of Aging, Cell Culture Repository (Coriell Institute, Camden, NJ, USA; Stampfer, 1985). HMEC strain AG11132 was established from normal tissue obtained at reduction mammoplasty, had a limited life span in culture, and failed to divide after approximately 20–25 passages. HMECs exhibit a low level of ER staining characteristic of normal mammary epithelial cells. HMECs were grown and mycoplasma testing was performed as previously reported (Seewaldt *et al*., 1997a, 1999b).

Single construct transduction The LXSN16E6 retroviral vector containing the HPV-16 E6 coding sequence was provided by D Galloway (Fred Hutchinson Cancer Research Center, Seattle, WA, USA) (Demers *et al*., 1996). HMECs were transduced with PA317-LXSN16E6 and PA317-LXSN and selected as described (Seewaldt *et al*., 1995). Transduced HMECs expressing the HPV-16 E6 construct were designated HMEC-E6 and vector control clones were designated HMEC-LXSN. All cells were maintained in the absence of G418 selection to minimize exposure to G418. All experiments were performed on mass cultures.

Double retroviral transductions Expression and selection of two retroviral constructs are adapted from previously published methods (Seewaldt *et al*., 2001b). Construction of retroviral vectors containing either the coding sequences for AKT1-Myr or AKT-DD was as described (Seewaldt *et al*., 1995). Transducing virions from either PA317-AKT-Myr or PA317-AKT-DD or the control PA317-LXSN (without insert) and PA317-LXSHE6 or PA317-LXSH were used for the first and second rounds of transduction, respectively (Figure 6a). At the completion of selection, all cells were removed from selection and used within three passages of the second transduction. Double transduced HMECs expressing the (1) LXSN/LXSH constructs were designated HMEC-LX/LX, (2) LXSN/HPV-16E6 constructs were designated HMEC-LX/E6, (3) LAKT-MyrSN/LXSH constructs were designated HMEC-Myr/LX, and (4) LAKT-MyrSN/HPV-16E6 constructs were designated HMEC-Myr/E6. Cells expressing the AKT-DD construct were designated either HMEC-DD/LX or HMEC-DD/E6.

Plasma membrane association of Tam and E2-BSA/FITC

Acutely transduced HMEC-E6s were plated in phenol-red-free media on glass Petri dishes. The cells were grown to 50% confluency and preincubated with 6.0 μM unlabeled Tam at 37°C for 10 min. After addition of 0.5 μM [^{3}H]Taz (B Katzenellenbogen, University of Illinois, Urbana, IL, USA), the incubation was continued for another 15 min. Next, the cells were washed with ice-cold PBS, trypsinized, pelleted, and resuspended in ice-cold homogenization buffer (50 mM Tris/10 mM sodium pyrophosphate/5 mM EDTA (pH 7.5), 150 mM NaCl, 1.0 mM Na orthovanadate, 10 mM NaF, 2 × Complete protease inhibitor). The resuspended cells were homogenized at 4°C with a Dounce homogenizer and the lysate, or respective supernatants, were centrifuged at 4°C for 10 min at 1000, 3000, and 20 000 *g*. The final supernatant was centrifuged for 60 min at 4°C and 100 000 *g* to produce microsomal and cytosolic fractions. All pellets were washed once by resuspending in homogenization buffer and repelleting. The washed pellets were resuspended in homogenization buffer, 5 μl of each fraction was counted in a scintillation counter, and the remainder was stored at −70°C. The crude nuclear fraction (1000 *g*) was subfractionated into an enriched nuclear fraction and a plasma membrane fraction by discontinuous sucrose density gradient centrifugation (Marquez and Pietras, 2001). The resulting fractions were assayed for the presence of DNA, 5'-nucleotidase activity, and LDH activity (Marquez and Pietras, 2001).

For binding of E2-BSA/FITC, cells were seeded in glass-bottomed microwell plates (MatTek, Ashland, MA, USA) at low density and allowed to attach for 1 day. The cells were fixed for 10 min in 1% formaldehyde in PBS at room temperature and then incubated for 15 min in room temperature PBS containing 10 μM BSA/FITC (Molecular Probes, Eugene, OR, USA), 0.2 μM E2-BSA/FITC, or 0.2 μM E2-BSA/FITC in the presence of either (1) 0.1 μM E2, (2) 1.0 μM Tam, 1.0 μM QTam, or (3) 1.0 μM E2-17-hemisuccinate-BSA as competitors. The cells were then washed rapidly twice with ice-cold PBS and observed at room temperature with a Nikon TE2000 fluorescence microscope (Nikon USA, Melville, NY,

USA) coupled to a Photometrics cooled CCD camera (Roper Scientific, Trenton, NJ, USA), using Metamorph software (Universal Imaging, Downingtown, PA, USA) and the preprogrammed settings for FITC.

SDS–PAGE and Western analysis

Three T-75 flasks of each cell type were grown to 50% confluency, treated for 1 h with 1.0 μM Tam, harvested as previously described (Seewaldt *et al*., 2001b), resuspended in immunoprecipitation buffer (homogenization buffer with 1.0% Triton X-100, 0.1 mM PMSF, 0.1 mM TLCK, 0.1 mM TPCK, 1 μg/ml pepstatin, 1 μg/ml leupeptin, 15 μg/ml calpain inhibitor I, 1 μg/ml aprotinin, 50 μg/ml bestain), aliquoted, and stored at -70°C until use. The lysate was separated by 10% SDS–PAGE and transferred to a PVDF membrane that was blocked overnight with 10% BSA (w/v) dissolved in Tris-buffered saline with 0.1% Tween-20 (TTBS). The blocked membrane was incubated with antibodies directed against AKT (#9272, Cell Signaling Technology, Beverly, MA, USA), AKT phosphoserine-473 (#9271, Cell Signaling Technology), or actin (sc-1616, Santa Cruz Biotechnology, Santa Cruz, CA, USA) in TTBS. To detect protein expression of the AKT-DD and AKT-Myr, the blocked membrane was incubated with anti-HA tag antibody (#2362, Cell Signaling Technology) and anti-Myc tag antibody (#2276, Cell Signaling Technology), respectively. Anti-HPV16 E6 antibody was used to detect HPV16 E6 protein (Santa Cruz, sc-1583). The membrane was washed in TTBS, incubated with a 1 : 6000 dilution of the appropriate secondary antibody conjugated to alkaline phosphatase (Santa Cruz Biotechnology), washed, and developed with LumiPhos WB (Pierce Chemical, Rockford, IL, USA). The image was digitized with a Kodak Digital Science IS 440 and quantitated using Kodak 1D™ software (Eastman Kodak, Rochester, NY, USA).

Measurement of apoptosis, caspase-9/-3 activity, and mitochondria depolarization

Apoptosis was measured by Annexin V binding and FACS after treatment with 1.0 μM Tam or 1.0 μM QTam for 18 h as previously described (Seewaldt *et al*., 1999a; Dietze *et al*., 2001). Caspase-9 was measured after 1 h treatment and caspase-3 was measured after 12–18 h treatment, as noted, with either 1.0 μM Tam or 1.0 μM QTam. Cells were harvested by trypsinization. The cells were washed once with 100 volumes of ice-cold PBS and pelleted. Caspase-9 and -3 activities were then assayed according to the manufacturer's instructions using a Caspase 9/6 (K2015) or Caspase 3 (K2026) assay kit (Clontech, Palo Alto, CA, USA). Mitochondrial depolarization was also measured as previously described (Dietze *et al*., 2001) on cells treated for 1–6 h, as noted, with 0.10 or 1.0 μM of either Tam or QTam.

Acknowledgements
We acknowledge the generous gifts of (1) J Woodgett for the AKT308D/S473D plasmid, (2) D Galloway for the LXSN16E6 retroviral vector containing the HPV-16 E6 coding sequence, and (3) B Katzenellenbogen for the [^{3}H]tamoxifen aziridine. This work is supported by NIH/NCI Grants 2P30CA14236-26 (VLS, ECD), R01CA88799 (VLS), R01CA98441 (VLS), NIH/NIDDK Grant 2P30DK 35816-11 (VLS), DAMD-98-1-851 and DAMD-010919 (VLS), American Cancer Society Award CCE-99898 (VLS), a V-Foundation Award (VLS), a Susan G Komen Breast Cancer Award (VLS, ECD), and a Charlotte Geyer Award (VLS).

References

Allen MC, Gale PA, Hunter AC, Lloyd A and Hardy SP. (2000). *Biochim. Biophys. Acta*, **1509,** 229–236.
Anderson E, Clarke RB and Howell A. (1998). *J. Mamm. Gland Biol. Neoplasia*, **3,** 23–35.
Aoudjet F and Vuori K. (2001). *Oncogene*, **20,** 4995–5004.
Aronica SM, Kraus WL and Katzenellbogen BS. (1994). *Proc. Natl. Acad. Sci. USA*, **91,** 8517–8521.
Behl C. (2002). *Nat. Rev. Neurosci.*, **3,** 433–442.
Boserma AWM, Nooter K, Oostrum RG and Stoter G. (1996). *Cytometry*, **24,** 123–130.
Brazil DP and Hemmings BA. (2001). *Trends Biochem. Sci.*, **26,** 657–664.
Campbell RA, Baht-Nakshatri P, Patel NM, Constantinidou D, Ali S and Naksahtri H. (2001). *J. Biol. Chem.*, **276,** 9817–9824.
Chambliss KL, Yuhanna IS, Anderson RGW, Mendelsohn ME and Shaul PW. (2002). *Mol. Endocrinol.*, **16,** 938–946.
Demers GW, Espling E, Harry JB, Etscheid BG and Galloway DA. (1996). *J. Virol.*, **70,** 6862–6869.
Dick GM, Hunter AC and Sanders KM. (2002). *Mol. Pharmacol.*, **61,** 1105–1113.
Dietze EC, Caldwell LE, Grupin SL, Mancini M and Seewaldt VL. (2001). *J. Biol. Chem.*, **276,** 5384–5394.
Doolan CM and Harvey BJ. (2003). *Mol. Cell. Endocrinol.*, **199,** 87–103.
Fernandez A, Cantabrana B and Hildago A. (1993). *Gen. Pharmacol.*, **24,** 391–395.
Fisher B, Constantino JP, Wickerham CDL, Redmond CK, Kavanah M, Cronin WM, Vogel V, Robidoux A, Dimitrov N, Atkins J, Daly M, Wieand S, Tan-Chiu E, Ford L and Wolmark N. (1998). *J. Natl. Cancer Inst.*, **90,** 1371–1388.
Friedman ZY. (1998). *Cancer Invest.*, **16,** 391–396.
Ho KJ and Liao JK. (2002). *Arterioscler. Thromb. Vasc. Biol.*, **22,** 1952–1961.
Hutchinson J, Jin J, Cardiff RD, Woodgett JR and Muller WJ. (2001). *Mol. Cell. Biol.*, **21,** 2203–2212.
Improta-Brears T, Whorton AR, Codazzi F, York JD, Meyer T and McDonnell DP. (1999). *Proc. Natl. Acad. Sci. USA*, **96,** 4686–4691.
Jarman M, Leung OT, LeClercq G, Devleeschouwer N, Stossel S, Coombes RC and Skilton RA. (1986). *Anti-Cancer Drug Des.*, **1,** 259–268.
Johnson LV, Walsh ML and Chen LB. (1980). *Proc. Natl. Acad. Sci. USA*, **77,** 990–994.
Kandel ES and Hay N. (1999). *Exp. Cell Res.*, **253,** 210–229.
Kato S, Endoh H, Masuhiro Y, Kitamoto T, Uchiyama S, Sasaki H, Masushige S, Gotoh Y, Nishida E, Kawashima H, Metzger D and Chambon P. (1995). *Science*, **270,** 1491–1494.
Kirk J, Syed SK, Harris AL, Jarman M, Roufogalis BD, Stratford IJ and Carmichael J. (1994). *Biochem. Pharmacol.*, **48,** 277–285.
Kousteni S, Chen JR, Bellido T, Han L, Ali AA, O'Brien CA, Plotkin L, Fu Q, Mancino AT, Wien Y, Vertino AM, Powers CC, Stewart SA, Ebert R, Parfitt AM, Weinstein RS, Jilka RL and Manolagas SC. (2002). *Science*, **298,** 843–846.
Kozikowski AP, Sun H, Brognard J and Dennis PA. (2003). *J. Am. Chem. Soc.*, **125,** 1144–1145.
Levin ER. (2002). *Steroids*, **67,** 471–475.

Li L, Haynes MP and Bender JR. (2003). *Proc. Natl. Acad. Sci. USA*, **100,** 4607–4812.
Linford N, Wade C and Dorsa D. (2000). *J. Neurocytol.*, **29,** 367–374.
Marquez DC and Pietras RJ. (2001). *Oncogene*, **20,** 5420–5430.
Okano J, Gaslightwala I, Birnbaum MJ, Rustgi AK and Nakagawa H. (2000). *J. Biol. Chem.*, **275,** 30934–30942.
O'Regan RM and Jordan VC. (2002). *Lancet Oncol.*, **3,** 207–214.
Pietras RJ, Nemere I and Szego CM. (2001). *Endocrine*, **14,** 417–427.
Razandi M, Alton G, Pedram A, Ghonshani S, Webb P and Levin ER. (2003a). *Mol. Cell. Biol.*, **23,** 1633–1646.
Razandi M, Oh P, Pedram A, Schnitzer J and Levin ER. (2002). *Mol. Endocrinol.*, **16,** 100–115.
Razandi M, Pedram A and Levin ER. (2000). *Mol. Endocrinol.*, **14,** 1434–1447.
Razandi M, Pedram A, Park ST and Levin ER. (2003b). *J. Biol. Chem.*, **278,** 2701–2712.
Ropero AB, Soria B and Nadal A. (2002). *Mol. Endocrinol.*, **16,** 497–505.
Scheid MP and Woodgett JR. (2003). *FEBS Lett.*, **546,** 108–112.
Schlegel A, Wang C, Katzenellenbogen BS, Pestell RG and Lisanti MP. (1999). *J. Biol. Chem.*, **274,** 33551–33556.
Schwartfeger KL, Richert MM and Anderson SM. (2001). *Mol. Endocrinol.*, **15,** 867–881.
Seewaldt VL, Caldwell LE, Johnson BB, Swisshelm K and Collins SJ. (1997a). *Cell Growth Diff.*, **8,** 631–641.
Seewaldt VL, Caldwell LE, Johnson BS, Swisshelm K, Collins SJ and Tsai S. (1997b). *Exp. Cell Res.*, **236,** 16–28.
Seewaldt VL, Dietze EC, Johnson BS, Collins SJ and Parker MB. (1999a). *Cell Growth Diff.*, **10,** 49–59.
Seewaldt VL, Johnson BS, Parker MB, Collins SJ and Swisshelm K. (1995). *Cell Growth Diff.*, **6,** 1077–1088.
Seewaldt VL, Kim J-H, Parker MB, Dietze EC, Srinivasan KV and Caldwell LE. (1999b). *Expt. Cell Res.*, **249,** 70–85.
Seewaldt VL, Mrózek K, Dietze EC, Parker MB and Caldwell LE. (2001a). *Cancer Res.*, **61,** 616–624.
Seewaldt VL, Mrózek K, Sigle R, Dietze EC, Heine K, Hockenbery DM, Hobbs KB and Caldwell LE. (2001b). *J. Cell Biol.*, **155,** 471–486.
Segars JH and Driggers PH. (2002). *Trends Endocrinol. Metab.*, **13,** 349–354.
Simoncini T, Hafezi-Moghandam A, Brazil DP, Ley K, Chin WW and Liao KJ. (2000). *Nature*, **407,** 538–541.
Song RX-D, Mcpherson RA, Adam L, Bao Y, Shupnik M, Kumar R and Santen RJ. (2002). *Mol. Endocrinol.*, **16,** 116–127.
Stampfer M. (1985). *J. Tissue Cult. Method*, **9,** 107–121.
Stocia GE, Franke TF, Wellstein A, Czubayko F, List HJ, Reiter R, Morgan E, Martin MB and Stoica A. (2003a). *Mol. Endocrinol.*, **17,** 818–830.
Stocia GE, Franke TF, Wellstein A, Morgan E, Czubayko F, List HJ, Reiter R, Martin MB and Stocia A. (2003b). *Oncogene*, **22,** 2073–2087.
Strange R, Netcalfe T, Thackeray L and Dang M. (2001). *Microsc. Res. Tech.*, **52,** 171–181.
Sun M, Wang G, Paciga JE, Feldman RI, Yuan ZQ, Ma XL, Shelley SA, Jove R, Tsichlis PN, Nicosia SV and Cheng JQ. (2001). *Am. J. Path.*, **159,** 431–437.
Testa JR and Bellacosa A. (2001). *Proc. Natl. Acad. Sci. USA*, **98,** 10983–10985.
West KA, Castillo SS and Dennis PA. (2002). *Drug Resist. Updates*, **5,** 234–248.
Whitehead JP, Molero JC, Clark S, Martin S, Meneily G and James DE. (2001). *J. Biol. Chem.*, **276,** 27816–27824.
Zhang Z, Maier B, Santen RJ and Song RX-D. (2002). *Biochem. Biophys. Res. Commun.*, **294,** 926–933.

Oncogene (2004) 23, 8743–8755

www.nature.com/onc

Interferon-regulatory factor-1 is critical for tamoxifen-mediated apoptosis in human mammary epithelial cells

Michelle L Bowie[1], Eric C Dietze[1], Jeffery Delrow[2], Gregory R Bean[1], Michelle M Troch[1], Robin J Marjoram[1] and Victoria L Seewaldt*[,1,3]

[1]*Division of Medical Oncology, Duke University, Durham, NC 27710, USA;* [2]*Fred Hutchinson Cancer Research Center, Seattle, WA 98120, USA;* [3]*Department of Pharmacology and Cancer Biology, Duke University, Durham, NC 27710, USA*

Unlike estrogen receptor-positive (ER(+)) breast cancers, normal human mammary epithelial cells (HMECs) typically express low nuclear levels of ER (ER poor). We previously demonstrated that 1.0 μM tamoxifen (Tam) promotes apoptosis in acutely damaged ER-poor HMECs through a rapid, 'nonclassic' signaling pathway. Interferon-regulatory factor-1 (IRF-1), a target of signal transducer and activator of transcription-1 transcriptional regulation, has been shown to promote apoptosis following DNA damage. Here we show that 1.0 μM Tam promotes apoptosis in acutely damaged ER-poor HMECs through IRF-1 induction and caspase-1/3 activation. Treatment of acutely damaged HMEC-E6 cells with 1.0 μM Tam resulted in recruitment of CBP to the γ-IFN-activated sequence element of the *IRF-1* promoter, induction of IRF-1, and sequential activation of caspase-1 and -3. The effects of Tam were blocked by expression of siRNA directed against IRF-1 and caspase-1 inhibitors. These data indicate that Tam induces apoptosis in HMEC-E6 cells through a novel IRF-1-mediated signaling pathway that results in activated caspase-1 and -3.
Oncogene (2004) **23,** 8743–8755. doi:10.1038/sj.onc.1208120
Published online 4 October 2004

Keywords: IRF-1; tamoxifen; CBP; breast cancer

Introduction

The 'classic' or genomic mechanism of β-estradiol (E2) action requires the presence of the estrogen receptor (ER), the E2/ER complex binding to an ERE, and changes in both transcription and translation. However, recent evidence suggests that estrogen and perhaps antiestrogens may also act through rapid, 'nonclassic' signaling pathways in mammary epithelial cells (Kelly and Levin, 2001). Tamoxifen (Tam) is an ER agonist/antagonist that has been characterized as an inhibitor of the classic E2 pathway. The Breast Cancer Prevention Trial demonstrated a decreased incidence of *in situ* and ER(+) breast cancer in the high-risk participants who were prescribed Tam for 5 years (Fisher *et al*., 1998). However, the molecular mechanism of Tam action in normal breast tissue is poorly understood. Normal human mammary epithelial cells (HMECs), unlike ER(+) breast cancers, typically express low nuclear levels of ER (ER poor) (Anderson *et al*., 1998). As a result, it is uncertain whether Tam is able to target the elimination of acutely damaged, ER-poor cells or whether Tam's action is restricted to mammary epithelial cells that express high levels of ER. We have previously shown that 1.0 μM Tam rapidly promotes apoptosis in acutely damaged, ER-poor HMECs but only induces growth arrest in HMEC controls (Dietze *et al*., 2001; Seewaldt *et al*., 2001). Here we further investigated the molecular mechanism of Tam-induced apoptosis in acutely damaged HMECs. Acute cellular damage was modeled via expression of the human papilloma virus (HPV) E6 protein (E6), which results in dysregulation of multiple signaling pathways crucial for cellular homeostasis. E6 protein affects these pathways by interacting with proteins such as p53, p300/CBP, Bak, IRF-3, and paxillin and provides a convenient model of acute cellular damage (Mantovani and Banks, 2001).

Interferons (IFNs) are a family of cytokines that have multiple biological effects including immunomodulatory, antiviral, antiproliferative, antigen modulation, cell differentiation, and apoptotic effects (Pestka *et al*., 1987; Stark *et al*., 1998; Chawla-Sarkar *et al*., 2003). Upon secretion from cells, IFNs bind to specific cell membrane receptors and activate the JAK-STAT pathway, which results in upregulation of IFN-stimulated genes (ISGs) (Darnell *et al*., 1994; Stark *et al*., 1998). Many of the biological effects from IFNs are mediated by these ISGs.

IFNs have also been shown to enhance the growth inhibitory actions of Tam (Gibson *et al*., 1993; Coradini *et al*., 1997; Iacopino *et al*., 1997). In studies by Lindner *et al*., treatment with Tam (1.0 μM) and IFN-β (100 IU/ml) resulted in growth inhibition in both ER(+) and ER(−) breast cancer cell lines. In ER(−) cell lines, Tam in combination with IFN-β treatment was significantly more effective in inhibiting cell growth than Tam alone. In addition, in MCF-7 cells resistant to IFN-β treatment, preincubation with Tam followed by IFN-β

*Correspondence: V Seewaldt, Duke University Medical Center, Box 2628, Durham, NC 27710, USA. E-mail: seewa001@mc.duke.edu
Received 20 May 2004; revised 2 August 2004; accepted 9 August 2004; published online 4 October 2004

treatment resulted in growth inhibition and upregulation of the ISGs 2′-5′-oligoadenylate synthetase, PKR, and IFN-induced protein (IFI) 56. Furthermore, *in vivo* studies using nude mice with established 6-week-old MCF-7 (ER(+)) and OVCAR-3 (ER(−)) breast tumors showed tumor regression only with combined Tam/IFN therapy (Lindner and Borden, 1997; Lindner *et al*., 1997). This synergistic cytotoxicity, combined with the observed induction of IFN genes in IFN-resistant cells, suggests possible cross-talk between the two pathways. Cross-talk with the IFN pathway has also been shown with other steroid/thyroid and death receptor modulators including retinoic acid (Kolla *et al*., 1996) and TRAIL/APO-2L (Kumar-Sinha *et al*., 2002).

ISGs exert their effects in many different ways, including promoting apoptosis. Signal transducer and activator of transcription-1 (STAT1) is activated upon IFN ligand binding to its receptor, and acts either in a complex with STAT2/p48 (ISGF3), or as a homodimer, to induce transcription of ISGs (Horvath, 2000). IFN-regulatory factor-1 (IRF-1) is a target of STAT1 transcriptional regulation (Pine *et al*., 1994). IRF-1 itself transcriptionally regulates additional ISGs and has been shown to promote apoptosis following DNA damage (Tanaka *et al*., 1994; Tamura *et al*., 1995; Henderson *et al*., 1997). Specifically, IRF-1 promotes apoptosis associated with caspase-1 activation (Tamura *et al*., 1995; Romeo *et al*., 2002). More recently, IRF-1 has been shown to be a tumor suppressor and critical for mammary gland involution (Yim *et al*., 1997; Nozawa *et al*., 1999; Hoshiya *et al*., 2003; Kim *et al*., 2004). Studies have also shown that IRF-1 expression is lowered or the gene is mutated in multiple cancers, including breast cancer (Doherty *et al*., 2001; Tzoanopoulos *et al*., 2002).

CREB-binding protein (CBP) has been shown to be a critical coactivator in IFN signaling (Horvai *et al*., 1997; Merika *et al*., 1998). CBP, located at chromosome band 16p13.3, is a transcriptional cofactor that regulates proliferation, differentiation, and apoptosis (Giles *et al*., 1997b; Yao *et al*., 1998). Chromosomal loss at 16p13 has been reported to occur in a majority of benign and malignant papillary neoplasms of the breast and loss or amplification of 16p is frequently observed in premalignant breast lesions (Lininger *et al*., 1998; Tsuda *et al*., 1998; Aubele *et al*., 2000). CBP acts as a key integrator of diverse signaling pathways including those regulated by retinoids, p53, and estrogen, and has been hypothesized to play a role in BRCA1-mediated DNA repair (Kawasaki *et al*., 1998; Robyr *et al*., 2000). CBP levels are tightly controlled and CBP is thought to be present in limiting amounts. It has been theorized that the many transcription factors requiring CBP compete for its binding (Giles *et al*., 1997a; Kawasaki *et al*., 1998; Yao *et al*., 1998; Robyr *et al*., 2000). Recent evidence indicates that CBP activity is also regulated by both phosphorylation and expression (Guo *et al*., 2001).

In this study, we aimed to identify potential mediators of Tam-induced apoptosis in acutely damaged HMEC apoptosis-sensitive cells expressing E6. Here we show that Tam promotes apoptosis in acutely damaged HMEC-E6 cells through IRF-1 induction and caspase-1 activation. These results provide evidence for a novel role for ISG signaling in targeting the elimination of acutely damaged HMECs.

Results

cDNA microarray analysis of Tam-induced gene transcripts

To investigate the molecular mechanism of Tam-induced apoptosis, we analysed the expression profiles of acutely damaged HMEC-E6 cells and passage-matched HMEC-LX controls treated with or without 1.0 μM Tam for 6 h. Analysis was performed using Hu6800 cDNA microarrays (Affymetrix™). As shown in Table 1, 20 ISGs were significantly upregulated in Tam-treated HMEC-E6 cells but not in HMEC-LX controls. The upregulated genes included (fold change >1.5; P-value <0.05) IFI9–27, IRF-1, ISG15, ISG-54, MX-A, IFN-γ inducible protein 16, STAT1 α, STAT1 β, IFI 6–16, and ISG12. Differential expression was confirmed by semiquantitative reverse transcriptase–polymerase chain reaction (RT–PCR) in triplicate, and normalized to β-actin (Figure 1). Based on these observations, we hypothesized that ISGs may (1) participate in or (2) be a marker for Tam-induced apoptosis in acutely damaged HMEC-E6 cells.

Table 1 Tamoxifen gene changes

Gene name	*GenBank™*	*Fold change*	
		HMEC-LX	HMEC-E6
IFI 9-27	J04164	—	4.5
IRF-1	L05072	—	4.0
ISG15	M13755	—	4.4
ISG-54	M14660	—	5.2
RANTES	M21121	—	1.9
IFI-56	M24594	—	2.3
MX-A	M33882	—	20.0
IFN-γ inducible protein 16	M63838	—	2.0
2′-5′-oligoadenylate synthetase 2, isoform p69	M87284	—	3.8
2′-5′-oligoadenylate synthetase 2, isoform p71	M87434	—	3.6
IRF-9	M87503	—	2.6
STAT1 α	M97935	—	2.0
STAT1 β	M97936	−3.1	12.7
IFN γ receptor 1	U19247	—	2.1
IFI 6-16	U22970	—	17.5
RIG-G	U52513	—	2.1
IRF-7	U53830	—	9.7
IFN-induced protein 35	U72882	—	2.6
2′,5′-oligoadenylate synthetase 1 (1.6 kb RNA)	X02874	—	4.5
2′,5′-oligoadenylate synthetase 1 (1.8 kb RNA)	X02875	—	4.2
IL-6 (IFN, β2)	X04602	—	—
IFN-induced transmembrane protein 2 (1–8 kDa)	X57351	—	—
ISG12	X67325	—	7.6
Proteasome subunit, β type 10	X71874	−1.6	—
Proteasome subunit, β type 8; LMP8	Z14982	−2.6	—

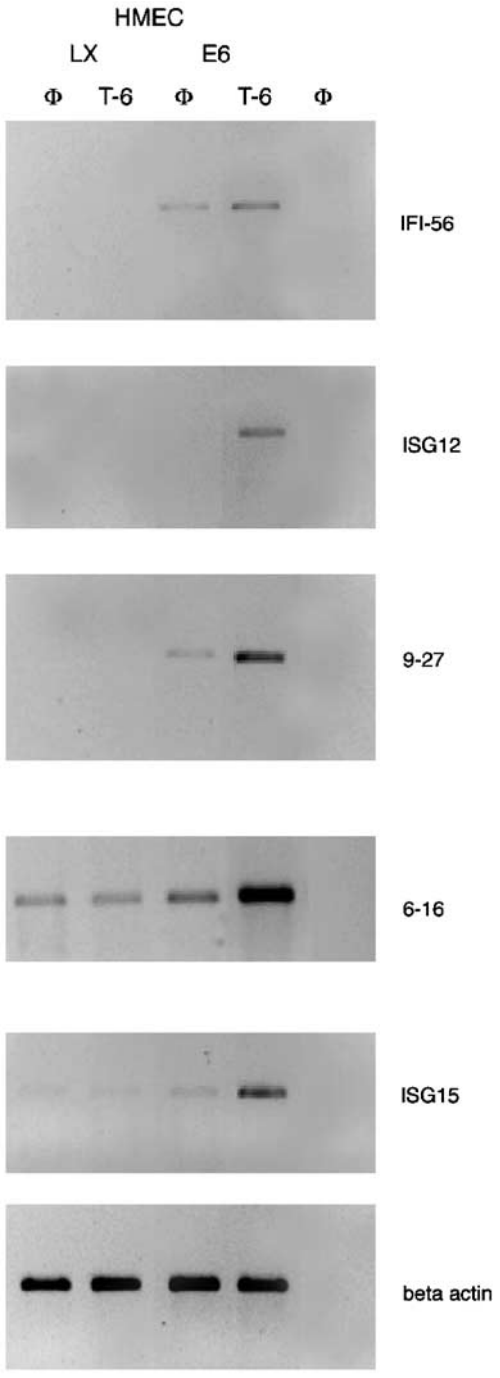

Figure 1 Semiquantitative RT–PCR analysis of ISG mRNA expression in early passage acutely damaged HMEC-E6 cells (passage 10) and HMEC-LX vector controls (passage 10). Treated with 1.0 μM Tam for 0 h (Φ) and 6 h (T-6). β-actin serves as a normalization control. These data are representative of three separate experiments

IFN-α, -β, and -γ are not induced by Tam treatment

The subset of ISGs induced by 1.0 μM Tam are only a few of the more than 300 genes shown to be upregulated by type I (IFN-α and -β) and type II (IFN-γ) IFNs (Der *et al*., 1998; de Veer *et al*., 2001). Our differential gene expression data indicated that IFN transcripts-α, -β, and -γ were not induced by 6 h Tam treatment (data not shown). ELISA assays were performed in Tam-treated HMECs to test whether IFNs were released following Tam treatment. Passage-matched apoptosis-sensitive HMEC-E6 cells and HMEC-LX controls were treated with 1.0 μM Tam for 24 h. Release of IFN-α, -β, and -γ was not detected following Tam treatment (data not shown). These data show that Tam promotes apoptosis and ISG induction in HMEC-E6 cells in the absence of IFN-α, -β, and -γ induction or release.

IRF-1 is induced by Tam

IRF-1 is a transcriptional regulator that has been shown to promote apoptosis following DNA damage and is critical for mammary gland involution (Kroger *et al*., 2002; Hoshiya *et al*., 2003). Differential gene expression studies demonstrated that IRF-1 mRNA was induced by Tam in acutely damaged HMEC-E6 cells at 6 h. Semiquantitative RT–PCR and Western analysis were performed to determine the kinetics of IRF-1 mRNA and protein induction. We observed that IRF-1 mRNA and protein were induced by 1.0 μM Tam in acutely damaged HMEC-E6 cells but not in HMEC-LX controls. IRF-1 mRNA induction in HMEC-E6 cells was first observed at 30 min (5.1-fold, P-value <0.01) and was maximally induced at 3 h (8.8-fold, P-value <0.0001) (Figure 2a and b). IRF-1 protein induction was first observed at 30 min (1.5-fold, P-value <0.025) and was maximally induced at 3 h (2.3-fold, P-value <0.001) (Figure 2c and d). These observations demonstrate that IRF-1 mRNA and protein are induced by Tam in acutely damaged HMEC-E6 cells starting at 30 min.

Tam promotes recruitment of CBP to the IFN consensus sequence 2/γ-IFN-activated sequence (ICS2/GAS) element of the IRF-1 promoter

Chromatin immunoprecipitation (ChIP) and immunoprecipitation studies were performed to identify coactivators that might participate in IRF-1 mRNA induction in apoptosis-sensitive HMEC-E6 cells. CBP is a known regulator of apoptosis and a coactivator for steroid/thyroid and type II IFN signaling (Horvai *et al*., 1997; Hiroi and Ohmori, 2003). STAT1 is a transcriptional regulator of IRF-1 and has been shown to interact with CBP through the (1) CREB-binding domain and (2) CH3 domain (Zhang *et al*., 1996). Recently, an IFN-inducible GAS element was identified in the *IRF-1* promoter that serves to activate IRF-1 transcription (Sims *et al*., 1993; Harada *et al*., 1994). Using ChIP and immunoprecipitation studies, we tested whether Tam treatment of HMEC-E6 cells may promote (1) CBP or STAT1 recruitment to this *IRF-1* promoter GAS element and (2) induction of IRF-1 mRNA expression at 0, 2, and 6 h. We observed that STAT1 was constitutively associated with the GAS element of the *IRF-1* promoter in HMEC-E6 cells and Tam treatment did not alter this association (Figure 3a). In contrast,

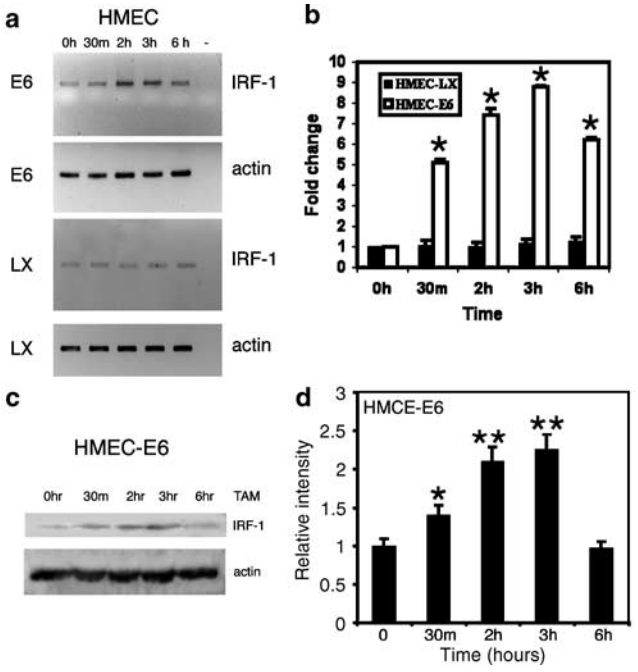

Figure 2 Tam induces expression of IRF-1 mRNA and protein in acutely damaged HMEC-E6 cells. (**a**) Semiquantitative RT–PCR analysis of IRF-1 mRNA expression in early passage acutely damaged HMEC-E6 cells (passage 10) and HMEC-LX vector controls (passage 10). Treated with 1.0 μM Tam for 0, 30 min, 2, 3, and 6 h. β-actin serves as a normalization control. The negative sample (−) contained no cDNA. These data are representative of three separate experiments. (**b**) Quantitation of IRF-1 mRNA expression in early passage HMEC-E6 cells and HMEC-LX vector controls treated with 1.0 μM Tam. Expression is normalized to β-actin. These data are the average of three separate determinations. (*P-value <0.01). (**c**) Expression of IRF-1 protein in early passage HMEC-E6 cells (passage 11) treated with 1.0 μM Tam for 0, 30 min, 2, 3, and 6 h. Equal amounts of protein lysate were added in each lane. β-actin serves as a loading control. (**d**) Quantitation of IRF-1 protein expression in early passage HMEC-E6 cells treated with 1.0 μM Tam. Expression is normalized to β-actin. These data are the average of three separate determinations. (*P-value <0.025; **P-value <0.001)

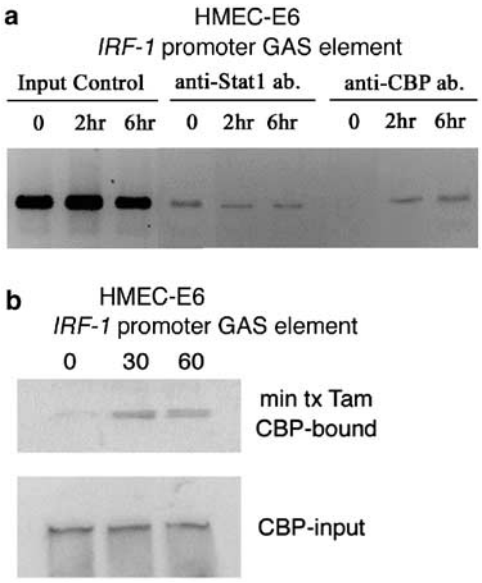

Figure 3 Tam promotes recruitment of CBP to the *IRF-1* promoter GAS element in acutely damaged HMEC-E6 cells. (**a**) ChIP was performed to test for STAT1 and CBP recruitment to the *IRF-1* GAS element as a function of Tam treatment. Early passage acutely damaged HMEC-E6 cells (passage 11) were treated with 1.0 μM Tam for 0, 2, and 6 h as described in Materials and methods. Input controls tested the integrity of the DNA samples. These data represent three separate experiments. (**b**) An immunoprecipitation time course using a biotin-labeled oligo, containing the *IRF-1* GAS promoter element, was performed to investigate the temporal correlation between CBP recruitment to the *IRF-1* promoter and IRF-1 mRNA induction in Tam treated early passage HMEC-E6 cells (passage 12) as described in Materials and methods. CBP-input controls are provided to assess the CBP content of protein lysates subjected to immunoprecipitation. CBP-bound assesses the amount of CBP bound to the *IRF-1* GAS promoter element oligo. These data are representative of three separate experiments

CBP was recruited to the *IRF-1* promoter 2 h following treatment of HMEC-E6 cells with 1.0 μM Tam (Figure 3a). Neither STAT1 nor CBP were recruited to the GAS element of the *IRF-1* promoter in HMEC-LX controls with Tam treatment (data not shown). The observation that STAT1 was constitutively bound to the IRF-1 GAS element in the HMEC-E6 cells suggested that it may be active at baseline. There are two known phosphorylation sites within STAT1, Tyr701 and Ser727. It has been shown that phosphorylation of Ser727 induces the highest transcriptional activation for STAT1 (Wen *et al*., 1995). Western analysis was performed to determine the phosphorylation status of STAT1 in the untreated acutely damaged HMEC-E6 cells. We observed that STAT1 is phosphorylated at Ser727 in the HMEC-E6 cells at baseline (Figure 4d). The activation of STAT1 in the HMEC-E6 cells at baseline may be a response to the expression of E6 in these cells.

An immunoprecipitation time course using a biotin-labeled oligo, containing the *IRF-1* GAS promoter element, was performed to precisely pinpoint the temporal correlation between (1) CBP recruitment to the *IRF-1* promoter and (2) IRF-1 mRNA induction in Tam-treated HMEC-E6 cells. CBP was recruited to the GAS element of the *IRF-1* promoter at 30 min after 1.0 μM Tam treatment (Figure 3b). STAT1 was again shown to be constitutively associated with the *IRF-1* promoter GAS element between 0 and 60 min (data not shown). CBP recruitment correlated with IRF-1 mRNA induction at 30 min (Figure 2). These observations demonstrate that Tam-mediated recruitment of CBP to the GAS element of the *IRF-1* promoter in acutely damaged HMEC-E6 cells is temporally concurrent with IRF-1 mRNA and protein induction.

IFI 6–16 is induced by Tam

IFNs have been shown to regulate the expression of the IFI 6–16 gene (Gjermandsen *et al*., 2000). Specifically, IRF-1 expression induces transcription of IFI 6–16 (Henderson *et al*., 1997). Our differential gene expression studies demonstrate that IFI 6–16 mRNA is

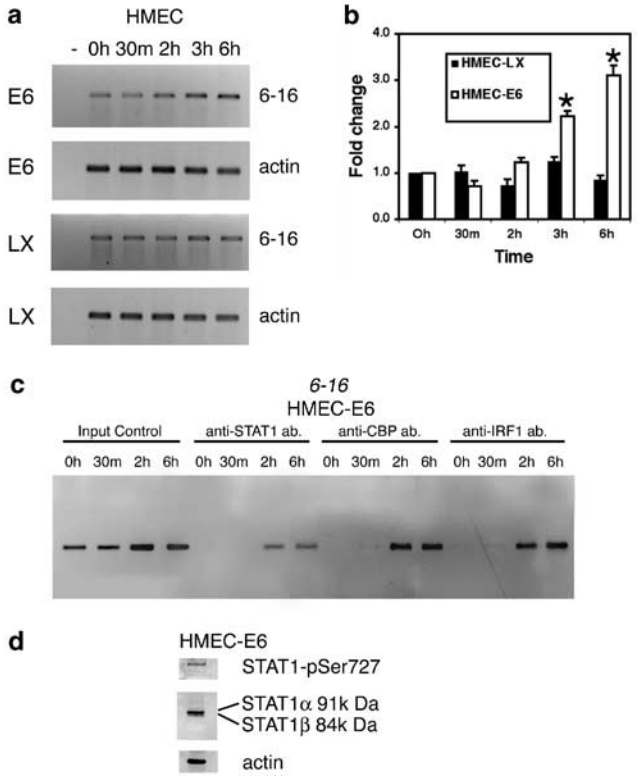

Figure 4 Tam promotes induction of IFI 6–16 mRNA and recruitment of STAT1, CBP, and IRF-1 to the ISRE element of the *IFI 6–16* promoter. (**a**) Semiquantitative RT–PCR analysis of IFI 6–16 mRNA expression in early passage acutely damaged HMEC-E6 cells (passage 10) and HMEC-LX vector controls (passage 10) treated with 1.0 μM Tam for 0, 30 min, 2, 3, and 6 h. β-actin serves as a normalization control. The negative control (−) contained no cDNA. These data are representative of three separate experiments. (**b**) Quantitation of IFI 6–16 mRNA expression in early passage HMEC-E6 cells and HMEC-LX vector controls treated with 1.0 μM Tam. Expression is normalized to β-actin. These data are the average of three separate determinations (*P-value <0.01). (**c**) ChIP was performed to test for STAT1, CBP, and IRF-1 recruitment to the *IFI 6–16* ISRE promoter element as a function of Tam treatment. Early passage acutely damaged HMEC-E6 cells (passage 11) were treated with 1.0 μM Tam for 0, 30 min, 2, and 6 h as described in Materials and methods. Input controls tested the integrity of the DNA samples. These data represent three separate experiments. (**d**) Baseline phosphorylation of STAT1 in early passage HMEC-E6 cells (passage 11). Membrane was incubated with antibodies specific for STAT1-phosphoserine-727 (STAT1-pSer727) and STAT1 (total STAT1). β-actin serves as a loading control

induced by treatment of acutely damaged HMEC-E6 cells with 1.0 μM Tam for 6 h. Semiquantitative RT–PCR was performed to determine the kinetics of IFI 6–16 mRNA induction. IFI 6–16 mRNA was induced by 1.0 μM Tam in acutely damaged HMEC-E6 cells but not in HMEC-LX controls (Figure 4). Induction of IFI 6–16 mRNA was (1) first observed in HMEC-E6 cells by 2 h, (2) statistically significant by 3 h (2.2-fold), and (3) maximally induced at 6 h (3.1-fold) (Figure 4a). These observations demonstrate that Tam induces IFI 6–16 mRNA in acutely damaged HMEC-E6 cells starting at 3 h.

Tam promotes recruitment of IRF-1, STAT1, and CBP to the IFI 6–16 *promoter IFN-stimulated response element (ISRE) element*

IRF-1 has been shown to complex with STAT1 and to induce ISG expression through binding to the ICS2/GAS element (Chatterjee-Kishore *et al*., 1998). In addition, IRF-1 has been shown to directly bind to the ISRE within the *IFI 6–16* promoter and induce transcription (Parrington *et al*., 1993). We observe induction of IFI 6–16 mRNA in HMEC-E6 cells by 3 h after treatment with 1.0 μM Tam. ChIP was performed to test whether recruitment of IRF-1, STAT1, and the coactivator CBP to the ISRE element of the *IFI 6–16* promoter temporally correlated with IFI 6–16 mRNA induction. We observed that IRF-1, STAT1, and CBP are simultaneously recruited to the ISRE element of the *IFI 6–16* promoter in acutely damaged HMEC-E6 cells after 2 h treatment with 1.0 μM Tam (Figure 4c). These observations demonstrate that Tam treatment of acutely damaged HMEC-E6 cells promotes recruitment of IRF-1, STAT1, and CBP to the *IFI 6–16* promoter at 2 h, followed by induction of IFI 6–16 mRNA by 3 h.

Caspase-1 and -3 are induced by Tam

IRF-1 is thought to mediate apoptosis through activation of caspase-1 (Karlsen *et al*., 2000; Kim *et al*., 2002). Recently, overexpression of IRF-1 in two mouse breast cancer cell lines has also shown to activate caspase-3 (Kim *et al*., 2004). We have previously shown that caspase-3 is activated by 1.0 μM Tam in acutely damaged HMEC-E6 cells starting at 6 h, maximally at 24 h, and precedes the appearance of marginated chromatin (early effector-phase apoptosis), first observed at 12 h (Dietze *et al*., 2001). In contrast, we observed that caspase-3 was not activated by Tam in HMEC-LX controls (Dietze *et al*., 2001).

Here we tested for caspase-1 activation in Tam-treated acutely damaged HMEC-E6 cells and HMEC-LX controls. Our gene chip data showed no increase in caspase-1 mRNA at 6 h, in either the HMEC-LX controls or the HMEC-E6 cells (data not shown). In HMEC-E6 cells, however, caspase-1 was activated by 1.0 μM Tam starting at 3 h (Figure 5a). This activation temporally correlated with maximal IRF-1 mRNA and protein induction observed at 2–3 h (Figure 2). In contrast, caspase-1 was not activated in passage-matched HMEC-LX controls (Figure 5a).

Caspase-1 inhibitor IV blocks Tam-induced apoptosis

HMEC-E6 cells were pretreated with caspase-1 inhibitor IV to test whether caspase-1 activation was required for Tam-induced apoptosis. HMEC-E6 cells treated with 15 nM caspase-1 inhibitor and 1.0 μM Tam for 4 h failed to show a significant increase in caspase-1 activation (Figure 5b). As previously observed, HMEC-E6 cells treated with 1.0 μM Tam showed activation of caspase-3 at 12 h, and underwent apoptosis as demonstrated by Annexin V binding at 18 h (Figure 5c and d) (Dietze

et al., 2001). Pretreatment with 15 nM caspase-1 inhibitor IV 3 h prior to treatment with 1.0 μM Tam for 12 and 18 h inhibited both the induction of caspase-3 activity (Figure 5c) and apoptosis as evidenced by a lack of Annexin V binding (Figure 5d). Caspase-1 inhibitor IV treatment alone did not alter the proliferation rate of HMEC-E6 cells and did not induce apoptosis (Figure 5d and data not shown). These data demonstrate that caspase-1 activation is required for Tam-induced apoptosis in acutely damaged HMEC-E6 cells.

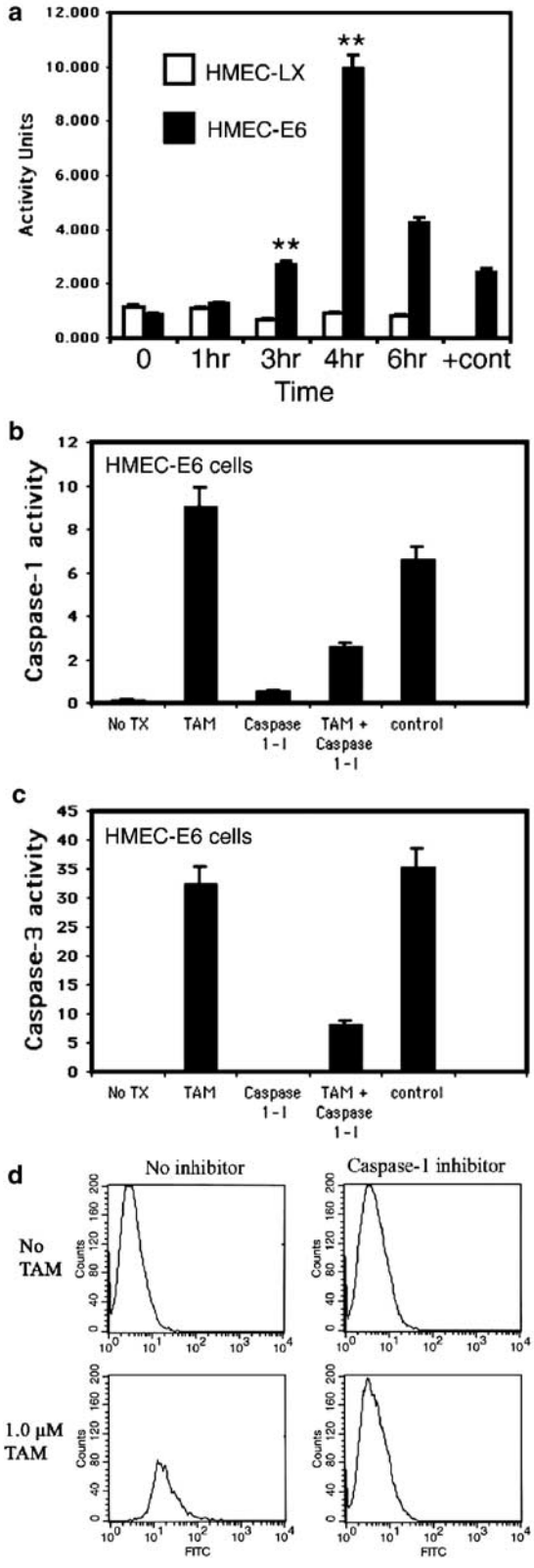

siRNA directed against IRF-1 blocks Tam-induced activation of caspase-1/3 and apoptosis

siRNA was used to test whether suppression of IRF-1 expression blocked Tam-mediated caspase activation and apoptosis in acutely damaged HMEC-E6 cells. Treatment of HMEC-E6 cells with siRNAs IRF-1 #1 and IRF-1 #4 sequences for 12 h resulted in suppression of IRF-1 protein and mRNA (Figure 6a and data not shown). We observed that 1.0 μM Tam activated caspase-1 at 3–4 h (Figure 5a). Suppression of IRF-1 expression in HMEC-E6 cells by IRF-1-specific siRNA blocked Tam-mediated caspase-1 activation at 3 and 4 h (Figure 6b). We previously demonstrated that caspase-3 is activated by 1.0 μM Tam in acutely damaged HMEC-E6 cells starting at 6 h and maximally at 24 h (Dietze *et al*., 2001). Suppression of IRF-1 expression in HMEC-E6 cells by IRF-1-specific siRNA blocked Tam-mediated caspase-3 activation at 12 h (Figure 6c). In previously published data, we showed that 1.0 μM Tam induced apoptosis in acutely damaged HMEC-E6 cells as demonstrated by Annexin V binding at 18 h (Dietze *et al*., 2001). Here we show that two siRNA sequences directed against IRF-1 blocked Tam-mediated apoptosis in HMEC-E6 cells (Figure 6d). These observations demonstrate that IRF-1 expression is required for Tam-induced caspase-1/3 activation and apoptosis in acutely damaged HMEC-E6 cells.

Figure 5 Tam promotes caspase-1 activation in acutely damaged HMEC-E6 cells. (**a**) HMEC-LX vector controls (passage 10) and HMEC-E6 cells (passage 10) were treated with either 1.0 μM Tam or an equivalent volume of solvent for 0–6 h to test for caspase-1 activity. Cells were harvested by trypsinization, washed, and pelleted. The pellets were lysed and assayed according to the manufacturer's instructions. Assays were performed in duplicate. A positive control was provided by THP-1 cells (+cont). These data are the mean of three separate experiments with standard deviation (**P-value <0.025). (**b**) Caspase-1 activation by Tam in acutely damaged HMEC-E6 cells (passage 11) is blocked by pretreatment with 15 nM caspase-1 inhibitor IV for 4 h. HMEC-E6 cells were treated with either 1.0 μM Tam (TAM) or an equivalent volume of solvent for 4 h. Caspase-1 activity was assayed as above. A positive control was provided by THP-1 cells. These data are the mean of three separate experiments performed in duplicate. (**c**) Caspase-3 activation by Tam in acutely damaged HMEC-E6 cells (passage 11) is blocked by pretreatment with 15 nM caspase-1 inhibitor IV for 3 h. HMEC-E6 cells were treated with either 1.0 μM Tam (TAM) or an equivalent volume of solvent. Caspase-3 activity was assayed as described in Materials and methods. These data are the mean of three separate experiments performed in duplicate. (**d**) Pretreatment with 15 nM caspase-1 inhibitor IV for 3 h blocks Tam-induced apoptosis in acutely damaged HMEC-E6 cells (passage 11). Cells were treated with or without 1.0 μM Tam and harvested after an 18 h treatment. Control cells received an equivalent volume of solvent. Detection of apoptotic cells was preformed with FITC-conjugated Annexin V as described in Materials and methods. These data are representative of three experiments

Discussion

While IFN signaling is important for eliminating cells that are damaged by viral infection, evidence suggests that IFN signaling, through STAT1, IRF-1, and other ISGs, may play a more comprehensive role in mammary gland homeostasis and response to DNA damage. Recently, a similar subset of IFN-regulated genes was induced by overexpression of BRCA1, in the absence of further IFN production (Andrews *et al*., 2002). This observation suggests that the loss of BRCA1 may facilitate the disruption of the IFN response. IFN-regulatory proteins such as IRF-1, STAT1, and ISG12 are dysregulated during breast carcinogenesis (Rasmussen *et al*., 1993; Watson and Miller, 1995; Doherty *et al*., 2001) and IFN exhibits cross-talk with estrogen and retinoid signaling (Kolla *et al*., 1996; Widschwendter *et al*., 1996; Bjornstrom and Sjoberg, 2002).

Here we report a novel role for the ISG, IRF-1, in regulating Tam-mediated apoptosis in acutely damaged HMEC-E6 cells. This finding is not completely unexpected. Recent reports have highlighted the ability of IRF-1 to mediate growth arrest and apoptosis in breast cancer cell lines (Kim *et al*., 2002, 2004; Hoshiya *et al*., 2003). In addition, evidence suggests that IRF-1 plays a role in mammary homeostasis, as IRF-1 is critical for mammary gland involution and loss of expression of IRF-1 is an early event in mammary carcinogenesis (Doherty *et al*., 2001). In this study, IRF-1 expression was induced by 60 min treatment with 1.0 μM Tam (Figure 2). IRF-1 was induced by Tam in acutely damaged HMEC-E6 cells 1–3 h prior to subsequent ISG induction, 9 h prior to caspase-3 induction, and 21 h prior to late effector-phase apoptosis (detection of apoptotic bodies) (Figure 2 and data not shown). Suppression of IRF-1 expression by siRNA sequences blocked the induction of apoptosis by Tam (Figure 6).

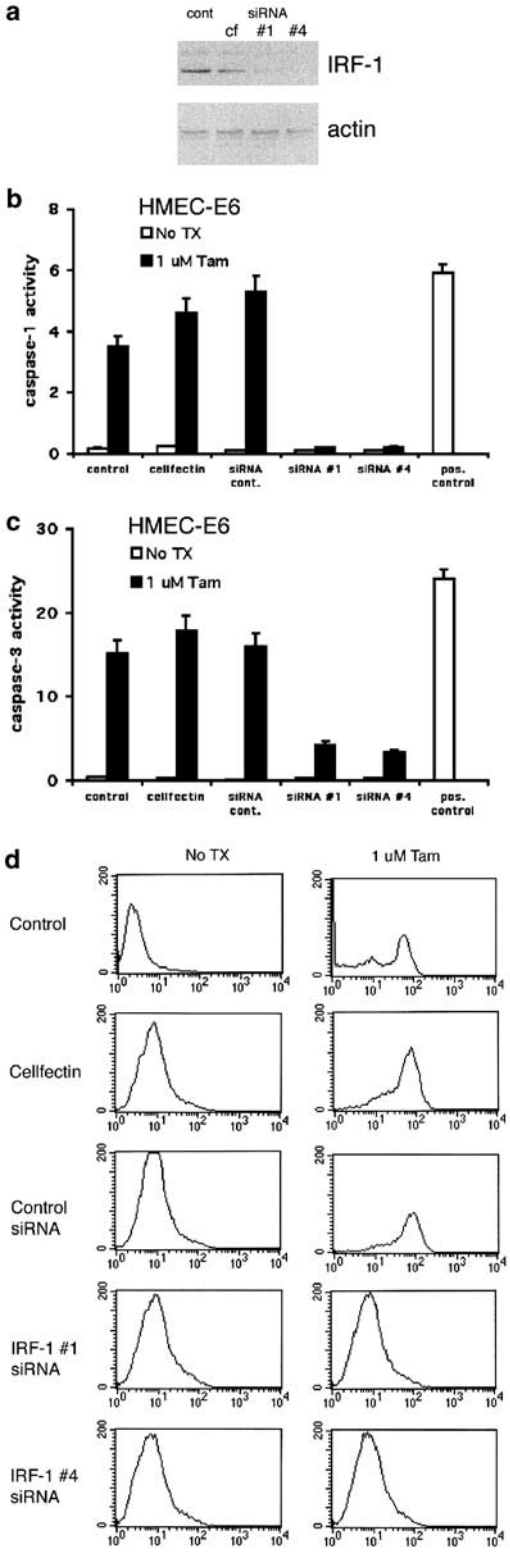

Figure 6 Inhibition of IRF-1 expression blocks Tam-induced caspase-1/3 activation and apoptosis in acutely damaged HMEC-E6 cells. (**a**) Suppression levels of IRF-1 protein expression in early passage HMEC-E6 cells (passage 11) treated with siRNA #1, siRNA #4, and Cellfectin™ for 12 h. Equal amounts of protein lysate were loaded in each lane. β-actin serves as a loading control. (**b**) siRNA directed against IRF-1 blocks Tam-mediated caspase-1 activation in acutely damaged HMEC-E6 cells (passage 11). Cells were treated with 1.0 μM Tam (Tam) or an equivalent volume of solvent (No TX) for 4 h. Caspase-1 activity was assayed as described in Materials and methods. A positive control was provided by THP-1 cells (pos. control). These data are the mean of three experiments performed in duplicate. (**c**) siRNA directed against IRF-1 blocks Tam-mediated caspase-3 activation in acutely damaged HMEC-E6 cells (passage 11). Cells were treated with 1.0 μM Tam (Tam) or an equivalent volume of solvent (No TX) for 12 h. Caspase-3 activity was assayed as per manufacturer's instructions using the caspase-3 assay kit (Clontech, Palo Alto, CA, USA). A positive control was provided by THP-1 cells (pos. control). These data are the mean of three experiments performed in duplicate. (**d**) siRNA directed against IRF-1 blocks Tam-induced apoptosis in acutely damaged HMEC-E6 cells (passage 11). Cells were treated with 1.0 μM Tam (Tam) or an equivalent volume of solvent (No TX) for 18 h. Detection of apoptotic cells was performed with FITC-conjugated Annexin V as described in Materials and methods. These data are representative of three experiments. In each experiment HMEC-E6 cells were pretreated with Cellfectin™, control siRNA, siRNA #1 or siRNA #4 for 12 h, and then treated with either 1.0 μM Tam (Tam) or an equivalent volume of solvent (No TX) for the time indicated. Control cells (Control) were not exposed to either siRNA or Cellfectin™. Cellfectin™ controls (Cellfectin) were exposed to Cellfectin™ alone

Taken together these results suggest a critical role for IRF-1 expression in mediating Tam-induced apoptosis in acutely damaged HMEC-E6 cells.

Recently, an IFN-inducible GAS element has been identified in the *IRF-1* promoter (Sims *et al*., 1993; Harada *et al*., 1994). STAT1 homodimers bind to this GAS element and induce transcription. At a similar IFN response element, called γRE element, a STAT1 dimer binds and recruits CBP to the promoter complex (Hiroi and Ohmori, 2003). STAT1 has been shown to interact with CBP through both the CREB-binding domain and CH3 domain (Zhang *et al*., 1996). IRF-1 in turn has been reported to complex with STAT1 to induce ISG expression by binding to the ICS2/GAS element (Chatterjee-Kishore *et al*., 1998). Based on these observations we hypothesized that (1) STAT1 and CBP may play a role in IRF-1 induction and (2) IRF-1/STAT1/CBP, in turn, may cooperatively promote induction of further ISGs.

ChIP and immunoprecipitation experiments demonstrated that STAT1 was constitutively bound to the GAS element of the *IRF-1* promoter in HMEC-E6 cells (Figure 3). In contrast, CBP was not associated with the *IRF-1* GAS element at baseline. ChIP and immunoprecipitation experiments demonstrated that CBP was recruited to the GAS element of the *IRF-1* promoter by 30 min after Tam treatment (Figure 3). Neither STAT1 nor CBP were associated at baseline or recruited to the *IRF-1* GAS element in HMEC-LX vector control cells. Based on these observations, we hypothesize that CBP recruitment to the *IRF-1* GAS element may be the crucial step in upregulation of IRF-1 mRNA following Tam treatment.

Induction of IRF-1 was closely followed by induction of a small set of ISGs (Table 1). IRF-1 has previously been shown to participate in the induction of the ISG, IFI 6–16, through recruitment of IRF-1 to the *IFI 6–16* promoter ISRE sequence (Parrington *et al*., 1993). Here we report that induction of IFI 6–16 mRNA temporally correlated with recruitment of STAT1, IRF-1, and CBP to the ISRE of the *IFI 6–16* promoter region (Figure 4). Tam induced IFI 6–16 mRNA expression at 3 h in acutely damaged HMEC-E6 cells but not in HMEC-LX controls (Table 1, Figures 1 and 4). ChIP analysis of untreated HMEC-E6 cells showed that IRF-1, STAT1, and CBP were not bound to the *IFI 6–16* ISRE at baseline (Figure 4c). However, when acutely damaged HMEC-E6 cells were treated with 1.0 μM Tam for 2 h, IRF-1, CBP, and STAT1 were recruited to the ISRE sequence in the *IFI 6–16* promoter (Figure 4) and this recruitment was followed by the induction of IFI 6–16 mRNA at 3 h. These observations demonstrate a potential role for Tam (1) in promoting IRF-1 recruitment to the *IFI 6–16* promoter and (2) perhaps in promoting IFI 6–16 mRNA expression. Work is ongoing in our laboratory to define (1) the requirement for IRF-1/STAT1/CBP in modulating IFI 6–16 expression and (2) whether IFI 6–16 directly participates in Tam-induced apoptosis in acutely damaged HMEC-E6 cells or whether it serves only as a marker of IRF-1 induction.

Caspase-1 and -3 have previously been shown to participate in IRF-1-mediated apoptosis (Kim *et al*., 2002, 2004). IRF-1 has been shown to be critical for caspase-1 mRNA induction from cytokine treatment (Karlsen *et al*., 2000). While caspase-3 is clearly an effector caspase, the role of caspase-1 in promoting effector-phase apoptosis is controversial. Caspase-1/ICE is traditionally considered an initiator caspase, well known for its inflammatory actions in activating both IL-1β and IL-18 cytokines (Creagh *et al*., 2003). Some earlier studies, however, suggest that it is also involved in apoptosis (Miura *et al*., 1993; Wang *et al*., 1994). There have also been several reports of sequential activation of caspase-1 and -3 (Kamada *et al*., 1997; Dai and Krantz, 1999; Pasinelli *et al*., 2000; Aiba-Masago *et al*., 2001; Zhang *et al*., 2003; Jiang *et al*., 2004). While the phenotype of the caspase-1 knockout mouse did not show major dysregulation of apoptosis, ICE(−/−) thymocytes were resistant to Fas-mediated apoptosis (Kuida *et al*., 1995). More recently, studies with IFN-γ have shown that caspase-1 is induced and activated in cells sensitive to apoptosis (Detjen *et al*., 2001, 2002; Kim *et al*., 2002).

Here we observed that caspase-1/3 are activated by Tam in acutely damaged HMEC-E6 cells by 3 and 12 h (Figure 5, Dietze *et al*., 2001), respectively, in the absence of IFN secretion (data not shown). Microarray analysis for both HMEC-LX and HMEC-E6 cells showed no induction of caspase-1 mRNA at 6 h (data not shown), however, caspase-1 was activated 2 h after the observed increase in IRF-1 protein levels (Figure 5a). Inhibition of caspase-1 activity with 15 nM caspase-1 inhibitor IV blocked Tam-induced (1) activation of caspase-1 and -3 and (2) effector-phase apoptosis (Figure 5). siRNA directed against IRF-1 also blocked Tam-mediated activation of caspase-1/3 and apoptosis (Figure 6). Taken together these data indicate that Tam-induced apoptosis in acutely damaged HMEC-E6 cells requires both induction of IRF-1 and a subsequent increase in caspase-1 activity.

We have previously shown that caspase-9 was induced by Tam treatment of HMEC-E6 cells (Dietze *et al*., 2001, 2004). Caspase-9 induction occurred within 1 h of Tam treatment and returned to baseline by 12 h after Tam treatment (Dietze *et al*., 2001). Caspase-9 has not been shown to process procaspase-1. Thus it is unlikely that caspase-9 is involved in the observed activation of caspase-1. Also, IRF-1(−/−) cells were still able to induce caspase-9 activity (Oda *et al*., 2000). Taken together with the kinetics of IFI 6–16 induction (Figure 4), it is unlikely that IRF-1 participates in caspase-9 activation. The exact relationship of caspase-9, -1, and -3 to each other and to the execution phase of apoptosis is under study in our laboratory.

In previously published studies, we have recently shown that Tam treatment of acutely damaged HMEC-E6 cells results in rapid loss of AKT Ser-473 phosphorylation and activity (Dietze *et al*., 2004). In this report we demonstrate that (1) Tam promotes recruitment of CBP to the GAS element of the *IRF-1* promoter and (2) this recruitment is temporally associated with induction

of IRF-1. It is known that CBP and its related coactivator, p300, are present in limiting amounts. The current paradigm of CBP/p300 action suggests that CBP/p300 activity is mediated by competition of various promoter elements for limited quantities of CBP/p300. However, recent studies suggest that the activity of CBP may also be controlled by phosphorylation, although correlation between specific sites of phosphorylation and alteration of function has been rare (Kovacs *et al*., 2003). Given our recent observations regarding (1) the role of AKT in regulating Tam-induced apoptosis and (2) Tam-modulated CBP recruitment to the *IRF-1* GAS element, we are currently investigating the potential role of AKT in promoting CBP recruitment and IRF-1 induction. AKT has been shown to phosphorylate the CBP analog p300 in the CH3 domain and block the transcriptional activity of C/EBPβ, which binds that domain (Guo *et al*., 2001). We are currently investigating the possibility that AKT functions in a similar fashion to promote CBP binding to the STAT1-bound *IRF-1* GAS element and thereby promote IRF-1 transcription in acutely damaged HMEC-E6 cells.

Materials and methods

Materials

All chemicals and cell culture reagents were obtained from Sigma-Aldrich (St Louis, MO, USA), DNA primers from Invitrogen (Carlsbad, CA, USA) or Qiagen Operon (Alameda, CA, USA), and cell culture plasticware from Corning (Corning, NY, USA) unless otherwise noted. A 1.0 mM stock solution of Tam was prepared in 100% ethanol and stored in opaque tubes at -70°C. Control cultures received equivalent volumes of the ethanol solvent. Stocks were used under reduced light. Caspase-1 inhibitor IV was obtained from EMD Biosciences Inc. (San Diego, CA, USA). IFN-γ was obtained from R&D Systems (Minneapolis, MN, USA), reconstituted to a 10 μg/ml stock with 1 × PBS (0.1% BSA), and stored at -70°C.

Cell culture and media

Normal HMEC strain AG11132 (M Stampfer #172R/AA7) was purchased from the National Institute of Aging, Cell Culture Repository (Coriell Institute, Camden, NJ, USA; Stampfer, 1985). HMEC strain AG11132 was established from normal tissue obtained at reduction mammoplasty, has a limited life span in culture, and fails to divide after approximately 20–25 passages. HMECs exhibit a low level of ER staining characteristic of normal mammary epithelial cells. HMECs were grown in mammary epithelial cell basal medium (Clonetics, San Diego, CA, USA) supplemented with 4 μl/ml bovine pituitary extract (Clonetics #CC4009), 5 μg/ml insulin (UBI, Lake Placid, NY, USA), 10 ng/ml epidermal growth factor (UBI), 0.5 μg/ml hydrocortisone, 10^{-5} M isoproterenol, and 10 mM HEPES buffer (Standard Media). G418 containing Standard Media was prepared by the addition of 300 μg/ml of G418 (Gibco, Grand Island, NY, USA) to Standard Media. Cells were cultured at 37°C in a humidified incubator with 5% CO_2/95% air. Mycoplasma testing was performed as previously reported (Seewaldt *et al*., 1997a).

Retroviral transduction

The LXSN16E6 retroviral vector containing the HPV-16 E6 coding sequence was provided by D Galloway (Fred Hutchinson Cancer Research Center, Seattle, WA, USA) (Demers *et al*., 1996). HMECs (passage 9) were plated in four T-75 tissue culture flasks in standard medium and grown to 50% confluency. Transducing virions from either the PA317-LXSN16E6 or the control PA317-LXSN (without insert) retroviral producer line were added at a multiplicity of infection at 1 : 1 in the presence of 4 μg/ml polybrene to log-phase cells grown in T-75 flasks. The two remaining T-75 flasks were not infected with virus. After 48 h two flasks containing transduced cells and one flask with untransduced cells were passaged 1 : 3 (passage 10) and selected with standard media containing 300 μg/ml G418. Cells were grown in G418 containing standard media for 4–7 days, until 100% of control untransduced cells were dead. The transduction efficiency was high during selection, cells were passaged 1 : 3 at the completion of selection (passage 11), and cells were maintained in the absence of selection before immediately proceeding to apoptosis experiments. The fourth flask of unselected, untransduced parental control cells was passaged in parallel with the selected, transduced experimental and vector control cells. Parental AG11132 cells were designated HMEC-P. Transduced AG11132 cells expressing the HPV-16 E6 construct were designated HMEC-E6 and vector control clones were designated HMEC-LX. All cells were maintained in standard media after transfection in the absence of G418 selection to ensure that any observed chromosomal abnormalities or apoptosis resistance was not due to continued exposure to G418. All experiments were performed on mass cultures.

Differential gene expression studies

Total RNA isolation was as previously described (Seewaldt *et al*., 1995). RNA integrity was confirmed by electrophoresis, and samples were stored at -70°C until used. All RNA combinations used for array analysis were obtained from cells that were matched for passage number, cultured under the identical growth conditions, and harvested at identical confluency. cDNA synthesis and probe generation for cDNA array hybridization were obtained by following the standardized protocols provided by Affymetrix (Affymetrix, Santa Clara, CA, USA).

Expression data for approximately 5600 full-length human genes were collected using Affymetrix GeneChip HuGeneFL™ arrays, and following the standardized protocols provided by the manufacturer. Data were collected in triplicate using independent biological replicates. Array images were processed using Affymetrix™ MAS 5.0 software, where we filtered for probe saturation, employed a global array scaling target intensity of 1000, and collected the signal intensity value (i.e., the 'average difference') for each gene. Pairwise 'treatment *vs* control' comparisons were made employing CyberT (Baldi and Long, 2001), a Bayesian *t*-statistic algorithm derived for microarray analysis. We employed a window size of 101 and used a confidence value of 10 in our CyberT analysis. Significant changes in expression were determined by ranking the assigned Bayesian *P*-values and applying a false discovery rate correction (FDR = 0.05) to account for multiple testing (Benjamini and Hochberg, 1995).

Semiquantitative RT–PCR

To confirm the microarray data, relative transcript levels were analysed by semiquantitative RT–PCR. Total RNA (5 μg) was

used in first-strand cDNA synthesis with Superscript™ II reverse transcriptase (Invitrogen). PCR reaction conditions were optimized for each gene product to determine the PCR cycle number of linear amplification for each primer set. The primer sets, cycling conditions, and cycle numbers used are indicated in Table 2. All PCR reactions were in 50 μl total volume. For ISG15, IFI56, and IFI 9–27, a reaction was set up containing 100 nM of each primer, 1.0 mM dNTPs, 10 mM Tris-HCl (pH 8.3), 1.5 mM $MgCl_2$, 50 mM KCl, 2.5 U Taq polymerase (Roche Applied Science, Indianapolis, IN, USA), and 2.0 μl cDNA. IFI 6–16 was amplified with 100 nM of each primer, 1.0 mM dNTPs, 1 × expand high fidelity buffer ($MgCl_2$) (Roche Applied Science), 0.5 mM $MgCl_2$, 10% DMSO, 2.0 U Taq polymerase, and 4.0 μl cDNA. Amplification of ISG12 was carried out with 100 nM of each primer, 1.0 mM dNTPs, 10 mM Tris-HCl (pH 8.3), 1.5 mM $MgCl_2$, 50 mM KCl, 2.0 U Taq polymerase, and 4.0 μl cDNA. IRF-1 cDNA was amplified with 200 nM of each primer, 1.0 mM dNTPs, 20 mM Tris-HCl (pH 8.4), 50 mM KCl, 1.0 mM $MgCl_2$, 2.5 U Taq polymerase, and 2.0 μl cDNA. Reaction conditions for β-actin were 300 nM of each primer (sequences obtained from Invitrogen), 1.0 mM dNTPs, 10 mM Tris-HCl (pH 8.3), 1.5 mM $MgCl_2$, 50 mM KCl, 2.5 U Taq polymerase, and 2.0 μl cDNA. Products were amplified with GeneAmp PCR Systems 2400 and 9700 (Applied Biosystems, Foster City, CA, USA). In all, 10 μl of PCR product was analysed by electrophoresis in 1.2–1.5% agarose (Invitrogen) gels containing ethidium bromide and visualized under UV light. All samples were performed in triplicate and normalized to β-actin control. Band quantitation was done using Kodak 1D™ Image Analysis Software (Eastman Kodak, Rochester, NY, USA).

ChIP assay

ChIP was performed by published methods with some modifications (Yahata *et al*., 2001). Preliminary experiments were run to determine optimal sonication and formaldehyde cross-linking time. Once optimized, cells were harvested, pelleted, and treated with 1% formaldehyde for 15 min to cross-link cellular proteins. Cells were then rinsed twice in ice cold PBS containing protease inhibitors, pelleted, and resuspended in Lysis Buffer (1% SDS, 10 mM EDTA, 50 mM Tris-HCl at pH 8.1, 1 × protease inhibitor cocktail (4 μg/ml epibestatin hydrochloride, 2 μg/ml calpain inhibitor II, 2 μg/ml pepstatin A, 4 μg/ml mastoparan, 4 μg/ml leupeptin hydrochloride, 4 μg/ml aprotinin, 1 mM TPCK, 1 mM phenymethylsulfonyl fluoride, and 100 μM TLCK)). Samples were then sonicated 3 × 15 s each with a 1 min incubation on ice in between pulses on a Branson sonifier model 250 at 50% duty and maximum mini probe power. A 20 μl aliquot of lysate was saved and used to determine the input DNA for each sample. Supernatants were diluted (1 : 10) in dilution buffer(1% Triton X-100, 2 mM EDTA, 150 mM NaCl, 20 mM Tris-HCl at pH 8.1, 1 × protease inhibitor cocktail), and precleared with 2 μg of sheared salmon sperm DNA (Gibco), 20 μl normal human serum, and 45 μl of protein A-sepharose (50% slurry in 10 mM Tris-HCl at pH 8.1, 1.0 mM EDTA). To precleared chromatin, 10 μl of either anti-CBP (A22,

Table 2 ISG primers

Gene name	*Primer set*	*Cycle conditions*	*PCR cycle number*
ISG15	F: 5′-AGTACAGGAGCTTGTGCCGT-3′	94°C, 2 min	
	R: 5′-GAAGGTCAGCCAGAACAGGT-3′	94°C, 30 s	
		58°C, 30 s	22
		72°C, 1 min	
		72°C, 7 min	
ISG12	F: 5′-GAATTAACCCGAGCAGGCAT-3′	94°C, 2 min	
	R: 5′-CTCTGGAGATGCAGAATTTGG-3′	94°C, 30 s	
		58°C, 30 s	27
		72°C, 1 min	
		72°C, 7 min	
IFI-56	F: 5′-GGTCAAGGATAGTCTGGAGCA-3′	94°C, 2 min	
	R: 5′-AGTGGCTGATATCTGGGTGC-3′	94°C, 30 s	
		58°C, 30 s	23
		72°C, 2 min	
		72°C, 7 min	
IFI 9-27	F: 5′-GAAACTGAAACGACAGGGGA-3′	94°C, 2 min	
	R: 5′-TGTATCTAGGGGCAGGACCA-3′	94°C, 30 s	
		58°C, 30 s	24
		72°C, 1 min	
		72°C, 7 min	
IFI 6-16	F: 5′-CAAGGTCTAGTGACGGAGCC-3′	94°C, 2 min	
	R: 5′-CTGCTGGCTACTCCTCATCC-3′	94°C, 30 s	
		58°C, 30 s	25
		72°C, 1 min	
		72°C, 7 min	
IRF-1	F: 5′-ACCCTGGCTAGAGATGCAGA-3′	94°C, 5 min	
	R: 5′-TTTTCCCCTGCTTGTATCG-3′	94°C, 30 s	
		51°C, 30 s	28
		72°C, 45 s	
		72°C, 7 min	
β-actin	F: 5′-GCTCGTCGTCGACAACGGCTC-3′	94°C, 2 min	
	R: 5′-AAACATGATCTGGGTCATCTTCTC-3′	94°C, 15 s	
		55°C, 30 s	18
		72°C, 30 s	
		72°C, 7 min	

Santa Cruz Biotechnology, Santa Cruz, CA, USA), anti-STAT1 (E23, Santa Cruz Biotechnology), or anti-IRF-1 (H205, Santa Cruz Biotechnology) was added, and the reaction was incubated overnight, followed by an addition of 45 μl of protein A-sepharose and 2.0 μg sheared salmon sperm and an additional 1 h incubation. Sepharose beads were then collected and washed sequentially for 10 min each in TSE I (0.1% SDS, 1% Triton X-100, 2 mM EDTA, 20 mM Tris-HCl at pH 8.1, 150 mM NaCl), TSE II (0.1% SDS, 1% Triton X-100, 2 mM EDTA, 20 mM Tris-HCl at pH 8.1, 500 mM NaCl), and buffer III (0.25 M LiCl, 1% NP-40, 1% deoxycholate, 1 mM EDTA, 10 mM Tris-HCl at pH 8.1). Beads were washed once with TE buffer and DNA eluted with 100 μl of 1% SDS–0.1 M $NaHCO_3$. Eluate was heated at 65°C overnight to reverse the formaldehyde cross-linking. DNA fragments were cleaned-up with the QIAquick PCR purification kit (Qiagen, Valencia, CA, USA) and amplified in a PCR reaction. Primers for the *IRF-1* and *IFI 6–16* promoters were (1) IRF-1 forward 5′-GTA CTT CCC CTT CGC CG-3′ and IRF-1 reverse 5′-GCG TAC TCA CCT CTG CTG C-3′ and (2) IFI 6–16 forward 5′-ATA CCC TTA GCG GCT CCA AA-3′ and IFI 6–16 reverse 5′-GCT GAA GGC TGG CTT TTT ATC-3′. In all, 30 μl of PCR product was analysed by electrophoresis in 1.5% agarose gels containing ethidium bromide and visualized under UV light using Kodak 1D™ Image Analysis Software. All reactions were performed in triplicate.

Western blotting

Preparation of cellular lysates and immunoblotting were performed as previously described (Seewaldt *et al*., 1997b, 1999b). For IRF-1 expression, the membrane was incubated with a 1 : 100 dilution of mouse anti-human IRF-1 (C-20, Santa Cruz Biotechnology). For CBP expression, the blocked membrane was incubated with a 1 : 200 dilution of the CBP antibody (C-20, Santa Cruz Biotechnology). For STAT1 expression the membrane was incubated with a 1 : 100 dilution of antibody to STAT1 (E-23, Santa Cruz Biotechnology). For STAT1 phosphoserine-727 detection the membrane was incubated with a 1 : 400 dilution of the Phospho-STAT1-Ser727 antibody (Cell Signaling Technology, Beverly, MA, USA). Loading control was provided by a 1 : 200 dilution of antibody to β-actin (I-19, Santa Cruz Biotechnology). The resulting film images were digitized and quantitated using Kodak 1D™ Image Analysis Software.

Suppression of IRF-1 with siRNA

Two double-stranded siRNA oligos were designed using Ambion Inc. software (Austin, TX, USA). Oligos were synthesized and annealed by Qiagen. IRF-1 #1 targets sequence: 5′-AAC TTT CGC TGT GCC ATG AAC-3′, and IRF-1 #4 targets sequence: 5′-AAG TGT GAG CGC CTT GGT ATG-3′. Control nonsilencing siRNA was provided by Qiagen. Early passage HMEC-E6 cells were transfected with IRF-1 #1 and #4 siRNAs (167–600 nM) and Cellfectin™ (Invitrogen). At 12 h after transfection, RNA was harvested using the Aurum™ Total RNA kit (Bio-Rad Laboratories, Hercules, CA, USA) and protein was harvested as previously described (Seewaldt *et al*., 1997b, 1999a). Western analysis (as described above) and RT–PCR were performed to confirm suppression of IRF-1 expression. cDNA was prepared for RT–PCR from 50 ng total RNA with Superscript™ II reverse transcriptase (Invitrogen). β-actin PCR reaction conditions were performed as described above except product was amplified for 24 cycles. IRF-1 amplification was reoptimized for lower input. The changes made to the reaction were as follows: (1) HotStarTaq™ polymerase (Qiagen) was used, (2) annealing temperature was increased to 57°C, and (3) amplification was carried out for 38 cycles. In all, 25 μl of PCR product was ran on either 2.0% or 1.2% agarose gels stained with ethidium bromide and visualized with Kodak 1D™ Image Analysis Software.

ELISA

Aliquots of tissue culture media were withdrawn from flasks at 0, 30 min, 1, 2, and 4 h and stored at −70°C. Manufacturer protocols for the commercial IFN-α, -β (Biosource International, Camarillo, CA, USA), and IFN-γ (BD Biosciences Pharmingen, San Diego, CA, USA) ELISA kits were followed. Duplicate standard curves were run on each plate, and media samples were assayed in triplicate.

IRF-1 *promoter immunoprecipitation*

HMEC-E6 cells and HMEC-LX controls were treated with 1.0 μM Tam and harvested at 0, 30, and 60 min. Preparation of cellular lysates and immunoblotting were performed as previously described (Seewaldt *et al*., 1997b, 1999b). A 25 bp section of the *IRF-1* promoter region, encompassing the GAS element (−134 to −109 bp upstream), was used to design biotin-labeled oligos. The complimentary oligos (Qiagen) were annealed in equal molar concentrations, heated to 95°C for 5 min, and allowed to cool to room temperature. Then 890 μg of total protein lysate was precleared with Strepavidin beads. The supernatant was subsequently incubated with *IRF-1* GAS-annealed oligos and Strepavidin beads for 2 h at 4°C. The beads were washed 3× with lysis buffer with protease inhibitors, boiled, and ran on an SDS–PAGE gel. Antibodies to CBP (C-20, Santa Cruz Biotechnology) and STAT1 (E-23, Santa Cruz Biotechnology) were used to detect bound protein.

Measurement of apoptosis and caspase-1/3 activity

Apoptosis was measured by Annexin V binding and FACS after treatment with 1.0 μM Tam for 18 h as previously described (Seewaldt *et al*., 1999a; Dietze *et al*., 2001). Caspase-1/3 assays were performed as follows: cells were harvested by trypsinization, washed once with 100 volumes of ice cold PBS, and pelleted. Caspase-1 and -3 activities were then assayed according to the manufacturer's instructions using a caspase-1 (EMD Biosciences Inc.) or caspase-3 (Clontech, Palo Alto, CA, USA) assay kit. For IRF-1 suppression studies, early passage HMEC-E6 cells were transfected with IRF-1 siRNAs 12 h prior to treatment with 1.0 μM Tam. Caspase-1 and -3 levels were measured at 4 and 18 h, respectively, after Tam treatment.

Acknowledgements
This work is supported by NIH/NCI grants 2P30CA14236–26 (VLS, ECD), R01CA88799 (VLS), R01CA984441 (VLS), NIH/NIDDK grant 2P30DK 35816-11 (VLS), DAMD-98-1-851 and DAMD-010919 (VLS), American Cancer Society Award CCE-99898 (VLS), a V-Foundation Award (VLS), a Susan G Komen Breast Cancer Award (VLS, ECD), and a Charlotte Geyer Award (VLS). The authors gratefully acknowledge Martha Stamfer's gift of normal human mammary epithelial cells and D Galloway for the LXSN16E6 retroviral vector containing the HPV-16E6 coding sequence.

References

Aiba-Masago S, Masago R, Vela-Roch N, Talal N and Dang H. (2001). *Cell Signal.*, **13,** 617–624.

Anderson E, Clarke RB and Howell A. (1998). *J. Mamm. Gland Biol. Neoplasia*, **3,** 23–35.

Andrews HN, Mullan PB, McWilliams S, Sebelova S, Quinn JE, Gilmore PM, McCabe N, Pace A, Koller B, Johnston PG, Haber DA and Harkin DP. (2002). *J. Biol. Chem.*, **277,** 26225–26232.

Aubele MM, Cummings MC, Mattis AE, Zitzelsberger HF, Walch AK, Kremer M, Hofler H and Werner M. (2000). *Diagn. Mol. Pathol.*, **9,** 14–19.

Baldi P and Long AD. (2001). *Bioinformatics*, **17,** 509–519.

Benjamini Y and Hochberg Y. (1995). *J. R. Stat. Soc. Ser. B – Methodological*, **57,** 289–300.

Bjornstrom L and Sjoberg M. (2002). *Mol. Endocrinol.*, **16,** 2202–2214.

Chatterjee-Kishore M, Kishore R, Hicklin DJ, Marincola FM and Ferrone S. (1998). *J. Biol. Chem.*, **273,** 16177–16183.

Chawla-Sarkar M, Lindner DJ, Liu YF, Williams BR, Sen GC, Silverman RH and Borden EC. (2003). *Apoptosis*, **8,** 237–249.

Coradini D, Biffi A, Pellizzaro C, Pirronello E and Di Fronzo G. (1997). *Tumor Biol.*, **18,** 22–29.

Creagh EM, Conroy H and Martin SJ. (2003). *Immunol. Rev.*, **193,** 10–21.

Dai C and Krantz SB. (1999). *Blood*, **93,** 3309–3316.

Darnell Jr JE, Kerr IM and Stark GR. (1994). *Science*, **264,** 1415–1421.

de Veer MJ, Holko M, Frevel M, Walker E, Der S, Paranjape JM, Silverman RH and Williams BR. (2001). *J. Leukoc. Biol.*, **69,** 912–920.

Demers GW, Espling E, Harry JB, Etscheid BG and Galloway DA. (1996). *J. Virol.*, **70,** 6862–6869.

Der SD, Zhou A, Williams BR and Silverman RH. (1998). *Proc. Natl. Acad. Sci. USA*, **95,** 15623–15628.

Detjen KM, Farwig K, Welzel M, Wiedenmann B and Rosewicz S. (2001). *Gut*, **49,** 251–262.

Detjen KM, Kehrberger JP, Drost A, Rabien A, Welzel M, Wiedenmann B and Rosewicz S. (2002). *Int. J. Oncol.*, **21,** 1133–1140.

Dietze EC, Caldwell LE, Grupin SL, Mancini M and Seewaldt VL. (2001). *J. Biol. Chem.*, **276,** 5384–5394.

Dietze EC, Troch MM, Bean GR, Heffner JB, Bowie ML, Rosenberg P, Ratliff B and Seewaldt VL. (2004). *Oncogene*, **23,** 3851–3862.

Doherty GM, Boucher L, Sorenson K and Lowney J. (2001). *Ann. Surg.*, **233,** 623–629.

Fisher B, Costantino JP, Wickerham DL, Redmond CK, Kavanah M, Cronin WM, Vogel V, Robidoux A, Dimitrov N, Atkins J, Daly M, Wieand S, Tan-Chiu E, Ford L and Wolmark N. (1998). *J. Natl. Cancer Inst.*, **90,** 1371–1388.

Gibson DF, Johnson DA, Goldstein D, Langan-Fahey SM, Borden EC and Jordan VC. (1993). *Breast Cancer Res. Treat.*, **25,** 141–150.

Giles RH, Dauwerse JG, Higgins C, Petrij F, Wessels JW, Beverstock GC, Dohner H, Jotterand-Bellomo M, Falkenburg JH, Slater RM, van Ommen GJ, Hagemeijer A, van der Reijden BA and Breuning MH. (1997a). *Leukemia*, **11,** 2087–2096.

Giles RH, Petrij F, Dauwerse HG, den Hollander AI, Lushnikova T, van Ommen GJ, Goodman RH, Deaven LL, Doggett NA, Peters DJ and Breuning MH. (1997b). *Genomics*, **42,** 96–114.

Gjermandsen IM, Justesen J and Martensen PM. (2000). *Cytokine*, **12,** 233–238.

Guo S, Cichy SB, He X, Yang Q, Ragland M, Ghosh AK, Johnson PF and Unterman TG. (2001). *J. Biol. Chem.*, **276,** 8516–8523.

Harada H, Takahashi E, Itoh S, Harada K, Hori TA and Taniguchi T. (1994). *Mol. Cell. Biol.*, **14,** 1500–1509.

Henderson YC, Chou M and Deisseroth AB. (1997). *Br. J. Haematol.*, **96,** 566–575.

Hiroi M and Ohmori Y. (2003). *J. Biol. Chem.*, **278,** 651–660.

Horvai AE, Xu L, Korzus E, Brard G, Kalafus D, Mullen TM, Rose DW, Rosenfeld MG and Glass CK. (1997). *Proc. Natl. Acad. Sci. USA*, **94,** 1074–1079.

Horvath CM. (2000). *Trends Biochem. Sci.*, **25,** 496–502.

Hoshiya Y, Gupta V, Kawakubo H, Brachtel E, Carey JL, Sasur L, Scott A, Donahoe PK and Maheswaran S. (2003). *J. Biol. Chem.*, **278,** 51703–51712.

Iacopino F, Robustelli della Cuna G and Sica G. (1997). *Int. J. Cancer*, **71,** 1103–1108.

Jiang B, Liu JH, Bao YM and An LJ. (2004). *Toxicon*, **43,** 53–59.

Kamada S, Washida M, Hasegawa J, Kusano H, Funahashi Y and Tsujimoto Y. (1997). *Oncogene*, **15,** 285–290.

Karlsen AE, Pavlovic D, Nielsen K, Jensen J, Andersen HU, Pociot F, Mandrup-Poulsen T, Eizirik DL and Nerup J. (2000). *J. Clin. Endocrinol. Metab.*, **85,** 830–836.

Kawasaki H, Eckner R, Yao TP, Taira K, Chiu R, Livingston DM and Yokoyama KK. (1998). *Nature*, **393,** 284–289.

Kelly MJ and Levin ER. (2001). *Trends Endocrinol. Metab.*, **12,** 152–156.

Kim EJ, Lee JM, Namkoong SE, Um SJ and Park JS. (2002). *J. Cell. Biochem.*, **85,** 369–380.

Kim PK, Armstrong M, Liu Y, Yan P, Bucher B, Zuckerbraun BS, Gambotto A, Billiar TR and Yim JH. (2004). *Oncogene*, **23,** 1125–1135.

Kolla V, Lindner DJ, Xiao W, Borden EC and Kalvakolanu DV. (1996). *J. Biol. Chem.*, **271,** 10508–10514.

Kovacs KA, Steinmann M, Magistretti PJ, Halfon O and Cardinaux JR. (2003). *J. Biol. Chem.*, **278,** 36959–36965.

Kroger A, Koster M, Schroeder K, Hauser H and Mueller PP. (2002). *J. Interferon Cytokine Res.*, **22,** 5–14.

Kuida K, Lippke JA, Ku G, Harding MW, Livingston DJ, Su MS and Flavell RA. (1995). *Science*, **267,** 2000–2003.

Kumar-Sinha C, Varambally S, Sreekumar A and Chinnaiyan AM. (2002). *J. Biol. Chem.*, **277,** 575–585.

Lindner DJ and Borden EC. (1997). *J. Interferon Cytokine Res.*, **17,** 681–693.

Lindner DJ, Kolla V, Kalvakolanu DV and Borden EC. (1997). *Mol. Cell. Biochem.*, **167,** 169–177.

Lininger RA, Park WS, Man YG, Pham T, MacGrogan G, Zhuang Z and Tavassoli FA. (1998). *Hum. Pathol.*, **29,** 1113–1118.

Mantovani F and Banks L. (2001). *Oncogene*, **20,** 7874–7887.

Merika M, Williams AJ, Chen G, Collins T and Thanos D. (1998). *Mol. Cell*, **1,** 277–287.

Miura M, Zhu H, Rotello R, Hartwieg EA and Yuan J. (1993). *Cell*, **75,** 653–660.

Nozawa H, Oda E, Nakao K, Ishihara M, Ueda S, Yokochi T, Ogasawara K, Nakatsuru Y, Shimizu S, Ohira Y, Hioki K, Aizawa S, Ishikawa T, Katsuki M, Muto T, Taniguchi T and Tanaka N. (1999). *Genes Dev.*, **13,** 1240–1245.

Oda E, Ohki R, Murasawa H, Nemoto J, Shibue T, Yamashita T, Tokino T, Taniguchi T and Tanaka N. (2000). *Science*, **288,** 1053–1058.

Parrington J, Rogers NC, Gewert DR, Pine R, Veals SA, Levy DE, Stark GR and Kerr IM. (1993). *Eur. J. Biochem.*, **214,** 617–626.

Pasinelli P, Houseweart MK, Brown Jr RH and Cleveland DW. (2000). *Proc. Natl. Acad. Sci. USA*, **97,** 13901–13906.
Pestka S, Langer JA, Zoon KC and Samuel CE. (1987). *Annu. Rev. Biochem.*, **56,** 727–777.
Pine R, Canova A and Schindler C. (1994). *EMBO J.*, **16,** 406–416.
Rasmussen UB, Wolf C, Mattei MG, Chenard MP, Bellocq JP, Chambon P, Rio MC and Basset P. (1993). *Cancer Res.*, **53,** 4096–4101.
Robyr D, Wolffe AP and Wahli W. (2000). *Mol. Endocrinol.*, **14,** 329–347.
Romeo G, Fiorucci G, Chiantore MV, Percario ZA, Vannucchi S and Affabris E. (2002). *J. Interferon Cytokine Res.*, **22,** 39–47.
Seewaldt VL, Caldwell LE, Johnson BS, Swisshelm K, Collins SJ and Tsai S. (1997a). *Exp. Cell Res.*, **236,** 16–28.
Seewaldt VL, Dietze EC, Johnson BS, Collins SJ and Parker MB. (1999a). *Cell Growth Differ.*, **10,** 49–59.
Seewaldt VL, Johnson BS, Parker MB, Collins SJ and Swisshelm K. (1995). *Cell Growth Differ.*, **6,** 1077–1088.
Seewaldt VL, Kim JH, Caldwell LE, Johnson BS, Swisshelm K and Collins SJ. (1997b). *Cell Growth Differ.*, **8,** 631–641.
Seewaldt VL, Kim JH, Parker MB, Dietze EC, Srinivasan KV and Caldwell LE. (1999b). *Exp. Cell Res.*, **249,** 70–85.
Seewaldt VL, Mrozek K, Dietze EC, Parker M and Caldwell LE. (2001). *Cancer Res.*, **61,** 616–624.
Sims SH, Cha Y, Romine MF, Gao PQ, Gottlieb K and Deisseroth AB. (1993). *Mol. Cell. Biol.*, **13,** 690–702.
Stampfer M. (1985). *J. Tissue Cult. Methods*, **9,** 109–121.
Stark GR, Kerr IM, Williams BR, Silverman RH and Schreiber RD. (1998). *Annu. Rev. Biochem.*, **67,** 227–264.
Tamura T, Ishihara M, Lamphier MS, Tanaka N, Oishi I, Aizawa S, Matsuyama T, Mak TW, Taki S and Taniguchi T. (1995). *Nature*, **376,** 596–599.
Tanaka N, Ishihara M, Kitagawa M, Harada H, Kimura T, Matsuyama T, Lamphier MS, Aizawa S, Mak TW and Taniguchi T. (1994). *Cell*, **77,** 829–839.
Tsuda H, Sakamaki C, Tsugane S, Fukutomi T and Hirohashi S. (1998). *Jpn. J. Clin. Oncol.*, **28,** 5–11.
Tzoanopoulos D, Speletas M, Arvanitidis K, Veiopoulou C, Kyriaki S, Thyphronitis G, Sideras P, Kartalis G and Ritis K. (2002). *Br. J. Haematol.*, **119,** 46–53.
Wang L, Miura M, Bergeron L, Zhu H and Yuan J. (1994). *Cell*, **78,** 739–750.
Watson CJ and Miller WR. (1995). *Br. J. Cancer*, **71,** 840–844.
Wen Z, Zhong Z and Darnell Jr JE. (1995). *Cell*, **82,** 241–250.
Widschwendter M, Daxenbichler G, Bachmair F, Muller E, Zeimet AG, Windbichler G, Uhl-Steidl M, Lang T and Marth C. (1996). *Anticancer Res.*, **16,** 369–374.
Yahata T, Shao W, Endoh H, Hur J, Coser KR, Sun H, Ueda Y, Kato S, Isselbacher KJ, Brown M and Shioda T. (2001). *Genes Dev.*, **15,** 2598–2612.
Yao TP, Oh SP, Fuchs M, Zhou ND, Ch'ng LE, Newsome D, Bronson RT, Li E, Livingston DM and Eckner R. (1998). *Cell*, **93,** 361–372.
Yim JH, Wu SJ, Casey MJ, Norton JA and Doherty GM. (1997). *J. Immunol.*, **158,** 1284–1292.
Zhang JJ, Vinkemeier U, Gu W, Chakravarti D, Horvath CM and Darnell Jr JE. (1996). *Proc. Natl. Acad. Sci. USA*, **93,** 15092–15096.
Zhang S, Liu J, Dragunow M and Cooper GJS. (2003). *J. Biol. Chem.*, **278,** 52810–52819.

Retinoic Acid Receptor-β2 Promoter Methylation in Random Periareolar Fine Needle Aspiration

Gregory R. Bean,[1] Victoria Scott,[1] Lisa Yee,[2] Brooke Ratliff-Daniel,[1] Michelle M. Troch,[1] Pearl Seo,[1] Michelle L. Bowie,[1] Paul K. Marcom,[1] Jaimie Slade,[1] Bruce F. Kimler,[3] Carol J. Fabian,[3] Carola M. Zalles,[3] Gloria Broadwater,[1] Joseph C. Baker Jr.,[1] Lee G. Wilke,[4] and Victoria L. Seewaldt[1]

[1]Division of Medical Oncology, Duke University Medical Center, Durham, North Carolina; [2]Department of Surgery and the Comprehensive Cancer Center, The Ohio State University, Columbus, Ohio; [3]University of Kansas Medical Center, Kansas City, Kansas; and [4]Department of Surgery, Duke University Medical Center, Durham, North Carolina

Abstract

Methylation of the retinoic acid receptor-β2 (RARβ2) P2 promoter is hypothesized to be an important mechanism for loss of RARβ2 function during early mammary carcinogenesis. The frequency of RARβ2 P2 methylation was tested in (a) 16 early stage breast cancers and (b) 67 random periareolar fine needle aspiration (RPFNA) samples obtained from 38 asymptomatic women who were at increased risk for breast cancer. Risk was defined as either (a) 5-year Gail risk calculation ≥1.7%; (b) prior biopsy exhibiting atypical hyperplasia, lobular carcinoma *in situ*, or ductal carcinoma *in situ*; or (c) known *BRCA1/2* mutation carrier. RARβ2 P2 promoter methylation was assessed at two regions, M3 (−51 to 162 bp) and M4 (104-251 bp). In early stage cancers, M4 methylation was observed in 11 of 16 (69%) cases; in RPFNA samples, methylation was present at M3 and M4 in 28 of 56 (50%) and 19 of 56 (38%) cases, respectively. RPFNAs were stratified for cytologic atypia using the Masood cytology index. The distribution of RARβ2 P2 promoter methylation was reported as a function of increased cytologic abnormality. Methylation at both M3 and M4 was observed in (a) 0 of 10 (0%) of RPFNAs with Masood scores of ≤10 (nonproliferative), (b) 3 of 20 (15%) with Masood scores of 11 to 12 (low-grade proliferative), (c) 3 of 10 (30%) with Masood scores of 13 (high-grade proliferative), and (d) 7 of 14 (50%) with Masood scores of 14 of 15 (atypia). Results from this study indicate that the RARβ2 P2 promoter is frequently methylated (69%) in primary breast cancers and shows a positive association with increasing cytologic abnormality in RPFNA. (Cancer Epidemiol Biomarkers Prev 2005;14(4):790–8)

Introduction

Recent studies suggest that breast cancer incidence may be substantially reduced in high-risk women by tamoxifen treatment and/or prophylactic mastectomy (1-3). Although these reports are encouraging, current prevention strategies are expensive and can be associated with significant side effects. Biomarkers are needed to accurately predict short-term breast cancer risk (a) so that women who are most likely to benefit from preventive therapy can be identified and (b) so that response to chemoprevention can be accurately assessed.

Retinoids are important mediators of growth and differentiation in normal human mammary epithelial cells (HMEC) and regulate the expression of many pharmacologic targets for prevention such as cyclooxygenase-2 (4-6). The majority of retinoid actions are mediated through specific nuclear retinoic acid receptors (RAR-α, RAR-β, and RAR-γ) and rexinoid X receptors (RXR-α, RXR-β, and RXR-γ). These nuclear receptors act as transcription regulators and establish genetic communication networks that are essential in regulating cell growth, differentiation, and apoptosis (4). The transcriptional activity of RARs and RXRs is primarily modulated through the formation of RAR/RXR heterodimers (4). These heterodimers have two distinct functions: (a) they modulate transcription initiation after binding to RAR elements in the promoter of target genes and (b) they promote ''cross-talk'' with other steroid signaling pathways, perhaps through promoting coactivator shifts.

RARβ2 is unique because it is (a) primarily expressed in epithelial cells and (b) positively regulated by retinoids and the RARβ2 P2 promoter RAR element (4). We have shown that RARβ2 is a tumor suppressor in breast cancer (7) and progressive loss of RARβ2 expression is observed during breast carcinogenesis (8, 9). Importantly, whereas retinoids and RARβ2 mediate growth arrest and differentiation in HMECs, restoration of RARβ2 function in breast cancer cells promotes apoptotic cell death (5, 10-12). Noncancerous epithelial cells adjacent to invasive breast cancer also exhibit markedly decreased RARβ2 mRNA expression (8, 9). This has led to the hypothesis that loss of RARβ2 expression may provide a local cellular environment (field effect) that promotes mammary carcinogenesis.

Tumorigenesis is thought to be a multistep process resulting from the accumulation of genetic losses and epigenetic changes. Epigenetic changes, mainly DNA methylation and modification of histones, are now recognized as playing a critical role in carcinogenesis (13). A multitude of studies using the candidate gene approach have established the importance of DNA hypermethylation in tumor suppressor gene silencing (13-24). Several important observations have been made. First, many tumor suppressor genes have been found to be hypermethylated in multiple tumor types. For example, *BRCA1* promoter hypermethylation has been observed in breast and ovarian cancer (16, 21). Second, DNA hypermethylation events occur early in carcinogenesis, which makes hypermethylation a potentially important marker of risk and a target for prevention. Third, evidence also suggests that hypermethylation of DNA repair genes may profoundly

Received 8/3/04; revised 10/28/04; accepted 11/18/04.

Grant support: NIH/National Cancer Institute grants CA68438-AV13 (AVON/National Cancer Institute Partners in Progress), 2P30CA14236-26 (V.L. Seewaldt), R01CA88799 (V.L. Seewaldt), R01CA98441 (V.L. Seewaldt), Susan G. Komen Breast Cancer award BCTR0402720 (V.L. Seewaldt), DAMD-98-1-851 and DAMD-010919 (V.L. Seewaldt), American Cancer Society award CCE-99898 (V.L. Seewaldt), V-Foundation award (V.L. Seewaldt), and a Charlotte Geyer Award (V.L. Seewaldt).

The costs of publication of this article were defrayed in part by the payment of page charges. This article must therefore be hereby marked advertisement in accordance with 18 U.S.C. Section 1734 solely to indicate this fact.

Note: L. Yee and B. Ratliff-Daniel made equal contributions as third authors.

Requests for reprints: Victoria L. Seewaldt, Duke University Medical Center, Box 2628, Durham, NC 27710. Phone: 919-668-2455; Fax: 919-668-2458. E-mail: seewa001@mc.duke.edu

affect overall and disease-free survival in patients with malignancy (13).

Loss of RARβ2 function in mammary epithelial cells is hypothesized to be the result of both genetic and epigenetic events. Two mechanisms have been proposed: (a) loss of heterozygosity and (b) promoter hypermethylation (6, 8, 9, 14, 15). Loss of heterozygosity at the RARβ2 locus (*3p24*) is frequently observed in invasive breast cancers and is thought to be a late mechanism for loss of RARβ2 expression (6, 8). In contrast, RARβ2 P2 promoter methylation has been observed in dysplastic mammary epithelial cells and is thought to be an important early mechanism for loss of RARβ2 expression (9, 14, 15). Previous studies have determined that the RARβ2 P2 promoter is CpG rich and includes four regions of hypermethylation unique to breast cancer cells and absent in normal mammary epithelial cells (14). Whereas other methods of regulating RARβ2 transcription surely exist, studies in cell lines suggest a negative relationship between methylation and message expression (14). These findings are supported by studies where cancer cell lines with suppressed RARβ2 reexpress message when treated with a demethylating agent such as 5′-aza-deoxycytidine (14, 15).

Random periareolar fine needle aspiration (RPFNA) is a research technique developed to repeatedly sample mammary cells from the whole breast of asymptomatic high-risk women to assess both (a) breast cancer risk and (b) response to chemoprevention (25, 26). RPFNA is distinct from diagnostic FNA: diagnostic FNA is a standard clinical technique used to evaluate a clinically identifiable breast mass, whereas breast RPFNA is analogous to a cervical Papanicolaou smear in its ability to obtain a representative sampling of cells from the entire breast of asymptomatic women. RPFNA has the advantage of being able to provide a ''snapshot'' of the whole breast, and unlike ductal lavage, (a) can be done successfully in a majority of high-risk women (72-85% cell yield for RPFNA versus 20-40% for ductal lavage) and (b) has been validated in long-term chemoprevention cohorts (25-27). A great strength of RPFNA is the willingness of high-risk women to undergo subsequent RPFNA; ~80% of women who undergo initial RPFNA undergo subsequent RPFNA (25, 26). Breast RPFNA has been successfully used to predict breast cancer risk in women at increased risk for breast cancer. The presence of any detectable cellular atypia in a breast RPFNA specimen is associated with a 5-fold increase in breast cancer risk in high-risk women (25). These observations validate the use of cellular atypia obtained by RPFNA as a surrogate marker of short-term breast cancer risk in high-risk populations.

The frequency of RARβ2 P2 promoter methylation and resulting loss of RARβ2 expression in breast RPFNA is currently unknown. RARβ2 P2 methylation is (a) frequently (74%) detected in fluid from mammary ducts containing ductal carcinoma *in situ* and invasive carcinomas and (b) observed in two of five (40%) atypical ductal lavage specimens (28, 29). Whereas these data are extremely limited (n = 5), they provide evidence for the feasibility of testing for RARβ2 P2 methylation in cytologic specimens. As described in this study, we show that RARβ2 P2 methylation (a) is observed in 69% of primary breast cancers and (b) correlates with the presence of increasing cytologic abnormality in RPFNA samples obtained in high-risk women.

Materials and Methods

Informed Consent. The study was approved by the Human Subjects Committee and Institutional Review Board at the Ohio State University (for biopsy assessment) and Duke University Medical Center (for RPFNA studies), in accordance with assurances filed with and approved by the Department of Health and Human Services.

Biopsy Tissue. Paraffin-embedded fixed breast biopsy tissue was tested from subjects with stage I or II invasive breast cancer.

Eligibility. To be eligible for screening by RPFNA, women were required to have at least one of the following major risk factors for breast cancer: (a) 5-year Gail risk calculation ≥ 1.7%; (b) prior biopsy exhibiting atypical hyperplasia, lobular carcinoma *in situ*, ductal carcinoma *in situ* (DCIS); or (c) known *BRCA1/2* mutation carrier. In subjects with prior invasive cancer, DCIS, or radiation, only the contralateral breast was aspirated, as the cell yield from radiated breast tissue is uniformly poor. In general, women were required to be between 30 and 60 years of age, as women younger than 30 years have a low short-term risk of breast cancer and women older than 60 years often have involutional breasts that are unlikely to yield sufficient cells for analysis (25). Women younger than 30 years could only be aspirated if they were within 10 years of the age of onset in a first-degree relative. Women older than 55 years could only participate if they had prior evidence of generalized proliferative breast disease. All women were required to have a mammogram interpreted as ''not suspicious for breast cancer'' within 2 months of entry, plus a breast examination on the day of aspiration that was interpreted as normal or not sufficiently abnormal to warrant a diagnostic biopsy. Clinical variables evaluated included age, menopausal status, hormone and oral contraceptive use, parity, age of menarche and menopause, lactation history, family cancer history (including family history of breast, ovarian, colon, and prostate cancer), radiation exposure, and other environmental exposures.

RPFNA. RPFNA was done as previously published (25, 26). All investigators were trained to perform RPFNA by Carol Fabian. To control for hormonal effects on mammary cell proliferation, menstruating women were aspirated between days 1 and 12 of their cycle. The breast was anesthetized with 5 mL of 1% lidocaine, immediately adjacent to the areola, at ~3 and 9 o'clock positions. Eight to 10 aspirations were done per breast for random sampling of epithelial cells. After the aspiration, cold packs were applied to the breasts for 10 minutes, and both breasts were bound in kerlex gauze for 12 to 24 hours. Epithelial cells were pooled and placed in modified CytoLyt (Cytyc Co., Boxborough, MA) with 1% formalin for 24 hours. Cells from the right and left breast were processed separately, so as to obtain one specimen per aspirated breast. Epithelial cells were split into two samples, with half designated for cytology and half designated for DNA extraction.

Cytologic Assessment. Slides for cytology were prepared by filtration and Papanicolaou stained as described previously (25, 26). A minimum of one epithelial cell cluster with at least 10 epithelial cells was required to sufficiently determine pathology; the most atypical cell cluster was examined and scored (25, 26). Cells were classified as nonproliferative, hyperplasia, or hyperplasia with atypia (30). Cytology preparations were also given a semiquantitative index score through evaluation by the Masood cytology index (25, 26). As previously described, cells were given a score of 1 to 4 points for each of six morphologic characteristics that include cell arrangement, pleomorphism, number of myoepithelial cells, anisonucleosis, nucleoli, and chromatin clumping (25, 26). Morphologic assessment, Masood cytology index scores, and cell count were assigned by a single dedicated pathologist from University of Kansas Medical Center (C.M.Z.) without knowledge of the subjects' clinical history.

Materials and Cell Culture Lines. Sodium bisulfite (Sigma, St. Louis, MO, A.C.S.) and hydroquinone (Sigma, >99%) were used under reduced lighting and stored in a dessicator. 2-Pyrrolidinone (>99%) was purchased from Fluka (Milwaukee, WI). HS578T and ZR751 cell lines were obtained from American

Type Culture Collection (Manassas, VA) and grown in supplemented αMEM (Life Technologies, Gaithersburg, MD) as previously described (5). HMEC-SR is a cell line derived from Human Papillomavirus E6-immortalized, normal HMEC strain AG11132 (M. Stampfer 172R/AA7; ref. 31). This cell strain was purchased from the National Institute of Aging, Cell Culture Repository (Coriell Institute, Camden, NJ) and grown in supplemented MEBM (Cambrex, Baltimore, MD) as previously described (11). E6-transduction is as previously described (32, 33).

DNA Extraction from Fixed Tissue. DNA was extracted from paraffin-embedded tissue using the Pico Pure DNA Extraction Kit (Arcturus, Mountain View, CA) according to manufacturer's instructions. The DNA was purified with a phenol-chloroform extraction, ethanol precipitated, and resuspended in 10 mmol/L Tris (pH 7.5). Samples were stored at −80°C.

DNA Extraction from RPFNA. The RPFNA samples were washed with unmodified CytoLyt to eliminate RBCs. The cells were treated with proteinase K digestion buffer [50 mmol/L Tris (pH 8.1), 1 mmol/L EDTA, 0.5% Tween 20, and 0.1 mg/mL proteinase K] and incubated overnight at 40°C (34). The proteinase K was inactivated by incubation at 95°C for 10 minutes, the samples were spun, and the supernatant was collected and stored at −80°C.

Confirmation of Genomic Integrity. To confirm the integrity of the extracted genomic DNA from fixed tissue, PCR analysis was used to detect β-actin. PCR reactions consisted of 50 ng DNA, 1× PCR buffer (Roche, Nutley, NJ), 250 μmol/L of each deoxynucleotide triphosphate, 200 nmol/L of each primer, and 2.5 units of Taq polymerase (Roche) in 30 μL total volume. Amplification was carried out in a GeneAmp PCR System 9700 (Applied Biosystems, Foster City, CA) as follows: initial 95°C for 5 minutes followed by 40 amplification cycles (94°C for 30 seconds, 59°C for 30 seconds, and 72°C for 1 minute) and a final extension of 72°C for 4 minutes. Primer sequences were as follows: 5′-CCCGCTACCTCTTCTGGTG-3′ (sense) and 5′-GGGGTGTTGAAGGTCTCAAA-3′ (antisense).

Bisulfite Treatment. Extracted DNA from both RPFNA and fixed tissue was sodium bisulfite treated following the protocol of Grunau et al., with some modifications (35). Treatments on positive and negative controls were done simultaneously. Commercially available, fully methylated human DNA (Amersham, Arlington Heights, IL) was used as a positive control. Briefly, 1 μg of genomic DNA was denatured with 3 mol/L NaOH for 20 minutes at 42°C followed by deanimation in saturated sodium bisulfite and 10 mmol/L hydroquinone solution (pH 5.0) for 4 hours at 55°C in the dark. The samples were desalted using the Wizard DNA Clean-Up System (Promega, Madison, WI) according to the manufacturer's protocol. The DNA was then desulfonated in 3 mol/L NaOH for 20 minutes at 37°C, ethanol precipitated, and resuspended in 1 mmol/L Tris (pH 8.0) for storage in aliquots at −20°C.

Methylation-specific PCR. This assay takes advantage of discriminatory primers for methylated and unmethylated DNA, as the primers bind or do not bind depending on methylation status. Previous work has elucidated four CpG regions where methylation is known to occur upstream from the *RARβ2* gene; region 3 (M3) includes the RAR element and TATAA box and region 4 (M4) includes the 5′ end of the transcribed message (14). Region 4 was first studied in the fixed tumor samples, whereas both regions 3 and 4 were investigated in the RPFNA samples. All PCR reactions consisted of 50 ng DNA, 1× PCR buffer (see Table 2), 250 μmol/L of each deoxynucleotide triphosphate, 200 nmol/L of each primer, and 2.5 units of HotStar Taq polymerase (Qiagen, Chatsworth, CA) in 30 μL total volume. Each PCR thermal cycle consisted of 95°C for 5 minutes followed by 40 amplification cycles (94°C for 1 minute, annealing temperature for 1 minute, and 72°C for 1 minute) and a final extension of 72°C for 4 minutes. See Table 1 for primer sequences and annealing temperatures (14). A GeneAmp PCR System 9700 (Applied Biosystems) was used for all amplifications. PCR products were visualized on 1.5% ethidium bromide agarose gels using an Image Station 440 (Kodak, Chicago, IL). Optimization with methylated primers was achieved using minute amounts of methylated positive control (~50 pg) to model RPFNA samples.

Methylation-specific PCR Sensitivity Experiment. Previous studies have investigated the methylation status of breast cancer cell lines at both regions 3 and 4 (14, 15). It was confirmed that cells of the HMEC-SR line were unmethylated at region 3, HS578T cells were unmethylated at region 4, and ZR751 cells were methylated at both regions. As an estimate of PCR sensitivity, two experiments were set up where known amounts of methylated cells were titrated in unmethylated cells of each negative type. For the purposes of testing, the RPFNA procedure was estimated to yield an average of two million epithelial cells. Thus, titrated amounts of ZR751 cells (0-100,000 cells) were used to spike two million cells of each negative type. Each sample was DNA extracted, bisulfite treated, and subjected to PCR as outlined above to determine the sensitivity of our method at each region.

Table 1. MS-PCR primer sequences and reaction conditions

	Sequences	1× Buffer (and additives)	Annealing temperature (°C)
M3	S 5′-GGTTAGTAGTTCGGGTAGGGTTTATC-3′, AS 5′-CCGAATCCTACCCCGACG-3′	16.6 mmol/L $(NH_4)_2SO_4$ 67 mmol/L Tris (pH 9.1) 3.0 mmol/L $MgCl_2$	57
U3	S 5′-TTAGTAGTTTGGGTAGGGTTTATT-3′, AS 5′-CCAAATCCTACCCCAACA-3′	15 mmol/L $(NH_4)_2SO_4$ 60 mmol/L Tris (pH 8.5) 4.5 mmol/L $MgCl_2$	57
M4	S 5′-GTCGAGAACGCGAGCGATTC-3′, AS 5′-CGACCAATCCAACCGAAACG-3′	15 mmol/L $(NH_4)_2SO_4$ 60 mmol/L Tris (pH 9.0) 3.5 mmol/L $MgCl_2$ 150 mmol/L 2-pyrrolidinone	55
U4	S 5′-GATGTTGAGAATGTGAGTGATTT-3′, AS 5′-AACCAATCCAACCAAAACA-3′	15 mmol/L $(NH_4)_2SO_4$ 60 mmol/L Tris (pH 8.5) 4.5 mmol/L $MgCl_2$	57

Abbreviations: S, sense; AS, antisense.

Table 2. Patient characteristics of early-stage breast cancer

Women enrolled in study	16
No. biopsy samples taken	17
	n = 16 (%)
Average age and range (y)	57 (34-82)
Race	
Caucasian	14 (88)
African American	2 (12)
Menopausal status	
Postmenopausal	11 (69)
Premenopausal	5 (31)
Stage of breast cancer	
Stage 0/DCIS	1 (6)
Stage I	8 (50)
Stage II	7 (44)
Average tumor size and range (cm)	3.2 (0.5-5.0)
Type of tumor	
Invasive ductal	12 (75)
Invasive lobular	1 (6)
Mixed ductal/lobular	2 (12)
DCIS	1 (6)
Tumor receptor status	
ER^+	11 (69)
PR^+	8 (50)
Lymph node–positive disease	5 (31)

Statistical Methods. The Wilcoxon rank sums test was used to compare the median Masood score with M3 methylation, M4 methylation, and a combination of both M3 and M4 methylation. Median cell counts and M3 or M4 methylation were also compared using the Wilcoxon rank sums test. The Spearman correlation coefficient was used to determine the association between cell count and Masood score.

Results

Study Demographics. Sixteen women with early stage breast cancer (stages 0-II) were enrolled at Ohio State University from April 1999 to December 1999. Six percent had stage 0 breast cancer (DCIS), 50% had stage I breast cancer, and 44% had stage II breast cancer. The average tumor size was 3.2 cm (range, 0.5-5 cm). Thirty-one percent of the women had lymph node positive disease. Sixty-nine percent of the tumors were estrogen receptor positive and 50% were progesterone receptor positive. The mean age of the women was 57 years old (range, 34-82 years). Eighty-eight percent of the women were Caucasian and 12% were African American. Sixty-nine percent of the women were postmenopausal. A summary of clinical characteristics of subjects with early stage breast cancers whose primary breast biopsy specimens were tested for RARβ2 P2 promoter methylation are listed in Table 2.

Thirty-eight women underwent RPFNA at Duke University Medical Center from March 2003 to March 2004. Clinical characteristics of subjects undergoing RPFNA are listed in Table 3. The mean age was 46 years (range, 29-64 years). Forty-seven percent of the women were either perimenopausal or postmenopausal; 53% were premenopausal. Seventy-four

Table 3. Clinical characteristics of patients undergoing RPFNA

A. Patient characteristics for RPFNA

Women enrolled in study	38
Bilateral RPFNA	28
Unilateral RPFNA	10
RPFNA samples collected	66
No. RPFNAs with insufficient epithelial cell count	10
No. RPFNAs submitted for analysis	56
	n = 38 (%)
Average age and range (y)	46 (29-64)
Race	
Caucasian	33 (87)
African American	5 (13)
Menopausal status	
Postmenopausal	18 (47)
Premenopausal/Perimenopausal	20 (53)
Hormone replacement use	
Current	2 (5)
Ever use	9 (24)
Never use	27 (71)
Antiestrogen therapy (at the time of RPFNA)	
Tamoxifen	2 (5)
Raloxifene	1 (3)
Aromatase inhibitor	2 (5)
Family history of breast cancer	17 (45)
Prior abnormal biopsies	
LCIS	1 (3)
DCIS	5 (13)
ADH	10 (26)
History of contralateral breast cancer	5 (13)

B. Characteristics of patients on prevention therapy at time of RPFNA

RPFNA sampling	Agent	Duration	Masood	Cell count	M3/M4 methylation
Unilateral	Tamoxifen	2 wk	14	500	+/+
Bilateral (L)	Raloxifene	2 y	10	<10	−/−
Bilateral (R)			10	10	−/−
Unilateral	Tamoxifen	2 wk	15	1,000	+/−
Unilateral	Aromatase inhibitor	1 y	NA	NA	−/−
Unilateral	Aromatase inhibitor	1 y	NA	NA	−/−

percent of the women had bilateral RPFNA (28 of 38), as RPFNA was not done on breast tissue with a history of invasive cancer or DCIS. Patients who underwent bilateral RPFNA contributed two separate samples for purposes of analysis. Eighty-seven percent (33 of 38) of the women were Caucasian and 13% (5 of 38) were African American. Five percent (2 of 38) of the women were currently on hormone replacement at the time of RPFNA. Twenty-four percent (9 of 38) of the women had been on estrogen replacement in the past and had a mean of 9 years of exposure (range, 1-25 years). Thirteen percent (5 of 38) received tamoxifen, raloxifene, or an aromatase inhibitor at time of RPFNA. The mean Masood cytology index was 12. Table 3B provides patient characteristics, duration of therapy, Masood score, and methylation for this subset of patients. Of the 66 RPFNA samples collected, 10 had insufficient epithelial cells for cytologic testing (one cell cluster with >10 epithelial cells); thus, 56 samples were submitted for full cytopathology analysis. Of the samples that contained insufficient cell counts for cytologic analysis, six samples both yielded methylation information and were positive for β-actin by PCR amplification (data not shown). Of the RPFNA samples, 33% (18 of 56) were from participants with a prior abnormal biopsy (20% ADH, 11% DCIS, 2% lobular carcinoma *in situ*), 8 of 56 had history of contralateral breast cancer, 20 of 56 had strong family history, and 2 of 56 were *BRCA2* mutation carriers.

Methylation Analysis. In this study, two known potential hypermethylation regions of the RARβ2 P2 promoter were examined in mammary epithelial cells. These regions are detailed in Fig. 1. Region 3 (M3) contains the RAR element (nucleotides, nt −52 to −36), TATAA box (nt −28 to −24), and the transcription start region; methylation region 4 (M4) contains an Sp1 element (nt 230-235; ref. 14). In the RPFNA samples, either only an unmethylated band or both methylated and unmethylated bands were observed. The presence of unmethylated RARβ2 promoter sequences confirmed the integrity of the DNA in all samples and was expected given the global nature of the sampling. A cellular sensitivity experiment was conducted with titrated amounts of a cell line known to be methylated to model the RPFNA samples. In this heterogeneous environment, the Methylation-specific PCR (MS-PCR) assay was sensitive enough to detect 0.005% methylation at region 3 (100 ZR751 cells in two million HMEC-SR cells) and 0.05% methylation at region 4 (1,000 ZR751 cells in two million HS578T cells). Similarly, MS-PCR was able to detect ~5 and ~50 pg, respectively, of a bisulfite-treated methylated positive control submitted to the same experimental conditions as the RPFNA samples.

Incidence of RARβ2 P2 Promoter Methylation in Primary Breast Cancers. The frequency of RARβ2 P2 promoter methylation was tested in primary breast cancer samples at methylation region 4 (M4; Fig. 2B). PCR amplification of β-actin was used to confirm DNA integrity (data not shown). MS-PCR analysis of these 16 samples showed methylation in 69% of primary breast cancers at region M4. These results are similar to previously published reports (14).

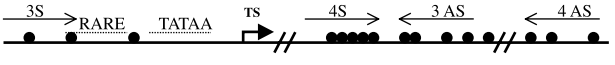

Figure 1. MS-PCR targets. MS-PCR primers were designed to amplify regions of known methylation regions in the RARβ2 P2 promoter (14). M3 region (methylated nt −51 to 162; unmethylated nt −49 to 162) includes the RARE, TATAA box, and transcription start region; M4 region (methylated nt 104-251; unmethylated nt 101-250) contains an Sp1 element. •, methylated CpGs were previously identified by sequencing of cell lines and primary tumor samples (14, 15).

Incidence of RARβ2 P2 Promoter Methylation in RPFNA. Methylation-specific PCR at the M3 and M4 regions was tested in 66 RPFNA specimens. Fifty-six of 66 samples (85%) had sufficient cellular material for cytologic analysis. MS-PCR analysis of these 56 samples showed methylation in 50% (28 of 56) of RPFNA samples at region M3 and 38% (21 of 56) of RPFNA samples at region M4. All included samples exhibited strong unmethylated bands at both regions, confirming both the presence of DNA and the promoter sequence itself (Fig. 2C). Sixty-four percent (36 of 56) of RPFNA samples showed methylation at either M3 or M4; 23% (13 of 56) showed methylation at both M3 and M4. Twenty-eight of the subjects had bilateral RPFNAs; 12 paired samples did not have sufficient cellular material so only 16 paired samples were analyzed. Of these samples, 5 of 16 (31%) showed methylation in RPFNA bilaterally, 7 of 16 (44%) showed methylation in RPFNA unilaterally, and 4 of 16 (25%) showed the absence of methylation in either breast.

Correlation of RARβ2 P2 Promoter Methylation in RPFNA with Masood Cytology Index Scores. RPFNA aspirates were stratified for cytologic atypia using the Masood cytology index. The distribution of RARβ2 P2 promoter methylation was reported as a function of increased cytologic abnormality. Figure 3A shows the number of samples with M3 region methylation for each Masood score. As the Masood score increased, the percentage of samples with M3 region methylation increased. Importantly, no sample with a Masood score of ≤10 exhibited RARβ2 P2 promoter methylation at either the M3 or M4 region. The 28 samples without M3 region methylation had a median Masood score of 11, whereas the 29 samples with M3 region methylation had a median Masood score of 13. There was a significant difference between the two groups (P = 0.0018). Figure 3B shows the number of samples with M4 region methylation for each Masood score. The 35 samples without M4 region methylation had a median score of 12, whereas the 20 samples with M4 region methylation had a median Masood score of 13.5 (P = 0.0002). Figure 3C shows the presence of both M3 and M4 region methylation for each Masood score. The 42 samples without methylation at both regions had a median Masood score of 12. The 13 samples with both M3 and M4 region methylation had a median Masood score of 14 (P = 0.0051).

Correlation of RARβ2 P2 Promoter Methylation in RPFNA with Cell Count. The presence of RARβ2 P2 promoter methylation was compared with total cell count of each corresponding RPFNA slide (Fig. 4A and B). The 22 samples without M3 or M4 region methylation had a median cell count of 10, whereas the 34 samples with either M3 or M4 region methylation had a median cell count of 300 (P = 0.003).

Correlation of Masood Score with Cell Count. RPFNA Masood scores were compared with the total cell count of each sample (Fig. 4C). The Spearman correlation coefficient is 0.67 and indicates a significant correlation between the cell count and the Masood score (P < 0.0001).

Discussion

Tumorigenesis is hypothesized to be a multistep process resulting from the accumulation of genetic losses and epigenetic changes. Epigenetic changes, mainly DNA methylation and modification of histones, are now recognized as playing a critical role in mammary carcinogenesis (13, 36). To better define the role of promoter hypermethylation in early mammary carcinogenesis, we prospectively tested (a) the frequency of RARβ2 P2 promoter hypermethylation in RFPNA specimens obtained from women at high-risk for breast cancer and (b) whether the presence of RARβ2 P2 promoter hypermethylation correlates with the presence of early cytologic changes.

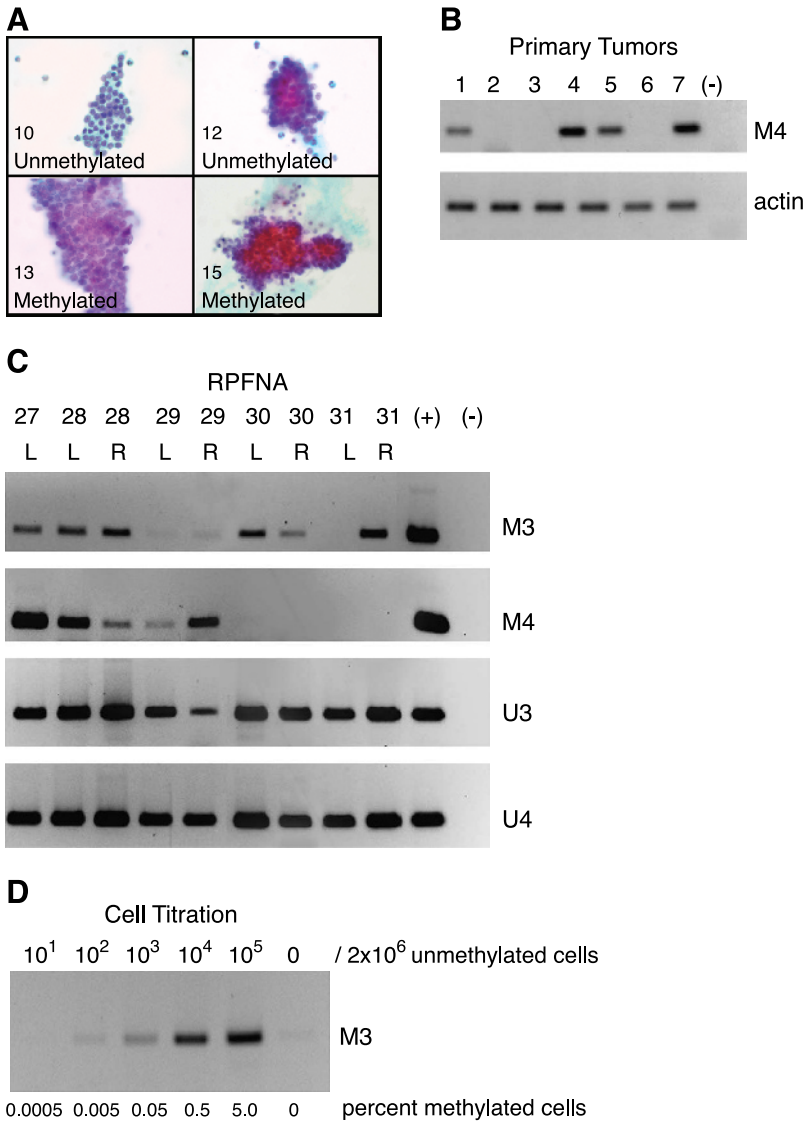

Figure 2. RPFNA cytology and methylation of RARβ2 P2 promoter. **A.** Representative RPFNA specimens in high-risk women. *Numeric value,* Masood cytology index score for this specimen. Presence of RARβ2 P2 promoter methylation at either the M3 or M4 region (*Methylated*). If neither region is methylated, the specimen is labeled *Unmethylated*. **B.** Hypermethylation of RARβ2 P2 promoter M4 region in early-stage breast cancer specimens. To confirm the integrity of the extracted genomic DNA, PCR analysis was used to detect β-actin (*actin*). **C.** Hypermethylation of RARβ2 P2 promoter M3 and M4 regions in RPFNA obtained from five representative high-risk women. **D.** Hypermethylation of RARβ2 P2 promoter M3 region in cellular sensitivity experiment to measure lowest threshold of methylation detection in a sea of unmethylated DNA, as explained in Materials and Methods. *M3* and *M4,* use of primers to identify methylated RARβ2 P2 regions 3 and 4, respectively. *U3* and *U4,* use of primers to identify unmethylated RARβ2 P2 regions 3 and 4, respectively. Methylated positive control in the M3 and M4 gels, HMEC-SR in the U3 gel, and HS578T in the U4 gel (+). Negative control (−).

In 1996, the late Helene Smith proposed a model of mammary carcinogenesis where breast cancer developed in a ''high-risk epithelial field'' in which some of the genetic and epigenetic aberrations found in cancer may also be present in the morphologically normal surrounding epithelium (8). Loss of heterozygosity of RARβ2 has been detected in normal epithelium adjacent to breast cancer but not in distal epithelium, supporting a ''field effect'' of increased risk (8). Yet, it has been found that loss of heterozygosity cannot fully account for the frequent loss of RARβ2 expression in breast cancer (37). Furthermore, the presence of methylation has been shown to correlate between tumor and the apparently normal adjacent tissue. For example, RARβ2 P2 promoter methylation has been detected in normal adjacent tissue of head and neck squamous cell carcinoma tumors where RARβ2 P2 promoter methylation was also present; RARβ2 P2 methylation was not detected in normal epithelium near unmethylated head and neck squamous cell carcinoma (38). Taken together, an early epigenetic change such as methylation may contribute to this ''field effect'' seen in breast cancer, and RARβ2 P2 promoter methylation occurs early enough along this progression to potentially serve as an effective biomarker.

In this study, we observe that RPFNA specimens obtained in women at high risk for breast cancer exhibit (a) a high frequency of methylation at the M3 and M4 regions of the RARβ2 P2 promoter and (b) a positive correlation between the presence of RARβ2 P2 promoter methylation and increasing Masood cytologic abnormalities (Fig. 3). RARβ2 P2 promoter methylation was also observed in 69% of primary low-risk breast cancers and, importantly, was not observed in 10 nonproliferative, cytologically normal RPFNA specimens (Masood index, ≤10). The frequency of RARβ2 P2 promoter methylation at the M3 region was unexpectedly high in RPFNA exhibiting low-grade proliferative changes (Masood index, 11-12) which may reflect the overall breast cancer risk of this cohort. However, the presence of both M3 and M4 RARβ2 P2 promoter methylation in RPFNA was 15% for specimens with low-grade proliferative changes and 30% for RPFNA specimens exhibiting high-grade proliferative changes (Masood index, 13). Studies are in progress to test whether the presence of RARβ2 P2 methylation can be used to further risk stratify high-risk patients with proliferative changes.

The diverse sample of patients in this study and their variable clinical histories mirror the heterogeneous nature of the population of women at an increased risk of developing breast cancer. Such heterogeneity poses a challenge to clinicians in diagnosing early breast disease, risk-stratifying patients, and deciding on appropriate treatment. Therefore, identifying biomarkers that account for such diversity while providing information on possible disease progression is a

worthy goal. Our sample size is currently too small to provide further analysis comparing RARβ2 P2 promoter methylation to patients' clinical histories. We attempted to compare Gail model risk calculations to methylation status but found that due to how the Gail model is calculated we could not obtain risk estimates on a majority of our patients. Risk calculations could not be done on (a) patients with a history of DCIS/lobular carcinoma *in situ* or invasive breast cancer, as the model did not incorporate them; (b) patients who are known and suspected *BRCA1/2* mutation carriers, as their Gail values do not accurately reflect their risk (39); (c) patients below the age of 35, as they were also not included in the development of the model; and (d) African American patients, as there is concern that the Gail model does not accurately reflect risk in African American women (40). Thus, only 47% (18 of 38) of our subjects were eligible for the Gail model risk assessment, and their findings were not enough to achieve statistical significance. Further subset analysis could not be accurately done on methylation status relative to other factors, such as history of breast disease or proportion of atypical cells per sample, due to limited sample size. A small percentage of patients (5 of 38) were on prevention therapy at the time of aspiration (see Table 3B); two patients were not included in the analysis due to insufficient epithelial cell count, two patients only just started antiestrogen therapy 2 weeks before RPFNA, and the exclusion of the final patient's results did not statistically alter our findings. Our hope is to serially follow these patients via RPFNA and observe any cytologic changes that occur as a result of treatment.

These studies used MS-PCR to detect the presence of RARβ2 P2 promoter methylation at two target regions. MS-PCR is an established method for detecting methylation in DNA sequences. The method has been successfully used to examine methylation in relatively homogenous samples such as cancer

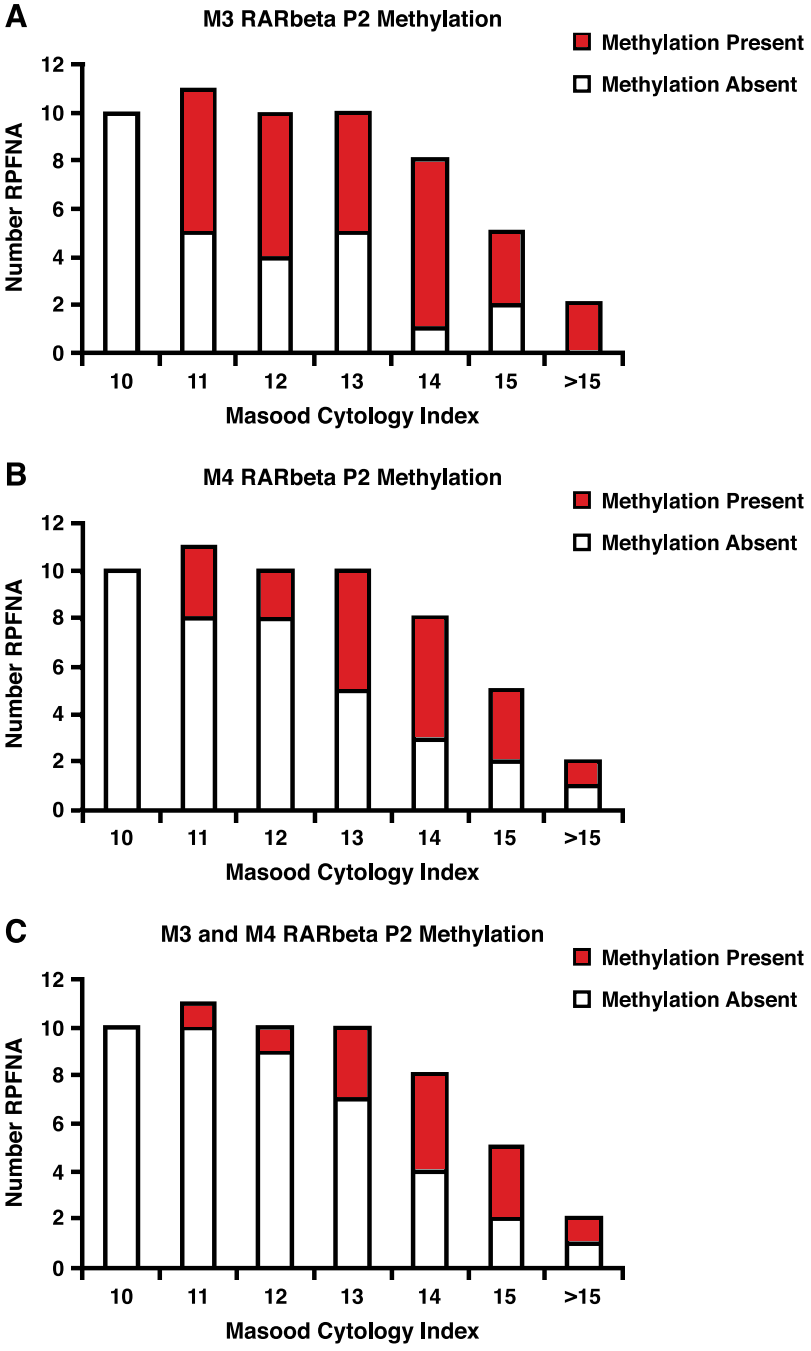

Figure 3. Correlation between RARβ2 P2 promoter methylation in RPFNA with Masood cytology index scores. RPFNA samples were assessed for cytologic atypia using the Masood cytology index. The distribution of RARβ2 P2 promoter methylation is depicted as a function of increased cytologic abnormality. **A.** Distribution of RFPNA samples with M3 region methylation relative to Masood cytology score. **B.** Distribution of RFPNA samples with M4 region methylation relative to Masood cytology score. **C.** RPFNA samples containing methylation at both the M3 and M4 regions relative to Masood cytology score.

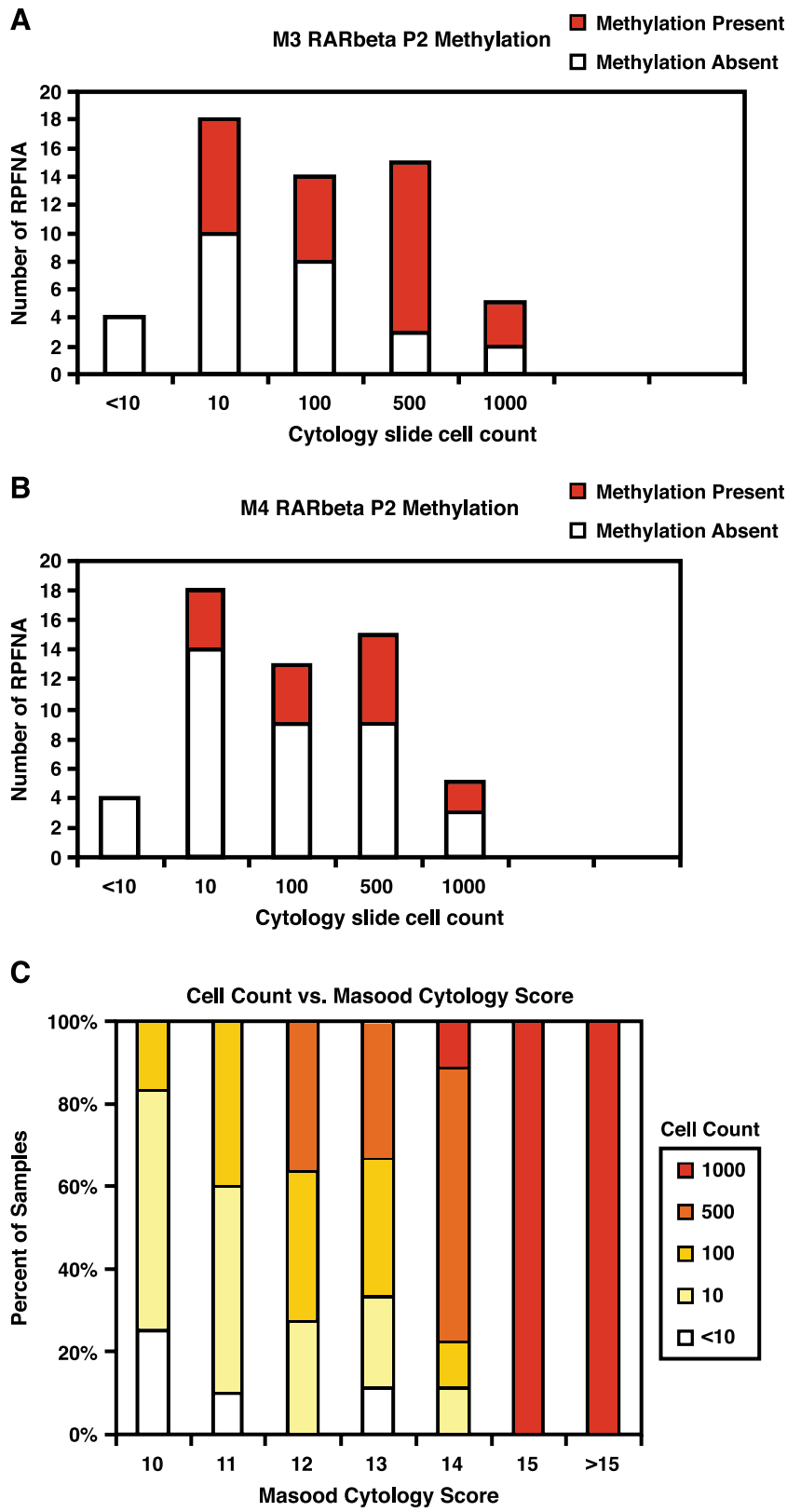

Figure 4. Correlation between RPFNA cell count and RARβ2 P2 promoter methylation and Masood score. **A** and **B.** Presence of RARβ2 P2 promoter methylation at the M3 (*A*) and M4 (*B*) region is depicted relative to total cell count of each RPFNA sample. **C.** RPFNA Masood cytology index scores are reported relative to the total cell count of each sample.

cell lines and tumor specimens. In such samples, primers anneal to plentiful ''target'' sequences readily. However, RPFNA samples consist of cells from the whole breast; a heterogeneous collection that may or may not include ''fields'' of increased risk. Assuming RARβ2 P2 promoter methylation is present in an RPFNA sample, MS-PCR primers would have far less ''target'' DNA to possibly bind, compared with in homogeneous samples with potentially greater amounts of target. MS-PCR in RPFNA samples is then complicated by two factors: (a) less target DNA and (b) a sea of presumably unmethylated DNA from the whole breast that partially impairs proper annealing of methylated primers. These factors are more easily overcome in cell lines and tumor specimens but require additional PCR optimization in RPFNA samples. It

is for these reasons that the PCR was optimized with such specific buffers and additives to refine the program and ensure small amounts of target-positive control could be amplified. Additionally, the cellular sensitivity experiment was set up for each region to gauge the effect of unmethylated DNA during amplification of the methylated target DNA. When optimized, the MS-PCR assay was able to detect 0.005% methylation at the M3 region and 0.05% methylation at the M4 region. Thus, the final optimized programs are quite sensitive, so each program was run in triplicate and only repeatable bands were counted as methylated.

Breast RPFNA has been used to predict both short-term breast cancer risk and monitor response to chemoprevention agents (25, 26). There are, however, some current limitations of breast RPFNA. First, much of the assessment of RPFNA samples has been focused on morphologic analysis. Molecular analysis of RPFNA samples may have the potential to enhance both the reproducibility and prognostic value of RPFNA. Second, many breast cancer prevention agents inhibit mammary cell proliferation and therefore have the potential to reduce the cell yield from RPFNA. As seen in our study as well as others' (29), MS-PCR studies on methylated genes such as *RARβ2* can still be done even when epithelial samples are inadequate for cytology. The statistically significant correlation between increasingly atypical morphologic appearance and the increase in rates of detectable methylation at the RARβ promoter site supports the concept that the methylation assay is accurately detecting an early step in carcinogenesis. The addition of MS-PCR–based marker analysis of RPFNA provides additional sensitivity to assist in determining whether a prevention agent (a) solely acted to decrease proliferation or (b) was also successful in eliminating abnormal cells. Thus, RPFNA coupled with methylation studies shows promise for the early detection of breast cancer risk and provides an extremely sensitive marker to track response to breast cancer prevention agents.

References

1. Fisher B, Costantino JP, Wickerham DL, et al. Tamoxifen for prevention of breast cancer: report of the National Surgical Adjuvant Breast and Bowel Project P-1 Study. J Natl Cancer Inst 1998;90:1371–88.
2. Rebbeck TR. Prophylactic oophorectomy in BRCA1 and BRCA2 mutation carriers. Eur J Cancer 2002;38 Suppl 6:S15–7.
3. Hartmann LC, Schaid DJ, Woods JE, et al. Efficacy of bilateral prophylactic mastectomy in women with a family history of breast cancer. N Engl J Med 1999;340:77–84.
4. Altucci L, Gronemeyer H. The promise of retinoids to fight against cancer. Nat Rev Cancer 2001;1:181–93.
5. Seewaldt VL, Johnson BS, Parker MB, et al. Expression of retinoic acid receptor β mediates retinoic acid-induced growth arrest and apoptosis in breast cancer cells. Cell Growth Differ 1995;6:1077–88.
6. Subbaramaiah K, Cole PA, Dannenberg AJ. Retinoids and carnosol suppress cyclooxygenase-2 transcription by CREB-binding protein/p300-dependent and -independent mechanisms. Cancer Res 2002;62:2522–30.
7. Treuting PM, Chen LI, Buetow BS, et al. Retinoic acid receptor β2 inhibition of metastasis in mouse mammary gland xenografts. Breast Cancer Res Treat 2002;72:79–88.
8. Deng G, Lu Y, Zlotnikov G, et al. Loss of heterozygosity in normal tissue adjacent to breast carcinomas. Science 1996;274:2057–9.
9. Widschwendter M, Berger J, Daxenbichler G, et al. Loss of retinoic acid receptor β expression in breast cancer and morphologically normal adjacent tissue but not in the normal breast tissue distant from the cancer. Cancer Res 1997;57:4158–61.
10. Seewaldt VL, Kim JH, Caldwell LE, et al. All-*trans*-retinoic acid mediates G_1 arrest but not apoptosis of normal human mammary epithelial cells. Cell Growth Differ 1997;8:631–41.
11. Seewaldt VL, Caldwell LE, Johnson BS, et al. Inhibition of retinoic acid receptor function in normal human mammary epithelial cells results in increased cellular proliferation and inhibits the formation of a polarized epithelium *in vitro*. Exp Cell Res 1997;236:16–28.
12. Dietze EC, Caldwell LE, Marcom K, et al. Retinoids and retinoic acid receptors regulate growth arrest and apoptosis in human mammary epithelial cells and modulate expression of CBP/p300. Microsc Res Tech 2002;59:23–40.
13. Kopelovich L, Crowell JA, Fay JR. The epigenome as a target for cancer chemoprevention. J Natl Cancer Inst 2003;95:1747–57.
14. Sirchia SM, Ferguson AT, Sironi E, et al. Evidence of epigenetic changes affecting the chromatin state of the retinoic acid receptor β2 promoter in breast cancer cells. Oncogene 2000;19:1556–63.
15. Widschwendter M, Berger J, Hermann M, et al. Methylation and silencing of the retinoic acid receptor-β2 gene in breast cancer. J Natl Cancer Inst 2000;92:826–32.
16. Esteller M, Silva JM, Dominguez G, et al. Promoter hypermethylation and BRCA1 inactivation in sporadic breast and ovarian tumors. J Natl Cancer Inst 2000;92:564–9.
17. Fackler MJ, McVeigh M, Evron E, et al. DNA methylation of RASSF1A, HIN-1, RAR-β, Cyclin D2 and Twist in *in situ* and invasive lobular breast carcinoma. Int J Cancer 2003;107:970–5.
18. Lapidus RG, Nass SJ, Butash KA, et al. Mapping of ER gene CpG island methylation-specific polymerase chain reaction. Cancer Res 1998;58:2515–9.
19. Lehmann U, Langer F, Feist H, et al. Quantitative assessment of promoter hypermethylation during breast cancer development. Am J Pathol 2002;160:605–12.
20. Liu ZJ, Maekawa M, Horii T, et al. The multiple promoter methylation profile of PR gene and ERα gene in tumor cell lines. Life Sci 2003;73:1963–72.
21. Mancini DN, Rodenhiser DI, Ainsworth PJ, et al. CpG methylation within the 5′ regulatory region of the BRCA1 gene is tumor specific and includes a putative CREB binding site. Oncogene 1998;16:1161–9.
22. Nass SJ, Herman JG, Gabrielson E, et al. Aberrant methylation of the estrogen receptor and E-cadherin 5′ CpG islands increases with malignant progression in human breast cancer. Cancer Res 2000;60:4346–8.
23. Sathyanarayana UG, Padar A, Suzuki M, et al. Aberrant promoter methylation of laminin-5-encoding genes in prostate cancers and its relationship to clinicopathological features. Clin Cancer Res 2003;9:6395–400.
24. Umbricht CB, Evron E, Gabrielson E, et al. Hypermethylation of 14-3-3 sigma (stratifin) is an early event in breast cancer. Oncogene 2001;20:3348–53.
25. Fabian CJ, Kimler BF, Zalles CM, et al. Short-term breast cancer prediction by random periareolar fine-needle aspiration cytology and the Gail risk model. J Natl Cancer Inst 2000;92:1217–27.
26. Fabian CJ, Kimler BF. Beyond tamoxifen new endpoints for breast cancer chemoprevention, new drugs for breast cancer prevention. Ann N Y Acad Sci 2001;952:44–59.
27. Dooley WC, Ljung BM, Veronesi U, et al. Ductal lavage for detection of cellular atypia in women at high risk for breast cancer. J Natl Cancer Inst 2001;93:1624–32.
28. Sirchia SM, Ren M, Pili R, et al. Endogenous reactivation of the RARβ2 tumor suppressor gene epigenetically silenced in breast cancer. Cancer Res 2002;62:2455–61.
29. Evron E, Dooley WC, Umbricht CB, et al. Detection of breast cancer cells in ductal lavage fluid by methylation-specific PCR. Lancet 2001;357:1335–6.
30. Zalles CM, Kimler BF, Kamel S, et al. Cytology patterns in random aspirates from women at high and low risk for breast cancer. Breast J 1995;1:343–9.
31. Stampfer MR. Isolation and growth of human mammary epithelial cells. J Tissue Cult Meth 1985;9:107–15.
32. Seewaldt VL, Mrozek K, Dietze EC, et al. Human papillomavirus type 16 E6 inactivation of p53 in normal human mammary epithelial cells promotes tamoxifen-mediated apoptosis. Cancer Res 2001;61:616–24.
33. Seewaldt VL, Mrozek K, Sigle R, et al. Suppression of p53 function in normal human mammary epithelial cells increases sensitivity to extracellular matrix-induced apoptosis. J Cell Biol 2001;155:471–86.
34. Lehmann U, Kreipe H. Real-time PCR analysis of DNA and RNA extracted from formalin-fixed and paraffin-embedded biopsies. Methods 2001;25:409–18.
35. Grunau C, Clark SJ, Rosenthal A. Bisulfite genomic sequencing: systematic investigation of critical experimental parameters. Nucleic Acids Res 2001;29:E65–5.
36. Widschwendter M, Jones PA. DNA methylation and breast carcinogenesis. Oncogene 2002;21:5462–82.
37. Yang Q, Yoshimura G, Nakamura M, et al. Allelic loss of chromosome 3p24 correlates with tumor progression rather than with retinoic acid receptor β2 expression in breast carcinoma. Breast Cancer Res Treat 2001;70:39–45.
38. Youssef EM, Lotan D, Issa JP, et al. Hypermethylation of the retinoic acid receptor-β(2) gene in head and neck carcinogenesis. Clin Cancer Res 2004;10:1733–42.
39. Breast Cancer Risk Assessment Tool [homepage on the Internet]. Bethesda: National Cancer Institute; c2000 [cited 2004 Oct 13]. Available from: http://bcra.nci.nih.gov/brc/.
40. Bondy ML, Newman LA. Breast cancer risk assessment models: applicability to African-American women. Cancer 2003;97:230–5.

CREB-binding protein regulates apoptosis and growth of HMECs grown in reconstituted ECM via laminin-5

Eric C. Dietze[1], Michelle L. Bowie[1], Krzysztof Mrózek[2], L. Elizabeth Caldwell[3], Cassandra Neal[3], Robin J. Marjoram[1], Michelle M. Troch[1], Gregory R. Bean[1], Kazunari K. Yokoyama[4], Catherine A. Ibarra[1] and Victoria L. Seewaldt[1,5,*]

[1]Division of Medical Oncology, Duke University, Durham, NC 27710, USA
[2]Division of Hematology and Oncology, Comprehensive Cancer Center, The Ohio State University, Columbus, OH 43210, USA
[3]Fred Hutchinson Cancer Research Center, Seattle, WA 98109, USA
[4]RIKEN, Tsukuba Institute, Ibaraki 305-0074, Japan
[5]Department of Pharmacology and Cancer Biology, Duke University, Durham, NC 27710, USA
*Author for correspondence (e-mail: seewa001@mc.duke.edu)

Accepted 3 August 2005
Journal of Cell Science 118, 5005-5022 Published by The Company of Biologists 2005
doi:10.1242/jcs.02616

Summary

Interactions between normal mammary epithelial cells and extracellular matrix (ECM) are important for mammary gland homeostasis. Loss of interactions between ECM and normal mammary epithelial cells are thought to be an early event in mammary carcinogenesis. CREB-binding protein (CBP) is an important regulator of proliferation and apoptosis but the role of CBP in ECM signaling is poorly characterized. CBP was suppressed in basal-cytokeratin-positive HMECs (CK5/6$^+$, CK14$^+$, CK8$^-$, CK18$^-$, CK19$^-$). Suppression of CBP resulted in loss of reconstituted ECM-mediated growth control and apoptosis and loss of laminin-5 α3-chain expression. Suppression of CBP in normal human mammary epithelial cells (HMECs) resulted in loss of CBP occupancy of the *LAMA3A* promoter and decreased *LAMA3A* promoter activity and laminin-5 α-3 chain expression. Exogenous expression of CBP in CBP-negative HMECs that have lost reconstituted ECM-mediated growth regulation and apoptosis resulted in (1) CBP occupancy of the *LAMA3A* promoter, (2) increased *LAMA3A* activity and laminin-5 α3-chain expression, and (3) enhancement of reconstituted ECM-mediated growth regulation and apoptosis. Similarly, suppression of laminin-5 α3-chain expression in HMECs resulted in loss of reconstituted ECM-mediated growth control and apoptosis. These observations suggest that loss of CBP in basal-cytokeratin-positive HMECs results in loss of reconstituted ECM-mediated growth control and apoptosis through loss of *LAMA3A* activity and laminin-5 α3-chain expression. Results in these studies may provide insight into early events in basal-type mammary carcinogenesis.

Key words: CBP, Basal cytokeratins, Basal-type breast cancer, Extracellular matrix, Apoptosis, Laminin-5

Introduction

Breast tissue is composed of mammary epithelial cells that rest on extracellular matrix (ECM), and interactions between epithelial cells and ECM regulate normal growth, polarity and apoptosis (Petersen et al., 1992; Strange et al., 1992; Zutter et al., 1995; Ilic et al., 1998; Farrelly et al., 1999; Stupack and Cheresh, 2002). Loss of ECM signaling is thought to be an early event in mammary carcinogenesis and to promote some of the phenotypic changes observed during malignant progression (Petersen et al., 1992; Howlett et al., 1995; Mercurio et al., 2001; Farrelly et al., 1999; Hood and Cheresh, 2002; Stromblad et al., 2002). Carcinogenesis is hypothesized to be a multistep process resulting from the progressive accumulation of genetic damage. Although loss or mutation of specific tumor suppressor genes such as *TP53* promotes mammary carcinogenesis (Fabian et al., 1996; Rohan et al., 1998), not all damaged epithelial cells progress to malignancy and many are thought to be eliminated by apoptosis (Thompson, 1995). Mammary gland homeostasis requires a coordinated balanced between proliferation and programmed cell death. ECM signaling is thought to play an important role in regulating this balance (Petersen et al., 1992; Howlett et al., 1995; Farrelly et al., 1999; Mercurio et al., 2001; Hood and Cheresh, 2002; Stupack and Cheresh, 2002). Loss of ECM signaling is thought to promote mammary carcinogenesis by preventing the apoptotic elimination of damaged mammary epithelial cells.

The majority of breast cancers are epithelial in origin. The normal mammary gland contains luminal epithelial cells that express luminal-type cytokeratins (CK7, CK8, CK18, CK19) and cells that express stratified epithelial cytokeratins (CK5/6, CK14, CK17) (Wazer et al., 1995; Anbazhagan et al., 1998; Abd El-Rehim et al., 2004). Epithelial breast cancers are broadly divided into those that express luminal keratins (luminal-type) and those that express stratified epithelial cytokeratins (basal-type) (Perou et al., 2000; Foulkes et al., 2003).

We previously used an in vitro model (Howlett et al., 1995; Weaver et al., 1995; Stampfer, 1985) to investigate the potential role of ECM-signaling in promoting apoptosis in basal-cytokeratin-positive human mammary epithelial cell strains (HMECs) that had acutely lost p53 function (Seewaldt et al.,

2001a). The HMEC strains used in our studies were isolated from reduction mammoplasty tissue by Martha Stampfer (Stampfer, 1985) and express basal-type cytokeratins (CK5/6$^+$ CK14$^+$ CK17$^+$) but not luminal-type cytokeratins (CK8$^-$ CK18$^-$ CK19$^-$) (Moll et al., 1982; Taylor-Papadimitriou and Lane, 1987; Wazer et al., 1995; Foulkes et al., 2003). These HMEC strains are distinguished from myoepithelial cells by (1) staining negatively for smooth muscle actin, (2) the presence of cytoplasmic vesicles that stain positively for lipid and exhibit an apical distribution in rECM culture by electron microscopy, and (3) the absence, when viewed by electron microscopy, of plasmalemmal vesicles and tracts of 5-7 nm actin microfilaments (Pitelka, 1983; Seewaldt et al., 1999b; Yee et al., 2003; Seewaldt et al., 2001a). Acute loss of p53 was modeled in these basal-cytokeratin-positive HMEC strains by either retroviral-mediated expression of the human papillomavirus type-16 (HPV-16) E6 protein (Band, 1995; Wazer et al., 1995) or treatment with p53-specific antisense oligonucleotides (AS ODNs). We observed that while p53$^+$ HMEC controls grown in reconstituted ECM (rECM) underwent growth arrest on day 7, HMEC-E6 and p53$^-$ HMECs underwent apoptosis (Seewaldt et al., 2001a). Although the acute expression of either HPV-16 E6 or suppression of p53 in HMECs promoted enhancement of rECM-mediated apoptosis, HMEC-E6 cells passaged in non-rECM culture rapidly lost both rECM-mediated growth arrest and apoptosis associated with loss of polarized expression of the laminin-5 receptor, α3β1-integrin, and loss of genetic material from chromosome 16 (Seewaldt et al., 2001a). These observations led us to hypothesize that laminin-5–α3β1-integrin growth regulation and polarity signals are critical for targeting the elimination of HMECs that have acutely suppressed levels of p53, and that 16p harbors a gene(s) whose loss and/or rearrangement might promote loss of rECM-mediated growth arrest and apoptosis.

Laminins are ECM glycoproteins that promote mammary gland homeostasis by regulating cell adhesion, migration, proliferation, differentiation and angiogenesis (Aberdam et al., 2000). Laminins have three distinct protein subunits, designated α, β and γ. Laminin-5 (α3A, β3 and γ2) is the most abundant ECM glycoprotein produced by mammary epithelial cells (D'Ardenne et al., 1991). Laminin-5 functions as a ligand for α3β1- and α6β4-integrins and has been implicated in adhesion, migration and invasion. Recent reports indicate that binding of the laminin-5 α3-chain globular LG3 domain to α3β1-integrin mediates cell adhesion and migration (Shang et al., 2001). Dysregulation of laminin-5 expression is observed during carcinogenesis. Whereas benign ductal and lobular epithelial cells demonstrate continuous laminin-5 staining at the epithelial-stromal interface, primary breast cancers and breast cancer cells exhibit loss of laminin-5 α3-chain expression (Martin et al., 1998). Loss of laminin-5 α3-chain expression has also been observed in prostate cancer (Hao et al., 2001), while epigenetic inactivation of all three laminin-5-encoding genes has been observed in lung cancer cells (Sathyanarayana et al., 2003). There is also evidence that increased laminin-5 γ2-chain expression and cleavage may be associated with tissue remodeling and tumor invasion. Matrix metalloproteinase (MMP)-dependent mammary gland involution coincides with binding of the laminin-5 γ2-chain MMP-cleavage fragment, DIII, to the epidermal growth factor receptor (Schenk et al., 2003). Mammary glands from β1,4-galactosyltransferase 1-null mice exhibit excess mammary gland branching associated with (1) decreased laminin-5 α3-chain expression, (2) increased expression and cleavage of laminin-5 γ2-chain, and (3) increased MMP expression (Steffgen et al., 2002). Increased expression of laminin-5 γ2-chain is observed at the invasive front of tumors associated with poor prognosis (Pyke et al., 1994; Yamamoto et al., 2001; Niki et al., 2002) and cooperative interactions between laminin-5 γ2-chain and MMPs are associated with an aggressive phenotype in melanoma (Seftor et al., 2001). These observations suggest that dysregulation of laminin-5 signaling are important for cancer progression.

Our prior studies indicated that laminin-5–α3β1-integrin-growth regulation signals may be critical for targeting the elimination of HMECs (Seewaldt et al., 2001a). Little is known about the regulation of laminin-5 gene transcription in normal mammary epithelial tissue or about the molecular mechanism underlying the loss of laminin-5 expression observed in early breast carcinogenesis. The human *LAMA3A* promoter is known to contain three binding sites of the dimeric transcription factor activating protein 1 (AP-1) (Virolle at al., 1998; Miller et al., 2001). It has been recently observed that the second AP-1-binding site present in the human *LAMA3A* promoter at position –185 bp is critical for baseline transcription of laminin-5 α3-chain (Miller et al., 2001). CREB-binding protein (CBP) is known to interact with AP-1 response elements (Benkoussa et al., 2002). However, the relationship between CBP and laminin-5 expression in mammary epithelial cells has not been studied.

Detailed cytogenetic analysis performed for this report indicated that chromosome 16p13 is the critical area whose loss and/or rearrangement promoted loss of rECM-mediated growth arrest and apoptosis (Seewaldt et al., 2001a). CBP is a nuclear protein located at chromosome band 16p13.3 that regulates proliferation, differentiation and apoptosis (Giles et al., 1997; Yao et al., 1998). CBP is a key integrator of diverse signaling pathways including those regulated by retinoids, p53, estrogen and BRCA1 (Kawasaki et al., 1998; Robyr et al., 2000). Chromosomal loss at 16p13 has been reported to occur in the majority of benign and malignant papillary neoplasms of the breast and loss or amplification of 16p is frequently observed in premalignant breast lesions (Lininger et al., 1998; Tsuda et al., 1998; Aubele et al., 2000). Taken together, these observations suggest that loss of CBP expression promotes mammary carcinogenesis.

This report describes a role for CBP in mediating laminin-5 α3-chain expression in basal-cytokeratin-positive HMEC strains and subsequent enhancement of rECM-mediated growth control and apoptosis. Observations in this model system may predict a critical role for CBP in regulating basal-cytokeratin-positive mammary epithelial cell homeostasis through modulation of laminin-5 α3-signaling.

Materials and Methods

Cell culture and media

Normal human mammary epithelial cell (HMEC) strains AG11132 and AG11134 (M. Stampfer #172R/AA7 and #48R, respectively) were purchased from the National Institute of Aging, Cell Culture Repository (Coriell Institute, National Institute of Aging, Camden, NJ) (Stampfer, 1985). HMEC strains AG11132 and AG11134 were

established from normal tissue obtained at reduction mammoplasty, have a limited life span in culture, and fail to divide after approximately 20 to 25 passages. HMECs exhibit a low level of estrogen receptor staining characteristic of normal mammary epithelial cells. HMECs were grown in Mammary Epithelial Cell Basal Medium (Clonetics, San Diego, CA) supplemented with 4 μl/ml bovine pituitary extract (Clonetics #CC4009), 5 μg/ml insulin (Sigma, St Louis, MO), 10 ng/ml epidermal growth factor (UBI, Lake Placid, NY), 0.5 μg/ml hydrocortisone (Sigma), 10^{-5} M isoproterenol (Sigma), and 10 mM HEPES buffer (Sigma) (Standard Media). Cells were cultured at 37°C in a humidified incubator with 5% CO_2/95% air.

Large-scale rECM culture

Large-scale rECM culture was used to prepare total RNA or protein lysate for analysis using techniques previously developed by the laboratory of Mina Bissell (Roskelley et al., 1994). Early and late passage HMEC-E6 cells and HMEC-LXSN controls were plated in T-75 flasks, previously treated with poly(2-hydroxyethyl methacrylate) (Poly-HEME). Cells were grown in Standard Media with 5% (vivo) rECM.

Cell growth and proliferation in rECM culture

Proliferation was assessed by Ki67 staining index, whereby 5 μm sections were immunostained with antibody directed against Ki-67. Cells were scored visually (100-500 cells) for immunopositive nuclei. The proliferation index was calculated by dividing the number of immunopositive cells as a percentage of the total number of cells scored. Growth was measured by counting the number of DAPI-stained nuclei per cell cluster in cryosections of cells grown in rECM by previously published methods (Weaver et al., 1997).

Detection of apoptosis

TUNEL staining in HMECs grown in rECM for 5-11 days was carried out as previously described (Seewaldt et al., 2001a). Two-hundred cells were scored. The apoptotic index was determined by expressing the number of TUNEL-positive cells as a percentage of the total number of cells scored. Electron microscopy was as previously described (Seewaldt et al., 1997a). Fifty colonies were scored for the presence of apoptosis by morphologic criteria that included (1) margination of chromatin, (2) nuclear condensation, (3) cell shrinkage, and (4) formation of apoptotic bodies (Majno and Joris, 1995).

Suppression of CBP expression

Nine antisense oligonucleotides (ODNs) to human CBP were generated by the PAS program (Ugai et al., 1999). The CBP antisense A3342V ODN (24-mer, nucleotide position 3342-3363) was initially chosen on the basis of selective inhibition of CBP protein expression in MCF-7 cells (data not shown); suppression was confirmed in HMECs. Inactive CBP ODN scrA3342V (22 mer, nucleotide position 3342-3363) was chosen to be the scrambled sequence of the antisense ODN to ensure identical nucleotide content and minimize differences potentially attributable to nucleic acid content, and based on lack of suppression of CBP in MCF-7 and HMECs. See Table 1 for a list of ODNs. The first and last three nucleotides of all ODNs were phosphorothioate modified to increase their stability in vitro. Early passage HMEC-LXSN controls and HMEC-E6 cells were plated in T-75 flasks in Standard Media. After allowing 24 hours for attachment, cell cultures were treated for 72 hours with either active or inactive ODNs (0.001 to 0.1 μM final concentration). Every 24 hours the culture media was replaced by new Standard Media containing fresh ODNs. Western analysis was performed to confirm suppression of CBP expression as described above and lack of suppression of the related coactivator p300. The resulting film images were digitized and quantitated using Kodak 1D Image Analysis Software (Eastman Kodak, Rochester, NY).

Table 1. CBP-specific antisense ODN sequences

Target gene	Sequences*	Size	Status
CBP			
A3342V	5′-CACTTCAGGTTTCTTTTCATCC-3′	22 bp	Active
scrA3342V	5′-ATTCTCATCATCGTCTTCGTTC-3′	22 bp	Inactive

*The first and last three base pairs of each ODN sequence were modified by phosphorothioate.

CBP suppression in rECM culture

Early passage HMEC-LXSN controls and HMEC-E6 cells were trypsinized and approximately 1×10^4 cells were resuspended in 100 μl rECM containing either active or inactive CBP-specific ODNs (0.01 to 0.1 μM final concentration) on ice. rECM cultures were prepared as above and overlayed with Standard Media containing active or inactive CBP-specific ODNs (0.01 to 0.1 μM final concentration). Overlay media were changed every 24 hours to ensure a constant supply of ODNs. The diameter of the growing colonies was determined and cells were prepared for electron microscopy and immunostaining.

Retroviral gene expression

Expression of HPV-16 E6 was as previously described (Seewaldt et al., 2001a). Exogenous expression of CBP in HMECs was as for HPV-16 E6 with the following modifications. The retroviral vector harboring the coding sequences for CBP was generated from the pcDNA3 recombinant plasmid by methods previously described (Seewaldt et al., 1995). The pcDNA3 plasmid was digested with *Bam*HI and the released plasmid inserted in the *Bam*HI cloning site of the dephosphorylated pLXSN plasmid. Correct orientation and sequence was verified by direct sequencing. Ten micrograms of purified pLCBPSN retroviral construct plasmid was transfected via Cellfectin™ (Invitrogen, Carlsbad, CA) into the PE 501 murine ecotropic retrovirus packaging cell line (Seewaldt et al., 1995). Expression of the exogenous construct was confirmed by PCR and protein expression was confirmed by western analysis (Seewaldt et al., 2001a; Seewaldt et al., 2001b).

Cytogenetic analysis of early and late passage HMECs

Spectral karyotypic analyses (SKY) of HMEC-LXSN controls (passages 10 and 16) and HMEC-E6 cells (passages 10 and 18) were performed as previously described (Mrózek et al., 1993; Schröck et al., 1996; Seewaldt et al., 2001a; Seewaldt et al., 2001b).

Western blotting

Preparation of cellular lysates and immunoblotting were performed as previously described (Seewaldt et al., 1997b; Seewaldt et al., 1999a). For CBP expression, the blocked membrane was incubated with 1:200 dilution of the CBP C20 antibody (Santa Cruz Biotechnology, Santa Cruz, CA). For laminin-5 expression, the membrane was incubated with a 1:100 dilution of the C19 antibody to the laminin-5 α3-chain (Santa Cruz Biotechnology). Loading control was provided by 1:200 dilution of the I19 antibody to β-actin (Santa Cruz Biotechnology). All CBP and laminin bands were normalized to actin. The resulting film images were digitized and quantitated using Kodak 1D Image Analysis Software (Eastman Kodak).

Immunostaining

Immunostaining was carried out as previously described (Seewaldt et

al., 2001a). Antibodies against integrin subunits α3 (P1F2, P1B5) and β1 (P4C10) were a generous gift of William Carter (Fred Hutchison Cancer Research Center, Seattle, WA) and have been previously described (Wayner and Carter, 1987; Wayner et al., 1988; Carter et al., 1990a; Carter et al., 1990b). Monoclonal antibody P5H10 directed against the α3-chain of laminin-5 was also a generous gift of William Carter.

Differential gene expression studies

Cells were grown in rECM using large-scale rECM culture techniques as described above. Isolation of total RNA was as previously described (Seewaldt et al., 1995). RNA integrity was confirmed by electrophoresis, and samples were stored at –80°C until used. All RNA combinations used for array analysis were obtained from cells that were matched for passage number, cultured under the identical growth conditions, and harvested at identical confluency. cDNA synthesis and probe generation for cDNA array hybridization were obtained by following the standardized protocols provided by Affymetrix™. Expression data for approximately 5600 full-length human genes was collected using Affymetrix GeneChIP® HuGeneFL™ arrays, following the standardized protocols provided by the manufacturer. Array images were processed using Affymetrix MAS 5.0 software. Probe-level signals were filtered for saturation and intra-array probe intensity data was scaled to a target intensity of 1000. Data was collected in triplicate using independent biological replicates and *P*-values were calculated for pair-wise comparisons using CyberT (Baldi and Long, 2001).

Semi-quantitative RT-PCR

To confirm microarray data, relative transcript levels were analyzed by semi-quantitative reverse transcriptase-polymerase chain reaction (RT-PCR). Five micrograms of total RNA was used in first-strand cDNA synthesis with Superscript II reverse transcriptase (Invitrogen). PCR reaction conditions were optimized for integrin-α3 (*ITGA3*), integrin-β1 (*ITGB1*), laminin-α3 (*LAMA3*), laminin-β3 (*LAMB3*), and laminin-γ2 (*LAMC2*). Primer sequences were obtained from published sources as follows: ITGA3 (Hashida et al., 2002), ITGB1 (Hsu et al., 2001), LAMA3 (Virolle et al., 2002), and LAMB3 and LAMC2 (Manda et al., 2000). A 50 μl reaction was set up containing 100 nM forward primer, 100 nM reverse primer, 250 μM of each dNTP, 10 mM Tris-HCl, 1.5 mM $MgCl_2$, 50 mM KCl, pH 8.3, 2.5 units Taq polymerase, and 2.0 μl cDNA. Reaction conditions for β-actin were 300 nM forward primer, 300 nM reverse primer, 250 μM of each dNTP, 10 mM Tris-HCl, 1.5 mM $MgCl_2$, 50 mM KCl, pH 8.3, 2.5 units Taq polymerase, and 2.0 μl cDNA in a total volume of 50 μl. Products were amplified with Applied Biosciences GeneAmp PCR system 2400 (Applied Biosciences). Preliminary reactions were performed to determine the PCR cycle number of linear amplification for each primer set. The primer sets, cycling conditions and cycle numbers used are indicated in Table 2. Ten microliters of PCR product was analyzed by electrophoresis in 1.2-1.5% agarose gels containing ethidium bromide, visualized under UV light, and quantitated. All samples were performed in triplicate and normalized to β-actin as the control.

LAMA3A reporter studies

A 1403 bp region of the laminin-5 α3-chain (*LAMA3*) promoter corresponding to GenBank accession number AF279435 was amplified with PCR primers, sense 5′-AAG CTT AAG TTT TCC CAT CCG CAA C-3′ and antisense 5′-TCT AGA GCT GAC CGC CTC ACT GC-3′. The PCR product was cloned into pCRII (Invitrogen),

Table 2. Laminin and integrin primers

Gene	Primer set	Cycle conditions	PCR cycle number
ITGA3	F: 5′-AAGCCAAGTCTGAGACT-3′ R: 5′-GTAGTATTGGTCCCGAGTCT-3′	94°C 3 min 94°C 30 sec 60°C 1 min 72°C 1 min 72°C 7 min	22
ITGB1	F: 5′-GCGAAGGCATCCCTGAAAGT-3′ R: 5′-GGACACAGGATCAGGTTGGA-3′	94°C 3 min 94°C 30 sec 54°C 30 sec 72°C 1 min 72°C 7 min	19
LAMA3	F: 5′-TGTGGATCTTTGGGGCAG-3′ R: 5′-TTGCCATAGTAGCCCTCCTG-3′	94°C 3 min 94°C 30 sec 58°C 30 sec 72°C 1 min 72°C 7 min	20
LAMB3	F: 5′-TGAGGTTCAGCAGGTACTGC-3′ R: 5′-TAACTGTCCCATTGGCTCAG-3′	95°C 3 min 95°C 1 min 55°C 1 min 72°C 1 min 72°C 7 min	23
LAMC2	F: 5′-CTGAGTATGGGCAATGCCAC-3′ R: 5′-GCTCTGGTATCAACCTTCTG-3′	95°C 3 min 95°C 1 min 55°C 1 min 72°C 1 min 72°C 7 min	22
β-actin	F: 5′-GCTCGTCGTCGACAACGGCTC-3′ R: 5′-CAAACATGATCTGGGTCATCTTCTC-3′ (Invitrogen)	94°C 2 min 94°C 15 sec 55°C 30 sec 72°C 30 sec 72°C 7 min	18

digested out with *Hin*dIII and *Bam*HI, and cloned into the reporter plasmid pBLCAT5 (American Type Culture Collection, Manassas, VA). Cells were transfected with the resultant pBLLAMA3aCAT5 reporter plasmid using previously published transfection conditions and controls (Seewaldt et al., 1997a). Transfection control was provided by the pCMV-GH plasmid (Seewaldt et al., 1997a). Transfected cells were plated in Standard Media in T-25 flasks pre-treated with Poly-HEME, treated with 5% (vivo) rECM for 24 hours, and harvested for CAT activity assays as previously described (Seewaldt et al., 1997a). CAT reporter activity was normalized to GH concentration (Nichols Institute, San Juan Capistrano, CA) and total protein as previously described (Seewaldt et al., 1997a).

LAMA3A chromatin immunoprecipitation

Occupancy of the AP-1-rich region of *LAMA3A* promoter from positions –387 to –127 bp was tested by chromatin immunoprecipitation (ChIP). ChIP was performed by published methods with some modifications (Yahata et al., 2001). Early and late passage HMEC-E6 cells and HMEC-LXSN controls were plated in T-25 flasks treated with Poly-HEME and grown in Standard Media with 5% (vivo) rECM. Preliminary experiments were run to determine optimal sonication and formaldehyde cross-linking time. Once optimized, cells were harvested, pelleted and treated with 1% formaldehyde for 15-20 minutes to crosslink cellular proteins. The formaldehyde was quenched by adding 1.0 ml of 250 mM glycine followed by a 5 minute RT incubation. Cells were then rinsed twice in ice-cold PBS containing protease inhibitor cocktail (4 μg/ml epibestatin hydrochloride, 2 μg/ml calpain inhibitor II, 2 μg/ml pepstatin A, 4 μg/ml mastoparan, 4 μg/ml leupeptin hydrochloride, 4 μg/ml aprotinin, 1 mM TPCK, 1 mM phenylmethylsulfonyl fluoride, and 100 μM TLCK), pelleted, and resuspended in lysis buffer (1% SDS, 10 mM EDTA, 50 mM Tris-HCl at pH 8.1, and 1× protease inhibitor cocktail). Samples were then sonicated 3×15 seconds each with a 1 minute incubation on ice in between pulses on a Branson sonifier model 250 at 50% duty and maximum mini probe power. Supernatants were diluted (1:10) in dilution buffer (1% Triton X-100, 2 mM EDTA, 150 mM NaCl, 20 mM Tris-HCl at pH 8.1, 1× protease inhibitor cocktail), and precleared with 2 μg of sheared salmon sperm DNA, 20 μl normal human serum, and 45 μl of protein A-Sepharose (50% slurry in 10 mM Tris-HCl at pH 8.1, 1 mM EDTA). Human anti-CBP antibody (A22, Santa Cruz) was added to the precleared lysate, and placed on a shaker at 4°C, followed by the addition of 45 μl of protein A-sepharose and 2.0 μg sheared salmon sperm DNA, and then incubated an additional 1 hour on a shaker at 4°C. Sepharose beads were then collected and washed sequentially for 10 minutes each in TSE I (0.1% SDS, 1% Triton X-100, 2 mM EDTA, 20 mM Tris-HCl at pH 8.1, 150 mM NaCl), TSE II (0.1% SDS, 1% Triton X-100, 2 mM EDTA, 20 mM Tris-HCl at pH 8.1, 500 mM NaCl), and buffer III (0.25 M LiCl, 1% NP-40, 1% deoxycholate, 1 mM EDTA, 10 mM Tris-HCl at pH 8.1). Beads were washed once with TE buffer and DNA eluted with 100 μl of 1% SDS-0.1 M $NaHCO_3$. The eluate was heated at 65°C overnight to reverse the formaldehyde crosslinking. DNA fragments were recovered by phenol/chloroform extraction followed by ethanol precipitation and then amplified by using PCR primers, sense 5′-AAG CTT AAG TTT TCC CAT CCG CAA C-3′ and antisense 5′-TCT AGA GCT GAC CGC CTC ACT GC-3′. Approximately 1.1% of the total chromatin was used as the input control and 16% was used for immunoprecipitation. Thirty microliters of PCR product were analyzed by electrophoresis in 1.5% agarose gels containing ethidium bromide and visualized under UV light. All samples were tested in triplicate.

Suppression of LAMA3 by siRNA

The double-stranded siRNA oligo targeting exon 29 of *LAMA3* mRNA was purchased from Ambion (Austin, TX). Control non-silencing siRNA was provided by Qiagen (Alameda, CA). Preliminary studies were conducted on HMEC cells. The total amount of *LAMA3* siRNA and time required for optimal suppression was determined to be 2.0 μg for 12 hours. HMEC cells were transfected with 2.0 μg of *LAMA3* siRNA using Cellfectin™ (Invitrogen). Twelve hours after transfection, RNA was harvested using the Aurum™ Total RNA kit (Bio-Rad Laboratories, Hercules, CA). Semi-quantitative RT-PCR was performed to confirm suppression of *LAMA3* expression. cDNA was prepared for RT-PCR from 50 ng total RNA with Superscript™ II reverse transcriptase (Invitrogen). β-Actin and *LAMA3* PCR reaction conditions were performed as described above except products were amplified for 24 and 29 cycles, respectively. Twenty microliters of PCR product were run on 1.5% agarose gels stained with ethidium bromide and visualized with Kodak 1D™ Image Analysis Software (Eastman Kodak). For initial *LAMA3* suppression studies, early passage HMECs were transfected with 2.0 μg of *LAMA3* siRNA, or control siRNA, 12 hours prior to culturing in rECM. For stable suppression of *LAMA3* in HMEC-E6 cells with siRNA, the pSilencer 4.1-CMV puro expression vector was purchased from Ambion. The *LAMA3* siRNA #2 sequence (target: 5′-AAGGCTAAAACACATTTCAAG-3′; Ambion; #8244), already shown to suppress *LAMA3* mRNA in transient transfection, was used to design two 55-mer DNA oligos to be annealed and inserted into the pSilencer 4.1-CMV puro vector. A hairpin siRNA template was created by annealing the following oligos: top-strand oligo, 5′-GAT CCG GCT AAA ACA CAT TTC AAG TTC AAG AGA CTT GAA ATG TGT TTT AGC CTT A-3′ and bottom-strand oligo, 5′-AGC TTA AGG CTA AAA CAC ATT TCA AGT CTC TTG AAC TTG AAA TGT GTT TTA GC CG-3′ (Qiagen). The annealed oligos were ligated to pSilencer 4.1-CMV through their *Hin*dIII and *Bam*HI ends. Transfection of expression plasmid was performed in HMEC-E6 cells by using Cellfectin™ (Invitrogen) and selection with puromycin. Suppression of *LAMA3* mRNA was confirmed by RT-PCR as described above.

Results

Late passage HMEC-E6 cells exhibit rearrangement of the CBP locus at chromosome 16p13 and a decrease in CBP protein expression

We previously performed SKY-based cytogenetic analysis on 35 unique late passage HMEC-E6 cells to identify rearrangements that might pinpoint the chromosomal location of potential gene(s) whose loss might promote loss of rECM-mediated growth control and apoptosis induction. The most frequent chromosomal losses involved (1) 16p (26/35 cells, 74%), (2) 12p (17/35 cells, 49%), (3) 21p (17/35 cells, 49%), and (4) 17p (14/35 cells, 40%) (Seewaldt et al., 2001a; Seewaldt et al., 2001b). These studies suggested that chromosome 16p harbored a gene(s) whose loss and/or rearrangement might play a role in loss of rECM-mediated growth control and apoptosis induction.

The predominant types of chromosomal changes involving chromosome 16p (and other chromosomes) were deletions, whole-arm translocations, and dicentric chromosomes with breakpoints in the pericentromeric and/or telomeric regions (Seewaldt et al., 2001a). However, two of 35 cells had specific translocations or deletions involving a more distal region of 16p. One cell exhibited a 16p deletion and retained material proximal to 16p1?2, and a second cell exhibited an unbalanced translocation der(16)t(13;16)(q1?2;p13) that affected band 16p13 (Fig. 1A,B). These observations indicated that the gene

of importance was possibly located in the distal region of 16p, at 16p13.

Chromosomal band 16p13 is the locus of the CBP gene (Giles et al., 1997; Yao et al., 1998). Since CBP is known to play a role in growth control and apoptotic signaling, we hypothesized that loss of CBP protein expression might promote loss of rECM-mediated growth control and apoptosis induction in HMEC-E6 cells. We found that these cells also had decreased levels of CBP by western blotting (Fig. 1C). The relative CBP level in late passage HMEC-E6 cells was 8% ($P<0.01$) and 5% ($P<0.01$) that of early passage HMEC-E6 and HMEC-LXSN cells, respectively. There was no significant difference ($P>0.05$) in the relative amount of CBP in early passage HMEC-E6 and HMEC-LXSN cells.

Laminin-5 expression is decreased in late passage HMEC-E6 cells

We previously observed that enhancement of rECM-mediated growth regulation and apoptosis in early passage HMEC-E6 cells required polarized expression of the laminin-5 receptor, α3/β1-integrin (Seewaldt et al., 2001a). Differential gene expression studies, semi-quantitative RT-PCR, and western analysis were performed to test whether the loss of rECM-mediated growth control and apoptosis and loss of CBP expression observed in late passage HMEC-E6 cells correlated with altered expression of laminin-5 and/or α3/β1-integrin mRNA. Differential gene expression studies demonstrated decreased expression of all three laminin-5 chains (α3, β3 and γ2) in apoptosis-resistant, late passage HMEC-E6 cells relative to early passage HMEC-LXSN controls and early passage HMEC-E6 cells grown in rECM (Fig. 2A, Table 3). Semi-quantitative RT-PCR

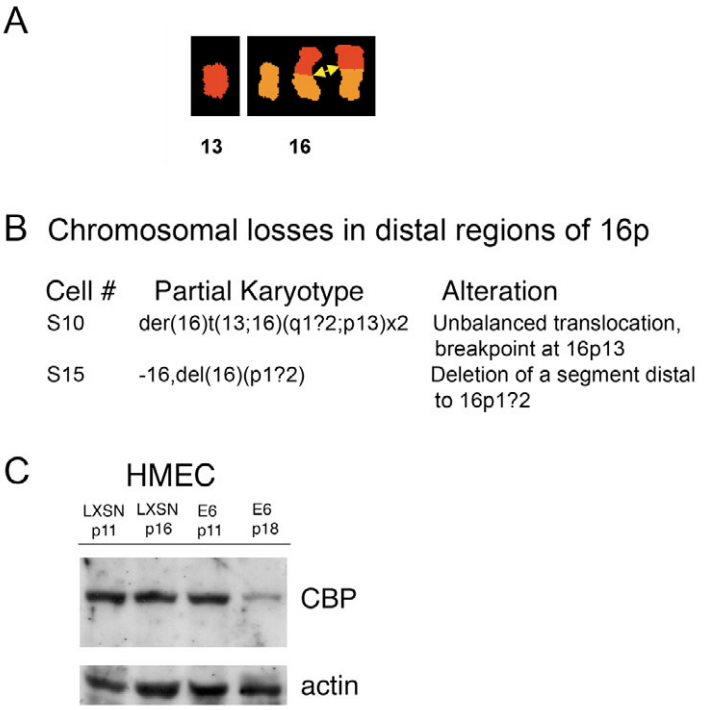

Fig. 1. Partial karyotype and CBP expression of late passage HMEC-E6 cells (passage 20). (A) Partial karyotype of a single mitotic cell demonstrating two copies of an unbalanced translocation between chromosomes 13 and 16 involving 16p13 (arrows). Spectral karyotyping in classification colors (red, chromosome 13 material; orange, chromosome 16 material). (B) Partial karyotypes of two cells that demonstrate either loss of a more distal region of 16p or rearrangement at the CBP locus, 16p13. (C) CBP protein expression is decreased in late passage HMEC-E6 cells. Early and late passage HMEC-LXSN vector controls (LXSN) (passages 11 and 16) and HMEC-E6 cells (E6) (passages 11 and 18) were analyzed for CBP protein expression as described in Materials and Methods. Equal amounts of protein lysate were loaded per lane. Actin was used as a loading control.

Table 3. Differential gene expression data

Expression
LXSN+MG vs E6E+MG

Affymetrix ID	Gene name	LX+MG (max)	LX+MG (min)	E6E+MG (max)	E6E+MG (min)	*P*-value	Fold*
L34155	Laminin-α3	27320.5	24983.1	12660.1	11419.4	3.15E-04	**–2.19**
U17760_rna1	Laminin-β3	20186.5	13978.7	6650.9	5177.5	2.60E-04	**–2.96**
U31201_cds1	Laminin-γ2	2113.7	1764.8	2210.2	1892.2	7.48E-01	+1.05
U31201_cds2	Laminin-γ2	12003.5	10606.4	6279.3	5727.3	5.49E-03	–1.91
M59911	Integrin-α3	3999.9	3699.8	4443.4	3507.5	7.74E-01	+1.05
X07979	Integrin-β1	17214.6	9457.1	16541.4	13266.4	8.79E-01	+1.03

Expression
LXSN+MG vs E6E+MG

Affymetrix ID	Gene name	LX+MG (max)	LX+MG (min)	E6L+MG (max)	E6L+MG (min)	*P*-value	Fold*
L34155	Laminin-α3	27320.5	24983.1	733.2	607.7	7.26E-08	**–38.0**
U17760_rna1	Laminin-β3	20186.5	13978.7	1310.3	811.2	2.92E-06	**–15.8**
U31201_cds1	Laminin-γ2	2113.7	1764.8	140.3	25.9	1.01E-05	**–18.9**
U31201_cds2	Laminin-γ2	12003.5	10606.4	793.8	687.3	3.18E-06	**–15.3**
M59911	Integrin-α3	3999.9	3699.8	6047.5	4928.4	1.06E-01	+1.37
X07979	Integrin-β1	17214.6	9457.1	20614.6	17432.6	1.41E-01	+1.36

*Values highlighted in bold indicate a fold change >2.0 with $P<0.01$.

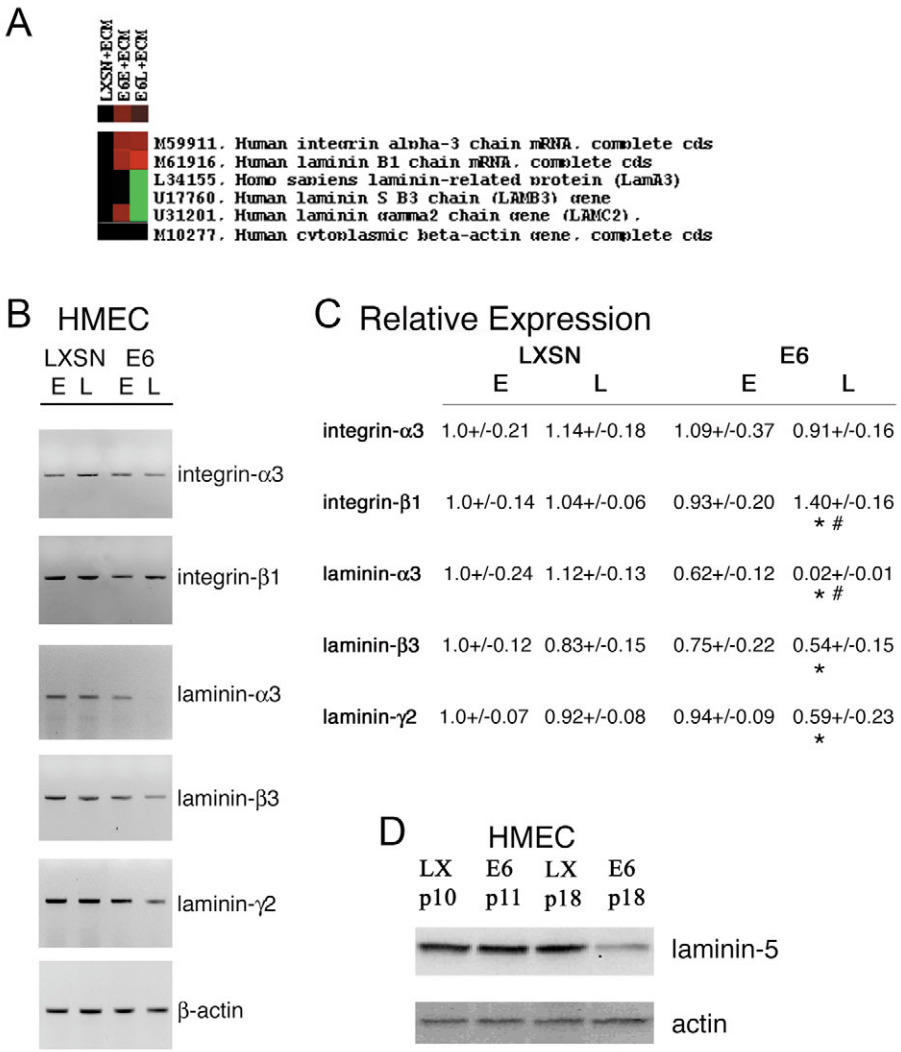

Fig. 2. Laminin-5 α3-chain expression is decreased in rECM-resistant, CBP-poor, late passage HMEC-E6 cells. (A) Analysis of differential gene expression in early (E6E) and late (E6L) passage HMEC-E6 cells (passage 10 and 18) relative to early passage HMEC-LXSN controls (passage 10) (LXSN). Cells were grown in contact with rECM and harvested for differential gene expression. All RNA combinations used for array analysis were obtained from cells that were matched for passage number, cultured under the identical growth conditions, and harvested at identical confluency. Data were collected in triplicate using independent biological replicates. Color-coding: green, downregulation of gene expression; red, induction; black, no significant change; grey, no data available. (B,C) Semi-quantitative RT-PCR analysis of integrin and laminin-5 mRNA expression in early (E) and late (L) passage HMEC-E6 cells (E6) (passage 10 and 18) and HMEC-LXSN controls (LXSN) (passage 10 and 16). Expression was normalized to β-actin. These data are representative of three separate experiments. *Significantly different from LXSN-E (P<0.05); #significantly different from E6-E (P<0.05). (D) Laminin-5 α3-chain protein expression is decreased in rECM-resistant, late passage HMEC-E6 cells (E6) (passage 18) relative to early passage HMEC-E6 cells (E6) (passage 11) and early and late passage HMEC-LXSN controls (LX) (passage 10 and 18). Western analysis was performed as described in Materials and Methods. Equal amounts of protein lysate were loaded per lane. Actin serves as a loading control.

confirmed a 98% decrease in laminin-5 α3-chain (P<0.01), a 46% decrease in laminin-5 β3-chain (P<0.01), and a 41% decrease in laminin-5 γ2-chain (P<0.01) mRNA expression relative to early passage HMEC-LXSN controls (Fig. 2B,C). Late passage HMEC-E6 cells also exhibited an 97% decrease in laminin-5 α3-chain (P<0.01), a 28% decrease in laminin-5 β3-chain (P>0.05), and a 37% decrease in laminin-5 γ2-chain (P>0.05) mRNA expression relative to early passage HMEC-E6 controls (Fig. 2B,C). There was no significant change (P>0.05) in the level of α3/β1-integrin mRNA expression (Fig. 2A-C).

Laminin-5 α3-chain protein has been previously shown to exhibit both a processed and unprocessed form (Aumailley et al., 2003). Western analysis demonstrated that late passage HMEC-E6 cells exhibited an 86% (P<0.01) decrease in unprocessed laminin-5 α3-chain protein relative to early passage HMEC-LXSN cells (Fig. 2D).

Loss of CBP expression in late passage HMEC-E6 cells correlates with a loss of CBP binding to the *LAMA3A* promoter and loss *of LAMA3A* promoter activity

We observed that late passage HMEC-E6 cells grown in rECM culture exhibit reduced levels of CBP protein expression and loss of laminin-5 α3-chain expression. We tested whether the observed decrease in CBP and laminin-5 α3-chain expression in late passage HMEC-E6 cells correlated with loss of CBP binding to the LAMA3A promoter and decreased LAMA3A promoter activity.

The human LAMA3A promoter contains three AP-1 sites at positions –387, –185 and –127 bp (Virolle et al., 1998; Miller et al., 2001). The AP-1 site at position –185 bp is critical for basal activity in mammary epithelial cells (Virolle et al., 1998; Miller et al., 2001). Chromatin immunopreciptation (ChIP) was performed in rECM-resistant, 'CBP-poor' late passage HMEC-E6 cells and controls to test whether the observed decrease in laminin-5 α3-chain expression and loss of LAMA3A activity correlated with a lack of CBP binding to the 277 bp AP-1-rich site of the LAMA3A promoter (position –402 to –125 bp) (Virolle et al., 1998; Miller et al., 2001). Early and late passage HMEC-LXSN control cells and rECM-sensitive, early passage HMEC-E6 cells grown in rECM demonstrated CBP binding to the AP-1-rich site of the LAMA3A promoter. By contrast, rECM-resistant, late passage HMEC-E6 cells, which expressed decreased CBP and low levels of laminin-5 α3-chain, demonstrated markedly

decreased CBP binding (Fig. 3A). These observations suggest that a decrease in CBP expression might promote loss of CBP occupancy of the AP-1-rich site of the LAMA3A promoter.

To test for LAMA3A promoter activity, early and late passage HMEC-E6 and passage-matched HMEC-LXSN controls were transiently transfected with a CAT reporter coupled to the LAMA3A promoter sequence (1403 bp, GenBank accession no. AF279435) and grown in rECM culture. Early passage HMEC-E6 cells and early and late passage HMEC-LXSN controls exhibited a similar level of LAMA3A activity (Fig. 3B). By contrast, late passage HMEC-E6 cells exhibited a 91% decrease (P<0.001) in LAMA3A promoter activity relative to early passage HMEC-E6 cells (Fig. 3B).

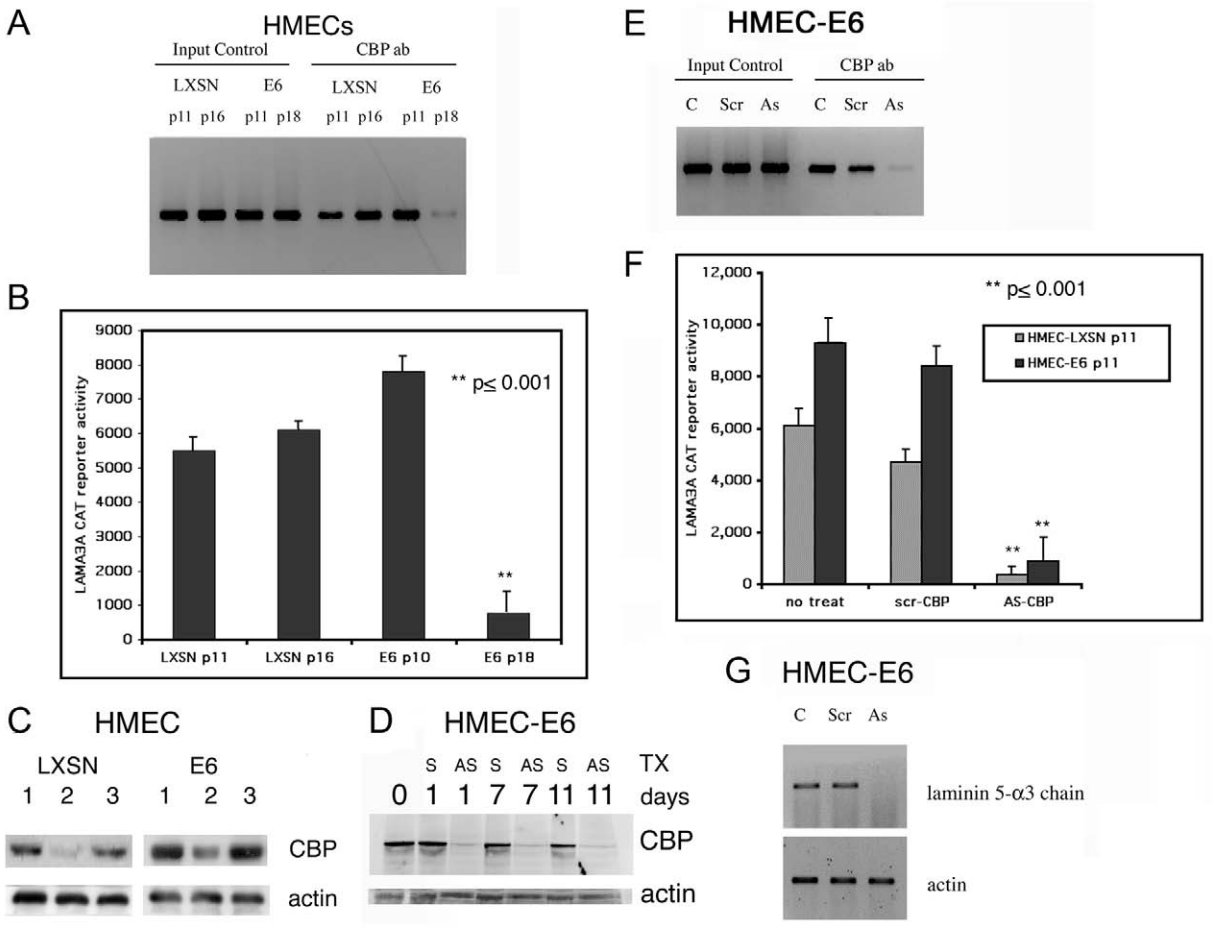

Fig. 3. Loss or suppression of CBP expression inhibits CBP occupancy of the *LAMA3A* promoter and suppresses *LAMA3A* promoter activity and laminin-5 expression. (A) Late passage HMEC-E6 cells do not exhibit CBP occupancy of the 277 bp AP-1-rich region of the *LAMA3A* promoter. ChIP was performed in HMEC-LXSN controls (LXSN) (passage 11 and 16), and early passage HMEC-E6 cells (E6) (passage 11) and compared with CBP-poor, late passage HMEC-E6 cells (E6) (passage 18). Input controls test the integrity of the DNA samples. (B) *LAMA3A* promoter activity was measured in early and late passage HMEC-LXSN controls (LXSN) (passage 11 and 16), and early passage HMEC-E6 cells (E6) (passage 10) and compared with CBP-poor, late passage HMEC-E6 cells (E6) (passage 18). Data represent two independent experiments performed in triplicate. (C) CBP protein expression is suppressed by antisense ODNs. HMEC-LXSN vector controls (LXSN) (passage 12) and early passage HMEC-E6 cells (E6) (passage 12) were cultured in the presence of (1) no treatment, (2) active CBP-specific ODN (A3342V), and (3) inactive CBP ODN (scrA3342V). Resultant cells were analyzed for CBP protein expression as described in Materials and Methods. Equal amounts of protein lysate were added per lane. Actin was used as a loading control. (D) CBP protein expression is suppressed in rECM culture on days 1-11. Early passage HMEC-E6 cells (passage 12) were cultured in rECM and treated daily with active CBP-specific ODN (A3342V) (AS) or inactive CBP ODN (scrA3342) (S). Resultant cells were tested for CBP protein expression as described in Materials and Methods. Equal amounts of protein lysate were added per lane and actin was used as a loading control. (E) Early passage HMEC-E6 cells (passage 10) were treated with CBP-specific ODN (A3342A; As) and inactive CBP ODN (scrA3342V; Scr), grown in contact with rECM, and tested by ChIP to determine whether suppression of CBP expression resulted in a loss of CBP binding to the AP-1-rich site of the *LAMA3A* promoter. Input controls test the integrity of the DNA samples. (F) Suppression of CBP expression results in decreased *LAMA3A* promoter activity. Early passage HMEC-LXSN controls (passage 11) and HMEC-E6 cells (passage 11) grown in rECM and treated with CBP-specific antisense ODNs (A3342V) (AS-CBP) exhibit decreased *LAMA3A* promoter activity relative to cells treated with inactive ODNs (scrA3342V) (scr-CBP). Data represent two independent experiments performed in triplicate. Error bars show standard error. (G) Laminin-5 α3-chain mRNA expression is suppressed by antisense ODNs. Early passage HMEC-E6 cells (passage 12) were cultured in the presence of no treatment (C), inactive CBP ODN (scrA3342V; Scr), and active CBP-specific ODN (A3342V; As). Resultant cells were analyzed for laminin-5 α3-chain mRNA expression by semi-quantitative RT-PCR as described in Materials and Methods. Actin was used as a loading control.

Direct suppression of CBP expression in early passage HMEC-E6 cells results in loss of CBP binding to the *LAMA3A* promoter, lack of *LAMA3A* promoter activity and suppression of laminin-5 α3-chain expression

Antisense ODNs were used to suppress CBP expression in HMECs to test whether direct suppression of CBP in early passage HMEC-E6 cells resulted in altered laminin-5 expression. We specifically tested for (1) loss of CBP binding to the AP-1-rich site of the *LAMA3A* promoter, (2) decrease in *LAMA3A* activity, and (3) suppression of laminin-5 α3-chain expression. Relative levels of CBP protein expression were tested by western analysis. Early passage HMEC-LXSN controls and early passage HMEC-E6 cells treated with the active, CBP-specific ODN, A3342V, exhibited a 98% (P<0.0001) and 81% (P<0.0001) respective decrease in CBP protein expression relative to untreated controls (Fig. 3C). Cells treated with the inactive CBP ODN, scrA3342V, did not exhibit a statistically significant decrease (P>0.05) in CBP protein expression (Fig. 3C). Early passage HMEC-E6 cells treated daily with CBP-specific ODN, A3342V, and grown in rECM culture exhibited a continued decrease in CBP protein expression at days 1, 7 and 11 (78%, 90% and 94%, respectively) (Fig. 3D).

Early passage HMEC-E6 cells treated with CBP-specific ODNs and grown in rECM demonstrated a loss of CBP occupancy of the AP-1-rich region of the *LAMA3A* promoter (Fig. 3E), a 94±7% decrease in *LAMA3A* promoter activity (Fig. 3F), and loss of laminin-5 α3-chain mRNA expression (Fig. 3G). By contrast, early passage HMEC-E6 controls treated with inactive ODNs and grown in rECM demonstrated CBP occupancy of *LAMA3A*, a statistically non-significant decrease (10%, P>0.05) in *LAMA3A* activity, and normal levels of laminin-5 α3-chain mRNA expression (Fig. 3E-G). These observations demonstrate that suppression of CBP expression in HMEC-E6 cells by antisense ODNs results in a loss of CBP occupancy of the AP-1-rich site of the *LAMA3A* promoter. Since the AP-1 site at position –185 is critical for basal activity in mammary epithelial cells (Virolle et al., 1998; Miller et al., 2001), these observations provide a potential mechanism by which loss of CBP expression might promote loss of *LAMA3A* promoter activity and laminin-5 α3-chain expression in HMECs.

Exogenous expression of CBP in late passage HMEC-E6 cells promotes CBP binding to the *LAMA3A* promoter, *LAMA3A* promoter activity and increased laminin-5 α3-chain expression

Retroviral-mediated gene expression was used to express CBP in late passage HMEC-E6 cells. This allowed us to test directly whether expression of physiologic levels of CBP promoted (1) CBP binding to the AP-1-rich site of the LAMA3A promoter, (2) LAMA3A activity, and (3) increased laminin-5 α3-chain expression. Western analysis and RT-PCR confirmed expression of exogenous expression of CBP (Fig. 4A and data not shown). As previously observed, late passage HMEC-E6 cells exhibited a 90% (P<0.001) decrease in CBP protein levels relative to early passage HMEC-E6 cells. Retroviral-mediated exogenous expression of CBP in late passage HMEC-E6 cells resulted in CBP protein levels that were similar (106%) to that of early passage HMEC-E6 cells. Since CBP protein levels are thought to be tightly regulated, it is important that the

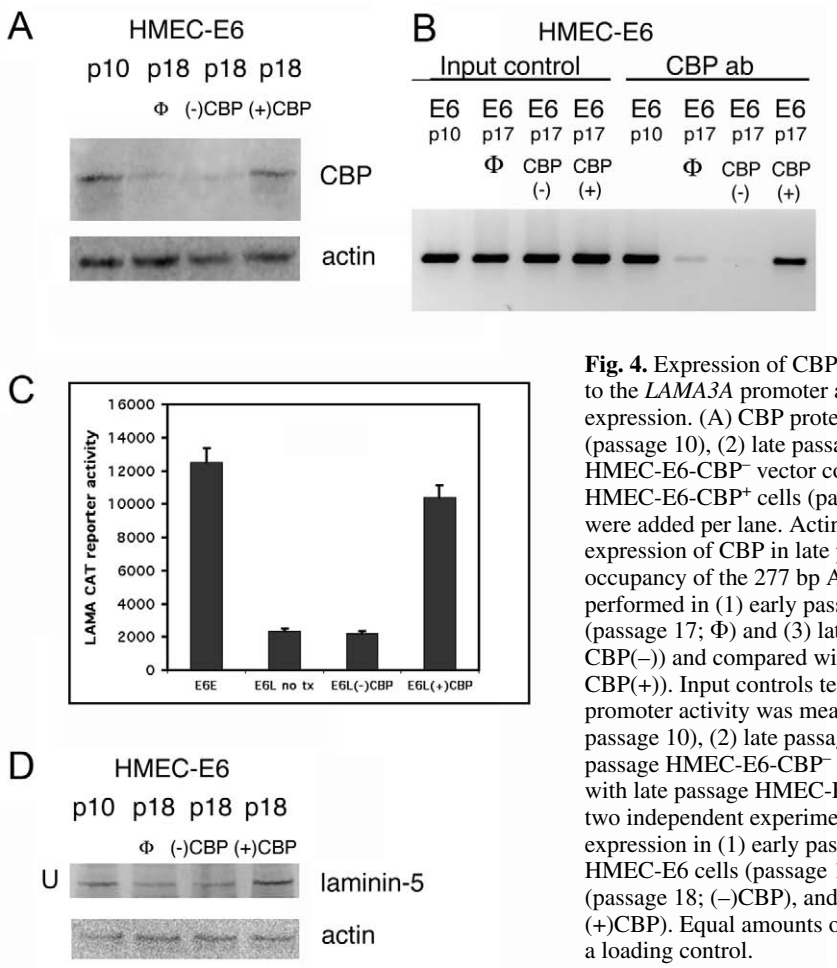

Fig. 4. Expression of CBP in late passage HMEC-E6 cells promotes CBP binding to the *LAMA3A* promoter and increases *LAMA3A* promoter activity and laminin-5 expression. (A) CBP protein expression in (1) early passage HMEC-E6 cells (passage 10), (2) late passage HMEC-E6 cells (passage 18; Φ), (3) late passage HMEC-E6-CBP$^-$ vector controls (passage 18; (–)CBP), and (4) late passage HMEC-E6-CBP$^+$ cells (passage 18; (+)CBP). Equal amounts of protein lysate were added per lane. Actin was used as a loading control. (B) Exogenous expression of CBP in late passage HMEC-E6-CBP$^+$ cells promotes CBP occupancy of the 277 bp AP-1-rich region of the *LAMA3A* promoter. ChIP was performed in (1) early passage HMEC-E6 cells, (2) late passage HMEC-E6 cells (passage 17; Φ) and (3) late passage HMEC-E6-CBP$^-$ vector controls (passage 17; CBP(–)) and compared with late passage HMEC-E6-CBP$^+$ cells (passage 17; CBP(+)). Input controls test the integrity of the DNA samples. (C) *LAMA3A* promoter activity was measured in (1) early passage HMEC-E6 cells (E6E; passage 10), (2) late passage HMEC-E6 cells (E6L no tx; passage 18), and (3) late passage HMEC-E6-CBP$^-$ vector controls (E6L(–)CBP; passage 18) and compared with late passage HMEC-E6-CBP$^+$ cells (E6L(+)CBP; passage 18). Data represent two independent experiments performed in triplicate. (D) Laminin-5 protein expression in (1) early passage HMEC-E6 cells (passage 10), (2) late passage HMEC-E6 cells (passage 18; Φ), (3) late passage HMEC-E6-CBP$^-$ vector controls (passage 18; (–)CBP), and (4) late passage HMEC-E6-CBP$^+$ cells (passage 18; (+)CBP). Equal amounts of protein lysate were added per lane. Actin was used as a loading control.

level of CBP protein expression in transduced late passage HMEC-E6 cells was not significantly greater than baseline CBP levels in early passage HMEC-E6 cells, HMEC-LXSN vector controls and parental HMECs (Fig. 4A and data not shown).

Late passage HMEC-E6-CBP$^+$ cells expressing exogenous CBP demonstrated CBP occupancy of the AP-1-rich region of the *LAMA3A* promoter (Fig. 4B). Expression of CBP in late passage HMEC-E6-CBP$^+$ cells resulted in *LAMA3A* promoter activity that was comparable (74%, $P<0.01$) with early passage HMEC-E6 cells (Fig. 4C). Finally, late passage HMEC-E6-CBP$^+$ cells exhibited laminin-5 expression α3-chain protein at levels that were equivalent (122%, $P<0.01$) to early passage HMEC-E6 cells (Fig. 4D). By contrast, late passage HMEC-E6 CBP$^-$ controls transduced with the empty LXSN retroviral vector lacked CBP occupancy of *LAMA3A*, and exhibited low levels of *LAMA3A* activity and laminin-5 α3-chain protein expression similarly to late passage HMEC-E6 cells (Fig. 4). These observations further demonstrate that CBP plays an important role in regulating *LAMA3A* promoter activity and laminin-5 α3-chain expression in HMECs.

Loss or suppression of CBP in HMECs grown in rECM results in a lack of polarized expression of laminin-5 α3 and integrin-α3 proteins

Early and late passage HMEC-LXSN controls and HMEC-E6 cells were grown in rECM and tested for laminin-5 α3-chain, and α3- and β1-integrin expression and distribution by immunocytochemistry. Early and late passage HMEC-LXSN controls and early passage HMEC-E6 cells exhibited polarized expression of laminin-5 α3-chain and α3- and β1-integrins on the basal surface (Fig. 5A and data not shown). By contrast, late passage, CBP-poor HMEC-E6 cells grown in rECM demonstrated disorganized plasma membrane and cytosolic expression of α3-integrin (Fig. 5A). As predicted by differential gene expression studies and western analysis, there was also a decrease in laminin-5 α3-chain expression in late passage HMEC-E6 cells relative to controls (Fig. 5A). Late passage HMEC-E6 cells that expressed low levels of CBP exhibited polarized basal β1-integrin expression but had increased cytosolic expression relative to early passage cells (data not shown).

Late passage HMEC-E6 cells grown in rECM culture

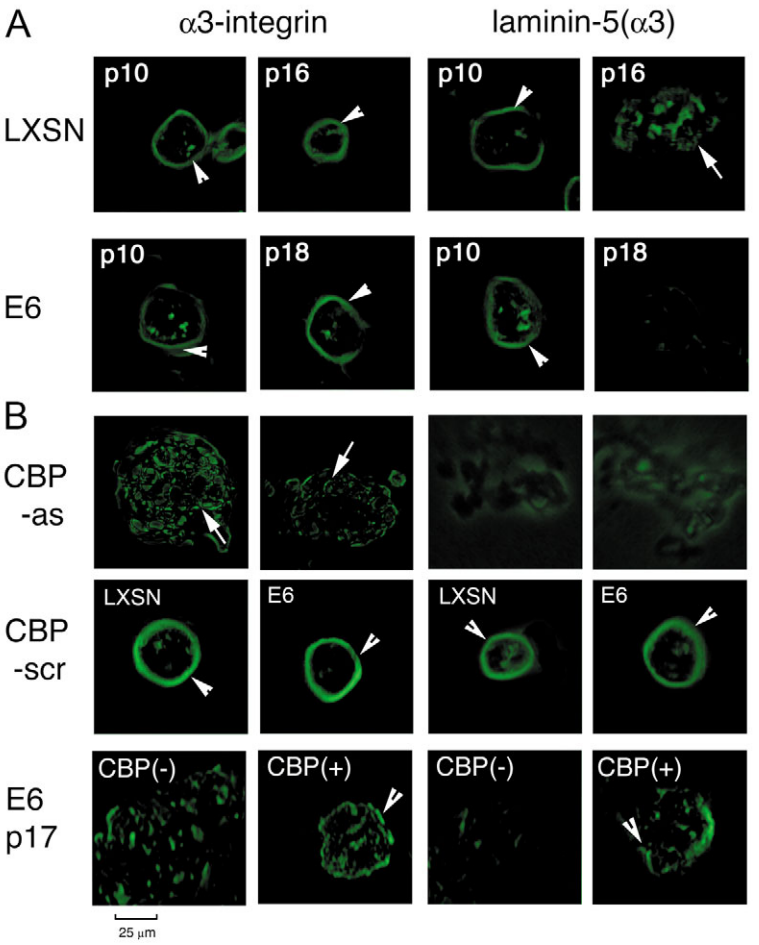

Fig. 5. Expression and distribution of α3-integrin and laminin-5 α3-chain in HMECs that express altered levels of CBP. (A) Immunofluorescence characterization of α3-integrin and laminin-5 α3-chain expression in cells sensitive and resistant to rECM-mediated growth arrest and apoptosis. Frozen section of early and late passage HMEC-LXSN controls (LXSN; passage 10 and 16) and HMEC-E6 cells (E6; passage 10 and 18) were grown in rECM for 6 days, cryosectioned, and immunostained for localization of α3-integrin and laminin-5 α3-chain expression. α3-integrin and laminin-5 α3-chain expression was primarily localized at the basal surface of early and late passage HMEC-LXSN and early passage HMEC-E6 cells (arrowheads). By contrast, CBP-poor late passage HMEC-E6 cells showed dispersed membrane and intracellular staining of α3-integrin (arrow) and qualitatively decreased laminin-5 α3-chain expression. (B) Immunofluorescent characterization of α3β1-integrin and laminin-5 α3-chain expression in HMECs treated with CBP antisense ODNs. Frozen section of early passage HMEC-LXSN vector controls (LXSN) (passage 11) and HMEC-E6 cells (E6) (passage 11) treated either with CBP antisense ODN (A3342V; CBP-as) or inactive CBP ODN (scrA3342V; CBP-scr). Cells were grown in rECM for 6 days, cryosectioned, and immunostained for α3-integrin or laminin-5 α3-chain. α3-integrin and laminin-5 α3-chain expression was primarily localized at the basolateral surface in HMEC-LXSN and HMEC-E6 cells treated with inactive CBP ODNs (arrowheads). By contrast, HMEC-LXSN and HMEC-E6 cells treated with antisense CBP ODNs demonstrated disorganized membrane and cytosolic staining of α3-integrin (arrows) and markedly reduced laminin-5 α3-chain expression. (C) Immunofluorescent characterization of α3β1-integrin and laminin-5 α3-chain expression in late passage HMEC-E6 cells expressing exogenous CBP. Frozen sections of immunostained late passage HMEC-E6-CBP$^-$ vector controls (CBP(–); passage 17) and late passage HMEC-E6-CBP$^+$ cells (CBP(+); passage 17). Cells were grown in rECM for 6 days, cryosectioned, and immunostained for α3-integrin or laminin-5 α3-chain. HMEC-E6-CBP$^-$ cells demonstrated disorganized membrane and cytosolic staining of α3-integrin and markedly reduced levels of laminin-5 α3-chain expression. By contrast, HMEC-E6-CBP$^+$ cells exhibited a qualitative increase in laminin-5 α3-chain expression. Although there was persistent membrane and cytosolic staining of α3-integrin and laminin-5 α3-chain, there was also increased localization at the basolateral surface (arrowheads).

exhibited reduced levels of CBP protein expression and disorganized expression of both laminin-5 α3-chain and α3-integrin. This observation led us to hypothesize that direct suppression of CBP in HMECs would alter laminin-5 α3-chain and α3-integrin expression and/or distribution in rECM culture. CBP protein expression was suppressed in early passage HMEC-E6 cells and HMEC-LXSN controls by treatment with CBP-specific, antisense ODN (A99424V). HMECs that had suppressed levels of CBP exhibited disorganized plasma membrane and cytosolic distribution of α3-integrin (Fig. 5B) and qualitatively reduced levels of laminin-5 α3-chain expression (Fig. 5B). β1-integrin expression was observed at the basal surface (data not shown). By contrast, early passage HMEC-LXSN controls and HMEC-E6 cells treated with inactive CBP ODN (scrA99424V) exhibited polarized basal expression of laminin-5 α3-chain and α3- and β1-integrins (Fig. 5B, and data not shown). These observations demonstrate that suppression of CBP protein expression in HMECs alters the distribution of both laminin-5 α3-chain and α3-integrin in rECM culture.

Expression of CBP in HMECs partially restores polarized expression of laminin-5 α3 and integrin-α3 proteins

Late passage HMEC-E6 cells, late passage HMEC-E6-CBP^{-} vector controls, and late passage HMEC-E6-CBP^{+} cells expressing exogenous CBP were grown in rECM and tested for laminin-5 α3-chain and α3- and β1-integrin expression and distribution by immunocytochemistry. Late passage, CBP-poor HMEC-E6 cells and late passage HMEC-E6-CBP^{-} control cells grown in rECM demonstrated disorganized plasma membrane and cytosolic expression of α3-integrin and a qualitative decrease in laminin-5 α3-chain expression (Fig. 5C). By contrast, late passage HMEC-E6-CBP^{+} cells expressing exogenous CBP exhibited partial but not fully polarized expression of laminin-5 α3-chain and α3-integrin on the basal surface (Fig. 5C and data not shown). As predicted by western analysis, there was also a qualitative increase in laminin-5 α3-chain expression in late passage HMEC-E6-CBP^{+} cells relative to controls (Fig. 5C).

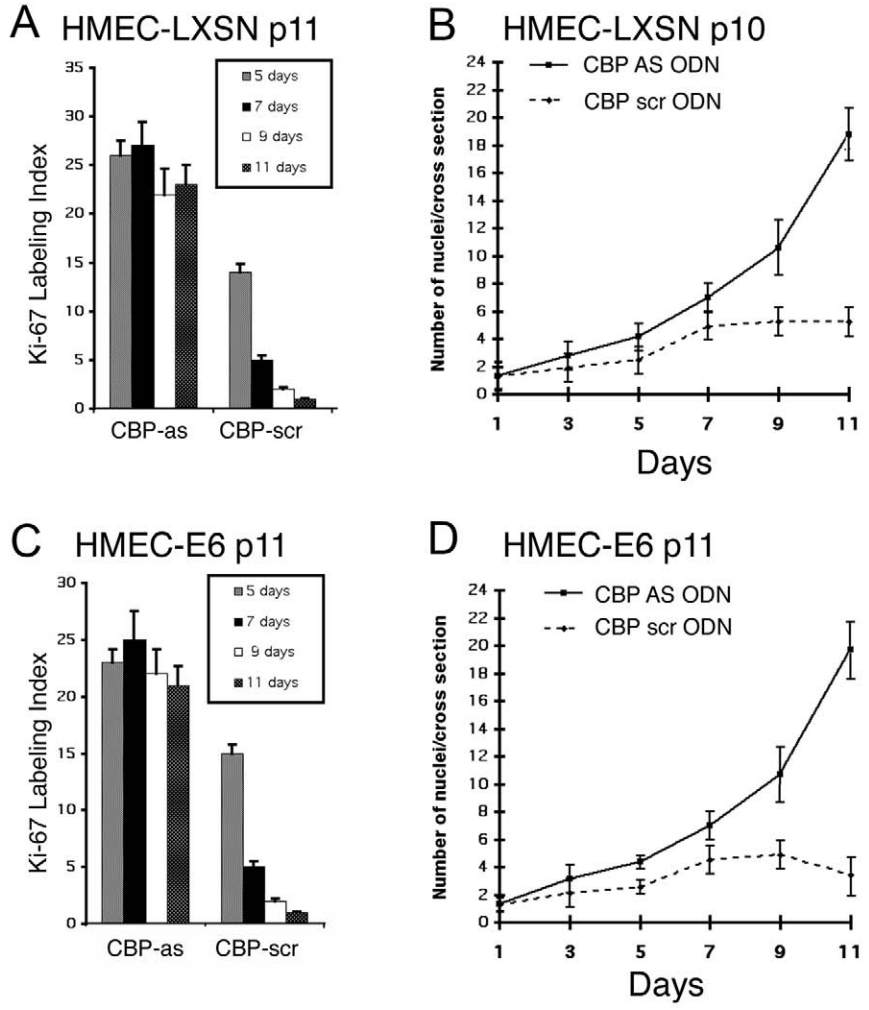

Fig. 6. Modulation of CBP expression alters proliferation in rECM culture. (A-D) Inhibition of CBP expression in HMECs by antisense ODNs results in enhanced proliferation in rECM. Ki-67 staining indices (A,C) in early passage HMEC-LXSN cells (passage 11) (A) and early passage HMEC-E6 cells (passage 11) (C). The mean number of nuclei per cell cluster (B,D) in early passage HMEC-LXSN vector controls (passage 10) (B) and early passage HMEC-E6 cells (passage 11) (D) treated with either CBP antisense ODN (A3342V; CBP AS) or inactive CBP ODN (scrA3342V; CBP scr). Two hundred cells were surveyed per time point and indices were calculated from an average of three independent experiments. Error bars show standard error.

Suppression of CBP expression results in dysregulated proliferation and inhibits apoptosis in rECM culture

Late passage HMEC-E6 cells lost both rECM-mediated growth arrest and apoptosis associated with loss of polarized expression of the laminin-5 receptor, α3β1-integrin (Seewaldt et al., 2001b), and loss of CBP expression. Loss or suppression of CBP in HMECs results in loss of laminin-5 expression. Based on these observations we hypothesized that direct suppression of CBP in early passage HMEC-E6 cells grown in rECM would result in dysregulated proliferation and block apoptosis.

Suppression of CBP expression in early passage HMEC-LXSN controls and HMEC-E6 cells resulted in enhanced proliferation in rECM-culture as measured by Ki-67 staining and DAPI staining of cell nuclei. Treatment of early passage HMEC-LXSN and HMEC-E6 cells with CBP-specific ODNs (A33243V) resulted in continued Ki-67 staining at 9 and 11 days in rECM culture (Fig. 6A,C). DAPI-stained early passage HMEC-LXSN controls and HMEC-E6 cells treated with active CBP-specific ODNs (A33243V) demonstrated a continued increase in the number of cells per cell cluster from day 7-11 (Fig. 6B,D). By contrast, early passage HMEC-LXSN

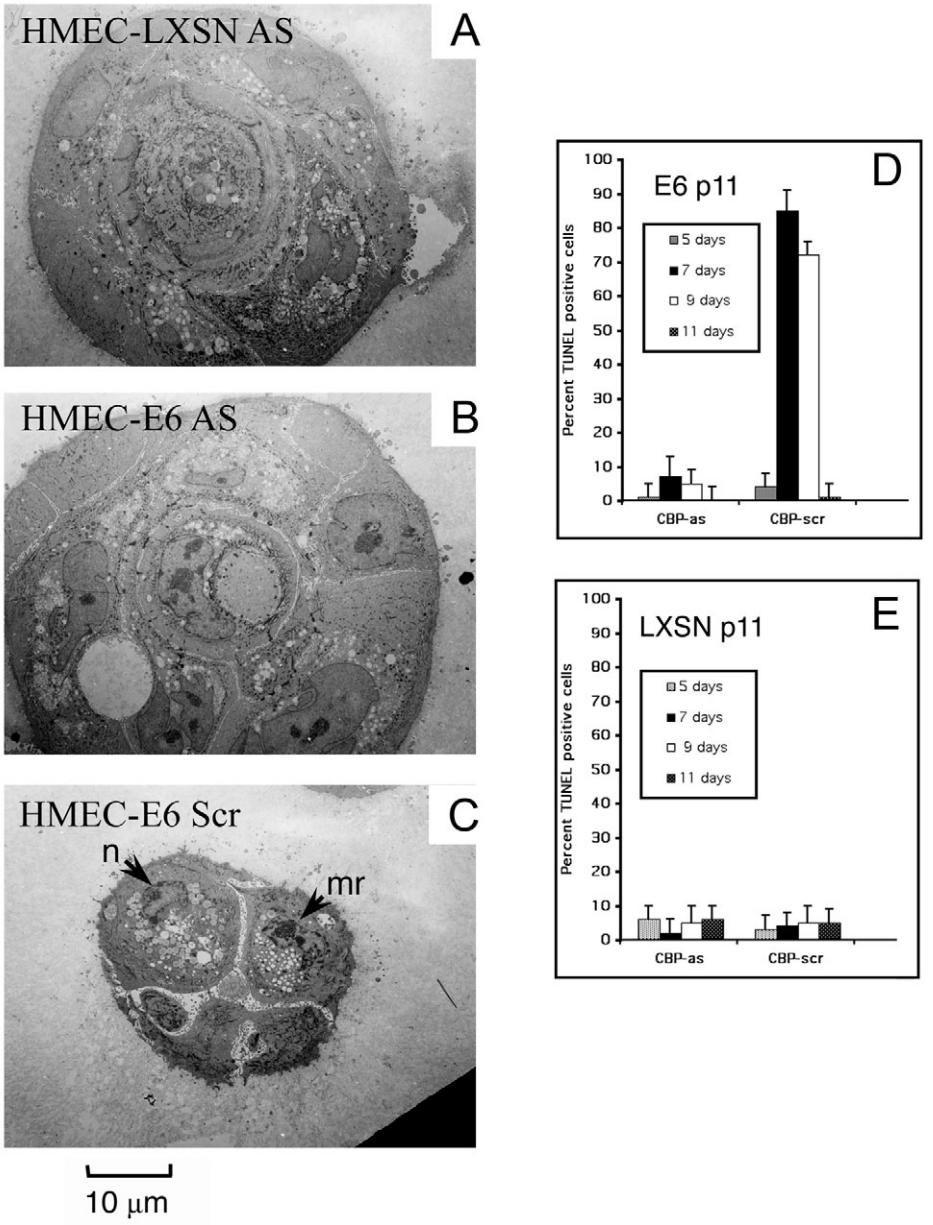

Fig. 7. Inhibition of CBP in early passage HMECs by antisense ODNs blocks apoptosis in rECM. Electron micrographs of early passage HMEC-LXSN control cells (passage 11) (A) and early passage HMEC-E6 cells (passage 11) (B) treated with CBP antisense (A3342V) ODN and grown in rECM for 9 days. Cells formed large, dense, irregularly shaped, multicellular colonies that have no central lumen (A,B). By contrast, early passage HMEC-E6 cells (passage 10) treated with inactive CBP ODN (scrA3342V) (C) underwent apoptosis when grown in rECM for 7 days as shown by (1) nuclear condensation (n), (2) cell shrinkage and separation, and (3) margination of chromatin (mr). Percentage of apoptotic cells in early passage HMEC-E6 cells (passage 11) (D) and early passage HMEC-LXSN controls (passage 11) (E) treated either with active (A3342V; CBP-as) or inactive (scrA3342V; CBP-scr) CBP-specific ODNs. Apoptosis was measured by TUNEL-staining. Apoptotic index was measured by calculating the percentage of TUNEL-stained cells relative to the total number of cells surveyed. Data represents an average of three independent experiments. Error bars show standard error.

controls and HMEC-E6 cells treated with inactive ODNs (scrA33243V) did not exhibit a continued increase in Ki-67 staining nor an increase in cell number per cell cluster after day 7 (Fig. 6). These observations show that suppression of CBP protein expression in early passage HMEC-E6 cells and HMEC-LXSN controls results in enhanced proliferation in rECM culture.

Early passage HMEC-E6 cells were treated with CBP-specific antisense ODNs to test whether suppression of CBP protein expression blocked apoptosis in rECM culture. Early passage HMEC-E6 cells treated with CBP-specific antisense ODNs (A33423V) formed large irregular clusters in rECM and did not undergo apoptosis on days 7-11 as assessed by electron microscopy and TUNEL-staining (Fig. 7B,D). By contrast, early passage HMEC-E6 cells treated with inactive CBP ODNs underwent apoptosis on day 7, as assessed by either morphologic criteria or TUNEL-staining (Fig. 7C,D). Similarly to early passage HMEC-E6 cells, early passage HMEC-LXSN cells treated with CBP-specific, antisense ODNs (A33423V) formed large irregular clusters in rECM and did not undergo apoptosis (Fig. 7A,E). Early passage HMEC-LXSN controls treated with inactive ODN (scrA33423V) formed morphologically organized structures and did not undergo apoptosis (Fig. 7E and data not shown). These observations demonstrate that suppression of CBP protein expression in HMEC-E6 cells by antisense ODNs blocks apoptosis in rECM culture.

A second HMEC strain, AG11134, was tested to ensure that these observations were not HMEC strain-specific. Similarly to HMEC strain AG11132 cells, early passage AG11134-E6 cells treated with inactive CBP ODN (scrA33423V) were sensitive to rECM-growth regulation and underwent apoptosis at day 7, early passage AG1134-LXSN controls treated with CBP-specific antisense ODN (A99424V) were resistant to

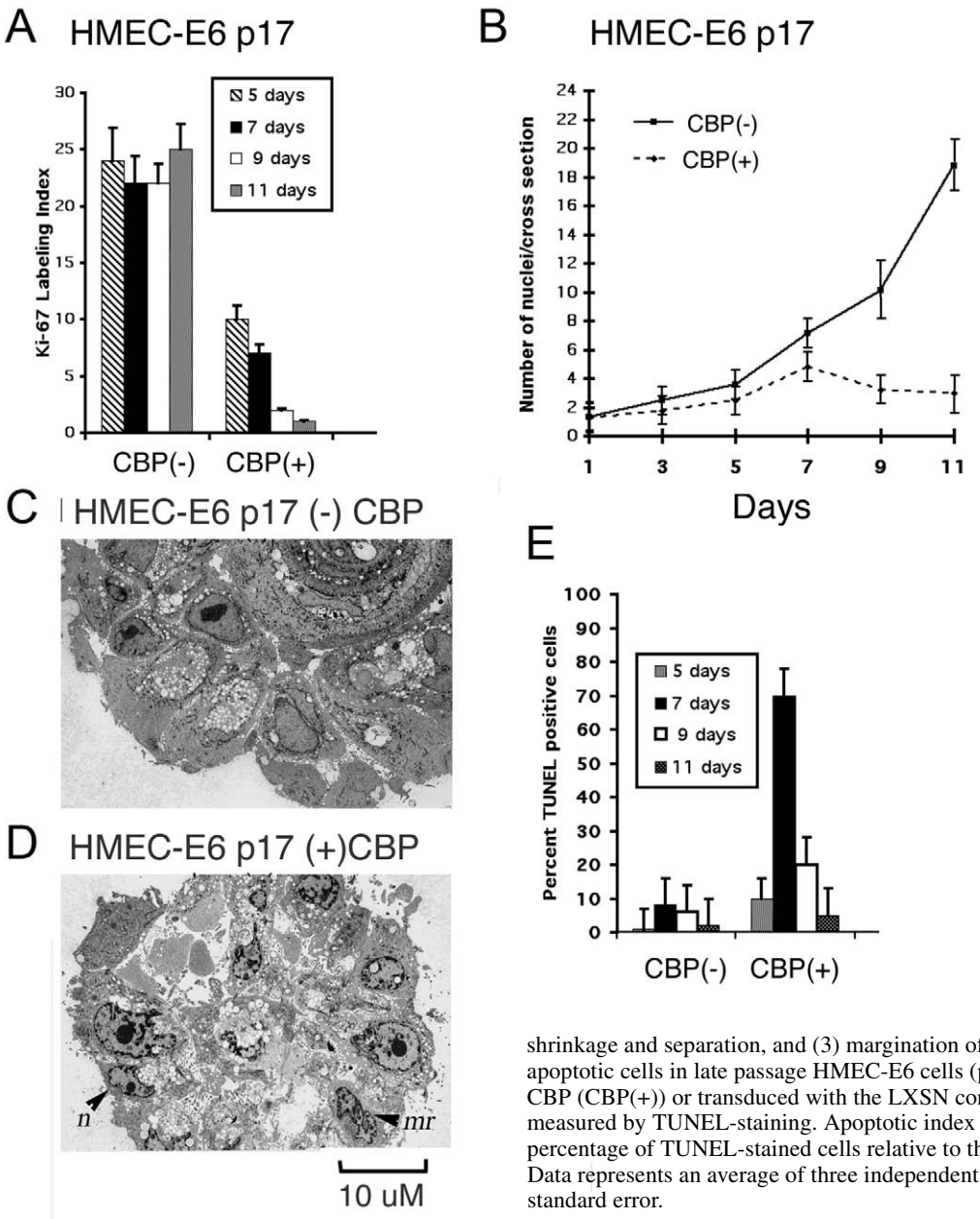

Fig. 8. Expression of CBP in late passage HMEC-E6 cells promotes growth regulation and apoptosis in rECM culture. (A,B) Exogenous expression of CBP in apoptosis-resistant late passage HMEC-E6 cells results in decreased growth in rECM culture. (A) Ki-67 staining indices in late passage HMEC-E6 cells (passage 17) expressing exogenous CBP (CBP(+)) or transduced with the LXSN control vector (CBP(–)). (B) The number of nuclei per cell cluster formed by late passage HMEC-E6 cells (passage 17) expressing exogenous CBP (CBP(+)) or transduced with the LXSN control vector (CBP(–)). Two hundred cells were surveyed per time point and indices were calculated from an average of three independent experiments. Error bars show standard error. (C,D) Electron micrographs of late passage HMEC-E6 cells (passage 17) expressing exogenous CBP ((+)CBP) or transduced with the LXSN control vector ((–)CBP) grown in rECM for 7 days. Late passage HMEC-E6-CBP(–) control cells formed large, dense, irregularly shaped, multicellular colonies that have no central lumen (C). By contrast, late passage HMEC-E6-CBP$^+$ cells underwent apoptosis when grown in rECM for 7 days (D) as shown by (1) nuclear condensation (n), (2) cell shrinkage and separation, and (3) margination of chromatin (mr). (E) Percentage of apoptotic cells in late passage HMEC-E6 cells (passage 16) expressing exogenous CBP (CBP(+)) or transduced with the LXSN control vector (CBP(–)). Apoptosis was measured by TUNEL-staining. Apoptotic index was measured by calculating the percentage of TUNEL-stained cells relative to the total number of cells surveyed. Data represents an average of three independent experiments. Error bars show standard error.

rECM growth arrest and did not undergo apoptosis on days 7-11, and early passage AG11134-LXSN controls treated with CBP-specific antisense ODNs were resistant to rECM-mediated growth regulation and did not undergo apoptosis (data not shown).

Expression of CBP in late passage HMEC-E6 cells promotes growth regulation and apoptosis in rECM culture

Exogenous expression of CBP in late passage HMEC-E6-CBP$^+$ cells resulted in reduced proliferation on days 5-11 relative to late passage HMEC-E6-CBP$^-$ controls transduced with the empty LXSN vector alone (Fig. 8A,B). Proliferation in rECM-culture was measured by Ki-67 staining and DAPI staining as above. Late passage HMEC-E6-CBP$^+$ cells expressing exogenous CBP exhibited a decrease in Ki-67 staining and did not exhibit an increase in the cell number per cell cluster after day 5 (Fig. 8A,B). By contrast, late passage HMEC-E6-CBP$^-$ vector control cells demonstrated continued Ki-67 staining and a continued increase in the number of cells per cell cluster on days 7-11 (Fig. 8A,B).

Late passage HMEC-E6-CBP$^+$ cells expressing exogenous CBP and late passage HMEC-E6-CBP$^-$ vector controls were tested for the presence of apoptosis by electron microscopy and TUNEL-staining. Late passage HMEC-E6-CBP$^+$ cells underwent apoptosis on day 7 as shown by morphological criteria, including nuclear condensation, cell shrinkage and margination of chromatin, and by TUNEL-staining (Fig. 8D,E). By contrast, late passage HMEC-E6-CBP$^-$ vector controls did not undergo apoptosis and formed large irregular clusters in rECM (Fig. 8C,E).

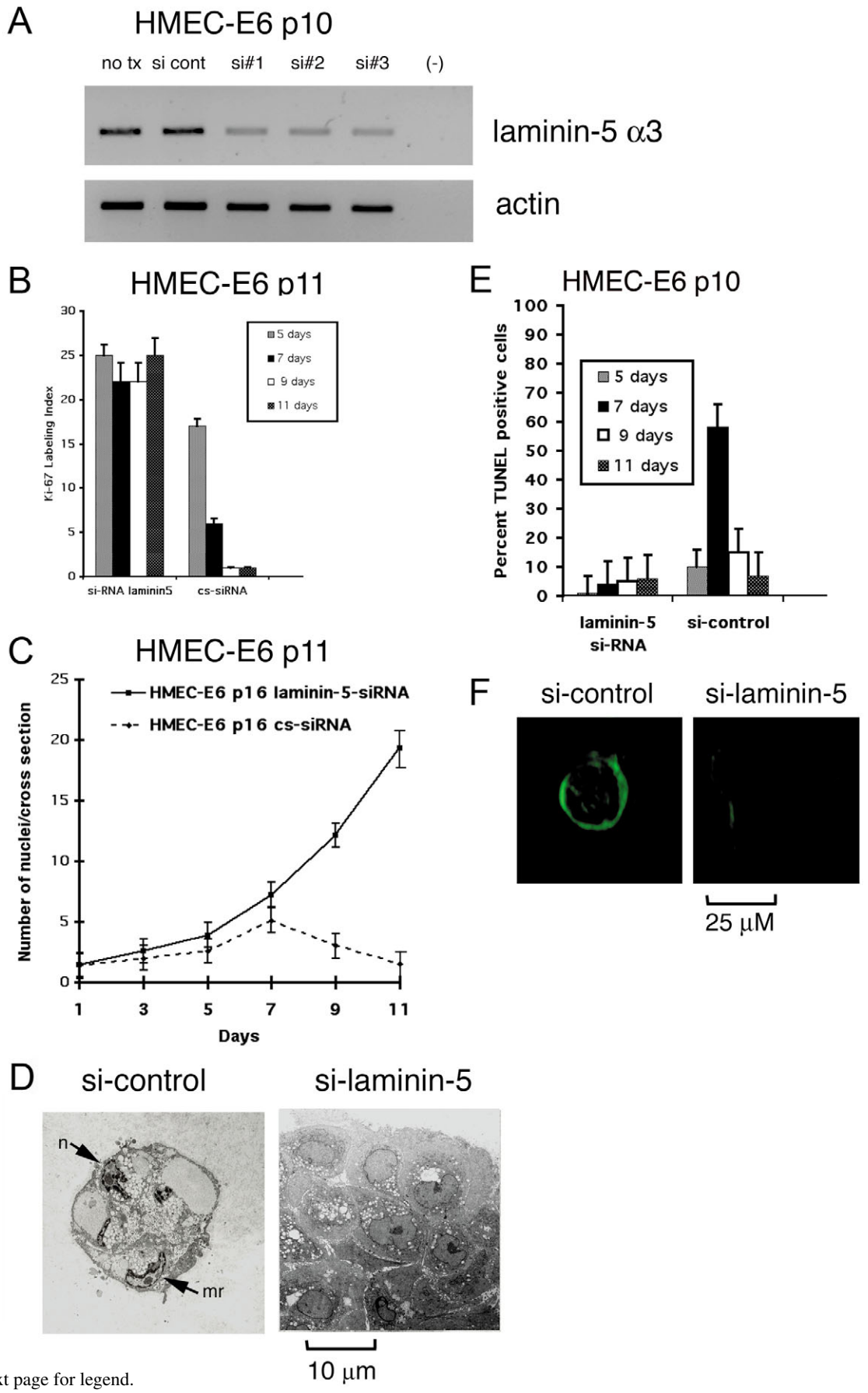

Fig. 9. See next page for legend.

Fig. 9. Suppression of laminin-5 α3-chain in early passage HMEC-E6 cells blocks apoptosis in rECM. (A) Laminin-5 α3-chain mRNA expression is compared by semi-quantitative RT-PCR in three early passage HMEC-E6 cells (passage 10) clones expressing siRNA sequences directed against laminin-5 α3-chain (si#1, si#2, si#3) or control siRNA (si-cont), and in HMEC-E6 control cells (no tx). Actin was used as a loading control. (B,C) Suppression of laminin-5 α3-chain expression in early passage HMEC-E6 cells results in increased proliferation in rECM culture. (B) Ki-67 staining indices in early passage HMEC-E6 cells (passage 11) expressing siRNA sequence #2 directed against laminin-5 α3-chain or siRNA control. (C) DAPI staining of cell nuclei demonstrates the number of nuclei per cell cluster formed by early passage HMEC-E6 cells (passage 11) expressing either siRNA sequence #2 directed against laminin-5 α3-chain or siRNA control. Two hundred cells were surveyed per time point and indices were calculated from an average of three independent experiments. Error bars show standard error. (D) Electron micrographs of early passage HMEC-E6 cells (passage 11) expressing siRNA sequence #2 directed against laminin-5 α3-chain (si-laminin-5) or control siRNA (si-control). Early passage HMEC-E6 cells expressing control siRNA underwent apoptosis when grown in rECM for 7 days as shown by (1) nuclear condensation (n), (2) cell shrinkage and separation, and (3) margination of chromatin (mr). By contrast, HMEC-E6 cells expressing siRNA directed against laminin-5 α3-chain did not undergo apoptosis and instead formed large, dense, irregularly shaped multicellular colonies that have no central lumen. (E) Relative levels of TdT-positive cells in early passage HMEC-E6 cells (passage 10) treated either with siRNA sequence #2 directed against laminin-5 α3-chain (laminin-5 si-RNA) or control siRNA (si-control). Apoptosis was measured by TUNEL-staining. Data represents an average of two independent experiments in triplicate. Error bars show standard error. (F) Immunofluorescent characterization of laminin-5 α3-chain expression in early passage HMEC-E6 cells (passage 12) expressing si-RNA directed against laminin-5 α3-chain (si-laminin-5) or control siRNA (si-control). Cells were grown in rECM for 6 days, cryosectioned, and immunostained for laminin-5 α3-chain. Laminin-5 α3-chain expression was primarily localized at the basolateral surface in early passage HMEC-E6 cells expressing control siRNA. By contrast, early passage HMEC-E6 cells expressing si-RNA directed against laminin-5 α3-chain exhibited markedly reduced laminin-5 α3-chain expression.

Inhibition of laminin-5 α3-chain expression in early passage HMEC-E6 cells results in loss of rECM-mediated growth control and apoptosis

Laminin-5 was directly inhibited in early passage HMEC-E6 cells using a siRNA construct targeted against the laminin-5 α3-chain. A 79% (P<0.01) decrease in laminin-5 α3-chain mRNA expression was observed in siRNA-expressing early passage HMEC-E6 cells relative to cells expressing control siRNA or untransduced cells (Fig. 9A). Early passage HMEC-E6 cells expressing siRNA directed against laminin-5 α3-chain grown in rECM exhibited a qualitative decrease in laminin-5 protein expression versus early passage HMEC-E6 cells expressing control siRNA (Fig. 9F). Suppression of laminin-5 expression in early passage HMEC-E6 cells blocked rECM-mediated growth regulation as measured by Ki-67 staining and DAPI staining of cell nuclei. Early passage HMEC-E6 cells treated with siRNA directed against laminin-5 exhibited continued Ki-67 staining and an increase in the cell number per cell cluster after day 5 (Fig. 9B,C). By contrast, early passage HMEC-E6 cells treated with control siRNA demonstrated a decrease in Ki-67 staining and a decrease in the number of cells per cell cluster on days 7-11 (Fig. 9B,C). Early passage HMEC-E6 cells treated with siRNA did not exhibit apoptosis by either electron microscopy or TUNEL-staining (Fig. 9D,E). HMEC-E6 cells treated with control siRNA exhibited apoptosis by both electron microscopy and TUNEL-staining (Fig. 9D,E). Taken together, these observations support a role for laminin-5 in regulating proliferation and apoptosis of HMECs in rECM culture.

Discussion

Here we demonstrate a mechanism by which loss of CBP expression in basal-cytokeratin-positive HMECs promotes loss of rECM-mediated growth regulation and apoptosis. CBP is a tightly regulated transcription factor that regulates proliferation, differentiation and apoptosis. Current models suggest that CBP is present in limiting amounts and transcriptional regulation may be, in part, achieved through competition for this cofactor (Kawasaki et al., 1998; Yao et al., 1998; Shang et al., 2000). In this report, we show that loss or suppression of CBP protein expression in basal-cytokeratin-positive HMECs results in loss of rECM-mediated growth regulation and apoptosis (Figs 6-8). Expression of CBP in CBP-poor late passage HMEC-E6 cells results in restoration of rECM-mediated growth regulation and apoptosis sensitivity (Fig. 8). Consistent with observations in this in vitro system, suppression of CBP protein levels in virgin $CBP^{+/-}$ heterozygote mice results in a 90% incidence of severe mammary gland hyperplasia and hyperlactation (T. P. Yao, personal communication). Taken together, these observations provide evidence that loss of CBP protein expression in mammary epithelial cells promotes loss of rECM-mediated growth regulation and apoptosis.

We observe that loss of CBP expression results in loss of CBP occupancy of the AP-1-rich region of the *LAMA3A* promoter and inhibits *LAMA3A* promoter activity and expression of laminin-5 α3-chain (Figs 2, 3, 5). This observation suggests a potential mechanism for CBP regulation of rECM-mediated growth regulation and apoptosis. Both the mouse and human *LAMA3A* promoter contain an AP-1-rich region (Virolle et al., 1998; Millet et al., 2001). The second AP-1 binding site present in both the mouse and human *LAMA3A* promoter is critical for baseline transcription of laminin-5 α3-chain (Virolle et al., 1998; Miller et al., 2001). We also show that suppression of CBP results in loss of CBP occupancy of the *LAMA3A* promoter, loss of *LAMA3A* promoter activity, and decreased laminin-5 α3-chain expression (Fig. 3). Conversely, exogenous expression of CBP in late passage HMEC-E6 cells that express low levels of CBP promotes CBP occupancy of the *LAMA3A* promoter, an increase in *LAMA3A* promoter activity, and laminin-5 α3-chain expression (Fig. 4). The decreased production of laminin-5 α3 correlated with loss of CBP occupancy of the AP-1-rich region of the *LAMA3A* promoter. Direct suppression of laminin-5 α3-chain expression resulted in dysregulated proliferation and loss of apoptosis sensitivity in rECM culture (Fig. 9). Taken together, these observations suggest that CBP occupancy of the *LAMA3A* promoter promotes laminin-5 α3-chain expression and loss of CBP occupancy inhibits laminin-5 α3-chain

expression and results in loss of growth regulation and apoptosis in rECM culture.

In contrast to our observation that suppression of CBP inhibits laminin-5 α3-chain expression in HMECs, it has been previously observed that overexpression of the related coactivator p300 inhibits laminin-5 production in MCF-10A cells (Miller et al., 2000). One potential explanation for these seemingly divergent results may lie in differences in cell type. MCF-10A is an immortalized human breast epithelial cell line that exhibits complex chromosomal rearrangements (Yoon et al., 2002). Our CBP suppression studies were performed in either early passage HMEC-LXSN control cells or in early passage HMEC-E6 cells. These transduced cell strains are not immortalized and previous cytogenetic analysis demonstrates the absence of chromosomal rearrangements in early passage transduced HMECs (Seewaldt et al., 2001b). It is also possible that the difference between these previous studies and our results can be accounted for by differences between CBP and p300 activities. Although p300 and CBP have many overlapping functions, there is ample evidence that they also have distinct activities. For example, CBP and p300 play distinct roles during retinoic-acid-induced differentiation in F9 cells (Kawasaki et al., 1998; Ugai et al., 1999), and p300, but not CBP, has been shown to be transcriptionally regulated by BRCA1 in breast cancer cell lines (Fan et al., 2002).

Observations in this model system are consistent with prior studies showing loss of laminin-5 α3-chain expression during early carcinogenesis (Sathyanarayana et al., 2003) but do not explain the seemingly paradoxical observation that increased laminin-5 γ2-chain expression and cleavage is associated with tumor invasion (Pyke et al., 1994; Seftor et al., 2001; Yamamoto et al., 2001). However, the rECM-resistant cells used in this model system are not transformed and do not exhibit invasion in in vitro assays and, therefore, do not represent a model of invasive cancer.

Tumorigenesis is thought to be a multistep process; there is increasing evidence that epigenetic changes, including DNA methylation and coactivator/corepressor shifts, may play an important role in modulating gene expression during carcinogenesis. For example, studies have shown that transcription of the E-cadherin gene is downregulated during early carcinogenesis by both promoter hypermethylation and modulation of coactivator/corepressor expression (Thiery, 2003). Similarly to this observation involving E-cadherin regulation, prior studies have demonstrated that laminin-5 α3-chain expression can be inhibited by hypermethylation (Sathyanarayana et al., 2003), and here we provide evidence for a second epigenetic mechanism that regulates expression of laminin-5 α3-chain – coactivator loss. In addition, there is evidence that loss of E-cadherin expression may be temporary and that epigenetic control over the expression of E-cadherin would make it possible for E-cadherin to be produced in aggressive primary and metastatic breast tumors (Thiery, 2003). This model of differential regulation of E-cadherin expression may be valuable in reconciling the potentially divergent observations that laminin-5 α3-chain expression is lost during early mammary carcinogenesis and increased laminin-5 γ2-chain expression is associated with tumor invasion and an aggressive phenotype (Pyke et al., 1994; Seftor et al., 2001; Yamamoto et al., 2001; Niki et al., 2002). Further studies will be necessary to determine the role of epigenetic silencing of laminin-5 α3-chain expression in early mammary carcinogenesis.

Observations in this model system may provide insights into the early biology of basal-type epithelial breast cancers. Basal-type epithelial breast cancers occur frequently in young African-American women and are also observed in women who are BRCA1 mutation carriers (Foulkes et al., 2003). Basal-type breast cancers are identified by the following characteristics: ER/PR$^{-/-}$, Her2/neu^{-}, p53^{-} and CK5/6$^{+/+}$ (Foulkes et al., 2003). Understanding the early biology of basal-type breast cancers is critical for developing effective prevention strategies. The primary HMEC strain used for these studies is AG11132/172R/AA7, a CK5/6$^{+/+}$, Her2/neu^{-}, basal-cytokeratin-positve HMEC strain that expresses low levels of ER/PR and was derived from the breast tissue of a young African-American woman (Seewaldt et al., 2001b). Here, we modeled loss of p53 function using expression of HPV-16 E6 to study the role of rECM signaling in mediating apoptosis in this basal-cytokeratin-positive HMEC strain. Importantly, in previous studies, we confirmed that p53-specific antisense ODNs and HPV-16 E6 resulted in the same apoptosis-sensitive phenotype (Seewaldt et al., 2001a). Since basal-type breast cancers typically arise in young African-American women and are ER/PR$^{-/-}$, p53^{-} and Her2/neu^{-}, modeling loss of p53 function in ER/PR-poor, Her2/neu^{-}, basal-cytokeratin-positive HMECs derived from a young African-American woman is a potentially relevant model of early basal-type breast carcinogenesis.

Observations in this model system predict that a partial reduction of CBP expression in basal-cytokeratin-positive HMEC strains results in (1) loss of CBP occupancy of the AP-1-rich region of the *LAMA3A* promoter, (2) decreased *LAMA3A* promoter activity, and (3) reduced expression of laminin-5 α3-chain protein. We also observe that loss of CBP/laminin-5 α3-chain expression blocks rECM-mediated growth control and apoptosis induction in vitro and thereby may promote the clonal expansion of 'damaged' HMECs in vivo. These observations have potential clinical implications and suggest that suppression of CBP in basal-cytokeratin-positive mammary epithelial cells promotes a cellular environment that may increase the risk of subsequent invasive basal-type breast cancer.

This work is supported by NIH/NCI grants 2P30CA14236-26 (V.L.S. and E.C.D.), R01CA88799 (V.L.S.), R01CA98441 (V.L.S.) and 5-P30CA16058 (K.M.), NIH/NIDDK grants 2P30DK 35816-11 (V.L.S.), DAMD-98-1-851 and DAMD-010919 (V.L.S.), an American Cancer Society Award CCE-99898 (V.L.S.), a V-Foundation Award (V.L.S.), a Susan G. Komen Breast Cancer Award (V.L.S., E.C.D.), and a Charlotte Geyer Award (V.L.S.). We are indebted to Judy Groombridge and Franque Remington for the preparation of electron microscopy specimens. We thank William Carter for the gift of integrin-specific antibodies, Jack and Marcia Slane for the generous gift of the Zeiss LSM 410 fluorescence microscope to the Duke University Comprehensive Cancer Center, and T. P. Yao for sharing his unpublished observations.

References

Abd El-Rehim, D. M., Pinder, S. E., Paish, C. E., Bell, J., Blamey, R. W., Robertson, J. F. R., Nicholson, R. I. and Ellis, I. O. (2004). Expression of luminal and basal cytokeratins in human breast cancer. *J. Pathol.* **203**, 661-671.

Aberdam, D., Virolle, T. and Simon-Assmann, P. (2000). Transcriptional regulation of laminin gene expression. *Microsc. Res. Tech.* **51**, 228-237.

Anbazhagan, R., Osin, P. P., Bartkova, J., Nathan, B., Lane, E. B. and Gusterson, B. A. (1998). The development of epithelial phenotypes in the human fetal and infant breast. *J. Pathol.* **184**, 197-206.

Aubele, M. M., Cummings, M. C., Mattis, A. E., Zitzelsberger, H. F., Walch, A. K., Kremer, M., Hofler, H. and Werner, M. (2000). Accumulation of chromosomal imbalances from intraductal proliferative lesions to adjacent in situ and invasive ductal breast cancer. *Diagn. Mol. Pathol.* **9**, 14-19.

Aumailley, M., El Khal, A., Knöss, N. and Tunggal, L. (2003). Laminin 5 processing and its integration into the ECM. *Matrix Biol.* **22**, 49-54.

Baldi, P. and Long, A. D. (2001). A Bayesian framework for the analysis of microarray expression data: regularized t-test and statistical inferences of gene changes. *Bioinformatics* **17**, 509-519.

Band, V. (1995). Preneoplastic transformation of human mammary epithelial cells. *Semin. Cancer Biol.* **6**, 185-192.

Benkoussa, M., Brand, C., Delmotte, M. H., Formstecher, P. and Lefebvre, P. (2002). Retinoic acid receptors inhibit AP1 activation by regulating extracellular signal-regulated kinase and CBP recruitment to an AP1-responsive promoter. *Mol. Cell. Biol.* **22**, 4522-4534.

Carter, W. G., Wayner, E. A., Bouchard, T. S. and Kaur, P. (1990a). The role of integrins alpha 2 beta 1 and alpha 3 beta 1 in cell-cell and cell-substrate adhesion of human epidermal cells. *J. Cell Biol.* **110**, 1387-1404.

Carter, W. G., Kaur, P., Gil, S. G., Gahr, P. J. and Wayner, E. A. (1990b). Distinct functions for integrins alpha 3 beta 1 in focal adhesions and alpha 6 beta 4/bullous pemphigoid antigen in a new stable anchoring contact (SAC) of keratinocytes: relation to hemidesmosomes. *J. Cell Biol.* **111**, 3141-3154.

D'Ardenne, A. J., Richman, P. I., Horton, M. A., McAulay, A. E. and Jordan, S. (1991). Co-ordinate expression of the alpha-6 integrin laminin receptor sub-unit and laminin in breast cancer. *J. Pathol.* **165**, 213-220.

Debnath, J., Muthuswamy, S. K. and Brugge, J. S. (2003). Morphogenesis and oncogenesis of MCF-10A mammary epithelial acini grown in three-dimensional basement membrane cultures. *Methods* **30**, 256-268.

Fabian, C. J., Kamel, S., Zalles, C. and Kimler, B. F. (1996). Identification of a chemoprevention cohort from a population of women at high risk for breast cancer. *J. Cell Biochem.* **Suppl. 25**, 112-122.

Fan, S., Ma, Y. X., Wang, C., Yuan, R. Q., Meng, Q., Wang, J. A., Erdos, M., Goldberg, I. D., Webb, P., Kushner, P. J. et al. (2002). p300 Modulates the BRCA1 inhibition of estrogen receptor activity. *Cancer Res.* **62**, 141-151.

Farrelly, N., Lee, Y. J., Oliver, J., Dive, C. and Streuli, C. H. (1999). Extracellular matrix regulates apoptosis in mammary epithelium through a control on insulin signaling. *J. Cell Biol.* **144**, 1337-1348.

Foulkes, W. D., Stefansson, I. M., Chappuis, P. O., Bégin, L. R., Goffin, J. R., Wong, N., Trudel, M. and Akslen, L. A. (2003). Germline BRCA1 mutations and a basal epithelial phenotype in breast cancer. *J. Natl. Cancer Inst.* **95**, 1482-1485.

Giles, R. H., Petrij, F., Dauwerse, H. G., den Hollander, A. I., Lushnikova, T., van Ommen, G. J. B., Goodman, R. H., Deaven, L. L., Doggett, N. A., Peters, D. J. M. et al. (1997). Construction of a 1.2-Mb contig surrounding, and molecular analysis of, the human CREB-binding protein (CBP/CREBBP) gene on chromosome 16p13.3. *Genomics* **42**, 96-114.

Hao, J., Jackson, L., Calaluce, R., McDaniel, K., Dalkin, B. L. and Nagle, R. B. (2001). Investigation into the mechanism of the loss of laminin 5 (alpha3beta3gamma2) expression in prostate cancer. *Am. J. Pathol.* **158**, 1129-1135.

Hashida, H., Takabayashi, A., Tokuhara, T., Taki, T., Kondo, K., Kohno, N., Yamaoka, Y. and Miyake, M. (2002). Integrin alpha3 expression as a prognostic factor in colon cancer: association with MRP-1/CD9 and KAI1/CD82. *Int. J. Cancer* **97**, 518-525.

Hood, J. D. and Cheresh, D. A. (2002). Role of integrins in cell invasion and migration. *Nat. Rev. Cancer* **2**, 91-100.

Howlett, A. R., Bailey, N., Damsky, C., Petersen, O. W. and Bissell, M. J. (1995). Cellular growth and survival are mediated by beta 1 integrins in normal human breast epithelium but not in breast carcinoma. *J. Cell Sci.* **108**, 1945-1957.

Hsu, S. L., Cheng, C. C., Shi, Y. R. and Chiang, C. W. (2001). Proteolysis of integrin alpha5 and beta1 subunits involved in retinoic acid-induced apoptosis in human hepatoma Hep3B cells. *Cancer Lett.* **167**, 193-204.

Ilic, D., Almeida, E. A. C., Schlaepfer, D. D., Dazin, P., Aizawa, S. and Damsky, C. H. (1998). Extracellular matrix survival signals transduced by focal adhesion kinase suppress p53-mediated apoptosis. *J. Cell Biol.* **143**, 547-560.

Kawasaki, H., Eckner, R., Yao, T. P., Taira, K., Chiu, R., Livingston, D. M. and Yokoyama, K. K. (1998). Distinct roles of the co-activators p300 and CBP in retinoic-acid-induced F9-cell differentiation. *Nature* **393**, 284-289.

Lininger, R. A., Park, W. S., Man, Y. G., Pham, T., MacGrogan, G., Zhuang, Z. and Tavassoli, F. A. (1998). LOH at 16p13 is a novel chromosomal alteration detected in benign and malignant microdissected papillary neoplasms of the breast. *Human Pathol.* **29**, 1113-1118.

Majno, G. and Joris, I. (1995). Apoptosis, oncosis, and necrosis. An overview of cell death. *Am. J. Pathol.* **146**, 3-15.

Manda, R., Kohno, T., Niki, T., Yamada, T., Takenoshita, S., Kuwano, H. and Yokota, J. (2000). Differential expression of the LAMB3 and LAMC2 genes between small cell and non-small cell lung carcinomas. *Biochem. Biophys. Res. Commun.* **275**, 440-445.

Martin, K. J., Kwan, C. P., Nagasaki, K., Zhang, X., O'Hare, M. J., Kaelin, C. M., Burgeson, R. E., Pardee, A. B. and Sager, R. (1998). Down-regulation of laminin-5 in breast carcinoma cells. *Mol. Med.* **4**, 602-613.

Mercurio, A. M., Bachelder, R. E., Chung, J., O'Connor, K. L., Rabinovitz, I., Shaw, L. M. and Tani, T. (2001). Integrin laminin receptors and breast carcinoma progression. *J. Mammary Gland Biol. Neoplasia* **6**, 299-309.

Miller, K. A., Chung, J., Lo, D., Jones, J. C. R., Thimmapaya, B. and Weitzman, S. A. (2000). Inhibition of laminin-5 production in breast epithelial cells by overexpression of p300. *J. Biol. Chem.* **275**, 8176-8182.

Miller, K. A., Eklund, E. A., Peddinghaus, M. L., Cao, Z., Fernandes, N., Turk, P. W., Thimmapaya, B. and Weitzman, S. A. (2001). Kruppel-like factor 4 regulates laminin alpha 3A expression in mammary epithelial cells. *J. Biol. Chem.* **276**, 42863-42868.

Moll, R., Franke, W. W., Schiller, D. L., Geiger, B. and Kerpler, R. (1982). The catalog of human cytokeratins: patterns of expression in normal epithelia, tumors and cultured cells. *Cell* **31**, 11-24.

Mrózek, K., Karakousis, C. P., Perez-Mesa, C. and Bloomfield, C. D. (1993). Translocation t(12;22)(q13;q12.2-12.3) in a clear cell sarcoma of tendons and aponeuroses. *Genes Chromosomes Cancer* **6**, 249-252.

Niki, T., Kohno, T., Iba, S., Moriya, Y., Takahashi, Y., Saito, M., Maeshima, A., Yamada, T., Matsuno, Y., Fukayama, M. et al. (2002). Frequent co-localization of Cox-2 and laminin-5 gamma2 chain at the invasive front of early-stage lung adenocarcinomas. *Am. J. Pathol.* **160**, 1129-1141.

Perou, C. M., Sørlie, T., Eisen, M. B., van de Rijn, M., Jeffrey, S. S., Rees, C. A., Pollack, J. R., Ross, D. T., Johnsen, H., Akslen, L. A. et al. (2000). Molecular portraits of human breast tumours. *Nature* **406**, 747-752.

Petersen, O. W., Rønnov-Jessen, L., Howlett, A. R. and Bissell, M. J. (1992). Interaction with basement membrane serves to rapidly distinguish growth and differentiation pattern of normal and malignant human breast epithelial cells. *Proc. Natl. Acad. Sci. USA* **89**, 9064-9068.

Pitelka, D. R. (1983). The Mammary Gland. In *Histology Cell and Tissue Biology.* 5th edn (ed. L. Weiss), pp. 944-965. New York: Elsevier Biomedical.

Pyke, C., Røsmer, J., Kallunki, P., Lund, L. R., Ralfkiaer, E., Danø, K. and Tryggvason, K. (1994). The gamma 2 chain of kalinin/laminin 5 is preferentially expressed in invading malignant cells in human cancers. *Am. J. Pathol.* **145**, 782-791.

Robyr, D., Wolffe, A. P. and Wahli, W. (2000). Nuclear hormone receptor coregulators in action: diversity for shared tasks. *Mol. Endocrinol.* **14**, 329-347.

Rohan, T. E., Hartwick, W., Miller, A. B. and Kandel, R. A. (1998). Immunohistochemical detection of c-erbB-2 and p53 in benign breast disease and breast cancer risk. *J. Natl. Cancer Inst.* **90**, 1262-1269.

Roskelley, C. D., Desprez, P. Y. and Bissell, M. J. (1994). Extracellular matrix-dependent tissue-specific gene expression in mammary epithelial cells requires both physical and biochemical signal transduction. *Proc. Natl. Acad. Sci. USA* **91**, 12378-12382.

Sathyanarayana, U. G., Toyooka, S., Padar, A., Takahashi, T., Brambilla, E., Minna, J. D. and Gazdar, A. F. (2003). Epigenetic inactivation of laminin-5-encoding genes in lung cancers. *Clin. Cancer Res.* **9**, 2665-2672.

Schenk, S., Hintermann, E., Bilban, M., Koshikawa, N., Hojilla, C., Khokha, R. and Quaranta, V. (2003). Binding to EGF receptor of a laminin-5 EGF-like fragment liberated during MMP-dependent mammary gland involution. *J. Cell Biol.* **161**, 197-209.

Schröck, E., du Manoir, S., Veldman, T., Schoell, B., Wienberg, J., Ferguson-Smith, M. A., Ning, Y., Ledbetter, D. H., Bar-Am, I.,

Soenksen, D. et al. (1996). Multicolor spectral karyotyping of human chromosomes. *Science* **273**, 494-497.

Seewaldt, V. L., Johnson, B. S., Parker, M. B., Collins, S. J. and Swisshelm, K. (1995). Expression of retinoic acid receptor beta mediates retinoic acid-induced growth arrest and apoptosis in breast cancer cells. *Cell Growth Differ.* **6**, 1077-1088.

Seewaldt, V. L., Caldwell, L. E., Johnson, B. S., Swisshelm, K., Collins, S. J. and Tsai, S. (1997a). Inhibition of retinoic acid receptor function in normal human mammary epithelial cells results in increased cellular proliferation and inhibits the formation of a polarized epithelium in vitro. *Exp. Cell Res.* **236**, 16-28.

Seewaldt, V. L., Kim, J. H., Caldwell, L. E., Johnson, B. S., Swisshelm, K. and Collins, S. J. (1997b). All-trans-retinoic acid mediates G1 arrest but not apoptosis of normal human mammary epithelial cells. *Cell Growth Differ.* **8**, 631-641.

Seewaldt, V. L., Dietze, E. C., Johnson, B. S., Collins, S. J. and Parker, M. B. (1999a). Retinoic acid-mediated G1-S-phase arrest of normal human mammary epithelial cells is independent of the level of p53 protein expression. *Cell Growth Differ.* **10**, 49-59.

Seewaldt, V. L., Kim, J. H., Parker, M. B., Dietze, E. C., Srinivasan, K. V. and Caldwell, L. E. (1999b). Dysregulated expression of cyclin D1 in normal human mammary epithelial cells inhibits all-trans-retinoic acid-mediated G0/G1-phase arrest and differentiation in vitro. *Exp. Cell Res.* **249**, 70-85.

Seewaldt, V. L., Mrózek, K., Sigle, R., Dietze, E. C., Heine, K., Hockenbery, D. M., Hobbs, K. B. and Caldwell, L. E. (2001a). Suppression of p53 function in normal human mammary epithelial cells increases sensitivity to extracellular matrix-induced apoptosis. *J. Cell Biol.* **155**, 471-486.

Seewaldt, V. L., Mrózek, K., Dietze, E. C., Parker, M. and Caldwell, L. E. (2001b). Human papillomavirus type 16 E6 inactivation of p53 in normal human mammary epithelial cells promotes tamoxifen-mediated apoptosis. *Cancer Res.* **61**, 616-624.

Seftor, R. E. B., Seftor, E. A., Koshikawa, N., Meltzer, P. S., Gardner, L. M. G., Bilban, M., Stetler-Stevenson, W. G., Quaranta, V. and Hendrix, M. J. C. (2001). Cooperative interactions of laminin 5 gamma2 chain, matrix metalloproteinase-2, and membrane type-1-matrix/metalloproteinase are required for mimicry of embryonic vasculogenesis by aggressive melanoma. *Cancer Res.* **61**, 6322-6327.

Shang, M., Koshikawa, N., Schenk, S. and Quaranta, V. (2001). The LG3 module of laminin-5 harbors a binding site for integrin alpha3beta1 that promotes cell adhesion, spreading, and migration. *J. Biol. Chem.* **276**, 33045-33053.

Shang, Y., Hu, X., DiRenzo, J., Lazar, M. A. and Brown, M. (2000). Cofactor dynamics and sufficiency in estrogen receptor-regulated transcription. *Cell* **103**, 843-852.

Stampfer, M. (1985). Isolation and growth of human mammary epithelial cells. *J. Tissue Cult. Methods* **9**, 107-115.

Steffgen, K., Dufraux, K. and Hathaway, H. (2002). Enhanced branching morphogenesis in mammary glands of mice lacking cell surface beta1,4-galactosyltransferase. *Dev. Biol.* **244**, 114-133.

Strange, R., Li, F., Saurer, S., Burkhardt, A. and Friis, R. R. (1992). Apoptotic cell death and tissue remodelling during mouse mammary gland involution. *Development* **115**, 49-58.

Strömblad, S., Fotedar, A., Brickner, H., Theesfeld, C., Aguilar de Diaz, E., Friedlander, M. and Cheresh, D. A. (2002). Loss of p53 compensates for alpha v-integrin function in retinal neovascularization. *J. Biol. Chem.* **277**, 13371-13374.

Stupack, D. G. and Cheresh, D. A. (2002). Get a ligand, get a life: integrins, signaling and cell survival. *J. Cell Sci.* **115**, 3729-3738.

Taylor-Papadimitriou, J. and Lane, E. B. (1987). Keratin expression in the mammary gland. In *The Mammary Gland: Development, Regulation, and Function* (ed. M. C. Neville and C. W. Daniel), pp. 181-215. New York: Plenum.

Thiery, J. P. (2003). Cell adhesion in cancer. *C. R. Phys.* **4**, 289-304.

Thompson, C. B. (1995). Apoptosis in the pathogenesis and treatment of disease. *Science* **267**, 1456-1462.

Tsuda, H., Sakamaki, C., Tsugane, S., Fukutomi, T. and Hirohashi, S. (1998). Prognostic significance of accumulation of gene and chromosome alterations and histological grade in node-negative breast carcinoma. *Jpn. J. Clin. Oncol.* **28**, 5-11.

Ugai, H., Uchida, K., Kawasaki, H. and Yokoyama, K. K. (1999). The coactivators p300 and CBP have different functions during the differentiation of F9 cells. *J. Mol. Med.* **77**, 481-494.

Virolle, T., Monthouel, M. N., Djabari, Z., Ortonne, J. P., Meneguzzi, G. and Aberdam, D. (1998). Three activator protein-1-binding sites bound by the Fra-2.JunD complex cooperate for the regulation of murine laminin alpha3A (*lama3A*) promoter activity by transforming growth factor-beta. *J. Biol. Chem.* **273**, 17318-17325.

Virolle, T., Coraux, C., Ferrigno, O., Cailleteau, L., Ortonne, J. P., Pognonec, P. and Aberdam, D. (2002). Binding of USF to a non-canonical E-box following stress results in a cell-specific derepression of the *lama3* gene. *Nucleic Acids Res.* **30**, 1789-1798.

Wayner, E. A. and Carter, W. G. (1987). Identification of multiple cell adhesion receptors for collagen and fibronectin in human fibrosarcoma cells possessing unique alpha and common beta subunits. *J. Cell Biol.* **105**, 1873-1884.

Wayner, E. A., Carter, W. G., Piotrowicz, R. S. and Kunicki, T. J. (1988). The function of multiple extracellular matrix receptors in mediating cell adhesion to extracellular matrix: preparation of monoclonal antibodies to the fibronectin receptor that specifically inhibit cell adhesion to fibronectin and react with platelet glycoproteins Ic-IIa. *J. Cell Biol.* **107**, 1881-1891.

Wazer, D. E., Liu, X.-L., Chu, Q., Gao, Q and Band, V. (1995). Immortalization of distinct human mammary epithelial cell types by human papilloma virus 16 E6 or E7. *Proc. Natl. Acad. Sci. USA* **92**, 3687-3691.

Weaver, V. M., Howlett, A. R., Langton-Webster, B., Petersen, O. W. and Bissell, M. J. (1995). The development of a functionally relevant cell-culture model of progressive human breast-cancer. *Semin. Cancer Biol.* **6**, 175-184.

Weaver, V. M., Petersen, O. W., Wang, F., Larabell, C. A., Briand, P., Damsky, C. and Bissell, M. J. (1997). Reversion of the malignant phenotype of human breast cells in tree-dimensional culture and in vivo by integrin blocking antibodies. *J. Cell Biol.* **137**, 231-245.

Yahata, T., Shao, W., Endoh, H., Hur, J., Coser, K. R., Sun, H., Ueda, Y., Kato, S., Isselbacher, K. J., Brown, M. et al. (2001). Selective coactivation of estrogen-dependent transcription by CITED1 CBP/p300-binding protein. *Genes Dev.* **15**, 2598-2612.

Yamamoto, H., Itoh, F., Iku, S., Hosokawa, M. and Imai, K. (2001). Expression of the gamma(2) chain of laminin-5 at the invasive front is associated with recurrence and poor prognosis in human esophageal squamous cell carcinoma. *Clin. Cancer Res.* **7**, 896-900.

Yao, T. P., Oh, S. P., Fuchs, M., Zhou, N. D., Ch'ng, L. E., Newsome, D., Bronson, R. T., Li, E., Livingston, D. M. and Eckner, R. (1998). Gene dosage-dependent embryonic development and proliferation defects in mice lacking the transcriptional integrator p300. *Cell* **93**, 361-372.

Yee, L. D., Guo, Y., Bradbury, J., Suster, S., Clinton, S. K. and Seewaldt, V. L. (2003). The antiproliferative effects of PPARγ ligands in normal human mammary epithelial cells. *Breast Cancer Res. Treat.* **78**, 179-192.

Yoon, D. S., Wersto, R. P., Zhou, W., Chrest, F. J., Garrett, E. S., Kwon, T. K. and Gabrielson, E. (2002). Variable levels of chromosomal instability and mitotic spindle checkpoint defects in breast cancer. *Am. J Pathol.* **161**, 391-397.

Zutter, M. M., Santoro, S. A., Staatz, W. D. and Tsung, Y. L. (1995). Re-expression of the alpha 2 beta 1 integrin abrogates the malignant phenotype of breast carcinoma cells. *Proc. Natl. Acad. Sci. USA* **92**, 7411-7415.

Interferon Regulatory Factor-1 Regulates Reconstituted Extracellular Matrix (rECM)-Mediated Apoptosis in Human Mammary Epithelial Cells

Michelle L. Bowie, Michelle M. Troch, Jeffrey Delrow, Eric C. Dietze, Gregory R. Bean, Catherine Ibarra, Gautham Pandiyan, and Victoria L. Seewaldt

Division of Medical Oncology [M.L.B., M.M.T., E.C.D., G.R.B., C.I., and V.L.S.] and Department of Pharmacology and Cancer Biology [G.P. and V.L.S.], Duke University, Durham, NC 27710, and Fred Hutchinson Cancer Research Center, Seattle, WA 98120 [J.D.]

Correspondence should be addressed to:

Victoria Seewaldt
Box 2628
Duke University Medical Center
Durham, NC 27710
Telephone: (919) 668-2455
Fax: (919) 668-2458
email: seewa001@mc.duke.edu

Running Title: IRF-1 Regulates ECM-Mediated Apoptosis in HMECs

Key Words: human mammary epithelial cells, IRF-1, apoptosis, extracellular matrix, and tamoxifen

Abstract

Interactions between extracellular matrix (ECM) and mammary epithelial cells are critical for the regulation of mammary gland homeostasis and apoptotic signaling. Interferon regulatory factor-1 (IRF-1) is a transcriptional regulator that promotes apoptosis during mammary gland involution and p53-independent apoptosis. We have recently shown that rapid cell surface tamoxifen (Tam) signaling promotes apoptosis in normal human mammary epithelial cells that were acutely damaged by expression of the Human Papillomavirus Type-16 E6 protein (*HMEC-E6) [Dietze et al., 2004]. Apoptosis was mediated by recruitment of CREB-binding protein (CBP) to the gamma-activating sequence (GAS) element of the *IRF-1* promoter, induction of IRF-1, and caspase-1 and -3 activation [Bowie et al., 2004]. Here we show that growth factor depleted, reconstituted ECM (rECM), similar to Tam, promotes apoptosis in *HMEC-E6 cells through induction of IRF-1. Apoptosis was temporally associated with recruitment of CBP to the GAS element of the *IRF-1* promoter, induction of IRF-1 expression, and caspase-1 and -3 activation. siRNA-mediated suppression of IRF-1 protein expression in *HMEC-E6 cells blocked 1) induction of IRF-1, 2) caspase-1 and -3 activation, and 3) apoptosis. These observations demonstrate that IRF-1 promotes rECM-mediated apoptosis and provide evidence that both rECM and rapid Tam signaling transcriptionally activates IRF-1 through recruitment of CBP to the IRF-1 GAS promoter complex.

Introduction

Interferon regulatory factor-1 (IRF-1) was originally identified as a DNA binding factor on the mouse *interferon beta* (*IFN*-β) promoter and is known to play an important role in promoting apoptosis in response to viral infections (Miyamoto et al., 1988). IRF-1 can be induced by type II-IFN (IFN-γ) (Romeo et al., 2002) and is known to participate in both p53-dependent and -independent apoptotic signaling in mouse models (Tanaka et al., 1996; Tamura et al., 1995). Recently, IRF-1 was shown to participate in both type II-IFN (IFN-γ) and anti-estrogen ICI 182,780 p53-independent apoptotic signaling in the human breast cancer cell lines, MCF-7 and T47D, respectively (Porta et al., 2005; Bouker et al., 2004). Taken together these observations suggest that IRF-1 plays a role in p53-independent apoptotic signaling in mouse and human mammary epithelial cells.

There is also growing evidence that IRF-1 plays an important role in mammary gland homeostasis and hormone responsiveness. IRF-1 promotes apoptosis during mammary gland involution in the rat (Hoshiya et al, 2003) and IRF-1 expression is decreased or lost in mouse (Kim et al., 2004; Yim et al., 1997) and human (Doherty et al., 2001; Yim et al., 2003; Bouker et al., 2004; Bouker et al., 2005; Connett et al., 2005) breast cancers. Doherty et al. demonstrated in human biopsy specimens that IRF-1 protein was expressed in normal mammary epithelial cells but that IRF-1 expression was lost in high-grade ductal carcinoma *in situ* and node-positive invasive breast cancers (Doherty et al., 2001). IRF-1 has also been implicated by Gu et al to be involved in ICI 182,780 antiestrogen resistance in breast cancer (Gu et al, 2002). More recently, IRF-1 has been shown to be induced by the estrogen agonist/antagonist, tamoxifen (Tam), and the pure estrogen antagonist, ICI 182,780 (Bowie et al., 2004; Bouker et

al., 2004). Specifically, ICI 182,780 was shown to induce IRF-1 expression in the estrogen receptor-positive (ER(+)) human breast cancer cell lines, MCF-7 and T47D (Bouker et al., 2004). Tam was shown to induce IRF-1 in human mammary epithelial cells (HMECs) that had been acutely damaged by the expression of human papillomavirus type 16 (HPV-16) E6 protein (*HMEC-E6) (Bowie et al., 2004). Taken together, these observations support the role of IRF-1 signaling in mammary gland homeostasis and estrogen/anti-estrogen signaling.

The "classic" or genomic mechanism of 17-β-estradiol (E2) action requires the presence of the estrogen receptor (ER), the E2/ER complex binding to an estrogen response element, and changes in both transcription and translation. However, recent evidence suggests that estrogen, and anti-estrogens, may also act through rapid, "non-classic" signaling pathways in human mammary epithelial cells (Kelly and Levin, 2001; Marquez and Pietras, 2001; Dietze et al., 2004; Marquez et al., 2006). Unlike ER(+) human breast cancers, HMECs typically express low nuclear levels of ER (ER-"poor"). While HMECs are ER-"poor", unlike ER(-) breast cancer cells, HMECs are not Tam-resistant. We recently demonstrated that while therapeutic levels of Tam (1.0 uM) promoted growth arrest in HMEC controls, equimolar concentrations of Tam induced apoptosis in ER-"poor" *HMEC-E6 through a rapid, "non-classic" signaling pathway (Dietze et al., 2001; Dietze et al., 2004; Bowie et al., 2004). We observed that 1.0 uM Tam induced apoptosis in *HMEC-E6 cells through 1) rapid cell-surface-mediated modulation of AKT phosphorylation, 2) recruitment of STAT1 and the co-activator, CBP, to the GAS element of the *IRF-1* promoter, and 3) induction of IRF-1 (Dietze et al., 2004; Bowie et al., 2004). These observations suggest a role for IRF-1 in regulating rapid Tam signaling and promoting p53-independent apoptosis in *HMEC-E6 cells.

Carcinogenesis is thought to be a multistep process resulting from the accumulation of genetic damage. However, not all damaged mammary epithelial cells progress to become invasive breast cancers and, instead, are thought to be eliminated by apoptosis. Breast tissue is composed of mammary epithelial cells that rest on extracellular matrix (ECM). Interactions between epithelial cells and ECM regulate mammary gland homeostasis by promoting a coordinated balance between proliferation and apoptosis (Folkman and Moscona, 1978; Petersen et al., 1992; Strange et al., 1992; Zutter et al., 1995; Ilic et al., 1998; Farrelly et al., 1999; Stupack and Cheresh, 2002). Laminins are heterotrimeric ECM glycoproteins that mediate many of the regulatory functions of ECM (Aberdam et al., 2000). Laminin-5 (α3A, β3, and γ2) is the most abundant ECM glycoprotein produced by mammary epithelial cells (D'Ardenne et al., 1991). Laminin-5 functions as a ligand for $\alpha3\beta1$- and $\alpha6\beta4$-integrins and has been implicated in adhesion, migration, and apoptotic signaling (Mercurio and Shaw, 1991; Howlett et al., 1995; Shang et al., 2001). Loss of ECM signaling (Petersen et al., 1992; Howlett et al., 1995; Mercurio et al., 2001; Farrelly et al., 1999; Hood and Cheresh, 2002) and dysregulation of laminin-5 expression is thought to be an early event in mammary carcinogenesis (Henning et al., 1999; Martin et al., 1998). While benign ductal and lobular epithelial cells demonstrate continuous laminin-5 staining at the epithelial-stromal interface, primary human breast cancers and human breast cancer cells exhibit loss/dysregulation of laminin-5 α3-chain expression (Martin et al., 1998; Henning et al., 1999).

Our prior studies showed that while contact with rECM promoted growth arrest in HMEC controls, contact between rECM and *HMEC-E6 cells promotes p53-independent apoptosis

through a laminin-5/α3β1-integrin signaling pathway; interruption of laminin-5/α3β1-integrin signaling blocked apoptosis (Seewaldt et al., 2001; Dietze et al, 2005). Given the observations that IRF-1 is important for response to acute cellular damage and p53-independent apoptotic signaling in mammary epithelial cells and our recent observation that Tam promotes p53-independent apoptosis in *HMEC-E6 cells through induction of IRF-1 (Dietze et al., 2004; Bowie et al., 2004), we hypothesized that rECM may also promote p53-independent apoptosis in *HMEC-E6 cells through induction of IRF-1. Here we show that rECM, similar to Tam, promotes recruitment of STAT1 and CBP to the GAS element of the *IRF-1* promoter and subsequent induction of IRF-1. These results provide evidence that Tam and rECM signal through IRF-1 and support a more global role of IRF-1 in mediating p53-independent apoptosis in mammary epithelial cells.

Results

*rECM activates caspases-1/-3 and induces apoptosis in *HMEC-E6 cells*

We have previously shown that 1.0 μM Tam promotes p53-independent apoptosis in *HMEC-E6 cells through activation of caspases-1 and -3 (Dietze et al. 2004; Bowie et al. 2004). Here we tested in large-scale 3-dimensional, high-density liquid rECM culture (3-hD) whether rECM, similar to Tam, activates caspases-1 and -3 and promotes apoptosis in *HMEC-E6 cells.

3-hD culture is an adaptation of the large-scale culture system developed by the laboratory of Mina Bissell (Roskelly et al., 1994). HMECs are plated at high density ($2.5 \times 10^7/25\ cm^2$) on a non-adhesive substrate as described in Materials and Methods, and treated with a 1:100 dilution of growth factor-depleted rECM in Standard Media. In this system, *HMEC-E6 cells and passage matched HMEC-LX controls detach from the non-adhesive substrate starting at 6 hr and spontaneously form 20-30 micron cellular aggregates in a liquid solution of growth-factor depleted rECM diluted in tissue culture media (Figs. 1A, F and data not shown). HMEC-LX controls and *HMEC-E6 cells undergo growth arrest starting between 6 and 7 hr ($p < 0.01$) while only *HMEC-E6 cells undergo apoptosis which occurs at 12-24 hr ($p < 0.05$) (Fig. 1B, C). This contrasts with our prior studies employing small scale 3-D rECM culture where HMECs are plated as single cell suspension in semi-solid growth factor-depleted rECM. In small scale 3-D rECM culture, *HMEC-E6 cells and HMEC-LX controls proliferate for 6 days until they form 20-30 micron ascinus-like structures, and then undergo growth arrest (Seewaldt et al., 2001; Dietze et al., 2005). While HMEC-LX controls undergo growth arrest alone starting on Day 6, passage-matched *HMEC-E6 cells undergo growth arrest on Day 6 followed by apoptosis on Day 6-7 (Seewaldt et al., 2001; Dietze et al., 2005). For the experiments described here, large-

scale 3-hD culture was chosen over small-scale 3-D culture due to the need to precisely synchronize our cells for promoter recruitment and differential gene expression studies. In large-scale 3-hD culture, apoptosis occurs starting at 12 hrs and occurs during a narrow window of time (versus 6-7 days for small-scale 3-D culture). Therefore, 3-hD culture allows for both precise temporal control and synchronization of gene expression prior to and during the induction of apoptosis.

We previously observed that 1.0 uM Tam promotes growth arrest and apoptosis in *HMEC-E6 cells but growth arrest alone in HMEC-LX cells (Dietze, et al., 2001). Evidence of apoptosis in Tam-treated *HMEC-E6 cells was first observed at 12 hr and maximally at 24 hr, as demonstrated by electron microscopy and Annexin V binding. Similarly, *HMEC-E6 cells grown in 3-hD culture demonstrated Annexin V binding first at 12 hr ($p < 0.05$) and maximally at 24 hr ($p < 0.001$) (Fig. 1C). In contrast, a significant increase in Annexin V binding was not observed in rECM-treated, passage-matched HMEC-LX vector controls at 24 hr ($p > 0.10$) (Fig. 1C). These observations provide evidence that *HMEC-E6 cells undergo apoptosis in 3-hD culture starting at 12 hr.

We also previously demonstrated that Tam-induced apoptosis in *HMEC-E6 cells was dependent on sequential activation of caspase-1 and -3 (Bowie et al., 2004). In addition, we have shown that rECM culture 1) promotes apoptosis in *HMEC-E6 cells through laminin-5/α3β1-integrin signaling and 2) interruption of laminin-5/α3β1-integrin signaling blocked apoptosis (Seewaldt et al., 2001a; Dietze et al, 2005). Here we tested whether rECM-induced apoptosis was similarly associated with caspase-1 and -3 activation, and whether α3- or β1-integrin

blocking antibodies could inhibit this caspase activation. *HMEC-E6 cells grown in 3-hD culture demonstrated caspase-1 activation first at 3 hr ($p < 0.0001$), with maximal activation at 4 hr ($p < 0.0001$), and pre-treatment of *HMEC-E6 cells with α3- or β1-integrin blocking antibodies inhibited the activation of caspase-1 ($p < 0.05$) (Fig. 1D). The effector-caspase, caspase-3, was activated in *HMEC-E6 cells starting at 12 hr ($p < 0.001$), maximally at 24 hr ($p < 0.001$), and pre-treatment with α3- or β1-integrin blocking antibodies blocked the activation of caspase-3 ($p < 0.01$) (Fig. 1E). Control non-immune mouse IgG did not block activation of caspases-1 and -3 ($p < 0.05$) (Fig. 1D-E). These data show that 1) rECM, similar to Tam, promotes apoptosis in *HMEC-E6 cells associated with activation of caspases-1 and -3 and 2) pre-treatment of *HMEC-E6 with α3- or β1-integrin blocking antibodies inhibited the activation of caspases-1 and -3.

cDNA microarray analysis of rECM-induced gene transcripts

To investigate the molecular mechanism of rECM-induced apoptosis in *HMEC-E6 cells, we analyzed the expression profiles of early passage *HMEC-E6 cells and passage-matched HMEC-LX vector controls in 3-hD rECM culture. Analysis was performed using HuGeneFL cDNA microarrays (Affymetrix™). We previously reported that treatment with 1.0 μM Tam induced interferon-stimulated genes (ISGs) in *HMEC-E6 cells (Bowie et al., 2004). Surprisingly, rECM treatment induced a similar subset of ISGs. As shown in Table 1, eighteen genes involved in the interferon pathway were significantly up-regulated by rECM (fold change >1.5 and p-value <0.05); 16 of these 18 rECM-induced ISGs were also induced in *HMEC-E6 cells by Tam, including IRF-1. This latter finding is important because we have previously shown that IRF-1 regulates Tam-induced, p53-independent apoptosis in *HMEC-E6 cells (Bowie et al., 2004).

Differential gene expression was confirmed by semi-quantitative RT-PCR in triplicate, and normalized to beta-actin, for 5 ISGs (Fig. 2A). *HMEC-E6 cells showed up-regulation of all 5 ISGs upon 6 hr rECM treatment. Unlike Tam-induced ISG expression, some ISGs were also slightly induced by rECM in HMEC-LX controls at 6 hr (Table 1 and Fig. 2A). However, the absolute levels of these transcripts in rECM-treated HMEC-LX cells are significantly lower than the absolute transcript levels in rECM-treated *HMEC-E6 early cells (Fig. 2A). Importantly, even though some ISGs are slightly induced by rECM in HMEC-LX controls, IRF-1 was not induced (Bowie et al., 2004). Based on these similar patterns of ISG induction, we hypothesized that both Tam- and rECM-mediated apoptosis in *HMEC-E6 cells may activate a similar downstream pathway that utilizes IRF-1 and possibly other ISGs.

rECM does not induce interferon-α, -β, or -γ and does not increase ERα expression

As in our previous work with Tam, we investigated whether rECM-mediated induction of IRF-1/ ISGs was due to the production and/or release of IFNs. Differential gene expression of *HMEC-E6 cells treated with rECM for 6 hr in 3-hD culture showed that transcription of IFN-α, -β, and -γ was not increased (data not shown). ELISA assays tested for IFN production. Passage-matched apoptosis-sensitive *HMEC-E6 cells and HMEC-LX controls were cultured in rECM and media was tested at 0, 30 min, 1 hr, 2 hr, and 4 hr. IFN-α, -β, and -γ production was not detected in either *HMEC-E6 cells or HMEC-LX controls grown in 3-hD rECM culture (data not shown). These observations are consistent with our previous observation that Tam promotes induction of IRF-1/ISGs and apoptosis in *HMEC-E6 cells in the absence of IFN production or secretion (Bowie et al., 2004). These data show that induction of IRF-1/ISGs, in *HMEC-E6 cells grown

in 3-hD rECM culture, occurs in the absence of IFN-α, -β, and -γ transcriptional activation and/or release.

Unlike ER(+) human breast cancers, HMECs typically express low nuclear levels of ER (ER-"poor"). While HMECs are ER-"poor", unlike ER(-) breast cancer cells, HMECs are not Tam-resistant and express low but detectable levels of ERα protein. Studies by Novaro et al. demonstrated that rECM increased expression of ERα in primary mouse mammary epithelial cells, but only in the presence of prolactin (Novaro et al., 2003). Differential gene expression and western analysis was performed to test whether rECM similarly increased ERα protein expression in *p53(-)HMEC-E6 cells. We observed that there was no increase in ERα mRNA or protein expression in *p53(-)HMEC-E6 cells grown in contact with rECM (data not shown). The lack of ERα induction is the expected result, as we do not culture our cells in the presence of prolactin, and Novaro et al. observed that prolactin was essential for induction of ERα.

Testing for Upstream Convergence of Tam and rECM Signaling

The upregulation of a similar subset of ISG genes lead us to investigate whether both Tam and rECM signal through the same upstream target or converge downstream at the level of transcription in *HMEC-E6 cells. Apoptosis sensitive *HMEC-E6 cells were pretreated with either estrogen and then cultured in rECM or pretreated with α3- or β1-integrin blocking antibodies and then treated with 1.0 uM Tam. Caspase-3 activation was measured 24 hr later. None of the pretreatments inhibited the rECM and Tam activation of caspase-3 in the *HMEC-E6 early cells ($p > 0.05$) (Fig. 2B, C). These experiments demonstrated that rECM and 1.0 uM Tam initiate apoptosis through different upstream targets. Based on these observations, we

hypothesized that rECM- and Tam-induced apoptosis converged at the level of transcriptional activation of IRF-1.

rECM promotes recruitment of CBP and STAT1 to the* IRF-1 *GAS element

Type II-IFN (IFN-γ) signaling has been shown to promote p53-independent apoptosis (Ossina et al., 1997; Porta et al., 2005). We previously demonstrated that treatment of *HMEC-E6 cells with 1.0 uM Tam promotes formation of a STAT1 complex on the *IRF-1* GAS element, recruitment of cofactor CBP, and up-regulation of IRF-1 mRNA. Here we investigated whether induction of IRF-1 by rECM in *HMEC-E6 cells grown in 3-hD culture was due to the formation of a similar transcriptional complex on the *IRF-1* GAS element. Western analysis was conducted to test for STAT1 expression and its phosphorylation. There are two known phosphorylation sites within STAT1, Tyr701 and Ser727. It has been shown that phosphorylation of Ser727 induces the highest transcriptional activation for STAT1 (Wen et al., 1995). As we previously reported for Tam-induced apoptosis (Bowie et al., 2004), STAT1 was active at baseline in untreated *HMEC-E6 cells (Fig. 3A). Treatment of *HMEC-E6 cells with rECM increased STAT1 phosphorylation at Ser727 by 2.5-fold ($p < 0.005$) at 1 hr, while total STAT1 levels remained unchanged (Fig. 3A, B).

Chromatin immunoprecipitation (ChIP) studies were performed to test whether rECM, similar to Tam, promotes the formation of a STAT1/CBP complex on the *IRF-1* GAS element. HMEC-LX control and *HMEC-E6 cells were grown in 3-hD rECM culture. Chromatin lysates were screened for STAT1 and CBP bound to the *IRF-1* GAS element. As shown in Fig. 3D, STAT1 was bound to the *IRF-1* GAS element in the *HMEC-E6 cells at baseline and during rECM

treatment while CBP was recruited to the GAS element only after rECM treatment. In contrast, neither STAT1 nor CBP were recruited to the *IRF-1* GAS element in HMEC-LX control cells (Fig. 3C). These observations indicate that STAT1 and CBP binding to the *IRF-1* GAS element may play a role in IRF-1 induction during rECM-mediated apoptosis in *HMEC-E6 cells.

To further test the association of STAT1 with the *IRF-1* GAS element, immunoprecipitation using a biotin-labeled oligonucleotide containing the *IRF-1* GAS promoter element was performed in *HMEC-E6 cells grown in 3-hD culture. Consistent with the ChIP results, STAT1 was associated with the GAS element at baseline (Figs. 3D, E). As seen in Fig. 3E, rECM promoted increased STAT1 association with the *IRF-1* promoter GAS element by 1 hr. These results show that 1) *HMEC-E6 cells exhibit baseline association of STAT1 binding to the *IRF-1* GAS element and 2) rECM promotes recruitment of CBP to the GAS element complex in *HMEC-E6 but not HMEC-LX cells.

IRF-1 induction and rECM

To further investigate the role of rECM in promoting apoptosis in *HMEC-E6 cells, we tested for mRNA and protein levels as a function of rECM treatment. Semi-quantitative RT-PCR showed that rECM promoted significant induction of IRF-1 mRNA in *HMEC-E6 cells at 1 hr (9.1-fold, p-value <0.05) but not in HMEC-LX cells (Fig. 4A, B). Consistent with mRNA expression results, rECM promoted a 2.5-fold increase in IRF-1 protein expression in *HMEC-E6 cells at 1 hr ($p < 0.0001$) (Fig. 4C, D).

Suppression of IRF-1 inhibits caspase-1 and -3 activation in *HMEC-E6 cells

We previously demonstrated that suppression of IRF-1 in *HMEC-E6 cells blocked Tam-induced activation of caspase-1 and -3 and apoptosis (Bowie et al., 2004). Here we similarly investigated whether suppression of IRF-1 in *HMEC-E6 cells blocked rECM-mediated caspase-1 and -3 activation and apoptosis in 3-hD culture. IRF-1 was suppressed using our previously published siRNA oligo sequences directed against IRF-1 (Bowie et al., 2004). Consistent with our prior results, treatment with IRF-1 #1 and IRF-1 #4 siRNA oligos for 12 hr suppressed baseline IRF-1 1) mRNA expression by 60% and 75%, respectively (Fig. 5A) and 2) protein expression by 95% and 97%, respectively (Fig. 5B). IRF-1 siRNAs #1 and #4 also blocked rECM-mediated induction of IRF-1 mRNA in *HMEC-E6 cells (Fig. 5C).

Suppression of IRF-1 with siRNA oligos in *HMEC-E6 cells blocked rECM-mediated apoptosis as evidenced by a lack of caspase-1 or -3 activation in 3-hD rECM culture. *HMEC-E6 cells pretreated with IRF-1 #1 or IRF-1 #4 siRNA oligos for 12 hr and grown in 3-hD rECM did not show activation of caspase-1 ($p < 0.002$) (Fig. 5D). Similarly, *HMEC-E6 cells pretreated with IRF-1 siRNA oligos also failed to fully activate caspase-3 at 12-24 hr after rECM culturing ($p < 0.002$) (Fig. 5E). In addition, we tested whether stable suppression of IRF-1 would inhibit rECM-induced activation of caspase-3 in *HMEC-E6 cells at 48 hr. *HMEC-E6 cells were transfected with the pSilencer4.1-CMV puro vector containing either the IRF-1 #1 siRNA target sequence or the Control siRNA non-specific sequence, and IRF-1 suppression was confirmed by western analysis (Fig. 6A). As shown in Fig. 6B, *HMEC-E6 cells with stable suppression of IRF-1 failed to activate caspase-3 upon 48h of rECM culturing ($p < 0.01$). These data show that IRF-1 expression is required for rECM-mediated activation of caspases-1 and -3 in *HMEC-E6 cells and are consistent with our previous observations demonstrating that suppression of IRF-1

in *HMEC-E6 cells blocked Tam-induced activation of caspase-1 and -3 as well as apoptosis (Bowie et al., 2004).

Based on the above observations, we next tested if overexpression of IRF-1 in HMEC-LX control cells sensitized them to rECM-mediated apoptosis. An exogenous IRF-1 construct was expressed in HMEC-LX cells using an IRES2 DsRed2 vector; control cells expressed the IRES2 DsRed2 empty vector alone. Transfection was confirmed by red fluorescence emission at 24 hr (Fig. 6C) and overexpression of IRF-1 in HMEC-LX cells expressing exogenous IRF-1 was confirmed by western analysis at 12 hr (Fig. 6D). As shown in Fig. 6E, overexpression of IRF-1 in HMEC-LX cells induced apoptosis in HMEC-LX cells 24 hr after transfection as evidenced by Annexin V binding ($p < 0.01$) and caspase-3 activation ($p < 0.01$) (Fig. 6E). This result is in line with recent reports showing that overexpression of IRF-1 induces apoptosis (Bouker et al., 2005; Pizzoferrato et al., 2004; Kim et al., 2004).

rECM induces IFI 6-16 mRNA

IRF-1 expression induces transcription of IFI 6-16, and it has been previously shown that IRF-1 directly binds to the interferon-stimulated response element (ISRE) within the *IFI 6-16* promoter (Parrington et al., 1993; Henderson et al., 1997). We previously demonstrated that treatment of *HMEC-E6 cells with 1.0 μM Tam promotes recruitment of IRF-1, STAT1, and CBP to the *IFI 6-16* IFN-stimulated response element (ISRE) promoter element followed by induction of IFI 6-16 mRNA (Bowie et al., 2004). These observations suggest that IFI 6-16 transcriptional activation can occur during Tam-induced apoptosis, associated with recruitment of IRF-1 to the *IFI 6-16* ISRE. We observe that Tam (Bowie et al., 2004) and rECM, as shown above, promote

apoptosis through recruitment of CBP to the *IRF-1* promoter, induction of IRF-1, and induction of apoptosis. Here we tested whether the downstream target of IRF-1, IFI 6-16 was activated by rECM, similar to our previously observations with Tam.

Differential gene expression data and semi-quantitative RT-PCR studies of *HMEC-E6 cells demonstrated that rECM, similar to Tam, induced a subset of ISGs, including IFI 6-16 (Table 1 and Fig. 2A). Since both Tam and rECM signals converge on the induction of IRF-1, we further investigated whether a downstream target of IRF-1, IFI 6-16, was similarly upregulated by rECM culturing in our *HMEC-E6 cells. Passage-matched HMEC-LX control and apoptosis-sensitive *HMEC-E6 cells were grown in 3-hD rECM culture and mRNA lysate harvested. Semi-quantitative RT-PCR was performed as described in Materials and Methods, in triplicate and normalized to β-actin. IFI 6-16 mRNA was induced in *HMEC-E6 cells at 1 hr ($p < 0.01$), while HMEC-LX control cells showed no induction of IFI 6-16 ($p > 0.05$) (Fig. 7A, B).

ISGF3 and IRF-1 binding to the ISRE in the* IFI 6-16 *promoter temporally correlates with transcriptional activation of IFI-6-16

IFI 6-16 has been shown to be strongly induced by Type I-IFN (IFN-α/β) signaling and weakly induced by Type II-IFN (IFN-γ) signaling (Kelly et al., 1986). Induction of IFI 6-16 expression by Type I IFNs has been shown to be mediated by binding of the ISGF3 complex (STAT1/STAT2/IRF-9) to the ISRE element of the *IFI 6-16* promoter (Kelly et al, 1986). It has been shown that upon IFN-α treatment, ISGF3 binds rapidly to the *IFI 6-16* ISRE, followed by the recruitment of IRF-1 at 1-2 hr (Kessler et al., 1988 and Levy et al., 1988). Furthermore, the binding of IRF-1 upon IFN-α treatment corresponds to maximal and sustained IFI 6-16 transcription. Without IRF-1 binding the level of IFI 6-16 transcription falls off suggesting that

IRF-1 is required to stabilize the ISGF3 complex (Imam et al., 1990). However, following treatment with IFN-γ, recruitment of IRF-1 alone to the *IFI 6-16* ISRE site also has been shown to promote IFI 6-16 expression (Henderson et al., 1997).

Here we tested in rECM-treated *HMEC-E6 cells whether the transcriptional activation of IFI 6-16 temporally correlated with recruitment of either the ISGF3 complex (STAT1/STAT2/IRF-9) or IRF-1/CBP to the *IFI 6-16* ISRE. *HMEC-E6 cells and HMEC-LX controls were grown in 3-hD rECM culture, cells harvested, and lysates tested for protein content and transcriptional factor binding. Western analysis demonstrated that exposure to rECM for 30 min was associated with a 3.1-fold and 2.2-fold respective increase in IRF-9 and STAT2 protein expression in *HMEC-E6 cells at 30 min (Fig. 7C). ChIP analysis demonstrated that in rECM-treated *HMEC-E6 cells, IRF-9 and STAT1 were recruited to the *IFI 6-16* ISRE promoter element by 30 min (Figs. 7D, E). IRF-9 is the final DNA binding factor recruited to the ISGF3 complex and is required for transcriptional activation (Veals et al., 1992). Therefore, these observations show that treatment of *HMEC-E6 cells with rECM for 30 min promotes recruitment of the ISGF3 complex to the *IFI 6-16* ISRE promoter element and precedes transcriptional activation of IFI 6-16 at 60 min.

We previously demonstrated that treatment of *HMEC-E6 cells with 1.0 μM Tam promoted recruitment of IRF-1, STAT1, and CBP to the *IFI 6-16* ISRE promoter element (Bowie *et al*, 2004). As described above, we observed that STAT1 was recruited to *IFI 6-16* ISRE promoter element in *HMEC-E6 cells after 30 min rECM treatment (Fig. 7E). We next tested the same lysates from *HMEC-E6 cells for the recruitment of IRF-1 and CBP to the *IFI 6-16* ISRE element. Both IRF-1 and CBP were recruited to the *IFI 6-16* ISRE promoter element in

*HMEC-E6 cells at 60 min, respectively (Fig. 7F). Recruitment was temporally associated with IFI 6-16 mRNA induction at 60 min (Fig. 7A-F). Taken together, these data show the ISGF3 complex is recruited to the *IFI 6-16* ISRE promoter element at 30 min, followed by IRF-1 and CBP recruitment by 60 min. The presence of this transcriptional complex correlates with the transcriptional activation of IFI 6-16 at 60 min. Since Tam also promotes recruitment of STAT1/CBP/IRF-1 to the *IFI 6-16* ISRE during the induction of IFI 6-16, this provides evidence that Tam- and rECM-signaling through IRF-1/CBP and target a common set of down-stream genes.

Discussion

Here we demonstrate that rECM promotes apoptosis in *HMEC-E6 cells through recruitment of CBP to the *IRF-1* GAS element and induction of IRF-1. Interactions between HMECs and ECM are known to regulate proliferation, polarity, and apoptosis (Petersen et al., 1992; Strange et al., 1992; Zutter et al., 1995; Ilic et al., 1998; Farrelly et al., 1999; Stupack and Cheresh, 2002) and loss of ECM signaling is observed during early mammary carcinogenesis (Petersen et al., 1992; Farrelly et al., 1999; Mercurio et al., 2001; Howlett et al., 1995; Hood and Cheresh, 2002). CBP is known to be a transcriptional regulator of both IFN and steroid/thyroid signaling (Robyr et al., 2000) and an important mediator of proliferation and apoptosis (Goodman and Smolik, 2000; Vo and Goodman, 2001). We previously demonstrated that suppression of CBP results in loss of rECM growth regulation, polarity, and apoptosis (Seewaldt et al., 2001). Recently we showed that CBP regulates mammary epithelial cell proliferation and apoptosis through recruitment of CBP to the *LAMA3A* promoter and transcriptional activation of laminin-5 (Dietze et al., 2005). These observations suggest that loss of CBP signaling may promote early mammary carcinogenesis through loss of sensitivity to rECM-mediated growth regulation and apoptosis.

We observe here that contact between *HMEC-E6 cells and rECM promotes recruitment of CBP to the *IRF-1* GAS element, IRF-1 induction, and apoptosis, while suppression of IRF-1 blocks apoptosis. CBP has been previously shown to be a transcriptional regulator of ISGs, including IRF-1. IRF-1 is known to play a critical role in eliminating damaged cells and participates in both p53-dependent and -independent apoptotic signaling (Tamura et al., 1995; Tanaka et al., 1996; Bouker et al., 2004; Porta et al., 2005). While IRF-1 was first identified as responding to IFNs (Romeo et al., 2002; Pizzoferrato et al., 2004), there is also growing evidence that IRF-1 plays an important role in mammary gland homeostasis and hormone responsiveness in the

absence of IFN treatment or production. IRF-1 promotes apoptosis during mammary gland involution while IRF-1 expression is downregulated or lost in both murine (Hoshiya et al., 2003; Kim et al., 2004; Yim et al., 1997;) and human (Yim et al., 2003; Doherty et al., 2001; Bouker et al., 2004; Bouker et al., 2005; Connett et al., 2005) breast cancers. IRF-1 is also induced by both Tam, an estrogen agonist/antagonist, and ICI 182,780, a pure estrogen antagonist (Bowie et al., 2004; Clarke et al., 2003; Bouker et al., 2004). Similar to our observation here with rECM, we recently observed that Tam promotes apoptosis in *HMEC-E6 cells, in the absence of IFN production, through recruitment of CBP to the GAS element of the *IRF-1* promoter and induction of IRF-1 (Bowie et al., 2004). Taken together, these observations support a role for IRF-1 signaling in mammary gland homeostasis and p53-independent apoptosis.

While p53 plays a pivotal role in apoptosis, not all apoptotic signaling requires the presence of p53. IRF-1 plays an important role in p53-independent response to DNA damage and is able to promote apoptosis in p53(-) cells (Tamura et al., 1995; Ossina et al., 1997; Kano et al., 1999; Pamment et al., 2002; Porta et al., 2005). Furthermore, mice lacking both IRF-1 and p53 exhibit a dramatic increase in spontaneous tumor formation relative to mice lacking p53 alone (Nozawa et al., 1999). IRF-1 has been shown to function as a tumor suppressor in breast cancer cells (Bouker et al., 2005). Suppression of IRF-1 in either MCF-7 (wild type p53) or T47D (mutant p53) cells resulted in increased growth and a decreased rate of apoptosis. Together, these results suggest that IRF-1 may act in parallel with p53 to promote apoptosis and that loss of IRF-1 would promote the survival of HMECs that had acutely lost p53 function. Since here we observe that recruitment of CBP to the *IRF-1* GAS element promotes induction of IRF-1, loss of CBP may also promote survival of p53(-) HMECs.

We observe that following exposure to rECM, IFI 6-16 mRNA is induced (Fig. 7). Traditionally IFI 6-16 is strongly induced by Type I IFNs and poorly induced by Type II IFNs (Kelly et al, 1986). However, induction of *IFI 6-16* promoter by IRF-1 alone has been seen in K562 cells using the -603 to +42 bp region of the *IFI 6-16* promoter (Henderson et al., 1997). In addition, treatment of human SV40 transformed fibroblasts with anti-IRF-1 antibody resulted in downregulation of IFI 6-16 expression (Tahara et al, 1995). Studies by Reid et al. showed that the core ISRE 39 bp region of the IFI 6-16 5'region could be stimulated by IFN-γ, but that the region from -603 to +437 bp was poorly induced (Reid et al., 1989). These data suggest that the intact, larger region of the *IFI 6-16* promoter may contain a repressor region which IFN-γ is not able to overcome in some cell types. Human foreskin fibroblasts show both ISGF3 (STAT1/STAT2/IRF-9) and IRF-1 binding to the IFI 6-16 ISRE in response to IFN-α yet the *IFI 6-16* promoter does not respond to IFN-γ (Imam et al., 1990). Thus, strong IRF-1 binding to the *IFI 6-16* promoter may require prior binding of ISGF3 in these cells. Since IFN-γ does not induce the formation of ISGF3, this could explain why IFI 6-16 mRNA is not induced well by IRF-1 alone in many cell types. Here, we observed binding of the ISGF3 complex and IRF-1/CBP to the *IFI 6-16* promoter ISRE after exposure to rECM. Binding of these co-activators was temporally associated with significant increase in IFI 6-16 mRNA. These observations suggest that ISGF3 as well as IRF-1/CBP participates in rECM-mediated transcriptional regulation of the *IFI 6-16* promoter ISRE .

Although extensive studies have focused on the *IFI 6-16* promoter, little is know about the biological function of IFI 6-16 during mammary carcinogenesis. Classically, Type I IFNs induce

growth arrest and apoptosis. IFI 6-16 is induced by Type I IFN-signaling, suggesting that it may play a role in apoptosis. However, IFI 6-16 is also upregulated in senescent human fibroblasts and recently, overexpression of IFI 6-16 was shown to correlate with resistance to apoptosis in cancer cell lines (Tahara et al., 2005). In the context of our work, we hypothesize that IFI 6-16 may be a marker of IRF-1 activity but may not be an essential component of the apoptotic response seen in the *HMEC-E6 cells. Further studies are underway to suppress IFI 6-16 and test for the requirement for IFI 6-16 expression in rECM-mediated apoptotic signaling.

In these studies, we observe that rECM, similar to rapid Tam-signaling, promotes apoptosis through induction of IRF-1. Both rECM and Tam-induced apoptosis are associated with induction of a subset of ISGs, including IFI 6-16, IFI 9-27, ISG15, IFI 35, TAP2, and ISG-54 (Table 1). Taken together, our studies show that both rECM and rapid Tam-signaling induce apoptosis through signaling pathways that converge on IRF-1 and are consistent with recent reports highlighting the importance of IRF-1-signaling in mammary gland homeostasis and estrogen signaling (Doherty et al., 2001; Tzonapoulous et al., 2002; Clarke et al., 2003, Pizzoferrato et al., 2004; Bouker et al., 2004; Bowie, et al., 2004, Bouker et al., 2005; Connett et al., 2005). In addition, these studies also provide evidence that IRF-1 promotes apoptosis in acutely damaged HMECs independent of p53 expression. IRF-1 and p53 are thought to participate in parallel damage response pathways. Therefore, if mammary epithelial cells are acutely damaged through loss of p53 function, IRF-1-signaling represents an alternative pathway to eliminate p53-damaged cells. Taken together, these results provide evidence that both Tam and rECM transcriptionally activate IRF-1 and support an important role for IRF-1 in mediating p53-independent apoptosis in mammary epithelial cells.

Materials and Methods

***Materials*-** All chemicals and cell culture reagents were obtained from Sigma-Aldrich (St. Louis, MO, USA), DNA primers from Invitrogen (Carlsbad, CA, USA) or Operon Biotechnologies (Alameda, CA, USA), and cell culture plasticware from Corning (Corning, NY, USA) unless otherwise noted. Caspase-1 inhibitor IV was obtained from EMD Biosciences Inc. (San Diego, CA, USA). IFN-γ was obtained from R&D Systems (Minneapolis, MN, USA), reconstituted to a 10 μg/ml stock with 1x PBS (0.1% BSA), and stored at -70^{o}C.

***Retroviral transduction*-** The LXSN16E6 retroviral vector containing the HPV-16 E6 coding sequence was provided by D. Galloway (Fred Hutchinson Cancer Research Center, Seattle, WA) (Demers et al., 1996). Retroviral transduction was performed as previously described (Dietze et al., 2001). HMECs (passage 9) were cultured in Standard Medium and grown to 50% confluency. Transducing virions from either the PA317-LXSN16E6 or the control PA317-LXSN (without insert) retroviral producer line were added at a multiplicity of infection of 1.0 in the presence of 4 ug/ml Polybrene to log-phase cells grown in T-75 flasks. After 48 hours, flasks containing transduced cells were passed 1:3 (passage 10) and selected with Standard Media containing 300 μg/ml G418. The transduced, selected cells were maintained in the absence of selection before immediately proceeding to experiments. Transduced AG11132 cells expressing the HPV-16E6 construct that are within three passages of retroviral transduction were designated *HMEC-E6 and corresponding vector control clones were designated HMEC-LX. All experiments were performed on mass cultures within three passages of transduction. All *HMEC-E6 cells and HMEC-LX controls were passed in parallel culture and all experimental

controls were passage matched.

Small scale semi-solid rECM culture- HMECs were grown in rECM by methods adapted from those developed by Bissell and others (Folkman and Moscona, 1978; Howlett et al., 1994; Howlett et al., 1995) as previously described (Seewaldt et al., 2001). In brief, 100 μl of rECM (Growth Factor Depleted Matrigel^{tm}, Discovery Labware, Bedford, MA) were added per well to a 48 well plate and allowed to gel at 37^{o}C for 20 min. Transduced HMECs were trypsinized, counted, and pelleted. Approximately 1 x 10^4 cells were resuspended in 100 μl rECM on ice, gently overlaid on the initial undercoating of extracellular matrix, and allowed to gel at 37^{o}C for 20 min. After addition of Standard Media, wells were inspected to ensure there was an equal distribution of cells in each well.

Large-scale high-density liquid rECM culture- Large-scale high-density liquid rECM culture (3-hD rECM) was utilized to prepare large-scale protein lysates using an adaptation of techniques previously developed by the laboratory of Mina Bissell (Roskelley et al., 1994). Cells were plated at high density (2.5 x 10^7/25 cm^2) in either T-25 or T-75 flasks or 24 well plates, previously treated with poly[2-hydroxyethyl methacrylate (poly-HEME)]. Cells were grown in Standard Media with 1:100 dilution (v:v) of growth factor-depleted rECM (Growth Factor Depleted Matrigel^{tm}, Discovery Labware, Bedford, MA).

Cell growth- Proliferation was assessed by Ki-67 staining index. HMEC-LX controls and *HMEC-E6 early passage cells were cultured in rECM. Cells were harvested and spun onto a coated microscope slide using a Shandon Cytospin® 4 Cytocentrifuge (Thermo Electron

Corporation, Pittsburg, PA, USA). Cells were fixed in acetone and immunostained with antibody directed against Ki-67. Cells were scored visually for immunopositive nuclei. The Ki-67 proliferative index was assessed by calculating the number of immunopositive cells as a percentage of the total number of cells.

***Integrin-blocking experiments*-** Approximately 5 x 10^4 cells were pelleted and resuspended in 100 μl Standard Media containing either antibodies (Ab) to α3- and β1-integrins (Chemicon International, Temecula, CA, USA) or control non-immune mouse IgG for 15 min at RT. Final concentration of α3-integrin blocking Ab (CDW496, clone P1B5) was 10 ug/ml and β1-integrin blocking Ab (CD29, clone JB1A) was 20 μg/ml. Cells were plated in poly-HEME coated 24 well plates and were grown in Standard Media with 1:100 dilution (v:v) of growth factor-depleted rECM (Growth Factor Depleted Matrigel™, Discovery Labware).

***Differential gene expression studies*-** Total RNA isolation was as previously described (Seewaldt et al., 1995). RNA integrity was confirmed by electrophoresis, and samples were stored at -70°C until used. All RNA combinations used for array analysis were obtained from cells that were matched for passage number, cultured under identical growth conditions, and harvested at identical confluency. cDNA synthesis and probe generation for cDNA array hybridization were performed by following the standardized protocols provided by Affymetrix (Affymetrix, Santa Clara, CA, USA).

Expression data for approximately 5,600 full-length human genes were collected using Affymetrix GeneChip HuGeneFL™ arrays and following the standardized protocols provided by

the manufacturer. Data were collected in triplicate using independent biological replicates. Array images were processed using Affymetrix™ MAS 5.0 software where we filtered for probe saturation, employed a global array scaling target intensity of 1000, and collected the signal intensity value (i.e., the "average difference") for each gene. Pair-wise "treatment vs control" comparisons were made employing CyberT (Baldi and Long, 2001), a Bayesian t-statistic algorithm derived for microarray analysis. We employed a window size of 101 and used a confidence value of 10 in our CyberT analysis. Significant changes in expression were determined by ranking the assigned Bayesian p-values and applying a false discovery rate correction (FDR = 0.05) to account for multiple testing (Benjamini et al., 1995).

***Semi-quantitative RT-PCR*-** To confirm the microarray data, relative transcript levels were analyzed by semi-quantitative RT-PCR as previously described (Bowie et al., 2004). Briefly, total RNA (5 ug) was used in first-strand cDNA synthesis with Superscript™ II reverse transcriptase (Invitrogen, Carlsbad, CA, USA). All PCR reactions were in 50 ul total volume. Products were amplified with GeneAmp PCR Systems 2400 and 9700 (Applied Biosystems, Foster City, CA, USA). In all, 10 ul of PCR product was analyzed by electrophoresis in 1.2-1.5% agarose (Invitrogen) gels containing ethidium bromide and visualized under UV light. All samples were performed in triplicate and normalized to β-actin control. Band quantitation was done using Kodak 1D™ Image Analysis Software (Eastman Kodak, Rochester, NY, USA).

For time-course semi-quantitative RT-PCR studies on IRF-1 and IFI 6-16, 50 ng of total RNA was used in first-strand cDNA synthesis with Superscript™ II reverse transcriptase. PCR reaction conditions were the same as previously described (Bowie et al., 2004) for IFI 6-16

amplification, except the product was amplified for 33 cycles. IRF-1 amplification had to be re-optimized for lower total RNA input. The changes made to the reaction were as follows: 1) HotStarTaq™ polymerase (Qiagen, Valencia, CA, USA) was used, 2) annealing temperature was increased to 57°C, 3) and amplification was carried out for 36 cycles. In all, 20 μl of PCR product was analyzed by electrophoresis in 1.5% agarose (Invitrogen) gels containing ethidium bromide and visualized under UV light. All samples were performed in triplicate and normalized to β-actin control. Band quantitation was done using Kodak 1D™ Image Analysis Software (Eastman Kodak).

IFN ELISA- Aliquots of tissue culture media, from both *HMEC-E6 and HMEC-LX cells cultured in rECM, were withdrawn from flasks at 0, 30 min, 1, 2, and 4 hr and stored at -70°C. Manufacturer protocols for the commercial IFN-α, IFN-β (Biosource International, Camarillo, CA, USA), and IFN-γ (Pharmingen, San Diego, CA, USA) ELISA kits were followed. Duplicate standard curves were run on each plate, and media samples were assayed in triplicate.

Measurement of apoptosis and caspase-1 and -3 activity- Apoptosis and caspase-3 were measured by using the ApopNexin™ FITC Apoptosis Detection Kit and the CaspaTag™ Caspase-3 *In Situ* Assay kit, respectively (Chemicon International, Inc). Briefly, *HMEC-E6 cells and control matched HMEC-LX cells were cultured in rECM for the determined times, harvested, spun down, washed in ice cold 1 x PBS and pelleted. The manufacture's protocol for fluorescence microscopy was followed, and cells were visualized on an inverted microscope, model Eclipse TE2000-U (Nikon, Melville, NY, USA). A digital camera (DXM1200F, Nikon) attached to the inverted microscope was used to take digital images of the cells. For Annexin-V

quantitation, 100 cells were counted for each time point and the percent of positive cells was determined.

For timecourse blocking antibody studies, caspase-1 and -3 assays were performed as follows: cells were harvested by trypsinization, washed once with 100 volumes of ice cold PBS and pelleted. Caspase-1 and -3 activities were then assayed according to the manufacturer's instructions using a caspase-1 (EMD Biosciences Inc.) or caspase-3 (Clontech, Palo Alto, CA, USA) assay kit. For IRF-1 suppression studies, early passage HMEC-E6 cells were transfected with IRF-1 siRNAs 12 hr prior to culturing in rECM. Caspase-1 and -3 levels were measured after cells were placed in rECM.

Chromatin immunoprecipitation assay (ChIP)- ChIP was performed by published methods with some modifications (Yahata et al., 2001) and as previously described (Bowie et al., 2004). Briefly, cells were cultured in rECM, harvested, pelleted, and treated with 1% formaldehyde for 15 min to cross-link cellular proteins. Cells were then rinsed twice in ice cold 1x PBS containing protease inhibitors, pelleted, and resuspended in Lysis Buffer. Samples were then sonicated 3 x 15 sec each with a 1 min incubation on ice in between pulses on a Branson sonifier model 250 at 50% duty and maximum mini probe power. A 20 ul aliquot of lysate was saved and used to determine the input DNA for each sample. Supernatants were diluted (1:10) in Dilution Buffer, and precleared with 2 μg of sheared salmon sperm DNA (Invitrogen), 20 ul normal human serum, and 45 ul of 50% slurry of protein A-sepharose. To the precleared chromatin, 10 μl of either anti-IRF-9 (H-143, Santa Cruz Biotechnology, Santa Cruz, CA,USA), anti-CBP (A-22, Santa Cruz Biotechnology), anti-STAT1 (E-23, Santa Cruz Biotechnology), or anti-IRF-1 (H-

205, Santa Cruz Biotechnology) was added, and the reaction was incubated overnight, followed by an addition of 45 ul of protein A-sepharose and 2.0 ug sheared salmon sperm and an additional 1 hr incubation. Sepharose beads were then collected and washed sequentially for 10 min each in TSE I, TSE II, and buffer III. Finally, beads were washed once with TE buffer and DNA eluted with 100 μl of 1% SDS-0.1 M $NaHCO_3$. Eluate was heated at 65°C overnight to reverse the formaldehyde cross-linking. DNA fragments were cleaned-up with the QIAquick PCR purification kit (Qiagen) and amplified in a PCR reaction. In all, 30 ul of PCR product was analyzed by electrophoresis in 1.5% agarose (Invitrogen) gels containing ethidium bromide and visualized under UV light using Kodak 1D™ Image Analysis Software (Eastman Kodak). All reactions were performed in triplicate.

Western blotting- Preparation of cellular lysates and immunoblotting were performed as previously described (Seewaldt et al., 1997; Seewaldt et al., 1999a). For protein expression, the membrane was incubated with the following antibodies: IRF-1 (C-20, Santa Cruz Biotechnology), STAT1 (E-23, Santa Cruz Biotechnology), phospho-STAT1-Ser727 antibody (Cell Signaling Technology, Beverly, MA, USA), IRF-9 (H-143, Santa Cruz Biotechnology) and STAT2 (A-7 Santa Cruz Biotechnology). Loading control was provided with antibody to GAPDH (V-18, Santa Cruz Biotechnology) or β-actin (I-19, Santa Cruz Biotechnology). After incubation with SuperSignal West Dura luminol substrate (Pierce Chemical, Rockford, IL, USA), the resulting membrane images were digitized with a Kodak 2000MM imager and quantitated using Kodak 1D™ Image Analysis Software (Eastman Kodak). The membrane was stripped with Restore™ Western Blot Stripping Buffer for 30 min, (Pierce) and reblocked overnight in 10% BSA in between screening for phospho-STAT1-Ser727 and total STAT1.

Suppression of IRF-1 with siRNA- Suppression of IRF-1 with siRNA oligos was done as previously described (Bowie et al., 2004). Briefly, early passage *HMEC-E6 cells were transfected with IRF-1 #1 and #4 siRNAs (2.0 ug and 1.5 ug, respectively) or control non-silencing siRNA (Qiagen) using Cellfectin™ (Invitrogen). Twelve hours after transfection, RNA was harvested using the Aurum™ Total RNA kit (Bio-Rad Laboratories, Hercules, CA, USA), and protein was harvested as previously described (Seewaldt et al., 1999b; Seewaldt et al., 1997). Western analysis (as described above) and RT-PCR were performed to confirm suppression of IRF-1 expression. cDNA was prepared for RT-PCR from 50 ng total RNA with Superscript™ II reverse transcriptase (Invitrogen). Beta-actin PCR reaction conditions were performed as described above except product was amplified for 24 cycles. IRF-1 RT-PCR reactions were done the same as the semi-quantitative RT-PCR time-course, except the program was run for 38 cycles. In all, 25 ul of PCR product were run on either 2.0% or 1.2% agarose gels stained with ethidium bromide and visualized with Kodak 1D™ Image Analysis Software (Eastman Kodak). Stable siRNA suppression was done as previously described (Dietze et al., 2005). Briefly, both the Control siRNA (Qiagen) and the IRF-1#1 siRNA target areas were used to design two 55-mer DNA oligos to be annealed and inserted into pSilencer 4.1-CMV puro vector (Ambion, Austin, TX, USA). A hairpin siRNA template was created by annealing the following oligos: Control siRNA top-strand, 5'-GAT CCT TCT CCG AAC GTG TCA CGT TTC AAG AGA ACG TGA CAC GTT CGG AGA ATT A-3', Control siRNA bottom strand, 5'- AGC TTA ATT CTC CGA ACG TGT CAC GTT CTC TTG AAA CGT GAC ACG TTC GGA GAA G-3', IRF-1 #1 siRNA top strand, 5'- GAT CCC TTT CGC TGT GCC ATG AAC TTC AAG AGA GTT CAT GGC ACA GCG AAA GTT A-3', and IRF-1#1 siRNA bottom strand, 5'- AGC TTA ACT

TTC GCT GTG CCA TGA ACT CTC TTG AAG TTC ATG GCA CAG CGA AAG G-3'. The annealed oligos were ligated to pSilencer 4.1-CMV puro through their HindIII and BamHI ends. Transfection of expression plasmid was performed in *HMEC-E6 cells using Cellfectin™ (Invitrogen) and selection with puromycin. Suppression of IRF-1 was confirmed by Western analysis as described above.

***Overexpression of IRF-1 cDNA*-** IRF-1 full length cDNA was PCR amplified from HMEC-LX control cells cDNA, using published primers with slight modification (Yokota et al., 2004). The forward primer 5'end was changed to an XhoI site while the reverse primer remained a 3'BamHI site. The full length IRF-1 cDNA was first cloned into the pCR2.1 vector (Invitrogen), and then subcloned into the IRES2 DsRed2 vector (DsRed-IRF-1) using the EcoRI ends from the pCR2.1 vector. Sequence was confirmed, and HMEC-LX cells were transfected with 10 μg of IRES2-DsRed2-IRF plasmid and empty IRES2-DsRed2 vector.

IRF-1 *promoter pull down*- *HMEC-E6 cells were cultured in rECM and harvested at 0 and 60 min. Preparation of cellular lysates and immunoblotting were performed as previously described (Seewaldt et al., 1997; Seewaldt et al., 1999a). A 25 bp section of the *IRF-1* promoter region, encompassing the GAS element (-134 to -109 bp upstream), was used to design biotin-labeled oligos. The complimentary oligos (Operon Biotechnologies) were annealed in equal molar concentrations by heating to 95°C for 5 min and being allowed to cool to room temperature. Then 890 μg of total protein lysate was precleared with Streptavidin beads. The supernatant was subsequently incubated with IRF-1 GAS-annealed oligos and Streptavidin beads for 2 hr at 4°C. The beads were washed 3x in lysis buffer with protease inhibitors, boiled, and run on an SDS-

PAGE gel. Anti-STAT1 (E-23, Santa Cruz Biotechnology) was used to detect bound protein. Loading control was provided with antibody β-actin (I-19, Santa Cruz Biotechnology).

Acknowledgements

This work is supported by NIH/NCI grants P30CA14236, P50CA68438, R01CA088799, R01CA098441, and R01CA114068 (to VLS), DAMD BC010919 (to VLS), Susan G. Komen Breast Cancer Foundation BCTR0402720 (to VLS and ECD), a V-Foundation award (to VLS), and a Charlotte Geyer award (to VLS). The authors gratefully acknowledge Martha Stamfer's gift of normal human mammary epithelial cells and Denise Galloway for the LXSN16E6 retroviral vector containing the HPV-16E6 coding sequence.

References

Aberdam D, Virolle T, and Simon-Assmann P. (2000). *Microscopy Res. Technique*, **51,** 228-237.

Baldi P and Long AD. (2001). *Bioinformatics*, **17,** 509-519.

Benjamini Y and Hochberg Y. (1995). *J. R. Stat. Soc. Ser. B - Methodological*, **57**, 289-300.

Bouker KB, Skaar, TC, Fernandez DR, O'Brien KA, Riggins RB, Cao DH, and Clarke R. (2004). *Cancer Res*., **64,** 4030-4039.

Bouker KB, Skaar TC, Riggins RB, Harburger DS, Fernandez DR, Zwart A, Wang A, and Clarke R. (2005). *Carcinogenesis*, **26,** 1527-1535.

Bowie ML, Dietze EC, Delrow J, Bean GR, Troch MM, Marjoram RJ, Seewaldt VL. (2004). *Oncogene*, **23**, 8743-8755.

Clarke R, Liu MC, Bouker KB, Gu Z, Lee RY, Zhu Y, Skaar TC, Gomez B, O'Brien K, Wang Y, and Hilakivi-Clarke LA. (2003). *Oncogene*, **22,** 7316-7339.

Connett JM, Badri L, Giordano TJ, Connett WC, and Doherty GM. (2005). *J. Interferon Cytokine Res*., **25**, 587-594.

D'Ardenne AJ, Richman PI, Horton MA, McAulay AE, and Jordan S. (1991). *J. Pathol*., **165,** 213-220.

Demers GW, Espling E, Harry JB, Etscheid BG, and Galloway DA. (1996). *J. Virol.*, **70,** 6862-6869.

Dietze EC, Caldwell LE, Grupin SL, Mancini M. and Seewaldt VL. (2001). *J Biol Chem*, **276,** 5384-5394.

Dietze EC, Troch MM, Bean GR, Heffner JB, Bowie ML, Rosenberg P, Ratliff B, and Seewaldt VL. (2004). *Oncogene*, **23**, 3851-3862.

Dietze EC, Bowie ML, Mrózek K, Caldwell LE, Neal C, Marjoram RJ, Troch MM, Bean GR, Yokoyama KK, Ibarra CA, and Seewaldt VL. (2005) *J. Cell Sci*., **118,** 5005-5022.

Doherty GM, Boucher L, Sorenson K, and Lowney J. (2001). *Ann. Surg.*, **233,** 623-629.

Farrelly N, Lee YJ, Oliver J, Dive C, and Streuli CH. (1999). *J. Cell Biol.*, **144**, 1337-1348.

Folkman J and Moscona A. (1978) *Nature*, **273**, 345-349.

Goodman RH and Smolik S. (2000). *Genes Devel*., **14,** 1553-1577.

Gu Z, Lee RY, Skaar TC, Bouker KB, Welch JN, Lu J, Liu A, Zhu Y, Davis N, Leonessa F, Brünner N, Wang Y, and Clarke R. (2002). *Cancer Research,* **62**, 3428-3437.

Henderson YC, Chou M, and Deisseroth AB. (1997). *Br. J. Haematol.*, **96,** 566-575.

Henning K, Berndt A, Katenkamp D, and Kosmehl H. (1999) *Histopathol*., **34,** 305-309.

Hood JD and Cheresh DA. (2002). *Nature Rev. Cancer,* **2**, 91-100.

Hoshiya Y, Gupta V, Kawakubo H, Brachtel E, Carey JL, Sasur L, Scott A, Donahoe PK, and Maheswaran S. (2003). *J. Biol. Chem.*, **278,** 51703-51712.

Howlett AR, Petersen OW, Steeg PS, and Bissell MJ. (1994). *J. Natl. Cancer Inst.*, **86**, 1838-1844.

Howlett AR, Bailey N, Damsky C, Petersen OW, and Bissell MJ. (1995). *J. Cell Sci.*, **108**, 1945-1957.

Ilic D, Almeida EA, Schlaepfer DD, Dazin P, Aizawa S, and Damsky CH. (1998). *J. Cell Biol.*, **143**, 547-560.

Imam AMA, Ackrill AM, Dale TC, Kerr IM, and Stark GR. (1990). *Nucleic Acids Res*., **18,** 6573-6580.

Kano A, Haruyama T, Akaike T, and Wantanabe Y. (1999). *Biochem. Biophys. Res. Commun*., **257,** 672-677.

Kelly MJ and Levin ER. (2001). *Trends Endocrinol. Metab.*, **12,** 152-156.

Kelly JM, Porter AC, Chernajovsky Y, Gilbert CS, Stark GR, and Kerr IM. (1986). *EMBO J.*, **5**, 1601-1606.

Kim PK, Armstrong M, Liu Y, Yan P, Bucher B, Zuckerbraun BS, Gambotto A, Billiar TR, and Yim JH. (2004). *Oncogene*, **23,** 1125-1135.

Kessler DS, Levy DE, and Darnell, JE. (1988). *Proc Natl. Acad. Sci. USA*, **85**, 8521-8525.

Levy DE, Kessler DS, Pine R, Reich N, and Darnell JE, Jr. (1988). *Genes and Develop*., **2**, 383-393.

Marquez DC and Pietras RJ. (2001). *Oncogene*, **20**, 5420-5430.

Marquez DC, Chen H-W, Curran EM, Welshons WV, and Pietras RJ. (2006). *Mol. Cell. Endocrinol.*, **246**, 91-100.

Martin KJ, Kwan CP, Nagasaki K, Zhang X, O'Hare MJ, Kaelin CM, Burgeson RE, Pardee AB, and Sager R. (1998). *Mol. Med*., **4,** 602-613.

Mercurio AM and Shaw LM. (1991). *Bioessays*, **13,** 469-473.

Mercurio AM, Bachelder RE, Chung J, O'Connor KL, Rabinovitz I, Shaw LM, and Tani T. (2001) *J. Mamm. Gland Biol. Neoplasia*, **6**, 299-309.

Miyamoto M, Fujita T, Kimura Y, Maruyama M, Harada H, Sudo Y, Miyata T, and Taniguchi T. (1988). *Cell*, **54**, 903-913.

Novaro V, Roskelley CD, and Bissell MJ. (2003). *J. Cell Sci*., **116**, 2975-2986.

Nozawa H, Oda E, Nakao K, Ishihara M, Ueda S, Yokochi T, Ogasawara K, Nakatsuru Y, Shimizu S, Ohira Y, Hioki K, Aizawa S, Ishikawa T, Katsuki M, Muto T, Taniguchi T, and Tanaka N. (1999). *Genes Dev*., **13**, 1240-1245.

Ossina NK, Cannas A, Powers VC, Fitzpatrick PA, Knight JD, Gilbert JR, Shekhtman EM, Tomei LD, Umansky SR, and Kiefer MC. (1997). *J. Biol. Chem.*, **272,** 16351-16357.

Parrington J, Rogers NC, Gewert DR, Pine R, Veals SA, Levy DE, Stark GR, and Kerr IM. (1993). *Eur. J. Biochem.*, **214,** 617-26.

Pamment J, Ramsay E, Kelleher M, Dornan D, and Ball KL. (2002). *Oncogene*, **21,** 7776-7785.

Petersen OW, Ronnov-Jensen L, Howlett AR, and Bissell MJ. (1992). *Proc Natl. Acad. Sci. USA*, **89**, 9064-9068.

Pizzoferrato E, Liu Y, Gambotto A, Armstrong MJ, Stang MT, Gooding WE, Alber SM, Shand SH, Watkins SC, Storkus WJ, and Yim JH. (2004). *Cancer Res.*, **64**, 8381-8388.

Porta C, Hadj-Slimane R, Nejmeddine M, Pampin M, Tovey MG, Espert L, Alvarez S, and Chelbi-Alix MK. (2005). *Oncogene*, **24,** 605-615.

Reid LE, Brasnett AH, Gilbert CS, Porter ACG, Gewert DR, Stark GR, and Kerr IM. (1989). *Proc. Natl. Acad. Sci. USA*, **86,** 840-844.

Robyr D, Wolffe AP, and Wahli W. (2000). *Mol. Endocrinol*., **14,** 329-347.

Romeo G, Fiorucci G, Chiantore MV, Percario ZA, Vannucchi S, and Affabris E. (2002). *J. Interferon Cytokine Res.*, **22,** 39-47.

Roskelley CD, Desprez PY, and Bissell MJ. (1994). *Proc. Natl. Acad. Sci. USA*, **91**, 12378-12382.

Seewaldt VL, Johnson BS, Parker MB, Collins SJ, and Swisshelm K. (1995). *Cell Growth Differ*., **6,** 1077-1088.

Seewaldt VL, Kim JH, Caldwell LE, Johnson BS, Swisshelm K, and Collins SJ. (1997). *Cell Growth Differ.*, **8,** 631-641.

Seewaldt VL, Kim JH, Parker MB, Dietze EC, Srinivasan KV, and Caldwell LE. (1999a). *Exp. Cell Res.*, **249,** 70-85.

Seewaldt VL, Dietze EC, Johnson BS, Collins SJ, and Parker MB. (1999b). *Cell Growth Differ.*, **10,** 49-59.

Seewaldt VL, Mrozek K, Sigle R, Dietze EC, Heine K, Hockenberry DM, Hobbs KB, and Caldwell LE. (2001). *J. Cell Biol.*, **155,** 471-486.

Shang M, Koshikawa N, Schenk S, and Quaranta V. (2001). *J. Biol. Chem.*, **276,** 33045-33053.

Strange R, Li F, Saurer S, Burkhardt A, and Friis RR. (1992) *Development*, **115**, 49-58.

Stupack DG and Cheresh DA. (2002). *J. Cell Sci.*, **115**, 3729-3738.

Tahara H, Kamada K, Sato E, Tsuyama N, Kim JK, Hara E, Oda K, and Ide T. (1995). *Oncogene*, **11,** 1125-1132.

Tahara E, Tahara H, Kanno M, Naka K, Takeda Y, Matsuzaki T, Yamazaki R, Ishihara H, Yasui W, Barrett JC, Ide T, and Tahara E. (2005). *Cancer Immunol. Immunotherapy*, **54,** 729-740.

Tamura T, Ishihara M, Lamphier MS, Tanaka N, Oishi I, Aizawa S, Matsuyama T, Mak TW, Taki S, and Taniguchi T. (1995). *Nature*, **376,** 596-599.

Tanaka N, Ishihara M, Lamphier MS, Nozawa H, Matsuyama T, Mak TW, Aizawa S, Tokino T, Oren M, and Taniguchi T. (1996). *Nature*, **382,** 816-818.

Tzoanopoulos D, Speletas M, Arvanitidis K, Veiopoulou C, Kyriaki S, Thyphronitis G, Sideras P, Kartalis G, and Ritis K. (2002). *Br. J. Haematol.*, **119,** 46-53.

Veals SA, Schindler C, Leonard D, Fu XY, Aebersold R, Darnell JE Jr., and Levy DE. (1992). *Mol. Cell Biol.*, **12**, 3315-3324.

Vo N and Goodman RH. (2001). *J. Biol. Chem.*, **273,** 13505-13508.

Wen Z, Zhong Z, and Darnell Jr JE. (1995). *Cell*, **82,** 241-250.

Yahata T, Shao W, Endoh H, Hur J, Coser KR, Sun H, Ueda Y, Kato S, Isselbacher KJ, Brown M, and Shioda T. (2001). *Genes Devel.*, **15,** 2598-2612.

Yim JH, Wu SJ, Casey MJ, Norton JA, and Doherty GM. (1997). *J. Immunol.*, **158,** 1284-1292.

Yim JH, Ro SH, Lowney JK, Wu SJ, Connett J, and Doherty GM. (2003). *J. Interferon Cytokine Res.*, **23**, 501-511.

Yokota S, Okabayashi T, Yokosawa N, and Fujii N. (2004). *J. Virol.*, **78**, 4591-4598.

Zutter MM, Santoro SA, Staatz WD, and Tsung YL. (1995). *Proc. Natl. Acad. Sci. USA*, **92**, 7411-7415.

Table 1: ISG gene changes with rECM or tamoxifen treatment.

			ECM treatment		Tam treatment	
Gene Name	Symbol	Genbank™	Fold change		Fold change	
			HMEC-LX	HMEC-E6	HMEC-LX	HMEC-E6
IFI 9-27	IFITM1	J04164	----	1.5	----	4.5
IRF-1	IRF1	L05072	----	2.0	----	4.0
ISG15	G1P2	M13755	----	2.5	----	4.4
ISG-54	IFIT2	M14660	----	3.4	----	5.2
RANTES	CCL5	M21121	----	----	----	1.9
IFI-56	IFIT1	M24594	2.7	3.2	----	2.3
MxA	MX1	M33882	3.7	13.3	----	20.0
IFI16	IFI16	M63838	----	1.7	----	2.0
OAS2, isoform p69	OAS2	M87284	----	----	----	3.8
OAS2, isoform p71	OAS2	M87434	----	----	----	3.6
IRF-9	ISGF3G	M87503	----	----	----	2.6
STAT-1 alpha	STAT1	M97935	----	----	----	2.0
STAT1-beta	STAT1	M97936	----	6.3	-3.1	12.7
IFNGR1	IFNGR1	U19247	2.8	2.7	----	2.1
IFI 6-16	G1P3	U22970	----	13.4	----	17.5
RIG-G	IFIT3	U52513	----	2.2	----	2.1
IRF-7	IRF7	U53830	4.7	4.7	----	9.7
IFI35	IFI35	U72882	----	1.8	----	2.6
OAS1, (1.6kb RNA)	OAS1	X02874	2.6	4.3	----	4.5
OAS1, (1.8kb RNA)	OAS1	X02875	----	3.5	----	4.2
IL6	IL6	X04602	----	----	----	----
IFITM2	IFITM2	X57351	----	----	----	----
ISG12	IFI27	X67325	----	----	----	7.6
PSMB10	PSMB10	X71874	----	1.5	-1.6	----
PSMB8	PSMB8	Z14982	----	2.1	-2.6	----
TAP2	TAP2	X66401	----	2.0	----	1.83

Titles and Legends to Figures.

Figure 1. rECM culture of *HMEC-E6 cells promotes growth arrest, apoptosis, and activation of caspase-1 and -3.

(A) *Small-Scale Semi-Solid rECM Culture:* Cells are embedded as single cells in three-dimensional, semi-solid growth factor depleted rECM at Day 0. HMEC-LX controls proliferate in rECM for 6 days in rECM, forming 20-30 micron acinus like structures, and then undergo growth arrest on Day 6-7. Passage-matched *HMEC-E6 cells are plated in rECM, caspase-3 is activated on Day 6-7 and apoptosis detected on Day 6-7 (Dietze et al., 2005). *Large-Scale High-Density Liquid rECM Culture (3-hD rECM):* Cells are plated at high density in poly-HEME (Sigma) coated flasks in Standard Media with a 1:100 dilution of growth factor depleted rECM. At 6 hrs both HMEC-LX and *HMEC-E6 cells detach from the non-adhesive substratum and spontaneously aggregate to form 20-30 micron, acinus -like structures. *HMEC-E6 cells exhibit evidence of apoptosis starting at 12 hr. **(B, C)** rECM promotes growth arrest and apoptosis in *HMEC-E6 cells but growth arrest alone in passage matched HMEC-LX controls. **(B)** Proliferation in 3-hD culture was measured by Ki-67 staining. The proliferation index was measured by calculating the number of Ki-67 staining cells relative to the total number of cells surveyed. Data represent an average of three experiments. ***** - significantly different from t = 0 h for $p < 0.01$. **(C)** Apoptosis was measured in 3-hD culture by Annexin V-staining of *HMEC-E6 cells and passage-matched HMEC-LX controls in 3-hD rECM as described in Materials and Methods and the percent of apoptotic cells measured. Data represent an average of three independent experiments. *Error bars* show standard error. ***** - significantly different from t = 0 h for $p < 0.05$. (D, E) Caspase-1 and -3 are activated in *HMEC-E6 cells grown in 3-hD rECM.

(D) Caspase-1 is induced by rECM in 3-hD culture starting at 3 hr. Treatment with α3- or β1-integrin blocking antibodies inhibited caspase-1 activation. ***** - statistically significant compared to NS IgG and control, $p < 0.05$. **(E)** Caspase-3 is induced by rECM starting at 12 hr. Treatment with α3- or β1-integrin blocking antibodies blocked caspase-3 activation. Cells were grown in rECM culture with or without preimmune IgG (NS IgG) or α3- or β1-integrin blocking antibodies. Control cells (control) received no treatment. Assays performed as described in Materials and Methods. These results are the mean of three independent experiments with standard deviation. ***** - statistically significant compared to NS IgG and control, $p < 0.01$. (**F**) Twenty-four hour rECM treatment induces caspase-3 activation in *HMEC-E6 cells. Qualitative caspase-3 activation was assayed as described in Materials and Methods and visualized on a fluorescence microscope. Light = total cells and FL= fluorescent positive cells. HMEC-LXSN control cells show no caspase-3 activation.

Figure 2 rECM and Tam signaling converge to upregulate a similar subset of genes in *HMEC-E6 early cells but do not share upstream initiation sites.

(A) Semiquantitative RT-PCR of selected interferon-stimulated genes in *HMEC-E6 cells **(*E6)** and passage matched HMEC-LX **(LXSN)** controls with either 1.0 μM Tam **(T)** treatment or growth in 3-hD rECM culture **(MG)** and compared to untreated cells **(Φ)**. Negative control reactions (no cDNA) are designated **Blk**. Gene expression studies were performed using Affymetrix Hu6800 gene chip arrays. Semiquantitative RT-PCR performed as described in Material and Methods. Results are representative of three independent experiments. **(B)** Pretreatment with estrogen does not block caspase-3 activation induced by rECM culturing in *HMEC-E6 cells. Cells were pretreated with or without 100 nM 17β–estradiol **(E2)** for 1 hr, and then cultured in rECM for 24 hr. Qualitative caspase-3 activation was assayed as described in Materials and Methods and visualized on a fluorescence microscope. **Light** = total cells and **FL*** = fluorescent positive cells. Results are representative of two independent experiments. **(C)** Pretreatment with α3- or β1-integrin blocking antibodies does not block caspase-3 activation induced by 1.0 uM Tam treatment in *HMEC-E6 cells. Cells were pretreated for 1 hr with preimmune IgG **(NS-IgG)**, α3- or β1-integrin blocking antibodies (**α3-bl** or **β1-bl**), and then treated with 1.0 uM Tam for 24 hr **(Tam)**. Control cells received no treatment **(No-Tx)**. Caspase-3 activation was assayed as described in Materials and Methods and visualized on a fluorescence microscope. Caspase-3 activation was measured by calculating the number of fluorescence positive nuclei relative to the total number of cells surveyed. Data represent an average of three experiments with standard deviation. There were no statistically significant differences between treatments, $p > 0.05$.

Figure 3. STAT1 phosphorylation and ChIP analysis of the *IRF-1* GAS element in *HMEC-E6 cells and HMEC-LX controls grown in3-hD rECM culture.

(A) Western analysis of STAT1α/β and STAT1-pSer727 showing constant STAT1α/β and increased STAT1-Ser727 phosphorylation after *HMEC-E6 cells **(*HMEC-E6)** are exposed to rECM for 1 hr. These results are representative of three independent experiments. **(B)** Quantitation of relative levels of STAT1-Ser727 phosphorylation in *HMEC-E6 cells **(*HMEC-E6)** after exposure to rECM for 1 hr. Results are the mean of three independent experiments with standard deviation. ***** - statistically significant compared to no rECM treatment, $p < 0.005$ **(C, D)** ChIP analysis in passage matched *HMEC-E6 cells and HMEC-LX vector controls of STAT1 and CBP recruitment to the *IRF-1* promoter GAS element as a function of rECM treatment. Cells are tested with **(+)** or without **(-)** exposure to rECM. Negative controls are designated **(N)**. **(C)** Vector control cells **(HMEC-LX)** show a lack of STAT1 or CBP recruitment to the *IRF-1* GAS element. Results are representative of three independent experiments. **(D)** In contrast, *HMEC-E6 cells **(*HMEC-E6)** demonstrate baseline association of STAT1 and recruitment of CBP to the *IRF-1* GAS element. Results are representative of three independent experiments. **(E)** Western blot of STAT1 binding to the *IRF-1* GAS element in lysates in precipitation experiments of *HMEC-E6 cells **(*HMEC-E6)** prepared with (+) and without (-) 1 hr exposure to rECM in 3-hD culture as described in Materials and Methods. *HMEC-E6 cells demonstrate baseline association increased binding of STAT1 and continued binding at 1 hr. Results are representative of two independent experiments.

Figure 4. Induction of IRF-1 mRNA and protein is observed in *HMEC-E6 cells grown in 3-hD rECM culture.

(A) Semiquantitative RT-PCR demonstrates that rECM promotes induction of IRF-1 mRNA starting at 60 min in *HMEC-E6 cells **(E6)** but not HMEC-LX controls **(LX)**. These results are representative of three separate experiments. **(B)** Quantitation of IRF-1 mRNA in *HMEC-E6 cells **(*HMEC-E6)** after exposure to rECM. These results are a mean of three independent experiments with standard deviation, * - significantly different from $t = 0$ h for $p < 0.01$. **(C)** Western analysis demonstrates that rECM promotes induction of IRF-1 protein in *HMEC-E6 cells at 1 hr **(*HMEC-E6)**. These results are representative of two separate experiments. **(D)** Quantitation of IRF-1 protein in *HMEC-E6 cells **(*HMEC-E6)** after exposure to rECM. These results are the mean of two independent experiments with standard deviation, * - significantly different from $t = 0$ h for $p < 0.01$.

Figure 5. Suppression of IRF-1 by siRNA blocks rECM-mediated apoptosis and caspase-1 and -3 activation in *HMEC-E6 cells.

(A) siRNA-mediated suppression of IRF-1 mRNA in *HMEC-E6 cells **(*HMEC-E6)** after 12 hr siRNA oligo treatment with either IRF-1 specific siRNA #1 **(si#1)** or IRF-1 specific siRNA #4 **(si#4)** relative to untreated control cells **(cont)**. These results are representative of two independent experiments. **(B)** siRNA suppression of IRF-1 protein in *HMEC-E6 cells **(*HMEC-E6).** Cells are pretreated for 12 hr with oligos, either IRF-1 specific siRNA #1 **(si#1)**, IRF-1 specific siRNA #4 **(si#4)**, or non-specific control siRNA **(cs).** Untreated cells are designated **(cont).** Data are representative of two independent experiments. **(C)** rECM-mediated induction of IRF-1 in *HMEC-E6 cells **(*HMEC-E6)** is blocked by pretreatment with siRNA. Cells are either untreated with rECM **(0)** or treated for 2 hr with rECM **(2h)**. Prior to rECM exposure, cells were pretreated for 12 hr with oligos, either IRF-1 specific siRNA #1 **(si#1)**, IRF-1 specific siRNA #4 **(si#4)**, or non-specific control siRNA **(cont siRNA).** These results are representative of three independent experiments. **(D, E)** rECM-mediated caspase-1 and caspase-3 activation in *HMEC-E6 cells is blocked by suppression of IRF-1. Prior to growth in 3-hD rECM culture, cells are pretreated for 12 hr with either IRF-1 specific siRNA oligos #1 **(siRNA #1)**, IRF-1 specific siRNA #4 **(siRNA #4)**, **(cellfectin)** cellfectin treatment alone, or non-specific control siRNA**(control siRNA).** Cells that do not receive siRNA or cellfectin are designated as control **(control)**. Caspase activity assays are performed as described in Materials and Methods. Data are the mean of three independent experiments with standard deviation. ***** - significantly different from controls, $p < 0.002$.

Figure 6. Stable suppression of IRF-1 blocks apoptosis in *HMEC-E6 cells while overexpression of IRF-1 promotes apoptosis in HMEC-LX cells.

(A) Stable siRNA suppression of IRF-1 protein in *HMEC-E6 cells **(*HMEC-E6).** Cells are transfected with pSilencer 4.1-CMV (**pSil**) containing either IRF-1 specific siRNA #1 **(si#1)**, or non-specific control siRNA **(cs)** target sequences. Untreated cells are designated (**cont**) and cells treated with Cellfectin only are designated **(CF).** Data are representative of two independent experiments. **(B)** rECM-mediated caspase-3 activation in *HMEC-E6 cells is blocked by stable suppression of IRF-1. Cells were transfected with pSilencer 4.1-CMV (**pSil**) containing either IRF-1 specific siRNA #1 **(si#1)**, or non-specific control siRNA **(cs)** target sequences; untreated cells are designated **(cont)**; cells treated with Cellfectin only are designated **(CF)**. Cells were cultured in rECM for 48h. Cells were harvested and assayed for caspase-3 activation as described in Materials and Methods. Data are representative of two independent experiments. ***** - statistically significant, $p < 0.01$. **(C)** Overexpression of IRF-1 in HMECs. HMEC-LX cells were transfected with IRES2-DsRed2-IRF-1 and control cells were transfected with the empty IRES2-DsRed2 vector. Qualitative DsRed expression in HMEC-LX cells expressing the DsRed empty vector **(DsRed-control)** and DsRed-IRF-1 **(DsRed-IRF1)** at 24h after transfection. Cells were visualized on a fluorescence microscope. Light = total cells and FL*= red fluorescence emission. **(D)** Expression of IRF-1 protein in HMEC-LX cells expressing the DsRed empty vector **(DsRed-control)** and DsRed-IRF-1 **(DsRed-IRF)**. **(E)** Overexpression of IRF-1 in HMEC-LX control cells induces apoptosis. HMEC-LX cells expressing DsRed-IRF-1 **(DsRed-IRF)** and the empty DsRed vector **(DS cont.)** were harvested 24h after transfection and assayed for caspase-3 activation **(Caspase-3)** and Annexin-V binding **(Annexin V)** as described in Materials and Methods. Data are representative of two independent experiments. Annexin V

binding is expressed as the percentage of Annexin V-FITC positive cells relative to total cells counted. Data are representative of three determinations. ***** - significantly different from controls $p < 0.002$.

Figure 7. rECM treatment of *HMEC-E6 cells promotes transcriptional activation of IFI 6-16 and coactivator recruitment to the *IFI 6-16* promoter ISRE.

(A) IFI 6-16 mRNA is induced by rECM in 3-hD culture at 60 min in *HMEC-E6 cells but not in HMEC-LX controls. Semiquantitative RT-PCR of IFI 6-16 mRNA expression in *HMEC-E6 cells **(*E6)** and passage matched HMEC-LX controls **(LX)**. Actin serves as a loading control. Data are representative of three separate experiments. **(B)** Quantitation of IFI 6-16 mRNA expression in *HMEC-E6 cells **(*HMEC-E6)** and passage matched HMEC-LX vector controls **(HMEC-LX)** after exposure to rECM. IFI 6-16 mRNA levels were normalized to actin. Data are the mean of three independent experiments with standard deviation, * - significantly different from $t = 0$ h for $p < 0.01$. **(C)** rECM treatment of *HMEC-E6 cells promotes increased expression of IRF-9 and STAT2 protein at 30 min. Western analysis of STAT2 and IRF-9 expression in *HMEC-E6 cells **(*HMEC-E6)** was performed as described in Materials and Methods. Actin serves as a loading control. **(D, E, F)** ChIP was performed to test for binding of the ISGF3 complex (STAT1/STAT2/IRF-9) as well as IRF-1 and CBP to the *IFI 6-16* ISRE element. *HMEC-E6 cells were treated with rECM, cells harvested, and lysates tested for transcriptional factor binding. Both IRF-9 **(D)** and STAT-1 **(E)** were recruited to the *IFI 6-16* ISRE promoter element in *HMEC-E6 cells at 30 min. In addition, IRF-1 and CBP were recruited to the *IFI 6-16* ISRE promoter element at 60 min **(F)**. These observations show that both the ISGF3 complex and IRF-1/CBP are recruited to the *IFI 6-16* ISRE promoter element. **(D)** MCF-7 cells **(M7)** treated with interferon-gamma **(+I)** serve as a positive control. A genomic DNA positive **(+)** and a negative with no DNA **(-)** were run as PCR controls. ChIP data are representative of three independent experiments

A

Small-Scale rECM Culture: HMECs are grown in semi-solid rECM in microtiter wells with media overlay

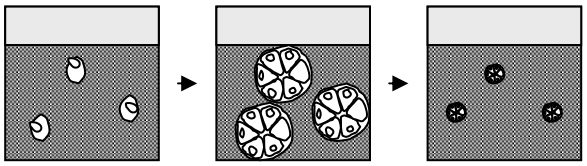

Day 0 Single Cells | Day 6 20-30 micron | Day 6-7 Apoptosis

Large-Scale High-Density Liquid rECM Culture (3-hD)- HMECs are grown in polyHEMA coated flasks with a 1:100 dilution of rECM in Standard Media

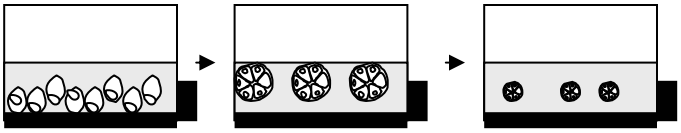

Time 0 Single Cells | 6 hr 20-30 micron | 12-24 hr Apoptosis

B

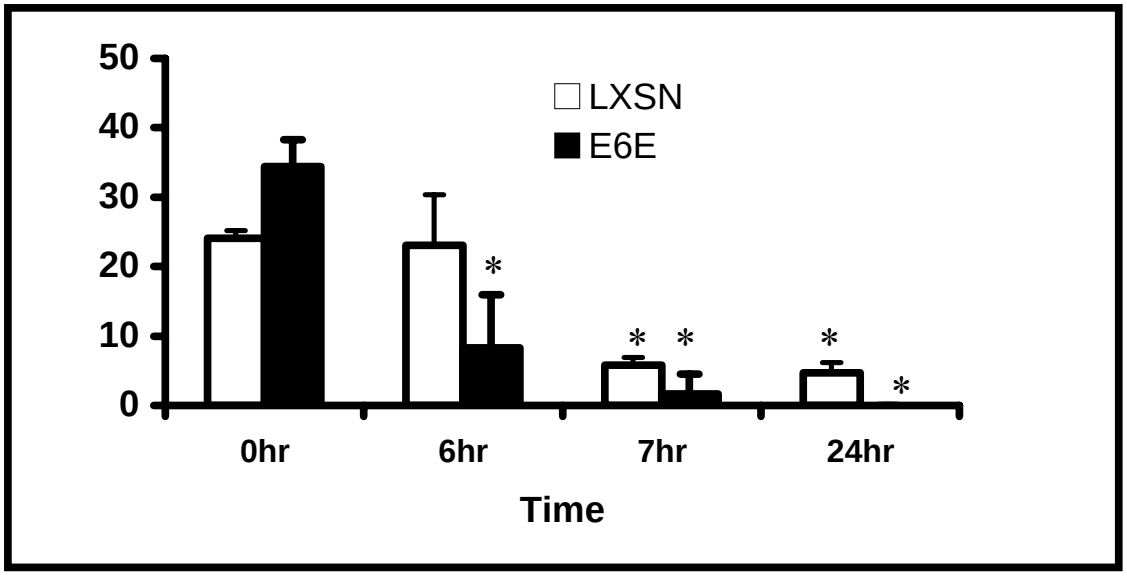

C

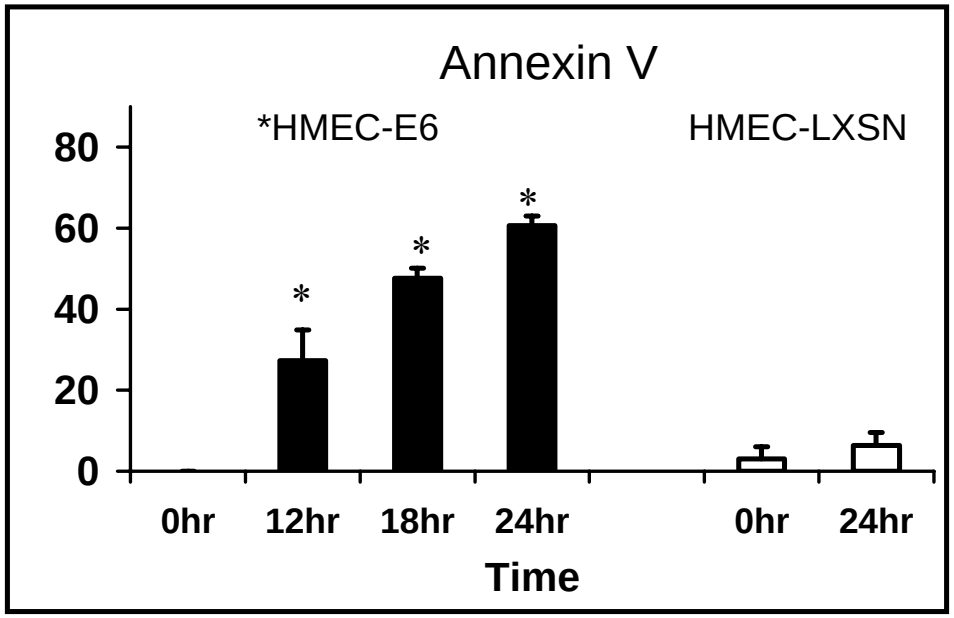

Fig. 1 A-C

D

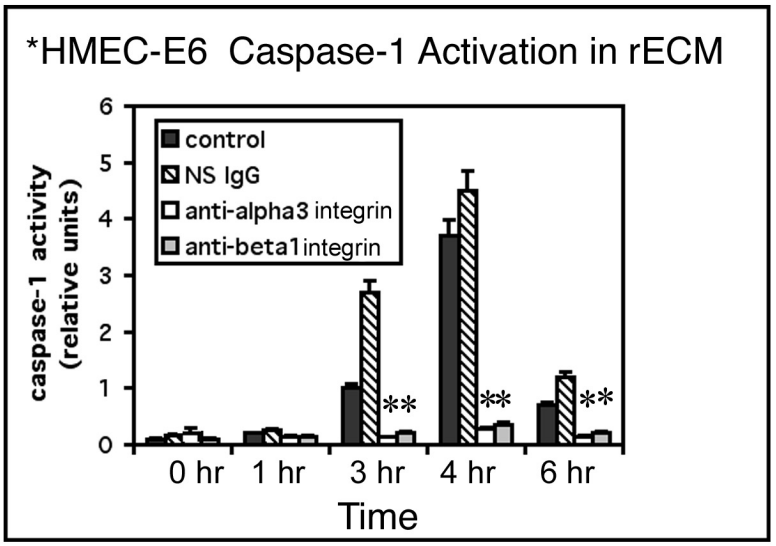
*HMEC-E6 Caspase-1 Activation in rECM
caspase-1 activity (relative units)
control
NS IgG
anti-alpha3 integrin
anti-beta1 integrin
0
1
2
3
4
5
6
**
**
**
0 hr
1 hr
3 hr
4 hr
6 hr
Time

E

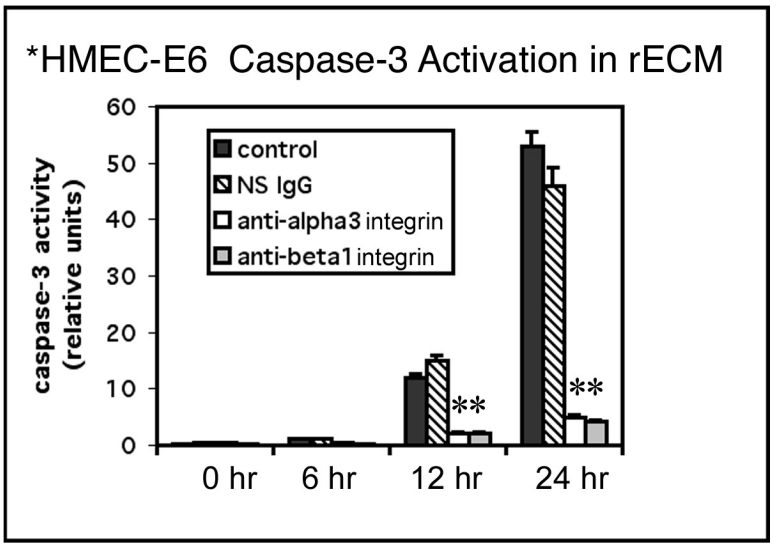
*HMEC-E6 Caspase-3 Activation in rECM
caspase-3 activity (relative units)
control
NS IgG
anti-alpha3 integrin
anti-beta1 integrin
0
10
20
30
40
50
60
**
**
0 hr
6 hr
12 hr
24 hr

F

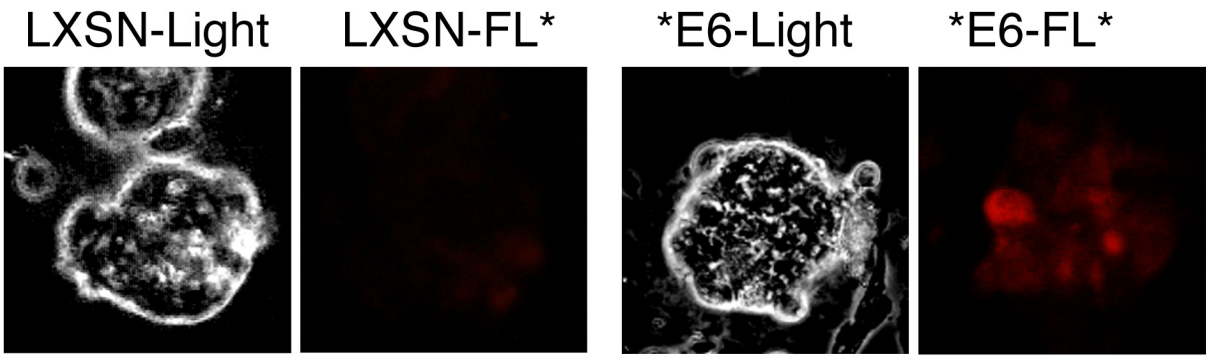
LXSN-Light
LXSN-FL*
*E6-Light
E6-FL
20 microns

Fig. 1 D-F

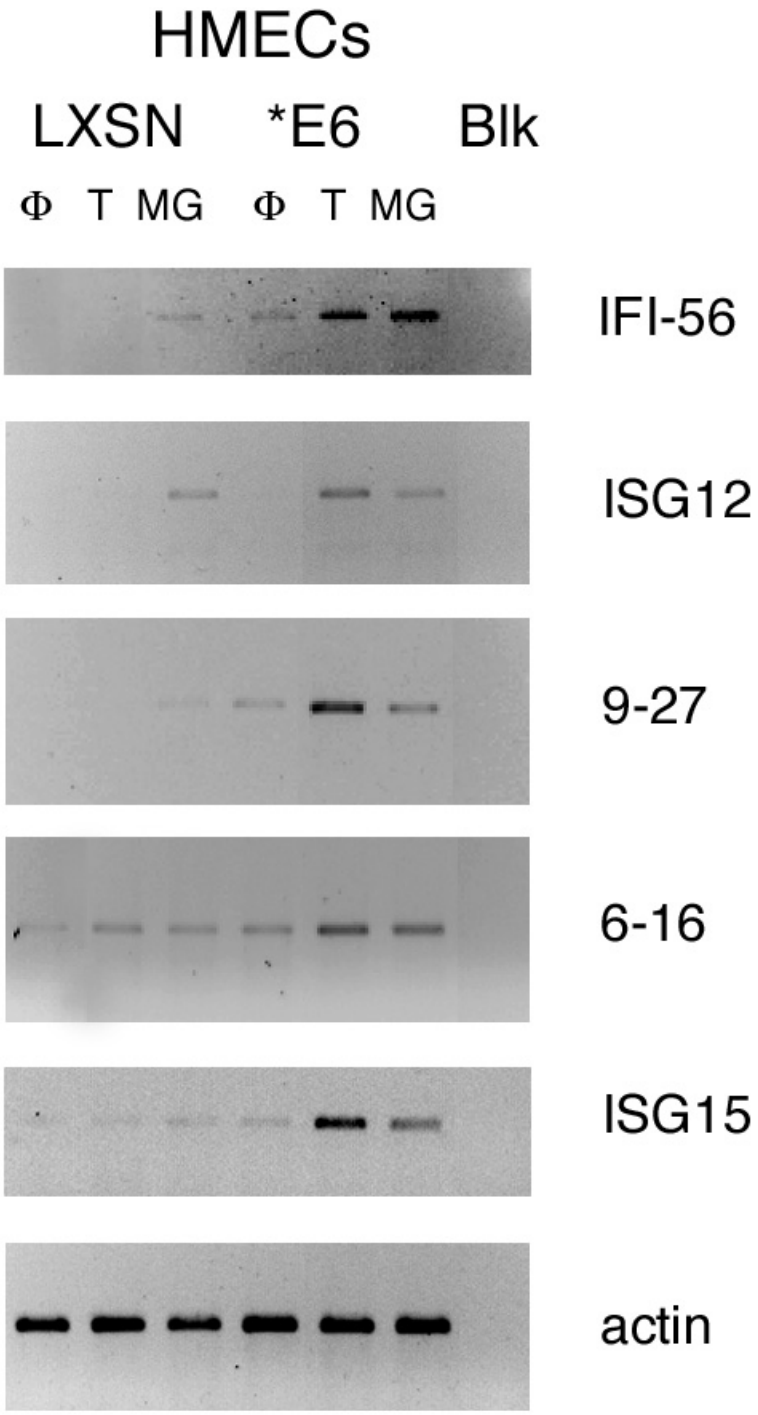

Fig. 2 A

B

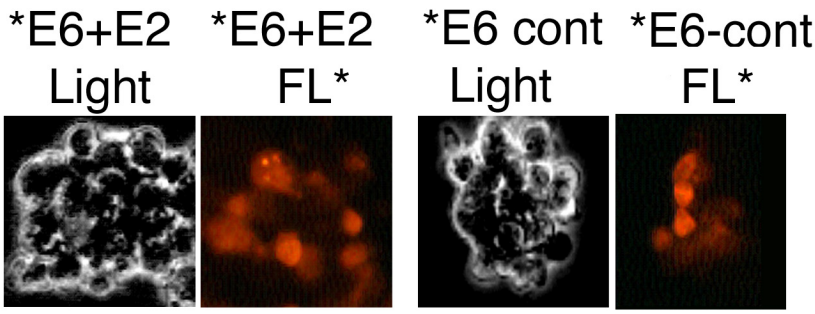

20 microns

C

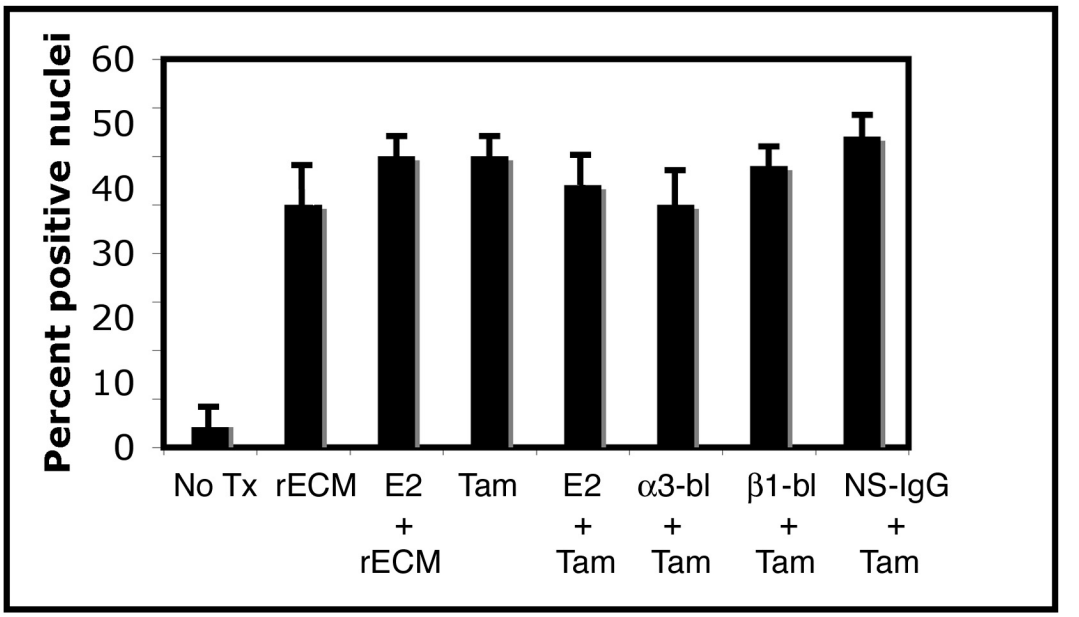

Fig. 2 B, C

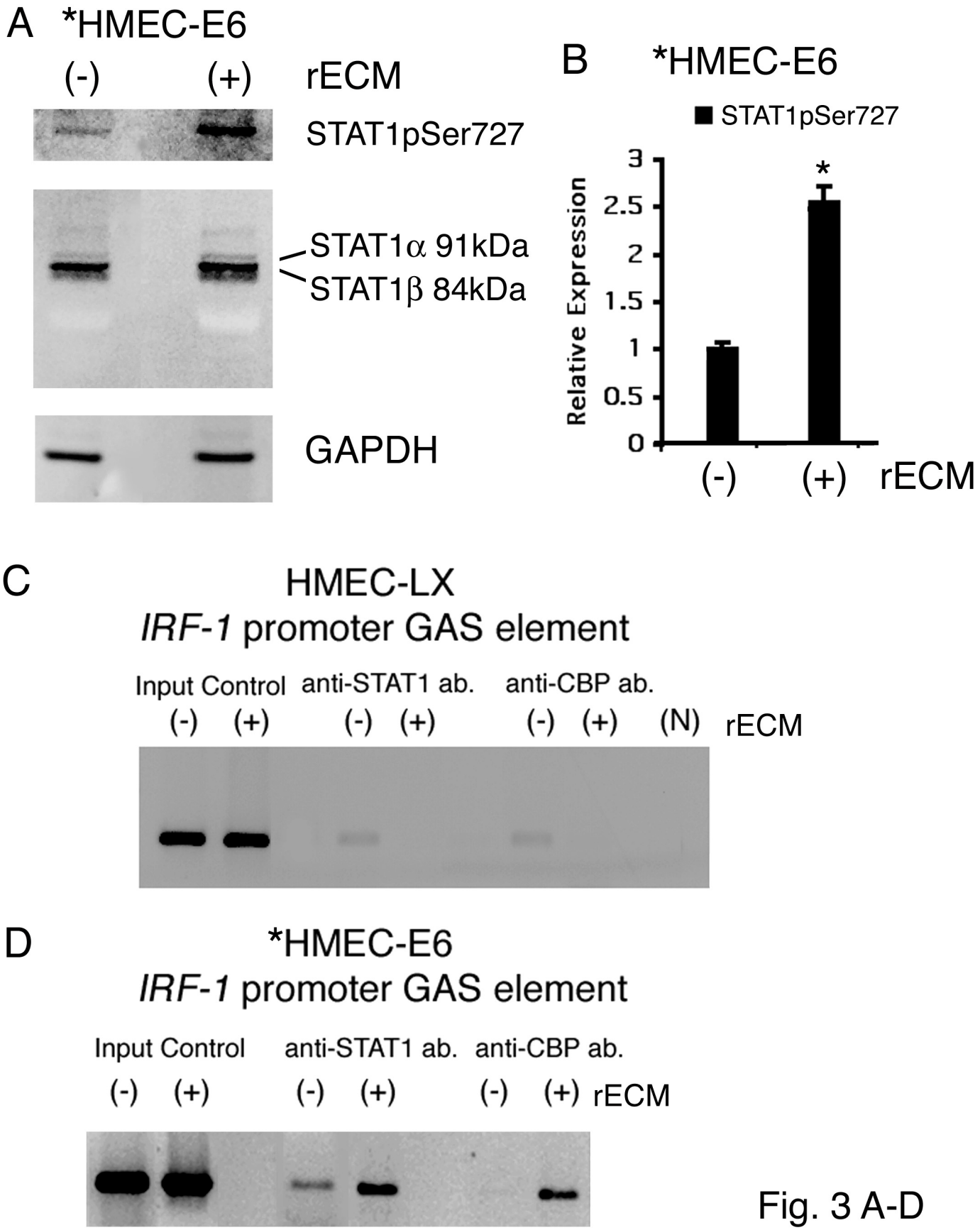
A
*HMEC-E6
(-)
(+)
rECM
STAT1pSer727
STAT1α 91kDa
STAT1β 84kDa
GAPDH
B
*HMEC-E6
STAT1pSer727
Relative Expression
3
2.5
2
1.5
1
0.5
0
*
(-)
(+)
rECM
C
HMEC-LX
IRF-1 promoter GAS element
Input Control
anti-STAT1 ab.
anti-CBP ab.
(-)
(+)
(-)
(+)
(-)
(+)
(N)
rECM
D
*HMEC-E6
IRF-1 promoter GAS element
Input Control
anti-STAT1 ab.
anti-CBP ab.
(-)
(+)
(-)
(+)
(-)
(+)
rECM

Fig. 3 A-D

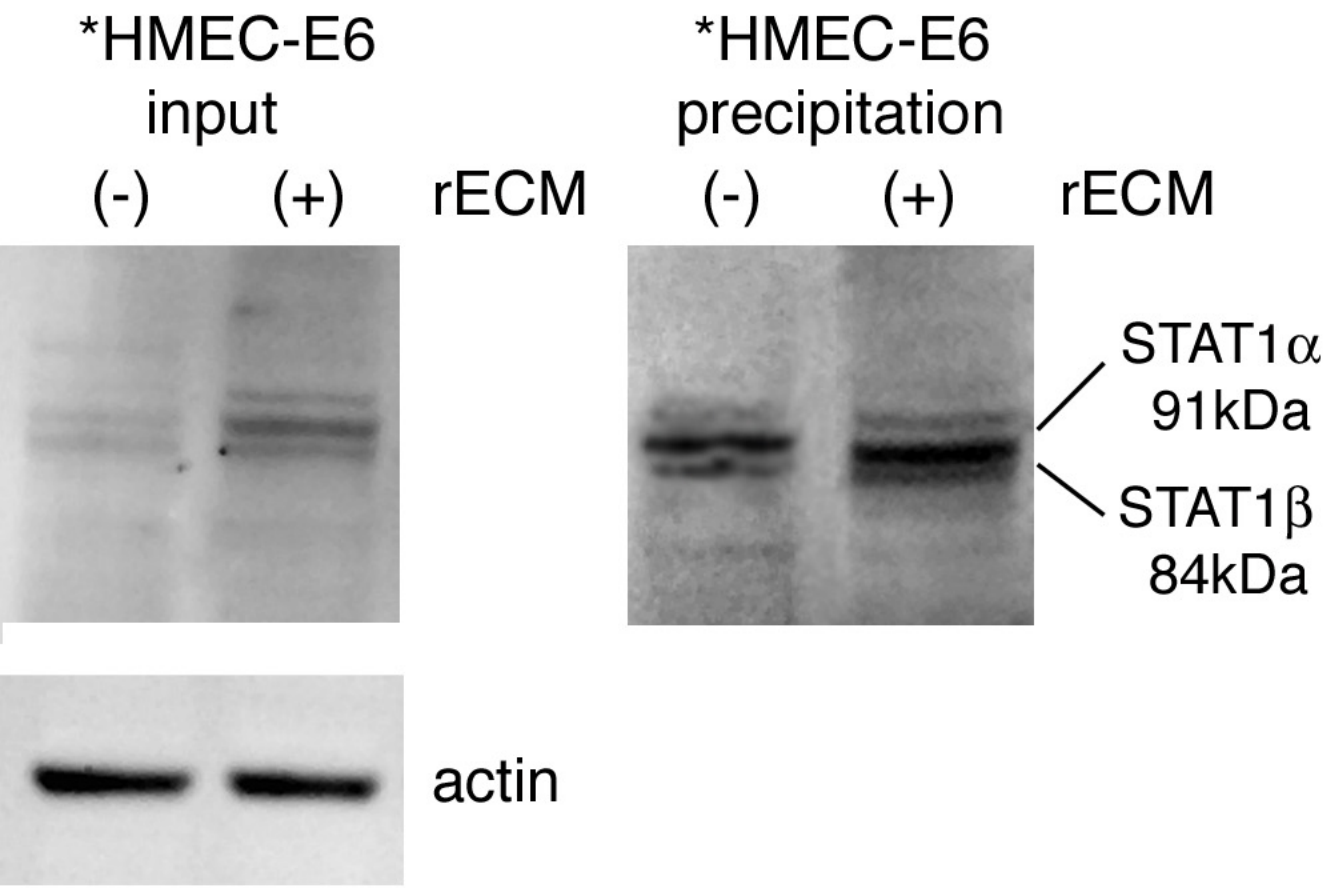
*HMEC-E6
input
(-)
(+)
rECM
*HMEC-E6
precipitation
(-)
(+)
rECM
STAT1α
91kDa
STAT1β
84kDa
actin

Fig. 3 E

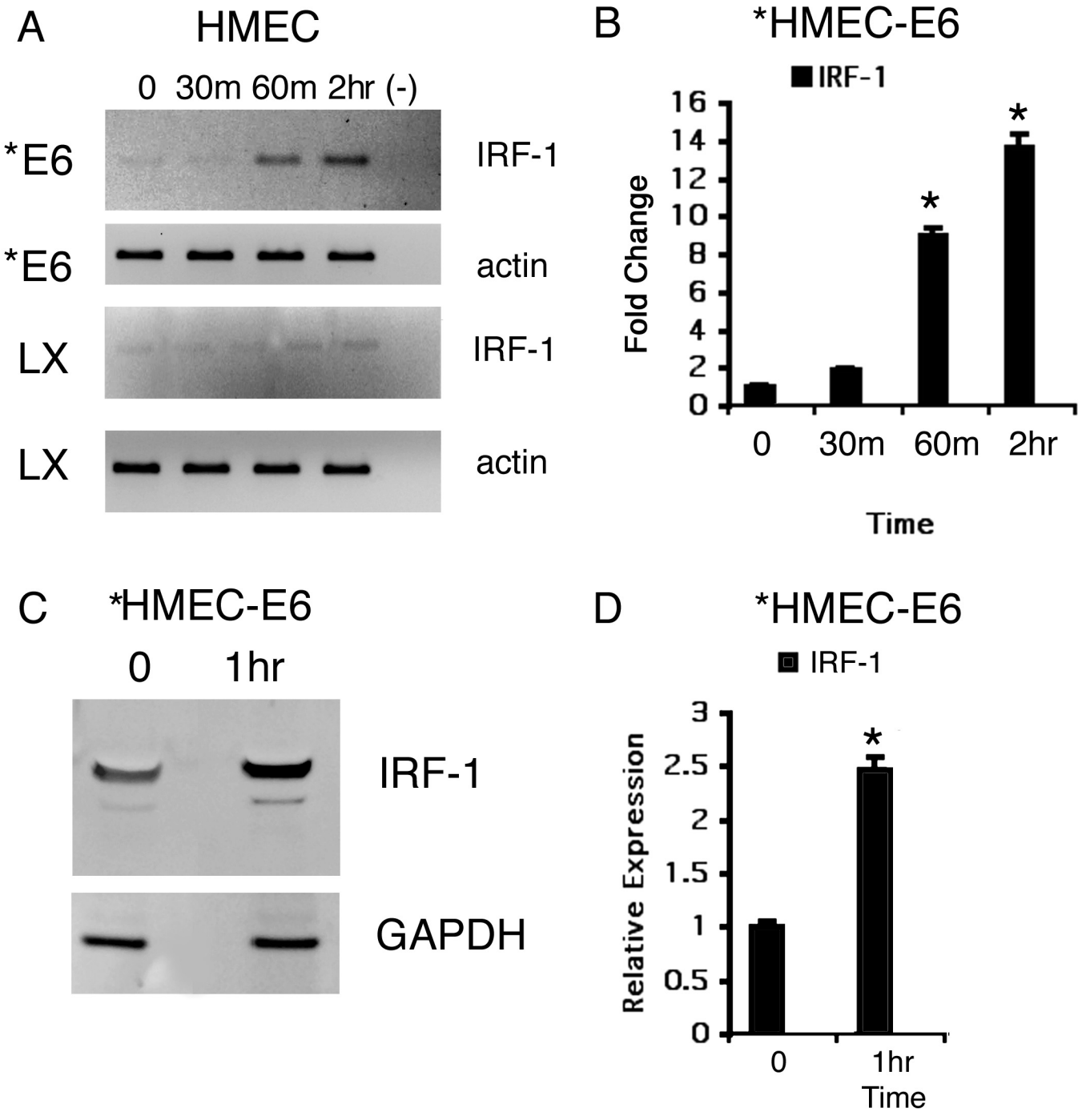
A
HMEC
0 30m 60m 2hr (-)
*E6
IRF-1
*E6
actin
LX
IRF-1
LX
actin
B
*HMEC-E6
IRF-1
Fold Change
16
14
12
10
8
6
4
2
0
0
30m
60m
2hr
Time
C
*HMEC-E6
0
1hr
IRF-1
GAPDH
D
*HMEC-E6
IRF-1
Relative Expression
3
2.5
2
1.5
1
0.5
0
0
1hr
Time

Fig. 4 A-D

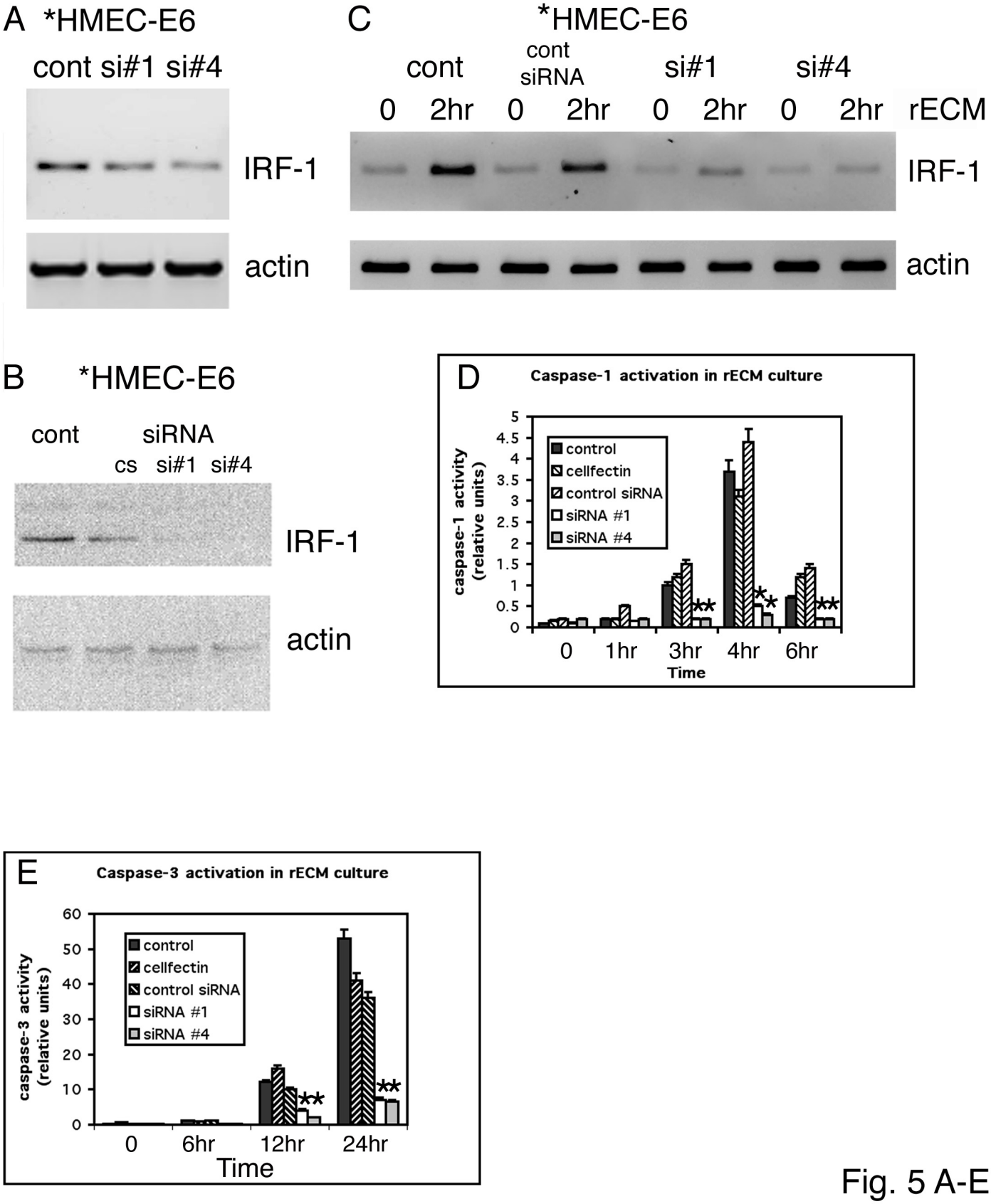
A *HMEC-E6
cont si#1 si#4
IRF-1
actin
C *HMEC-E6
cont
cont siRNA
si#1
si#4
0 2hr 0 2hr 0 2hr 0 2hr rECM
IRF-1
actin
B *HMEC-E6
cont siRNA
cs si#1 si#4
IRF-1
actin
D
Caspase-1 activation in rECM culture
caspase-1 activity (relative units)
control
cellfectin
control siRNA
siRNA #1
siRNA #4
0 1hr 3hr 4hr 6hr
Time
E
Caspase-3 activation in rECM culture
caspase-3 activity (relative units)
control
cellfectin
control siRNA
siRNA #1
siRNA #4
0 6hr 12hr 24hr
Time

Fig. 5 A-E

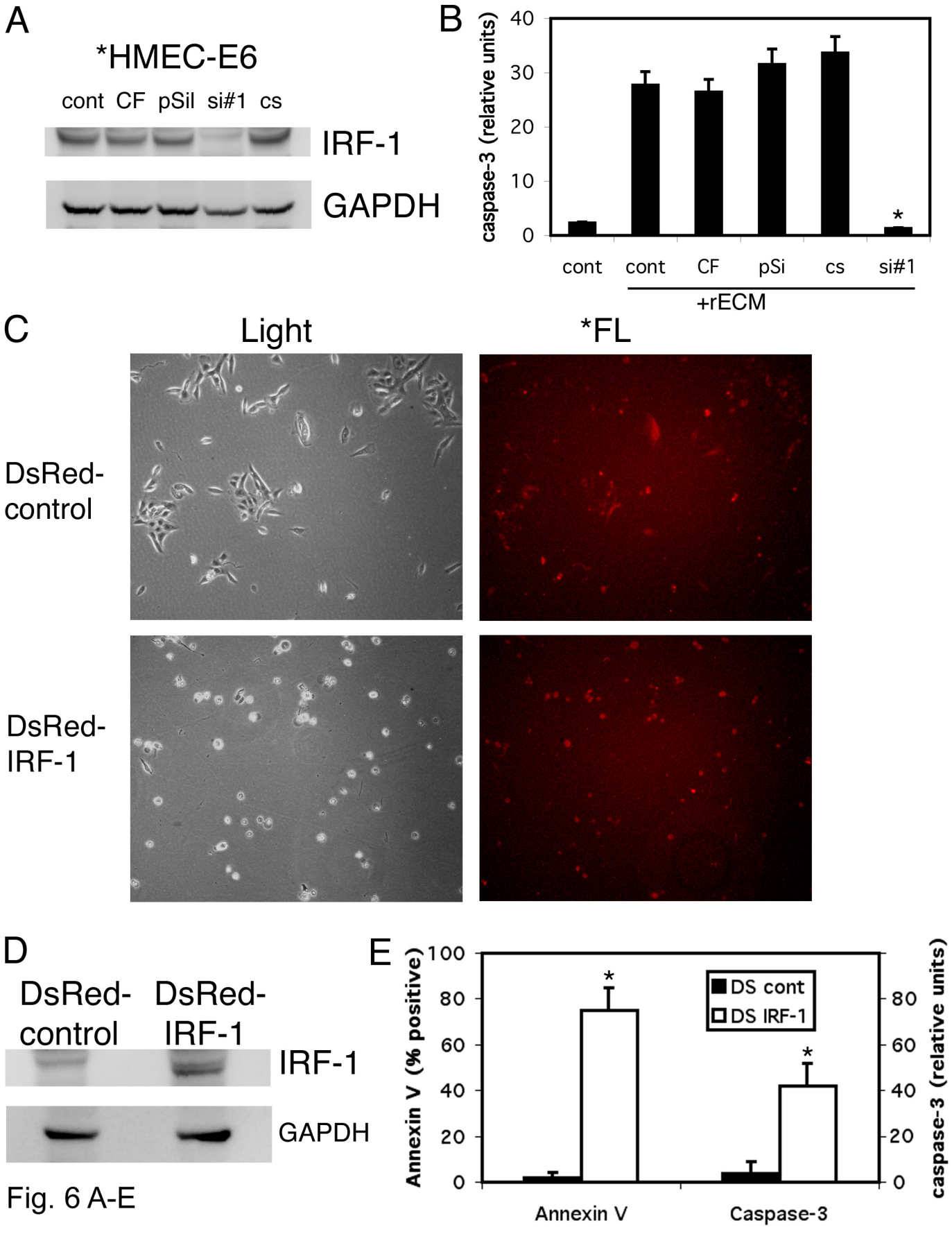
A
*HMEC-E6
cont CF pSil si#1 cs
IRF-1
GAPDH
B
caspase-3 (relative units)
40
30
20
10
0
*
cont cont CF pSi cs si#1
+rECM
C
Light
*FL
DsRed-control
DsRed-IRF-1
D
DsRed-control
DsRed-IRF-1
IRF-1
GAPDH
E
Annexin V (% positive)
100
80
60
40
20
0
DS cont
DS IRF-1
caspase-3 (relative units)
Annexin V
Caspase-3

Fig. 6 A-E

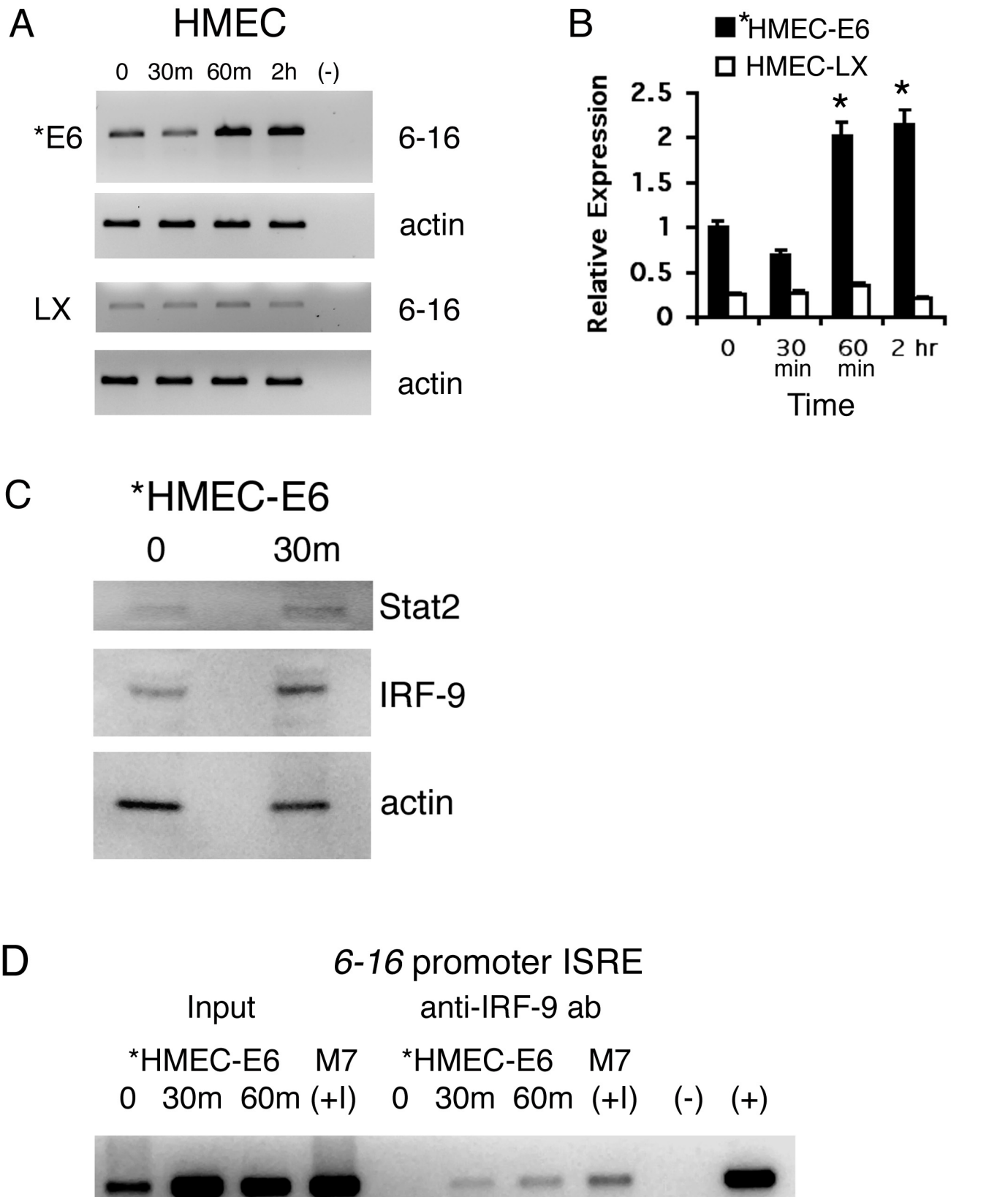
A
HMEC
0 30m 60m 2h (-)
*E6
6-16
actin
LX
6-16
actin
B
*HMEC-E6
HMEC-LX
Relative Expression
2.5
2
1.5
1
0.5
0
*
*
0
30 min
60 min
2 hr
Time
C
*HMEC-E6
0 30m
Stat2
IRF-9
actin
D
6-16 promoter ISRE
Input
anti-IRF-9 ab
*HMEC-E6 M7 *HMEC-E6 M7
0 30m 60m (+I) 0 30m 60m (+I) (-) (+)

Fig. 7 A-D

E

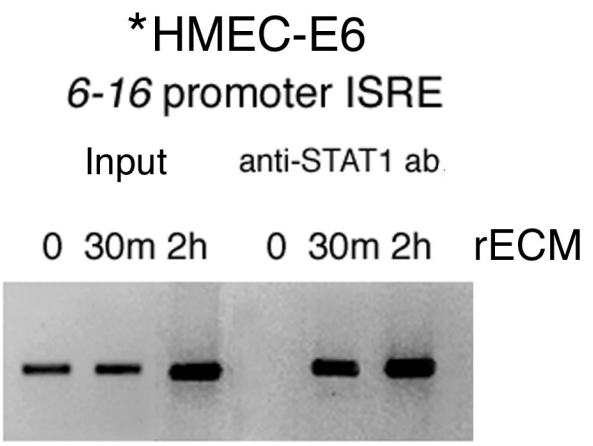
*HMEC-E6
6-16 promoter ISRE
Input
anti-STAT1 ab
0 30m 2h 0 30m 2h rECM

F

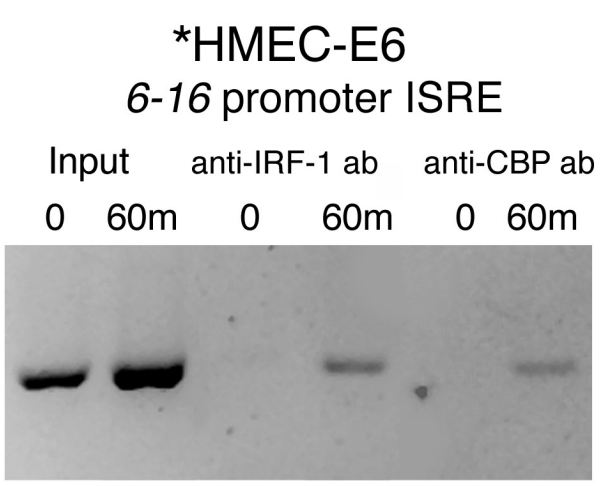
*HMEC-E6
6-16 promoter ISRE
Input
anti-IRF-1 ab
anti-CBP ab
0 60m 0 60m 0 60m

Fig. 7 E,F